TESE DE DOUTORAMENTO

DETERMINATION OF TRANSFORMATION PRODUCTS FORMED DURING WATER DISINFECTION BY CHROMATOGRAPHIC TECHNIQUES COUPLED TO QUADRUPOLE TIME-OF-FLIGHT MASS SPECTROMETRY

Benigno José Sieira Nóvoa

ESCOLA DE DOUTORAMENTO INTERNACIONAL

PROGRAMA DE DOUTORAMENTO EN CIENCIA E TECNOLOXÍA QUÍMICA

Santiago de Compostela
2020

USC
UNIVERSIDADE
DE SANTIAGO
DE COMPOSTELA

DECLARACIÓN DO AUTOR/A DA TESE

DETERMINATION OF TRANSFORMATION PRODUCTS FORMED DURING WATER DISINFECTION BY CHROMATOGRAPHIC TECHNIQUES COUPLED TO QUADRUPOLE TIME-OF-FLIGHT MASS SPECTROMETRY

D. Benigno José Sieira Nóvoa

Presento a miña tese seguindo o procedemento axeitado ao Regulamento, e declaro que:

1) A tese abarca os resultados da elaboración do meu traballo.
2) De selo caso, na tese faise referencia ás colaboración que tivo este traballo.
3) Confirmo que a tese non incorre en ningún tipo de plaxio doutros autores nin de traballos presentados por min para a obtención doutros títulos.

En Santiago de Compostela, 06 de Outubro de 2020

Asdo. Benigno José Sieira Nóvoa

USC
UNIVERSIDADE
DE SANTIAGO
DE COMPOSTELA

AUTORIZACIÓN DO DIRECTOR / TITOR DA TESE

DETERMINATION OF TRANSFORMATION PRODUCTS FORMED DURING WATER DISINFECTION BY CHROMATOGRAPHIC TECHNIQUES COUPLED TO QUADRUPOLE TIME-OF-FLIGHT MASS SPECTROMETRY

Dna. Mª del Rosario Rodil Rodríguez

D. José Benito Quintana Álvarez

INFORMAN:

Que a presente tese correspóndese co traballo realizado por D. Benigno José Sieira Nóvoa, baixo a nosa dirección, e autorizamos a súa presentación, considerando que reúne os requisitos esixidos no Regulamento de Estudos de Doutoramento da USC, e que como directores desta, non incorre nas causas de abstención establecidas na Lei 40/2015

En Santiago de Compostela, 06 de Outubro de 2020

Asdo. Mª del Rosario Rodil Rodríguez

Asdo. José Benito Quintana Álvarez

USC
UNIVERSIDADE
DE SANTIAGO
DE COMPOSTELA

AGRADECIMIENTOS

Cuando me metí de cabeza en el mundo del doctorado, era consciente de que estaba entrando en una carrera de fondo, un camino de mucha distancia y esfuerzo que, sin duda, estaba dispuesto a emprender. Años más tarde, tras tropezar con alguna que otra piedra, aquí estoy, redactando el fruto de esta caminata, momento que llevo esperando como el que más todo este tiempo. Y no lo he hecho solo.

No podría empezar esta parrafada sin darle las gracias a mis directores José Benito Quintana y Rosario Rodil… los puntos de luz en el suelo para saber por dónde caminar, Tito y Charo para mí. Gracias por haberme acogido desde que tenía 20 años en aquellas prácticas de 3º de grado y estar dispuestos a aguantarme durante TFG, TFM y, ahora, en esta Tesis. Estar a vuestro lado y bajo vuestra dirección todo este tiempo no sólo ha sido para mí un avance en el mundo académico, ha sido mucho más que eso. De verdad, gracias.

Isaac y María, aunque no pongáis la firma en esta tesis, habéis puesto un sello en mi vida al poder compartir con vosotros tanto el espacio en el laboratorio como otros puntos de vista y pensamiento. *Sharing is caring*, y vosotros lo habéis hecho conmigo.

Al padre de nuestro grupo, Rafael. Decir que eres un referente para mí es poco. Además de darme el verdadero placer de estar rodeado de los mejores equipos durante años, me has puesto los pies en la tierra más de una vez cuando más lo necesité, ayudándome y aconsejándome en lo personal y en lo profesional.

There are also people outside Spain I want to give thanks too. To Professor Hervé Gallard, for supporting me in Poitiers, knowing another country, another city, another lab. Florence, Clement and, of course, Arnaud, thank you so much.

Dentro de casa, mi verdadera casa, Papá y Mamá, qué decir de vosotros… en las buenas y en las malas, en las alegrías y en las discusiones, desde 2010 fuera del nido y cada fin de semana que agradezco poder bajar a veros, desconectar con vosotros. 28 años a vuestro lado no son suficientes. No tengo palabras para vosotros. Os quiero.

Uxi, mi hermanita del alma… para ti tengo que escribir aparte, y es que lo mejor que me pudo pasar es que nacieras antes que yo, y que así me advirtieses sobre el mundo. Literalmente mi consejera en la distancia, desde Dublín aguantándome estos años, poniendo la voz de la experiencia y enseñándome cómo afrontar las situaciones más complicadas de este mundo. Gracias irmán, las más sinceras que nunca te dará nadie.

A toda mi demás familia, porque no sólo dentro del "2º" me han estado apoyando. Mis abuelos, mis tíos, mis primos… Mi tía María, mi segunda madre, siempre pendiente de mí, Petete. A mi tío Jon, quien, desde pequeñito, bien pequeñito, me enseñó que la música es parte del mundo, parte de la vida, que siempre habrá una canción, un disco, un grupo, que encaje perfectamente con el momento en el que estás. *Let it be*.

Dentro del laboratorio, de puertas para dentro. Estar tanto tiempo aquí metido me ha hecho conocer mucha gente, cada uno de su padre y de su madre desde luego, pero mucha gente al final y con los que todos he conseguido intimar. Tania, Eugenia y Jorge, vosotros fuisteis de los primeros a los que enganché cuando crucé la puerta por primera

vez, además de mi pequeña madrastra, Inés, la que sin duda me animó a empezar, continuar y terminar en este mundo. Hace ya tiempo que nuestros caminos se separaron, pero el haberos conocido fue parte de la decisión de permanecer en esta pequeña casa. Iría e Inma, que desde la carrera os conozco por ser mis profes de prácticas y, al final, ¡compartiendo laboratorio! Y como no voy a agradecer a las que cierran este círculo de verdaderas marujas, Tamara, Sara y Rosita… madre mía que pandillita. Os juro que voy a echar de menos los descansos en todas sus formas y colores: en la planta de arriba, en la mesa redonda y, ¿por qué no? En psicología con unas cañas. Gracias a todos, de verdad.

Al colectivo que me rodea, los que compartieron y comparten el mismo mundo que yo por igual. Vero, Andrea, Miguel… avanzad pequeños, ¡avanzad! Mirad siempre hacia delante, que nada os pare ni os impida seguir caminando en este mundo, llegar hasta el final, sois capaces de eso y más, lo veo en vosotros. Espero que nos encontremos fuera y podamos celebrar hasta la última tesis. Mis pequeñajos Leti y Javi, vosotros habéis vivido conmigo más de una experiencia, buena y mala, tirones de pelos y alegrías. Pero al final, esto es lo que nos ha unido Gracias, chicos, en serio.

Gabriela… bah, que pereza escribir sobre ti :rata:. Si tuviera que escribir todo lo que tengo que agradecer, me saco otra tesis. Y ojalá estuviera exagerando. Desde el máster en el mismo laboratorio, como dos pequeñajos que crecen juntos, que se enfrentan de la mano al mundo en el que estamos y, desde luego, del que saldremos como adultos para cambiarlo. Muchos desayunos, muchas comidas, y alguna que otra bronca… pero muchas horas compartidas. Gracias, pero más gracias que nunca, más de las que nunca te podrán dar, por convertirte en mi mejor amiga, mi verdadero apoyo. No me importa que nuestros caminos se puedan separar, sólo podrá ser en espacio, porque abandonar, lo que viene siendo abandonar, te la vas a creer si piensas que va a ser así. Me da igual Carballo que Trondheim, tú háblame, ¿eh? Te voy a menos de echar mucho.

Pero no todo va a ser de puertas para dentro. O bueno, en realidad sí, pero de otras puertas, y es que dentro de mi propia casa hay gente a la que quiero mencionar, gente que está detrás de una pantalla, detrás de un micrófono en Discord, pero apoyos, al fin y al cabo. A la gente de VR/EU y añadidos, que desde 2017 llevan aguantándome como compañero de equipo y, desde luego, como amigo. A los Salmon Runners que “caminan” conmigo por el orgullo de Mr. Grizz. Para mí, sois parte de este camino. Para vosotros, soy Beni en vez de Thinsky.

En Santiago, mi ciudad durante 10 años… no creo que pueda agradecerle lo suficiente al destino que haya decidido colocarme aquí y permitirme conocer a la pandillita con la que hoy en día comparto terrazas, y con las que espero seguir haciéndolo. Cartas, Chechu (mi eterno compañero de prácticas, de ti también me acuerdo), Iago, Martín, Núñez, Samuel, Torres, eternamente agradecido chavules. A otros que no estudiaban conmigo, pero que estuvieron cada día como si lo hiciesen: Andrea, por ser nuestra madre en funciones en la facultad, Manuel, Alberto… gracias. A los más cercanos en esta tropa, Cristina, Roi, que hasta hemos vivido juntos… ¿qué más se puede compartir? Y, como no, Nurita, de las primeras de la pandilla en defender, de las primeras en ser una heroína, de las primeras en demostrarme que en este mundo se entra, pero también se sale. Vas a ser una profesora increíble.

A Claudia, de quien, por supuesto no me puedo olvidar, el mejor médico de Madrid. Finalmente, tras “vivir como un bicho, pensar como un bicho, convertirme en un bicho”, lo he conseguido, y sin duda alguna has tenido un poquito que ver durante muchos años, al igual que Goyo. Espero que de aquí salgan los frutos más grandes, jugosos y posiblemente super inteligentes que jamás conoció el hombre.

Al igual que un círculo, voy a terminar cerrando dónde empecé todo: Ribeira, mi mar, mi Dorna, mi casa. Cómo hacer una tesis si no es por el infinito apoyo de todos y cada uno de ellos, de mis Steaua de Fondevila. Literalmente sin vosotros, no sé qué habría hecho. Y bueno, “sé que, como Rey, no debería tener favoritos… pero, los tengo”, Alei y David, vosotros dos habéis sido mis secuaces, mis guardaespaldas. No me dejéis solo, nunca.

Es mucha la gente a la que quiero agradecer este camino. Sin alguno de vosotros, esto no habría salido adelante, de eso estoy seguro. Por ello no quiero que ninguno me faltéis en el futuro. Quién sabe dónde estaré, qué me espera ahí fuera, cuál será mi próximo reto…

Pero, de cualquier manera, siempre os tendré en la cabeza para decir:

Booyah!

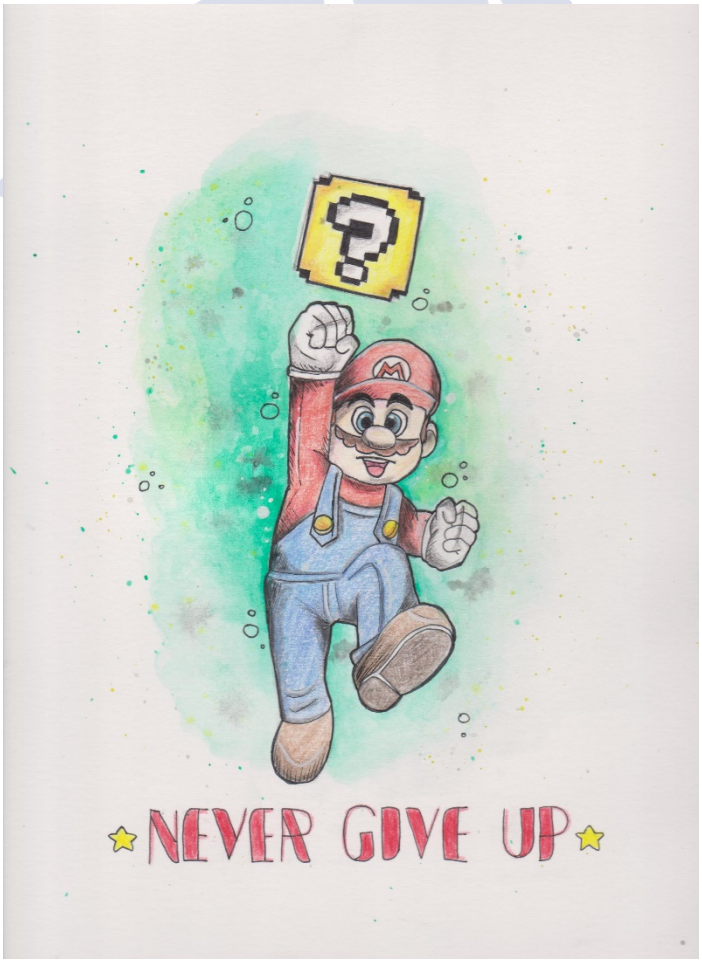

USC
UNIVERSIDADE
DE SANTIAGO
DE COMPOSTELA

FUNDING

This thesis was possible due to the funding provided by:

- Xunta de Galicia, Consellería de Cultura, Educación e Universidades (ref. GRC2013-020, ED431C2017/36, EM2014/004)
- Ministerio de Ciencia, Innovación e Universidades - Agencia Estatal de Investigación (ref. CTM2014-56628-C3-2-R, CTM2017-84763-C3- 2-R, JPIW2013-117, UNST15-DE-3350)
- Water Challenges for a Changing World Joint Program Initiative (Water JPI) Pilot Call (ref. WATERJPI2013 – PROMOTE)
- European Regional Development Funds (ERDF/FEDER), which cofounded several of the above projects
- European Cooperation in Science and Technology (COST) for funding my research stay in Poitiers through COST action ES1307

USC
UNIVERSIDADE
DE SANTIAGO
DE COMPOSTELA

INDEX

USC
UNIVERSIDADE
DE SANTIAGO
DE COMPOSTELA

INDEX

USC
UNIVERSIDADE
DE SANTIAGO
DE COMPOSTELA

INDEX OF FIGURES

INDEX OF TABLES

USC
UNIVERSIDADE
DE SANTIAGO
DE COMPOSTELA

ABBREVIATIONS

USC
UNIVERSIDADE
DE SANTIAGO
DE COMPOSTELA

ABBREVIATIONS

A	
AA	*4-aminoantipyrine*
AAA	*4-acetoamidoantipyrine*
ACN	*Acetonitrile*
AcOEt	*Ethyl acetate*
AOP	*Advanced oxidation process*
APCI	*Atmospheric pressure chemical ionization*
B	
BP	*4-bromophenol*
C	
CEC	*Contaminant of emerging concern*
CI	*Chemical ionization*
D	
DBE	*Double-bond equivalent*
DBP	*Disinfection by-product*
DCF	*Diclofenac*
DCAN	*Dichloroacetonitrile*
DCM	*Dichloromethane*
DDD	*Defined daily dose*
DOC	*Dissolved organic carbon*
DPG	*1,3-diphenylguanidine*
DTG	*1,3-di-o-tolylguanidine*
DWTP	*Drinking water treatment plant*
E	
ECD	*Electron capture detector*
ECHA	*European Chemicals Agency*
EI	*Electron impact*
EIC	*Extracted Ion Chromatogram*
EEO	*Electrical energy per order*
EPA	*Environmental Protection Agency*
ESI	*Electrospray ionization*
F	
FAA	*4-formylaminoantipyrine*
FET	*Fish embryo acute toxicity*
FT-ICR	*Fourier transform ion cyclotron resonance*
FWHM	*Full width half maximum*
G	
GC	*Gas chromatography*
GC-MS	*Gas chromatography – Mass spectrometry*
H	
HAA	*Haloacetic acid*
HAN	*Haloacetonitrile*

HPF	*Hour post-fertilization*
HPLC	*High-performance liquid chromatography*
HRMS	*High-resolution mass spectrometry*
I	
IBU	*Ibuprofen*
IDL	*Instrumental detection limit*
IQL	*Instrumental quantification limit*
IS	*Internal standard*
IT	*Ion Trap*
L	
Laser	*Light amplification by stimulated emission of radiation*
LC	*Liquid chromatography*
LC-MS	*Liquid chromatography – Mass spectrometry*
LOD	*Limit of detection*
LOQ	*Limit of quantification*
LSD	*Least significant difference*
M	
MAA	*4-methylaminoantipyrine*
MBR	*Membrane bioreactor*
MDL	*Method detection limit*
MeOH	*Methanol*
MQL	*Method quantification limit*
MS	*Mass spectrometry*
MS/MS	*Tandem mass spectrometry*
N	
NDBA	*N-Nitrosodibutylamine*
N-DBP	*Nitrogenous disinfection by-product*
NDEA	*N-Nitrosodiethylamine*
NDMA	*N-Nitrosodimethylamine*
NDPA	*N-Nitrosodipropylamine*
NIST	*National Institute of Standards and Technology*
NMEA	*N-Nitrosoethylmethylamine*
NMOR	*N-Nitrosomorpholine*
NMR	*Nuclear magnetic resonance*
NPIP	*N-Nitrosopiperidine*
NPYR	*N-Nitrosopyrrolidine*
NSAID	*Non-steroideal anti-inflamatory drug*
P	
PAC	*Powdered activated carbon*
PBT	*Persistent bioaccumulative and toxic*
PCI	*Positive chemical ionization*
PDA	*Photodioide array detector*
PFTBA	*Perfluorotributylamine*
Phe	*Phenazone*
PMOC	*Persistent and mobile organic compound*
PM(T)	*Persistent and mobile (and potentially toxic)*

PPE	*2-piperazin-1-ylethanamine*
PrPhe	*Propyphenazone*
PVDF	*Polyvinylidene fluoride*
Q	
Q	*Quadrupole*
QSAR	*Quantitative structure-activity relationship*
QTOF	*Quadrupole – time-of-flight*
QTRAP	*Linear ion trap*
R	
REACH	*Registration, evaluation, authorisation and restriction of Chemicals*
RSD	*Relative standard deviation*
S	
SD	*Standard deviation*
SE	*Standard error*
SPE	*Solid-phase extraction*
SPME	*Solid-phase microextraction*
S/N	*Signal-to-noise ratio*
T	
TBP	*2,4,6-Tribromophenol*
TC	*Total carbon*
T.E.S.T.	*Toxicity estimation software tool*
THM	*Trihalomethane*
TIC	*Total ion chromatogram*
TP	*Transformation product*
TQ	*Triple quadrupole*
U	
UF	*Ultrafiltration*
UV	*Ultraviolet*
V	
VP	*1-vinyl-pyrrolidin-2-one*
W	
WHO	*World Health Organization*
WWTP	*Wastewater treatment plant*

USC
UNIVERSIDADE
DE SANTIAGO
DE COMPOSTELA

ABSTRACT

USC
UNIVERSIDADE
DE SANTIAGO
DE COMPOSTELA

ABSTRACT

The interest of the scientific community on the presence, fate and effects of the so called "contaminants of emerging concern" (CECs, also called "emerging contaminants") has been a matter of extensive interest in the last two decades. CECs comprise a wide range of chemicals of emerging interest, lacking regulation (or when regulation has only arisen in the last few years in some cases) which includes pharmaceuticals, industrial chemicals, personal care products, UV filters, flame retardants and many others. The fate of CECs is particularly relevant as regards the water cycle, because of their easy spread from wastewater to surface and groundwater and finally drinking water, if they are persistent and mobile (i.e. polar). Thus, they may constitute both a risk for the environment and human health.

Therefore, it is evident that waterworks, both wastewater and drinking water treatment plants play a major role in controlling the spread of those chemicals. These facilities incorporate several treatments, including tertiary treatments such as disinfection aiming at avoiding microbiological hazards, but where reaction of CECs and organic matter may end up in the formation of disinfection by-products (DBPs) and transformation products (TPs) in general. Hence, even when some CECs are apparently removed during treatment, they can lead to the formation of TPs and regulated DBPs, which may be in some cases even more toxic than their precursor CECs themselves. Therefore, it is necessary to investigate those transformation reactions, identifying the potential to generate DBPs and TPs and the (eco)toxicological implications.

In this context, the development of quadrupole-time of flight (QTOF) mass spectrometry (MS) instruments (and high-resolution MS in general) coupled to chromatographic techniques has permitted to reach those goals for some treatment and CECs combination, but still many research is needed.

This thesis aims at filling part of this gap in knowledge on the formation of TPs and DBPs from CECs by developing and applying analytical methods based on QTOF instruments, focusing on some selected analgesic pharmaceuticals and metabolites and industrial chemicals and chlorine- and UV-based disinfection reactions.

Thus, five different chapters are included in the results section covering the following research:

- The development of a novel gas chromatography-QTOF method capable of determining N-nitrosamines (a relevant class of N-DBPs) at trace level (**Chapter IV.1**)
- Shedding light to the reaction of chlorinated disinfection agents (chlorine and chloramine, also covering the potential presence of bromide) with analgesic drugs and metabolites (**Chapter IV.2**) and the two industrial chemicals 1,3-diphenylguanidine and 1,3-di-o-tolylguanidine (**Chapter IV.3**) in terms of TPs and DBPs characterization
- Testing the performance of UV-C laser for water treatment for the removal of ibuprofen as first case study and characterizing the TPs formed (**Chapter IV.4**)
- Investigating the reactivity of up to 12 prioritized high production volume industrial chemicals with UV light and the transformation pathway and predicted

toxicological implications of 2 of those chemicals, 1-vinylpyrrolidin-2-one and 2-piperazin-1-ylethanamine (**Chapter IV.5**)

RESUME

USC
UNIVERSIDADE
DE SANTIAGO
DE COMPOSTELA

RESUME

A preocupación pola presenza de contaminantes no medio ambiente converteuse nun tema en continuo crecemento nas últimas décadas. Ao longo do día utilízanse unha gran cantidade de compostos nas diferentes actividades humanas, tales como procesos industriais, en produtos de coidado persoal nos fogares ou debido ao uso de medicamentos e fármacos, por citar algúns exemplos. Estes compostos son vertidos nas augas e polo tanto poden constituír unha vía de contaminación e de ameaza para a saúde humana e para os ecosistemas (acuáticos). Moitos destes compostos non están regulados, o que se traduce nunha maior dificultade no control da súa presenza e posibles efectos ambientais, constituíndo o que se veu en chamar como contaminantes de preocupación emerxente.

Polo tanto, as augas son unha vía de contaminación medioambiental se non son tratadas adecuadamente. Para poñer solución a este problema, as prantas de depuración de augas residuais fan uso de diferentes métodos de depuración, incluíndo desinfección, para poder obter auga ao final do proceso que se poida utilizar de novo nas actividades diarias. De maneira similar, as prantas de potabilización de auga constan de diversas etapas que deben garantir que a auga, unha vez tratada, é segura para o consumo humano, incluíndo, entre outros, procesos de desinfección que garantan a seguridade desde o punto de vista microbiolóxico, pero que á súa vez afectan á calidade química da auga potabilizada.

A contaminación das masas de auga ten nas descargas das estacións depuradoras de augas residuais unha das principais vías de entrada. Por tanto, se estes métodos non son efectivos, os contaminantes poden chegar aos efluentes finais, converténdose nunha ameaza. Son moitos os métodos que se poñen en práctica para reducir e eliminar os diferentes contaminantes, pero aínda é necesaria a exploración de novas técnicas que constitúan unha solución completa neste ámbito. É debido a isto que os/as investigadores/as traballan cada día por atopar novos procesos cada vez máis efectivos na eliminación destes contaminantes co fin de obter augas con menor contaminación antropoxénica. Técnicas de carácter físico que consistan na separación de residuos sólidos da auga, acompañada de procesos biolóxicos e (foto)químicos de oxidación dan lugar á degradación dos contaminantes. É nesta parte (foto)química onde esta tese pon o foco, pola súa capacidade de transformar os contaminantes noutros de propiedades e estruturas moitas veces descoñecidas.

Dentro deste campo das oxidacións químicas existen diferentes técnicas de desinfección como pode ser o uso de dióxido de cloro, ou unha moi coñecida e moi utilizada a nivel europeo como é o uso de cloro libre, un potente oxidante non selectivo usado na inactivación de patóxenos. Mediante a incorporación de cloro libre ás mostras de auga, ademais, os contaminantes presentes nela reaccionan e pode ser parcialmente eliminados. Porén, esta aparente eliminación ten como posible consecuencia a produción de novas estruturas procedentes do composto orixinal que, en moitas ocasión, posúan un grado de toxicidade maior que as substancias de partida. Estes produtos de transformación (TPs), nalgúns casos coñecidos como subprodutos de desinfección, son tamén, polo tanto, un tema de preocupación no ámbito da química ambiental e da saúde humana. Por isto, deben desenvolverse novas técnicas de desinfección que atopen o balance entre a eliminación dos contaminantes orixinais e a minimización dos TPs potencialmente tóxicos producidos.

Como alternativa, atopamos o uso de cloraminas, sendo a máis coñecida a monocloramina (NH_2Cl), un composto de menor capacidade oxidante en comparación co cloro libre, pero que tende a producir unha menor cantidade de TPs. Non obstante, a monocloramina é una substancia inestable, polo que debe ser xerada diariamente, ademais de que os tempos requiridos para a depuración das augas son máis longos. Ademais, as cloraminas foron amplamente relacionadas ca formación de N-nitrosaminas, sendo a máis coñecida a N-nitrosodimetilamina (NDMA), una substancia altamente carcinóxenica.

É polo tanto necesario estudar os procesos de transformación dos contaminantes e os TPs producidos, debido a isto, na comunidade científica trabállase nos diferentes métodos para a determinación de contaminantes e dos TPs formados. A maioría dos métodos de determinación de compostos consisten en técnicas de cromatografía (ben de líquidos ou de gases) seguidas de diferentes detectores como poden ser as lámpadas ultravioleta, pero sendo a máis coñecida a espectrometría de masas (MS). Esta clase de detectores asentáronse como os máis selectivos e de maior sensibilidade na determinación de substancias orgánicas, polo que existen diferentes tipos de MS dependendo de distintos compoñentes tales como a fonte de ionización ou o analizador de masas.

Analizadores de masas como o triplo cuadrupolo (QqQ) son moi utilizados na cuantificación de compostos xa que proporcionan unha alta selectividade na medida de transicións de masas. Por contra, non son tan vantaxosos na identificación de novas estruturas e en termos cualitativos en xeral. Neste ámbito, a alternativa de maior éxito é a espectrometría de masas de alta resolución (HRMS), con analizadores capaces de medir masas exactas, que axudan na obtención de fórmulas empíricas e facilitando a identificación de novos compostos. Analizadores como o tempo-de-voo (TOF), ou o Orbitrap, son capaces de medir estas masas cunha alta capacidade resolutiva, que en combinación cas técnicas cromatográficas previas para a separación dos compostos presentes na mostra, forman unha técnica híbrida moi asentada no día de hoxe.

Os TPs que se forman como consecuencia dos procesos de depuración poden resultar ser máis tóxicos que os compostos orixinais, polo que, ademais da súa identificación e control, é importante traballar na estimación da súa toxicidade. Existen diferentes métodos para o cálculo de parámetros referidos á toxicidade. Un moi utilizado consiste na estimación *in silico* mediante cálculos de cuantificación da relación estrutura-actividade (QSAR) con programas informáticos. Estes programas proporcionan unha predición dos valores de toxicidade de acordo ca estrutura do composto que, sendo un valor estimado, serve para comparar co composto de partida, traducíndose nunha comparativa directa entre o contaminante orixinal e os TPs formados. Dado que estes programas traballan en base a estrutura do composto, é importante encontrar unha estrutura fiable para estes TPs. Aínda que estas estimacións *in silico* son moi útiles, ao non ter que realizar laboriosos experimentos (eco)toxicolóxicos, deben ser considerados coma unha primeira aproximación (cribado) e deberían confirmarse posteriormente de mineira experimental.

Tendo en consideración o mencionando anteriormente, nesta tese doutoral abórdanse traballos relacionados coa formación de TPs e a súa determinación, relacionados con contaminantes de preocupación emerxente de diversa índole e procesos de desinfección con oxidantes clorados e radiación UV. Ademais de na identificación de TPs, traballouse na

estimación da súa toxicidade, completando unha serie de cinco capítulos, os cales se discuten brevemente a continuación:

1. **Determinación de N-nitrosaminas mediante cromatografía de gases acoplada a espectrometría de masas con analizador cuadrupolo-tempo-de-voo en mostras de auga.**

Neste primeiro capítulo considerouse a familia de compostos das N-nitrosaminas. Estes compostos con actividade carcinoxénica son unha fonte de preocupación no ámbito ambiental e da saúde humana, presentes nas augas e producidas por diferentes vías como poden ser en procesos de combustión no cociñado de certos alimentos, ou en procesos de oxidación química das estacións depuradoras. Nos últimos anos, a comunidade científica traballou no desenvolvemento de métodos de extracción destes compostos das augas, así como na súa determinación. O propio organismo da Axencia de Protección Ambiental (*Environmental Protection Agency)* dos Estados Unidos (US EPA) publicou no 2004 un método de extracción e determinación das nove N-nitrosaminas máis coñecidas, baseado no proceso da extracción en fase sólida (SPE) de mostras de auga con cartuchos de carbón activo (*Coconut Charcoal*), seguidos da elución con diclorometano (DCM) (*US EPA-method 521*). Para a súa determinación, a US EPA propón o uso da cromatografía de gases (GC) seguido de detección mediante MS con analizador de trampa de ións (IT), traballando cunha fonte de ionización química en modo positivo (PCI). Ao utilizar unha IT, é posible a análise mediante espectrometría de masas en tándem (MS/MS), facendo máis selectivo o método global.

Este capítulo centrou o seu traballo na parte referida á determinación destes mesmos compostos descritos pola US EPA en mostras de augas residuais, considerando distintos equipos de análise baseados todos no sistema GC-MS. As diferenzas principais nestes sistemas utilizados atópanse nos dous compoñentes mencionados anteriormente: a fonte de ionización e o analizador de masas.

No referido á fonte de ionización, traballouse con dúas diferentes, sendo estas a ionización electrónica (EI) e a PCI, usando metano como gas de ionización. Así mesmo, contouse con dous equipos GC-MS con analizador de masas de distinto tipo, sendo un deles unha IT (analizador de baixa resolución) e tendo por outro lado o analizador QTOF (analizador de alta resolución). Combinando as fontes de ionización cos analizadores de masas, foi posible a comparación de ata catro sistemas de análise.

Así pois, este traballo puxo o foco na comparación destes sistemas na determinación das N-nitrosaminas en mostras de augas residuais, reflexando os resultados en termos dos límites de detección e cuantificación (LODs e LOQs) coa fin de obter un método máis selectivo e sensible. Para o desenvolvemento deste traballo, considerouse o protocolo de extracción mediante SPE descrito pola US EPA, polo que se realizaron diferentes probas de extracción en auga ultrapura para o desenvolvemento do método.

Finalizadas as probas, os LODs e LOQs demostraron que a combinación de GC-PCI-MS cun analizador de alta resolución como o (Q)TOF proporcionou os mellores resultados, sendo o sistema escollido neste traballo para o análise final en mostras reais.

Co método descrito e validado, o capítulo remata co análise de mostras de auga residual de distintos tipos, considerando así mostras de auga de entrada da estación depuradora de aguas residuais (influente) e, dado que o uso de cloro e cloraminas nas estacións depuradoras se relaciona coa formación de N-nitrosaminas, tamén se tomaron mostras de auga de saída da mesta planta (efluente). Por outra banda, tamén se consideraron augas da billa locais co fin de detectar estes compostos nelas. Ademais, considerando que os niveis de cloro poden cambiar ao longo do día, estas mostras foron tomadas a diferentes horas.

Todo e traballo detallado atópase descrito no **Capítulo IV.1**

2. Reacción de fármacos fenazónicos e os seus metabolitos con cloro e monocloramina

Os compostos con estrutura de tipo fenazónico son fármacos utilizados na vida diaria de modo notable a nivel mundial. Dentro deste grupo existen unha gran cantidade de substancias, entre as cales pódense destacar a propia fenazona (Phe), a propifenazona (PrPhe), ou outros compostos como a aminopirina ou dipirona, máis coñecida coma metamizol.

Este último composto, sometido a certas restricións a nivel global no seu uso, metabolízase no organismo a outra estrutura (4-metilaminoantipirina, MAA), que á súa vez da lugar a dous metabolitos: 4-formilantipirina (FAA) e 4-aminopirina (AA), posteriormente transformado en 4-acetoamidoantipirina (AAA). Polo tanto, estas substancias son as finalmente excretadas polo organismo, e as que poderían chegar a ser contaminantes medioambientais.

Neste capítulo traballouse principalmente no estudo da transformación da Phe, PrPhe, AA, FAA e AAA con axentes desinfectantes usados nas estacións depuradoras como poden ser o cloro e, ademais, as cloraminas, considerando a monocloramina como o principal oxidante desde grupo.

Este estudio tomou como base un artigo previo do noso equipo de investigación de 2012, no que se describe o estudo cinético da Phe e da PrPhe con cloro, polo que neste capítulo se considerou no tratamento con cloraminas para estes dous compostos, e con cloro e monocloramina para AA, FAA e AAA.

A monocloramina usada neste traballo, dado que é un composto relativamente inestable en auga, foi necesario preparala diariamente. A preparación da monocloramina é un proceso delicado no que se deben ter en conta factores como o punto de rotura do cloro, un nivel de cloro libre determinado a partir do cal non se pode obter monocloramina. Outros factores como o pH debe ser tamén controlado, dado que inflúe na formación dunha especie en concreto, dando lugar á posible formación de dicloramina, unha especie menos reactiva.

Os 5 compostos considerados neste traballo foron sometidos á reacción con monocloramina a diferentes valores de pH da mostra, considerando un ácido, un neutro e un básico (pH 5,7, 7,0 e 8,3). Dado que a cloramina ten unha menor capacidade de oxidación comparado co cloro, os tempos de contacto foron máis longos, considerando horas e días. Do mesmo modo, AA, FAA e AAA foron sometidos tamén á reacción con cloro libre, obtendo reaccións moi rápidas, da orde de segundos como tempos de vida media.

Posteriormente ao estudio cinético, levouse a cabo unha procura dos TPs formados como consecuencia das degradacións destes compostos. No caso da Phe e PrPhe observáronse, en xeral, a maioría de TPs descritos anteriormente para a cloración dos mesmos. Do mesmo modo, para o AA, FAA e AAA, realizouse unha busca mediante un protocolo non-dirixido e comparación estatística de mostras non tratadas e tratadas, combinados con experimentos de MS/MS, identificándose tentativamente unha serie de produtos comúns na degradación con cloro e con monocloramina.

Coa estrutura proposta para os TPs, realizouse tamén unha estimación da toxicidade para todos os compostos mediante QSAR, facendo así unha comparativa fronte os compostos de partida. Todos estes resultados atópanse descritos no **Capítulo IV.II**.

3. Cloración e bromación da 1,3-difenilguanidina e 1,3-di-o-tolilguanidina

Este traballo foi realizando en colaboración coa Universidade de Poitiers (Francia) na estadía de tres meses realizada baixo a supervisión do Prof. Hervé Gallard.

1,3-difenilguanidina (DPG) e 1,3-di-o-tolilguanidina (DTG) son dous compostos utilizados nos procesos de vulcanización do caucho e outras etapas relacionadas coa manufactura de polímeros. Ambos están rexistrados no REACH (Rexistro, avaliación, autorización e restrición de sustancias químicas) da Axencia Europea de Produtos Químicos (ECHA) con altos niveis de produción. Ademais, estudos recentes demostraron que estes dous compostos están presentes nas augas en concentracións do nivel do ng L^{-1}, polo que o seu estudo está sendo un recente tema de interese. Estes dous compostos foron incluídos na lista de compostos priorizados no proxecto europeo PROMOTE, da convocatoria piloto Water JPI.

En vista da falta de antecedentes no referido á reacción destas dúas sustancias nas estacións depuradoras, neste traballo abordouse o estudo cinético da reacción destes dous compostos nas auga cloradas para a súa desinfección. Ademais, é sabido que as augas naturais conteñen niveis variables de bromuro, os cales poderían reaccionar co cloro libre presente para dar lugar a especies oxidantes de bromo, dando lugar a unha nova vía de reacción e, por ende, a un posible novo grupo de TPs bromados.

Neste traballo descrito en detalle no **Capítulo IV.3**, realizáronse diferentes experimentos. Nunha primeira etapa levouse a cabo o estudo cinético na cloración e bromación de ambos compostos nun amplo intervalo de pH (dende 5.0 ata 11.0). Ademais, foi posible realizar unha estimación dos valores da constante cinética mediante a elaboración dun modelo teórico sobre a cal se situaron os valores conseguidos experimentalmente, obtendo un axuste moi bo, e confirmando así o deseño dun modelo correcto e das principais especies envolvidas na reacción.

Nas seguintes etapas do traballo considerouse a busca dos TPs partindo de ambos compostos orixinais e considerando tanto os procesos de cloración como de bromación. Así pois, detectouse unha alta cantidade de produtos, sendo máis extensa a lista para o DTG, que demostrou ser máis reactivo que o DPG no estudo cinético. Ademais dos TPs, investigouse

tamén a formación de posibles DBPs, observándose a posible formación neste caso de trihalometanos e dicloroacetonitrilo.

Obtida a lista de TPs, realizáronse experimentos de MS/MS de cada un deles para atopar unha estrutura fiable, co fin de facer unha estimación da toxicidade mediante QSAR. Ademais, tamén se realizaron ensaios experimentais de toxicidade co test Microtox®, confirmándose a maior toxicidade dos TPs producidos.

4. Tratamento de augas con ibuprofeno mediante irradiación con radiación pulsada láser UV-C

O seguinte traballo, recollido no **Capítulo IV.4** foi realizado en colaboración co grupo Photonics4life, da Universidade de Santiago de Compostela e o Instituto de Ciencia de Materiales de Aragón (centro mixto CSIC-Universidad de Zaragoza), no cal se describe o estudo cinético na degradación dun dos compostos mais coñecido e usado no grupo dos fármacos antiinflamatorios non esteroideos (NSAIDs), o ibuprofeno (IBU). Existen numerosos artigos que describen o proceso de eliminación desde fármaco das augas usando distintos oxidantes, incluíndo tratamentos fotoquímicos. Neste traballo, recóllense os resultados referidos á degradación do IBU usando unha fonte láser de radiación pulsada que emite a 266 nm (rexión UV-C do espectro electromagnético).

No grupo de Photonics4life realizáronse os respectivos experimentos de degradación do IBU en mostras de auga ultrapura, para a seu posterior análise no laboratorio do grupo de Cromatografía e Quimiometría. Os resultados demostraron unha efectiva e rápida degradación do IBU, obtendo unha total eliminación no rango dos 15 minutos. Posteriores probas foron realizadas tamén en auga real, considerando o efluente de estacións depuradoras de auga residual para a validación final do método, onde tamén se demostrou que o láser pode ser unha fonte de radiación efectiva neste tipo de tratamentos.

Así pois, como etapa posterior ao estudo cinético, realizouse unha busca de TPs tanto manual, en base a TPs previamente descritos na bibliografía, como mediante algoritmos de software, obtendo un listado de 5 TPs tentativamente identificados, que ademais desaparecen a tempos de radicación de 15 minutos.

Posteriormente, co obxectivo de coñecer as implicacións colaborouse tamén co grupo de Miguel Santos no *Centre of Marine and Environmental Research* (CIIMAR) da Universidade do Porto (Portugal), que confirmaron mediante ensaios con embrións de peixe cebra unha clara redución da toxicidade nas mostras tratadas.

5. Transformación de 1-vinil-2-pirrolidona e 2-piperazin-1-iletilamina con radiación UV

Neste último traballo recóllense os resultados (**Capítulo IV.5**) do estudo da reacción de dous compostos potencialmente persistentes no medio ambiente como son 1-vinil-2-pirrolidona (VP) e 2-piperazin-1-iletilamina (PPE) coa radiación UV.

Inicialmente, o estudo considerou un total de 12 substancias priorizadas no proxecto PROMOTE anteriormente mencionado, como compostos potencialmente persistentes e móbiles no ciclo da auga. Poren, durante as probas preliminares demostrouse que só dous dos doce compostos daban lugar a reacción significativa coa radiación UV, reducindo a lista do estudo a estes dous compostos (VP e PPE).

O estudo da fotorreacción destes dous compostos realizouse por separado en mostras de 25 mL de auga ultra pura, obtendo unha cinética para cada un deles na que se demostra que VP ten unha máis rápida reacción que PPE, como se esperaba tendo en conta o espectro de absorbancia dos compostos.

De modo análogo aos capítulos anteriores, a busca de TPs realizouse tamén neste caso, obtendo un listado de produtos para os cales se propuxeron estruturas tras os ensaios MS/MS.

Para a estimación da toxicidade destes TPs utilizouse QSAR con dous software diferentes co fin de obter a maior cantidade de datos posible para a comparativa dos produtos respecto ao composto orixinal. Neste caso empregáronse para a estimación da toxicidade as ferramentas T.E.S.T. e ECOSAR da US EPA, en ámbolos dous casos, onde os resultados reflexan unha maior toxicidade nalgúns dos TPs, especialmente os derivados de PPE.

USC
UNIVERSIDADE
DE SANTIAGO
DE COMPOSTELA

I. INTRODUCTION

USC
UNIVERSIDADE
DE SANTIAGO
DE COMPOSTELA

I. INTRODUCTION

I.1. The urban water cycle

The water cycle is one of the most relevant hydrogeochemical cycles. However, as many others it has received a large impact from human activities. For instance, water is used at home in many household activities (drinking, cooking, bathing, washing, etc.), by industry, agriculture, etc. All these activities are translated into water being contaminated with substances or other chemicals, which is further directly discharger into surface water and groundwaters or reach wastewater treatment plants (WWTPs). As shown in **Figure I.1**, when treated at WWTPs, effluents are then discharged into creeks, rivers or other surface waters or groundwater in general. Thus, this water is further used for producing drinking water, closing the cycle.

A major problem of this anthropized cycle relies on the fact that some contaminants may not be completely removed at WWTPs. Then, if these contaminants are not eliminated, they will reach surface or groundwater, as mentioned, which are further used for producing drinking water. Hence, besides the ecotoxicological concern of contaminated surface water, this could end up posing a risk for human health, since those contaminants may not be eliminated at drinking water treatment plants (DWTPs) either.

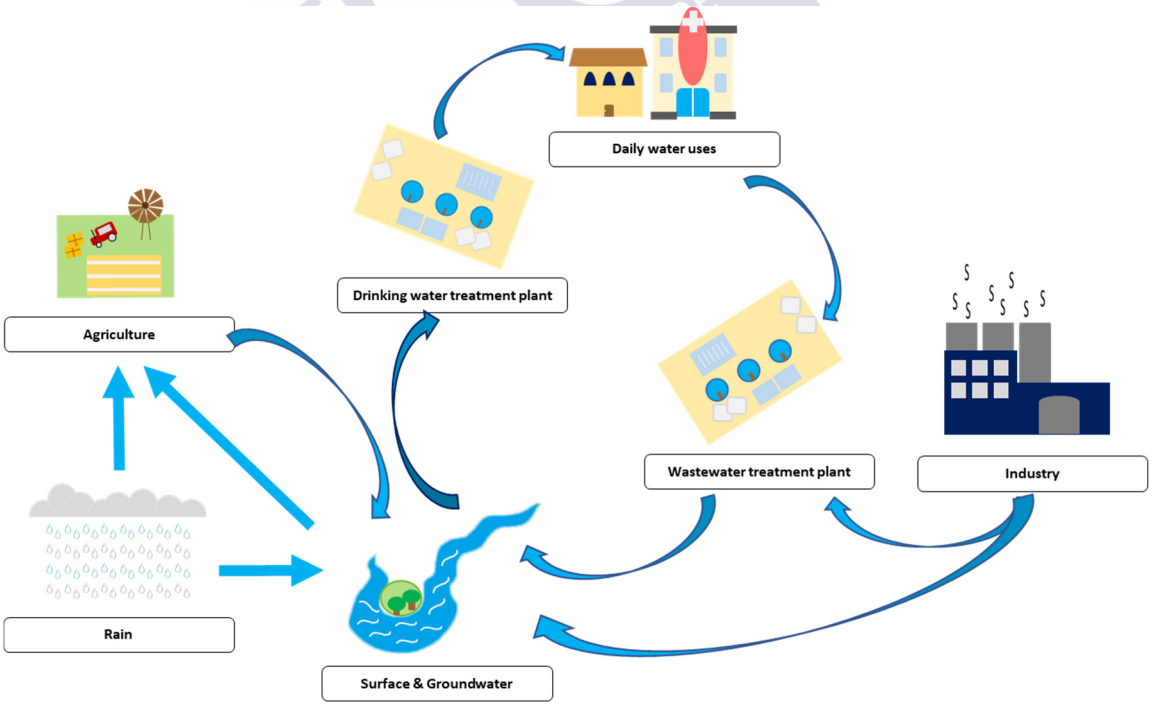

Figure I.1. Scheme of the anthropized water cycle

Even when WWTPs and DWTPs may seem efficient in removing several contaminants and organic matter in general, such apparent removal can still produce a large amount of transformation products (TPs). This thesis is mainly focused on potential removal of organic contaminants and the TPs that could be produced during disinfection

treatments, widely used at WWTPs and DWTPs, given the fact that these facilities have a major impact on water quality. Further discussion to typical operations employed for water treatment are provided in the sections below.

I.2. Water treatment

The concept of water treatment is related to the processes involved in WWTPs or DWTPs aiming at generating clean water for specific purposes. In most occasions, the main aim of water treatment is to either produce safe drinking water, at DWTPs, or safe water to be discharged into the environment, or for future reuse, at WWTPs[1].

In recent years, there has been a growing concern about organic contaminants in the environment, in which WWTPs are considered as the major point sources, because they are not specifically designed to remove organic contaminants and even because TPs are generated during water treatment processes. In some cases that TPs could be even more dangerous than the initial compounds[2]. In the following sections, different treatments used both in WWTPs and DWTPs will be described.

Although wastewater can have different sources, such as domestic/municipal wastewater (sewage), hospitals, and/or industrial wastewater[3], it is characterized by its high load of organic and inorganic compounds. Wastewater treatment converts such wastewater (or sewage) into an effluent that can be returned to the water cycle with an acceptable impact on the environment or reused for various purposes (water reclamation). Wastewater treatment typically includes primary and secondary treatment stages and, in some cases, also a tertiary treatment, including disinfection.

The main role of the DWTPs is to remove all the pollutants (organisms, particles, etc.) and pathogens from water, that could be hazardous for human health, making it chemically and biologically safe[3]. In DWTPs, raw water is up taken from surface water (e.g. rivers, lakes or dumps) and/or groundwater[4]. The methodologies used at DWTPs depend on the quality of raw water and local practices, but the most typical steps include aeration, flocculation, sedimentation, filtration and disinfection[1,3]. The cleaner the water is, the fewer steps that will be required. Anyway, one of the most important steps performed at DWTPs is disinfection, typically applied at the end of the treatment process. Disinfection aims at making water free of pathogens by a tertiary treatment, most often consisting of application of chemical oxidants (e.g. chlorine or ozone) and/or UV radiation.

I.2.1. Main treatment steps employed during water treatment

This section describes some of the treatment methodologies employed during wastewater/drinking water treatment. There are three key steps employed in water treatment which are: primary treatment, secondary treatment, and tertiary treatment (also known as advanced treatment), the most frequently used ones being summarized in **Table I.1**. Also, it is quite normal to include other previous steps such as the preliminary treatment or even steps afterwards dedicated to the management of solids, including the sludge

generated during the whole process. Each key treatment contains different steps and methods that are connected, providing a workflow from the raw water entering the DWTP/WWTP to the ending treated water. As an example, the scheme of a WWTP is shown in **Figure I.2**.

Table I.1. Main processes and steps employed at wastewater/drinking water treatment plants

Primary treatment
Sedimentation
Flotation
Coagulation-flocculation
Filtration
Secondary treatment
Activated sludge
Trickling filters
Constructed wetlands
Rotating biological contactor
Anaerobic digestors
Tertiary (chemical) treatment
Chemical oxidation: chlorination, chloramination, chlorine dioxide and other chemical oxidants (iron oxides, permanganate ions, etc.)
Photochemical treatments: UV
Advanced oxidation processes: ozone, Fenton, photo-Fenton
Membrane technologies: reverse osmosis, ultrafiltration

I.2.1.1. Pre-treatment

The pre-treatment removes the constituents of grease, sand and objects with a certain size that constitute raw water, whose presence can cause maintenance and operation problems. The procedures that are carried out for the elimination of these residues are: grinding, grit removal, flow equalization and fat and grease removal.

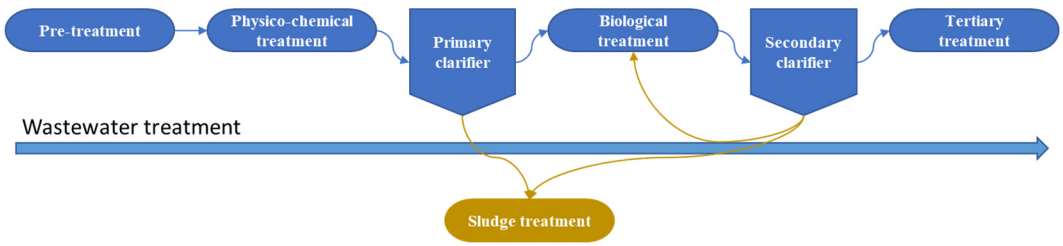

Figure I.2. Treatment scheme of a WWTP

I.2.1.2. Primary treatment

Primary water treatment separates by physical and/or chemical procedures the substances in suspension not retained by the pre-treatment, especially sedimentary and floating matter. In some cases, these treatments require the addition of chemicals or coagulants that break the colloidal state of the particles and form larger particles that settle or float more efficiently. Primary treatment includes processes such as coagulation – flocculation, sedimentation, and floatation. This procedure takes place in large tanks, commonly called "pre-settling basins", "primary sedimentation tanks" or "primary clarifiers" (**Figure I.3**)[5]. In this phase, the most frequently used method is sedimentation, which is able to remove organic and inorganic solids by passing the wastewater through tanks and filters[6]. In this step, around 50% of the residues are collected as sludge and fed into a digester, which could be treated in furthers processes[7]. This water goes then into the secondary treatment stages.

Figure I.3. Picture of a sedimentation tank employed during primary treatment (*Picture from Touzeen Hussain (2007) on flickr.com gallery)*

I.2.1.3. Secondary treatment

Secondary treatment consists of a set of biological processes that aim at eliminating organic matter, usually applied at WWTPs[5,8]. These biological processes consist of the metabolization of diverse chemicals by some bacteria and microorganisms. Processes included as secondary treatments could be aerobic or anaerobic depending on the microorganisms used, e.g. bacteria, algae, etc.

- Aerobic processes are carried out in the presence of oxygen, so it is necessary to introduce it into the tanks where the water is. In this stage, organic matter is partly degraded to be incorporated into the microorganism's biomass or yielding water and CO_2, and the elimination of nitrogenous products takes place.
- Anaerobic processes are carried out in the absence of oxygen. Under such conditions, fermentative reactions in which organic matter is transformed into energy, methane, and carbon dioxide can take place.

Wastewater is placed into bioreactors under different conditions for a favourable environment for the microorganism, allowing reproduction and keeping the oxidation processes active[8]. Although these methods are also efficient for the elimination of some pollutants, some residues of organic substances and pathogens could remain[9]. The main operations used in secondary treatment include:

- Activated sludge: this is an aerobic process that consists of an aeration tank containing a suspension of the wastewater and microorganisms, vigorously mixed by aeration devices which also supply oxygen to the suspension. Following the aeration step, the microorganisms are separated from the water by sedimentation, obtaining the clarified secondary effluent.
- Trickling filters: this is also an aerobic process that consists of a basin or a tower filled with support media, such as stones, wooden slats, or plastic shapes where the microorganism grow causes a layer or microbial slime (biofilm). Wastewater is applied intermittently or continuously over this device maintaining the aerobic conditions.
- Constructed wetlands: these are artificial wetlands that use vegetation, soil, and other organisms to treat wastewater. These wetlands are irrigated with wastewater. Vegetation in a wetland provides a substrate (roots, stems, and leaves) upon which microorganisms can grow as they break down organic chemicals.
- Rotating biological contactors: they consist of fixed-film reactors like trickling filters in that organisms are attached to support media. The rotating plastic disks are mounted so that they are partially submerged in flowing wastewater in the reactor, being exposed for an alternate process between air and wastewater, providing a layer of bacteria to grow on the disk.
- Anaerobic digestors: this is an anaerobic process that takes place in completely closed tanks. Bacteria that produce methane when degraded the organic matter are used.

Some secondary treatment methods include a secondary clarifier to settle out and separate biological floc or filter material grown in the secondary treatment bioreactor (**Figure I.4**).

Figure I.4. Secondary wastewater clarifier (*picture from Annabel (2011) Wikimedia Commons)*

I.2.1.4. Tertiary treatment

The purpose of tertiary treatment is to provide a final treatment stage to further improve the effluent quality before it is discharged to the receiving environment. Tertiary treatment consists mainly in the elimination of pathogens, especially faecal bacteria, and nutrients. This treatment is optional and is usually done when the water is going to be reused, so that it will not pose a danger to human health, or to the environment. More than one tertiary treatment process may be used at any treatment plant[10].

The most popular tertiary treatments are described in the following sections.

I.2.1.4.1. Chemical oxidation

It typically aims at eliminating microorganisms through the application of oxidant chemicals, which in turn can also react with natural organic matter and chemical pollutants. The main oxidant chemicals are described below.

I.2.1.4.1.1. Chlorine

Chlorine was first used as method for water disinfection in the XIX century[11]. Nowadays, chlorination is probably the most popular technique employed during water disinfection, as more than 90% of the DWTPs in Europe use this methodology.

Chlorine reacts with the organic matter present in water leading to its oxidation. Its application is normally performed either as free chlorine by application of its gaseous form or as sodium hypochlorite[12].

When chlorine is added to water, there are two main species present, the hypochlorite ion (OCl^-) and hypochlorous acid (HOCl), formed due to Cl_2 disproportionation if applied as gas, being HOCl the most efficient one for disinfection[12]. Despites its ability for disinfection, the main drawback of chlorination is the reaction with natural organic matter, which leads to the formation of disinfection by-products (DBPs), many of which have been proven to lead to human toxicity and therefore, needed to be regulated[13–15]. DBPs and other TPs are further discussed in **I.3.3**.

Furthermore, when chlorine is added to water containing (low levels of) bromine, a reaction between both substances occurs leading to the formation of hypobromous acid, as shown in **Equation I.1.**

Eq.I.1 $HOCl + Br^- \rightarrow HOBr + Cl^-$

Such reaction of HOCl with the bromide present in water to produce HOBr is a favourable reaction ($k = 1.55 \times 10^3\ M^{-1}\ s^{-1}$)[16]. Hence, HOBr, can also act as disinfectant, but can also lead to the formation of brominated DBPs, besides chlorinated ones.

I.2.1.4.1.2. Chloramines

Since chlorination leads to the formation of many DBPs, different techniques have been investigated to find out alternative disinfectants with reduced formation of DBPs. One of them is the use of chloramines, and more particularly monochloramine (NH_2Cl)[17].

Monochloramine is a water-unstable compound produced normally by the reaction of a nitrogen source (i.e. ammonia) and chlorine[18]. In the lab, it should be prepared daily by reaction between sodium hypochlorite (NaOCl) and ammonium chloride (NH_4Cl) as shown in **Equation I.2**.

Eq.I.2 $NaOCl + NH_4Cl \rightarrow \mathbf{NH_2Cl} + NaCl + H_2O$

This reaction has some requirements to be successful, thus, the pH should be adjusted to obtain monochloramine as main species. If the pH is lower than 8.5, an equilibrium between mono and dichloramine ($NHCl_2$) and trichloramine (NCl_3) occurs, as presented in **Figure I.5**. These species are less efficient than NH_2Cl for water disinfection[19]. Addition of chlorine during chloramine generation must also be performed drop by drop and with vigorous stirring to avoid breakpoint chlorination, defined as the level of chlorine that provides an overdose, commonly related to swimming-pools. When breakpoint chlorination occurs, chloramines present in water are degraded and other chlorinated substances are produced, leading to a mixture of free chlorine and other combined chlorine species (**Figure I.6**)[19].

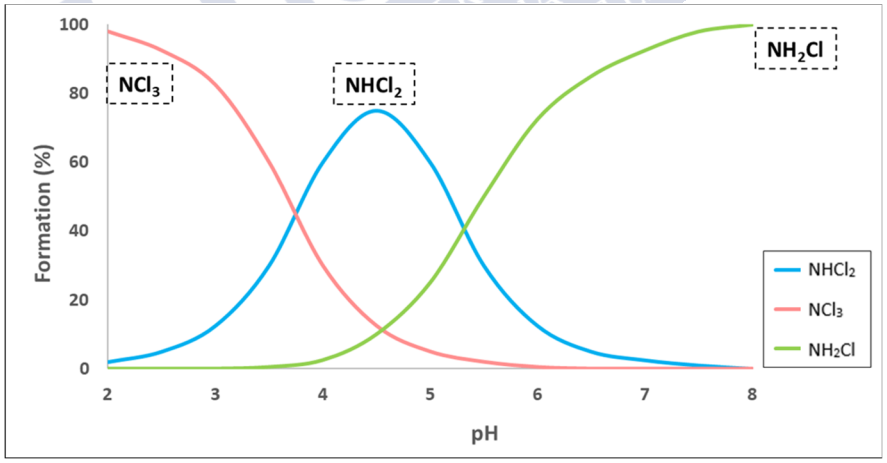

Figure I.5. pH dependence in chloramine formation

Chloramines can react with some organic contaminants without producing trihalomethanes (THMs) and haloacetic acids (HAAs) but, in turn, the amount of nitrogenous DBPs (N-DBPs) becomes more relevant, and even formation of bromate if water contains high levels of bromide is possible[15,17,20]. Among N-DBPs, an important one is N-nitrosodimethylamine (NDMA), the most relevant N-nitrosamine, a family of carcinogenic compounds that is further described in **I.3.3.1.1.** because of its relevance[20] in the context of this thesis.

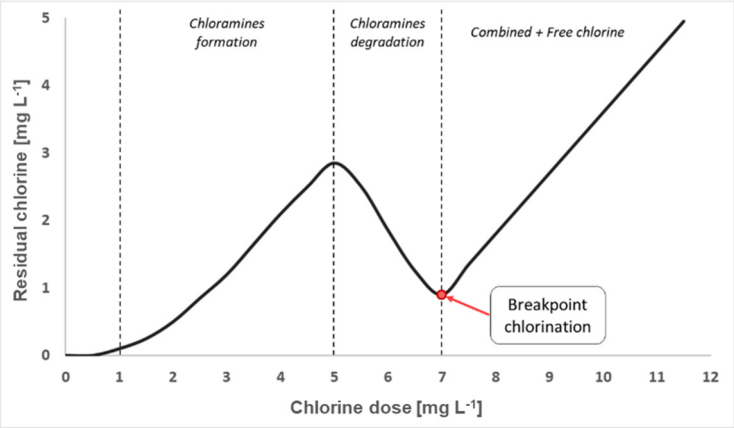

Figure I.6. Breakpoint chlorination curve

I.2.1.4.1.3. Chlorine dioxide

Mainly used for drinking water disinfection, chlorine dioxide (ClO_2) is a low-cost oxidant which is able to reduce the load of natural organic matter and to inactivate virus or bacteria, while its oxidizing capacity also allows to control taste and odor[21,22]. Chlorine dioxide is frequently used in combination with chlorine to minimize the formation of DBPs[23]. The main disadvantage of using ClO_2 for disinfection is, however, the formation of inorganic DBPs such as chlorite (ClO_2^-) or chlorate (ClO_3^-)[21].

ClO_2 is also used in waters with high concentration of bromide since it does not convert this substance into hypobromous acid.

I.2.1.4.1.4. Other oxidants

Besides those disinfectants already mentioned there are many other chemicals that could be used for this purpose, which are briefly mentioned here.

Permanganate (frequently added as potassium permanganate, $KMnO_4$) is a strong low-cost oxidant (Mn is in oxidation state VII) that could react with organic micropollutants and its typically used for odour and taste control, and also for biological control, mostly in DWTPs[24]. When used, halogenated DBPs are avoided. Also, MnO_2 is produced, but this chemical may help to physically remove pollutants while being easily separated by techniques such as filtration[25].

Typically, permanganate is used for peroxidation treatment leading to selective reactions linked to double bonds or aromatic rings, being a strong oxidant (stronger than chlorine) at natural water pH. As an example, Rodríguez-Álvarez et al. investigated permanganate reaction with non-steroidal anti-inflammatory drugs (NSAIDs) in water samples[24]. Due to its high oxidant capacity, several TPs could be produced[25].

Another oxidant used for water treatment is ferrate, i.e. Fe in oxidation state VI. This chemical pose also a high oxidant capacity, like permanganate, but is more dependent

on the pH. Its main product is $Fe(OH)_3$, which can also be used as coagulant and flocculant agent. In turn, the main disadvantage of ferrate is its lower stability[25].

I.2.1.4.2. Photochemical treatment

An alternative to the use of chemicals for water disinfection is the use of ultraviolet (UV) radiation or sunlight. Here the use of UV radiation from conventional sources and Lasers is discussed, given the fact that both are considered in this thesis.

I.2.1.4.2.1. UV radiation

The commonest photochemical method for water disinfection is the use of UV light. UV radiation is used in both DWTPs and WWTPs for the inactivation of pathogens, but can also lead to the removal (or transformation) of organic compounds[26].

According to the electromagnetic spectrum, shown in **Figure I.7**, it can be distinguished between UV-A, UV-B and UV-C radiation, depending on the wavelength:

- UV-A: this part of the UV spectra (ca. 315-400 nm) is not used for water disinfection because of its low energy (longer wavelength). In fact, UV-A radiation is present in the solar spectrum, not being adsorbed by the ozone layer, representing 5% of it[27].
- UV-B: in the 280-315 nm region, is perhaps the most widely studied part of the spectra. Solar UV-B radiation is mostly adsorbed by the ozone layer. Although more energetic than UV-A, its applications in water treatment are also very limited.
- UV-C: in the100-280 nm range, being the most energetic zone of the UV region, is the most relevant portion of the UV spectrum for water treatment. The UV-C radiation produced by the Sun is fully blocked in the ozone layer.

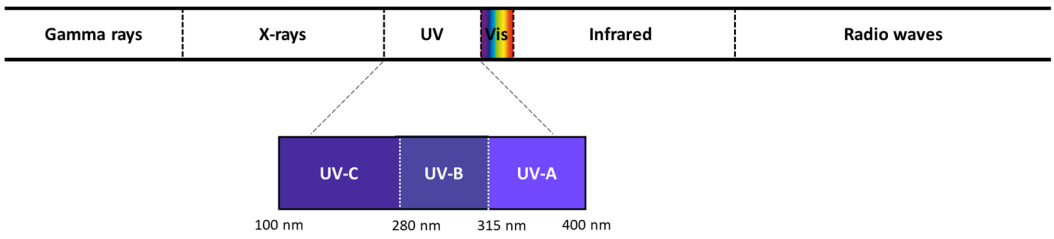

Figure I.7. UV radiation within the electromagnetic spectrum

Although UV-C is an energetic radiation, a higher dose is required, when compared to other methods, and reactivity depends on the structure of the organic contaminants to be removed[26]. When UV radiation is applied, reaction (and degradation) of organic matter and micropollutants may be produced by either direct photolysis, if the compound absorbs the UV radiation (absorption of a photon), or indirect photolysis, if there are other transient species between the radiation and the contaminant to be removed[28].

In water treatments, UV radiation is usually obtained from a mercury lamp emitting at 254 nm. In addition, UV light can also be used in combination with hydrogen peroxide (H_2O_2) at low concentrations, such as ca. 5 mg L^{-1}, that results into the generation of hydroxyl radicals (HO·) and which react very effectively with organic matter[26,29,30].

In indirect photolysis, the major contributors to the degradation of organic micropollutants are hydroxyl radicals (HO·), that then react with those micropollutants[31].

I.2.1.4.2.2. Laser sources

Water treatment (as mentioned) as well as most scientific research based on UV photo treatment has been performed by using continuous sources. An alternative, however, would be the use of pulsed sources[32], one of them being Lasers.

Lasers (acronym for Light Amplification by Stimulated Emission of Radiation) emit monochromatic spatially coherent radiation in a pulsed way. So far, there is not too much literature reporting the use of lasers in water treatment. Some few examples are the work of Unkroth et al. reporting in 1997 a first use in wastewater treatment for water mineralization by oxidation of textile dyes[33]. More than a decade later, Pascu et al. reported on the direct modification of phenothiazines using pulsed solid state Nd:YAG lasers emitting on their second (532 nm), third (355 nm) and forth (266 nm) harmonics, as well as a pulsed nitrogen gas laser emitting at 337 nm[34]. Similarly, a work published by Smarandache et al. reported on the degradation of thioridazine and BG1188 pharmaceutical compounds using direct laser irradiation emitted from a pulsed solid state Nd:YAG laser in its third harmonic at 355 nm[35]. Also, in 2002, Chu reported a patent in which a laser is used for microorganism degradation by irradiating water samples[36].

The potential use of laser radiation for micropollutants removal will be considered as a part of this thesis in **Chapter IV.4**.

I.2.1.4.3. Advanced Oxidation Processes (AOPs)

The methods described in the previous sections have some limitations as regards micropollutants removal and formation of TPs and DBPs. Thus, advanced oxidation processes (AOPs) are designed to achieve an improved removal of organic compounds based on different methods that generate very reactive, non-selective oxidants, such as hydroxyl radicals (HO·), which are able to react with many organic compounds[31,37–40]. This can be achieved in many ways, some of which are described below.

I.2.1.4.3.1. Ozone (O_3)

Ozonation is a common disinfection method used as tertiary treatment where ozone (O_3) is normally produced from a generator[41]. Ozone has a strong oxidation efficiency and has gained a lot of attention since the last years, especially for the elimination of both acidic

and basic compounds, such as phenols or amines[15,42–45]. Compared to chlorine in terms of removal efficiency, the use of O_3 is translated into a removal enhancement of the DBPs precursor instead of minimizing DBPs formation by the generation of HO· radicals in water solutions[46,47]. O_3 could also be used to produce other oxidants previously mentioned, e.g. HOBr, by the reaction of potassium bromide (KBr) and O_3[23].

As regards TPs, the use of O_3 avoids the generation of halogenated ones but produces oxidative TPs instead by inserting -OH groups, attacking molecules with double bonds or aromatic rings, and several functional groups, as e.g. amines[48].

O_3 is frequently described in the literature for the elimination of phenols from water samples. Phenolic substances are commonly found in industry for manufacturing processes or even for drug production. Because of this reason, phenol and its derivates reach wastewaters, becoming an environmental risk and being study for the community[42,43,45,49].

Since the reaction mechanism of O_3 mostly relies on HO· radicals generation, which are non-selective species but very reactive, some studies have considered the use scavengers in order to inactivate these radicals, for example, using *tert*-butanol[29,50].

I.2.1.4.3.2. Fenton reaction

The Fenton reaction is a non-photochemical AOP that involves a reaction between hydrogen peroxide (H_2O_2) and a metal, usually, Fe^{2+} under acidic conditions, to produce HO· radicals in solution[38,40]. There are other metals that could be used in this process to produce HO· radicals, but the "Fenton reagent", originally proposed by Henry J. Fenton, refers to Fe^{2+} [40].

In the whole process, several reactions take place, starting with the oxidation of Fe^{2+} to Fe^{3+} to produce HO· radicals from H_2O_2, as shown in **Equation I.3**.

Eq.I.3 $Fe^{2+} + H_2O_2 \rightarrow OH^- + Fe^{3+} + HO\cdot$

Then, Fe^{2+} is regenerated again in a further reaction of Fe^{3+} with H_2O_2 as shown in **Equation I.4**.

Eq.I.4 $Fe^{3+} + H_2O_2 \rightarrow Fe^{2+} + HO_2^{\cdot} + H^+$

Thus, Fe^{2+} works as a catalyst in the production of HO· radicals from H_2O_2. This reaction is an effective method for the removal of pharmaceuticals and other microcontaminants due to the generation of HO· radicals, its first application for this purpose being published in 1960[37,40].

I.2.1.4.3.3. Photo-Fenton reaction

Since the Fenton reaction is an effective technique for water treatment, several Fenton-based reactions were studied by the scientific community in order to further improve its efficiency.

One of the most important variants is the Photo-Fenton reaction, which is a Fenton-based method that includes UV light in the process to produce additional HO· radicals in solution, being, in this way, more efficient than conventional Fenton or direct UV irradiation[37,38]. The main advantage of the Photo-Fenton process relies on an accelerated regeneration of Fe^{2+} from Fe^{3+} by using, in this case, UV-A light[38].

In terms of water treatment, the photo-Fenton method can be applied for instance for the elimination of pesticides from the Directive 2013/39/EU list[38].

I.2.1.4.4. Membrane technologies

Besides techniques based on oxidative processes, there are also methods for tertiary treatment that include some physical barriers from which it is worth mentioning membrane-based technologies. These techniques are able to remove compounds with high efficiency, but they are restricted to the pore size of the membrane[51]. The two main membrane treatment methodologies are described below.

I.2.1.4.4.1. Reverse osmosis

Reverse osmosis is a method based on the use of semipermeable membrane. In natural osmosis process, found for example in cells, the liquid flows throughout the membrane from the lowest to the highest concentration side in order to equilibrate the concentrations of different substances between both sides of the membrane. During osmosis, the liquid flows generating a pressure between both sides, which is known as osmotic pressure.

Reverse osmosis works in the inverse direction in comparison to natural osmosis. This can be achieved by applying to the system a pressure higher than the osmotic pressure forcing pollutants to stay in one side of the membrane.

This technique is used as a tertiary water treatment for removing salts and a high percentage of pharmaceuticals and also viruses[10,52,53]. Some studies have investigated its efficiency in the removal of several organic micropollutants including N-nitrosamines, where removal was incomplete, especially for NDMA, which is only removed up to 65% by this way[54,55].

I.2.1.4.4.2. Ultrafiltration

Ultrafiltration is another tertiary method for the removal of pathogens and relatively large organic contaminats[10,51]. Thus, this technique can be also used for drinking water reclamation because of its efficiency in natural organic matter removal[56].

The main disadvantage of ultrafiltration and other membrane methods is membrane issues mostly due to the adsorption of compounds to the membrane and fouling that reduce the efficiency of the process along time[56]. This is the main reason why ultrafiltration is

commonly employed in combination with other pre/post-treatment, such as (powdered or granular) activated carbon[57]. Actually, a combination of powdered activated carbon with ultrafiltration (PAC/UF) allows to remove chemicals with low mass that would not be achieved by ultrafiltration only[57].

I.3. Contaminants of emerging concern

Since the last decades, the term of "contaminants of emerging concern" (CECs), also "emerging contaminants", has been used by the scientific community in thousands of articles[38]. According to the NORMAN Network, a CEC is considered "a substance currently not included in routine environmental monitoring programmes and may be candidate for future legislation due its adverse effects and/or persistency"[58]. Nowadays, more than 700 CECs, their metabolites and TPs, are listed as present in the European aquatic environment[59]. CECs are categorized into more than 20 classes related to their origin being the more prominent classes: pharmaceuticals, pesticides, DBPs, wood preservation and industrial chemicals[59]. Many CECs have been detected in the environment with potential risk to the human health[60], including both natural or anthropogenic substances.

Trace amounts of these contaminants are being discovered in water throughout the world, being detected at levels typically ranging from the ng L^{-1} to µg L^{-1} [38]. Considering the potential impact of these substances on aquatic life and human health and the lack of knowledge regarding their behaviour in the environment, action is urgently required at multiple levels. In the European Union, a watch list of CECs requiring further attention due to their high frequency of occurrence, the expected risk for human health and/or aquatic life, and/or for a lack of analytical techniques has been elaborated by the Water Framework Directive for national monitoring programs (Directive, 2000)[61].

Another matter of concern as regards CECs is the fact that they may get transformed in the human body (e.g. metabolism of drugs), the environment or during water treatment, resulting new TPs, i.e. more compounds to be monitored. As a result, tens of thousands of substances would need to be monitored and eventually regulated[62].

Detection, identification and quantification of CECs and their TPs in the various environmental compartments is essential for gaining knowledge on their occurrence and fate.

This thesis will put the focus on TPs (including DBPs) formed from pharmaceuticals and high production volume industrial chemicals during water disinfection.

I.3.1. Pharmaceuticals

Pharmaceuticals, including human and veterinary drugs, are continuously introduced into the environment via feces or urine after their consumption by humans and

animals. After their administration, pharmaceuticals can be excreted without being transformed or they can be metabolized by in two steps (**Figure I.8**): a first one (Phase I) by oxidation, reduction, hydrolysis, and alkylation; and a second one (Phase II) by (e.g. glucuronide or sulphate) conjugates formation, and excreted in the form of more polar and hydrophilic derivatives, as a metabolite or as a mixture of multiple metabolites.

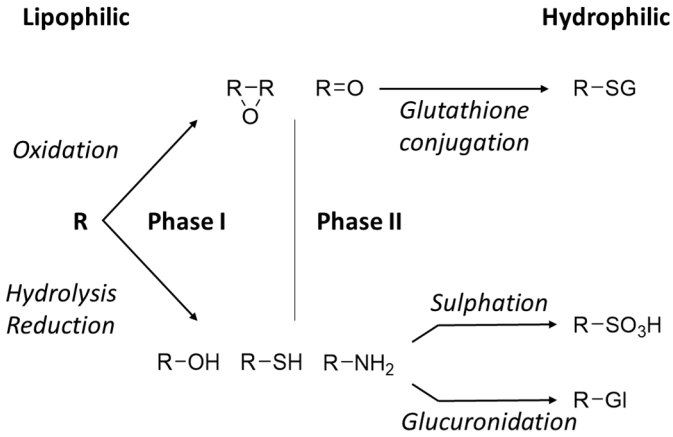

Figure I.8: Phases I and II of the metabolism

A large variety of pharmaceuticals and their metabolites have been detected in water samples at very low concentrations of ng L^{-1} to low μg L^{-1} range[63]. The therapeutic groups most commonly detected are: (I) anti-inflammatories and analgesics; (II) antidepressants; (III) antiepileptics; (IV) lipid-lowering drugs; (V) β-blockers; (VI) antiulcer drugs and antihistamines; (VII) antibiotics; and then (VIII) other substances.

Anti-inflammatories and analgesics are among the most consumed therapeutic subgroups. Among them, some few of those drugs account for most of the consumption, particularly paracetamol and, into a lesser extent, metamizole. Moreover, during the last 25 years, a significant increase has been produced in the consumption of NSAIDs, particularly ibuprofen (IBU), which are used with the same indications (analgesics and antipyretics). In general terms, as can be observed in **Figure I.9**, a continuous and significant increase in the use of this group of drugs is observed during the last 25 years. IBU consumption increased from 0.39 defined daily doses (DDD) per 1,000 inhabitants per day in 1992 to 26.49 DDD per 1,000 inhabitants per day in 2009. However, from that year its consumption decreased to 13.67 DDD per 1,000 inhabitants per day in 2016. The consumption of paracetamol has varied from 2.92 DDD per 1,000 inhabitants per day in 1992 to 25.67 DDD per 1,000 inhabitants per day in 2018. Regarding metamizole, a linear increase in consumption throughout the period studied is observed from 1 DDD per 1,000 inhabitants per day in 1992 to 5.54 DDD per 1,000 inhabitants per day in 2018 (**Figure I.9**)[64].

Among the anti-inflammatories and analgesics, IBU and phenazone-type drugs (also called pyrazolone drugs) including phenazone (also called, aminoantipyrine, Phe),

propyphenazone (PrPhe), aminopyrine and metamizole (also called dipyrone), are considered in this thesis because of their relevance.

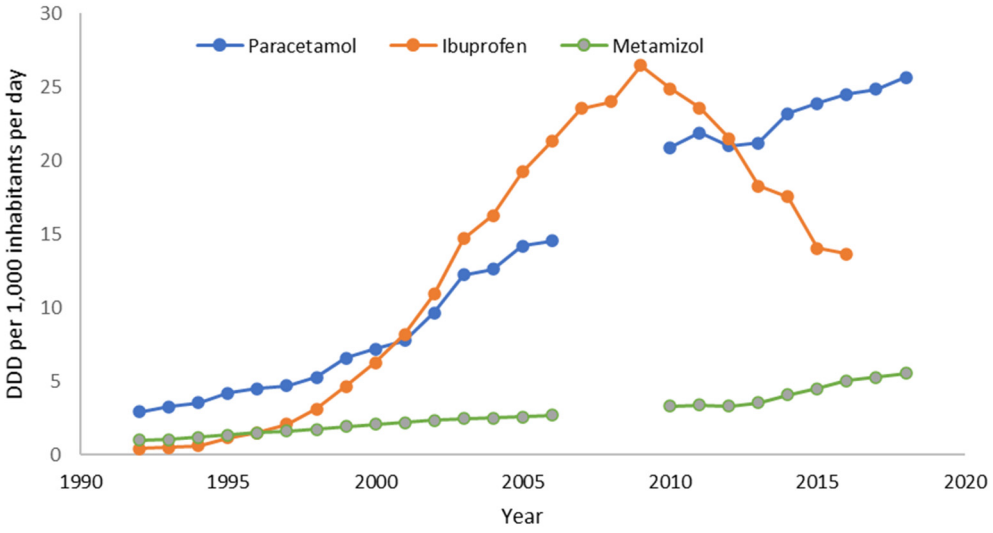

Figure I.9: Prescription of the anti-inflammatories and analgesics most consumed in Spain between 1992 and 2018 (expressed in defined daily doses (DDD) per 1,000 inhabitants per day). Data on drugs dispensed with a prescription from the National Health System and does not include prescription data in care private medical or hospital setting[64].

In the human body, up to 15% of IBU is excreted as an unchanged form or glucuronide and thiol conjugates or as metabolites, i.e., hydroxyibuprofen, carboxyibuprofen, and carboxyhydratropic acid. Nevertheless, conjugates of ibuprofen are further hydrolyzed in the environment[65].

Table I.2: Summary of typical concentrations and removals of the selected pharmaceuticals and metabolites in WWTPs and surface water

Compound	Sampling site	WWTP Influent (ng L^{-1})	WWTP effluent (ng L^{-1})	Removal in WWTP (%)	Surface water (ng L^{-1})	Ref.
IBU	EU, China, Korea, USA	4 - 603,000	ND - 55,000	72 - 100	ND - 1417	66,68, 70-75
Phe	EU	ND - 2,500	ND - 2,760	15 - 98	ND - 1989	76-78
PrPhe	Germany	ND -120	ND - 480	15 - 87	ND - 100	79
AA	EU	28 -780	ND - 9,286	54	ND - 630	79
AAA	EU	730 - 5,390	ND - 25,030	15 - 77	ND - 939	76,80,81
FAA	EU	410 - 2,580	ND - 10,114	5 - 30	ND - 803	76

IBU occurs in WWTP influents in the concentration range between 0.004 and 603 µg L^{-1} (**Table I.2**). For instance, it was the most abundant compound detected in the influent of four WWTPs in Spain, with the concentration levels ranging from 3.73 to 603

μg L^{-1} [66]. At WWTPs, IBU exhibited high removal with an average removal efficiency of 91.4%, being consistent and commonly higher than 70%[67]. The concentrations in WWTP effluents were one to two orders of magnitude lower than those in influent. However, this implies that it is still discharged at relatively high concentrations. Due to river water dilution, IBU occurs at levels at least one order of magnitude lower than effluent levels. IBU has also been found in finished waters from drinking water treatment at maximum occurrence concentrations below 100 ng L^{-1} [67].

Several advanced technologies have been evaluated for the removal of IBU at WWTPs, such as AOPs, coagulation-flocculation, membrane processes and membrane bioreactors (MBR)[67–69].

After oral intake, in humans, aminopyrine and metamizole are rapidly metabolized in a non-enzymatic process to 4-methylaminoanitipyrine (4-MAA) (**Figure I.10**). Then, in the liver, 4-MAA is metabolized to 4-formylaminoantipyrine (FAA) and 4-aminoantiyprine (AA) and further transformed to 4-acetoamidoantipyrine (AAA)[82–84]. So, after oral application, the major metabolites of metamizole and aminopyrine are detected in urine with the following proportions as percent of original dose: 20-48% for AAA, 11-29% for FAA, 4-9% for AA and 2-4% for 4-MAA[82,84–87].

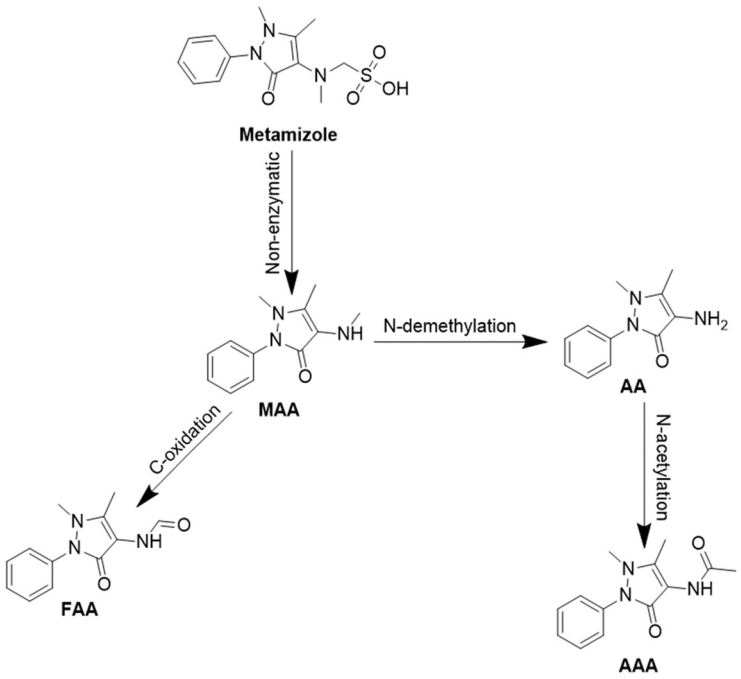

Figure I.10. Metabolism of metamizole (adapted from [88])

The occurrence of phenazone-type drugs and their metabolites has been considered in a lesser extent (**Table I.2**). Phenazone and propyphenazone are very polar, hardly biodegradable, and known to be mostly persistent through conventional activated sludge WWTPs. Phenazone-type pharmaceuticals are partly removed by conventional WWTPs: up to 30% for phenazone, up to 15% for propyphenazone and FAA, and 15 to 40% for AAA. Their removal could be increased by membrane bioreactor pilot plants[89].

I.3.2. High production volume industrial chemicals

The Registration, Evaluation, Authorisation and Restriction of Chemicals (REACH) regulation registers, evaluates, authorizes, and restricts the use of all substances manufactured or imported into the EU[89]. Different types of CECs with widely varying physico-chemical properties are included: organic chemicals, inorganic compounds and particulate contaminants. Among the organic chemicals, in the last 50 years, regulations and studies have been focused on persistent bioaccumulative and toxic (PBTs) substances. However, these PBT- chemicals can be readily removed from water by sorption processes during water treatment or in the environment.

On the other hand, persistent and mobile (and potentially toxic) substances (PM(T) substances), also known as persistent and mobile organic compounds (PMOCs), can persist in the environment but they are not removed from water due to their high water solubility[90]. TPs with increasing polarity from natural and artificial transformation processes can be included within this group of PM(T) substances. In recent years, several efforts have been put on achieving an increasing knowledge for PMOCs[91–93]. In Europe, there is a currently ongoing discussion on whether or not PMT substances should be regulated under the European Union chemical regulation, REACH, in a similar way as is the case for PBT substances[94].

This thesis will consider some of these PMT substances. However, since the number of compounds that could be classified in this group is extremely high, a prioritization approach to select the compounds to be studied under the project Water JPI PROMOTE was applied. Three criteria were selected: (1) high production volume PMT substances registered under REACH[95], (2) predicted TPs of high production volume derived by hydrolysis fulfilling the PMT criteria[62], and (3) environmental relevance based on occurrence studies of PMT substances[91]. The selected substances are shown in **Table I.3**.

Among these prioritized substances, two groups of compounds are discussed below in more detail due to their importance in this thesis, i.e.: 1,3-diphenylguanidine (DPG), 1,3-di-o-tolylguanidine (DTG), 1-vinylpyrrolidin-2-one (VP) and 2-piperazin-1-ylethanamine (PPE).

DTG and DPG are chemicals used as accelerators in the vulcanization processes of rubber and other polymers manufacture, with a registered production in Europe in the 100 - 1000 tons and 1000 - 10,000 tons range, respectively. DPG has been identified as major chemical migrating from polyethylene pipes in China and leaching from tire wear particles[62,96]. Little information about their environmental occurrence is available. In the frame of the project PROMOTE[97], the presence of these compounds in environmental water samples across Europe is reported. These two compounds were detected in all the surface water samples analyzed at concentrations below 10 ng L^{-1} for DTG and up to 100 ng L^{-1} for DPG[91]. Moreover, DPG was found in drinking water in China at levels up to 0.74 mg L^{-1} [96]. On the other hand, DPG showed to be stable against hydrolysis and biotransformation and low extend photodegraded[62].

Table I.3: Selected high production volume industrial chemicals

Compound Name	CAS Number	Structure	Justification for inclusion	Use	REACH production
3-Amino-3,5,5-trimethylcyclohexanamine	2855-13-2	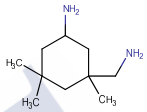	High production	Other; Intermediates	10,000 - 100,000
1,3,5,7-Tetraazatricyclo[3.3.1.1(3,7)]decane	100-97-0		High production	Fuels and fuel additives; Process regulators, used in vulcanization or polymerization processes	10,000 - 100,000
1-vinylpyrrolidin-2-one (VP)	88-12-0	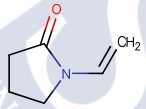	High production	Intermediates; Laboratory chemicals; Solvents	10,000
2-piperazin-1-ylethanamine (PPE)	140-31-8	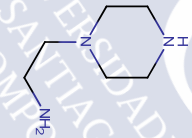	High production	Laboratory chemicals; Fixing agents; Binding agents; Anti-set off and adhesive agents	1,000 - 10,000
1,4-bis[(2-ethylhexyl)oxy]-1,4-dioxobutane-2-sulfonate *(sodium salt)*	577-11-7	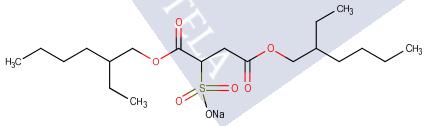	High production	Other; Surface active agents	1,000 - 10,000
1,3,5-tris(2-hydroxyethyl)-1,3,5-triazinane-2,4,6-trione	839-90-7	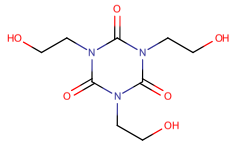	High production	Intermediates; Other	10,000 - 100,000

Table I.3 (cont.): Selected high production volume industrial chemicals

Compound Name	CAS Number	Structure	Justification for inclusion	Use	REACH production
1,3-ditolylguanidine	97-39-2	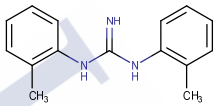	Environmental relevance	Process regulators, used in vulcanisation or polymerisation processes	100 -1,000
1,3-diphenylguanidine	102-06-7	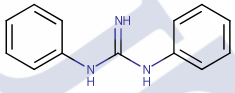	High production	Process regulators, used in vulcanization or polymerisation processes	1,000 - 10,000
6-phenyl-1,3,5-triazine-2,4-diamine	91-76-9	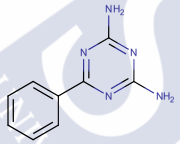	High production	Other; Intermediates; Stabilizers; Laboratory chemicals; Plating agents and metal surface treating agents	10,000 - 100,000
N-methylhydrazinecarbothioamide	6610-29-3	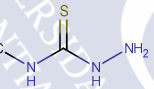	Hydrolysis TP	Intermediates	1,000 -,10,000
N',N'''-methylenebis{1-[3-(hydroxymethyl)-2,5-dioxoimidazolidin-4-yl]urea}	39236-46-9	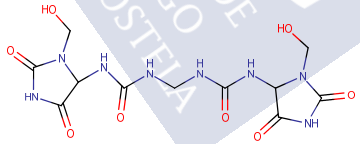	Hydrolysis TP	Intermediates; Other	100 – 1,000
4-hydroxy-2,2,6,6-tetramethylpiperidine-1-ethanol	52722-86-8	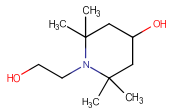	Environmental relevance	Intermediates; Other	1,000 – 10,000
Tartrazin *(disodium salt)*	1934-21-0	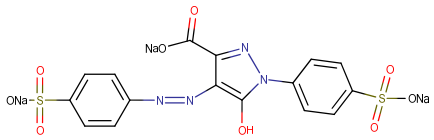	Environmental relevance	Dye	100 – 1,000

VP is the monomer of the widely deployed polymer polyvinylpyrrolidone and otherwise used in washing and cleaning products with a registered production in Europe of 10,000 tons. PPE is used in adhesives and sealants, coating products, paints ad polymers with a registered production in Europe in the 1,000 - 10,000 tons range. These two compounds have not been reported as environmental water pollutants. Only one work reported PPE in surface water samples with a low frequency of detection (28%)[91]. On the other hand, PPE and VP showed to be photodegraded after simulated solar irradiation, however in the case of VP hydrolysis is more probably to be the dominant degradation pathway. PPE was also removed by reaction with MnO_2[62].

I.3.3. Transformation products (TPs)

All the methodologies described in **Section I.2.1** could be potentially used for contaminants removal. However, a major problem, particularly when using oxidative treatments is the formation of the so-called TPs and DBPs.

TPs are chemicals which are produced upon the reaction (and apparent removal) of a precursor contaminant (present in water), where there is a change in its molecular structure[98,99]. Since the last two decades, the study of TPs formation, occurrence and fate has gained popularity, since their (eco)toxicological properties are largely unknown. Thus, the fact that a contaminant is removed from water is not relevant whenever its removal leads to the formation of TPs which are equally or more toxic that the original contaminant itself[100]. Moreover, TPs may even be more mobile in water and persistent than their precursor chemicals (normally TPs are more polar than their precursor chemicals), thus facilitating its travelling through surface and groundwater and spread along the water cycle[101].

Since the TPs and DBPs produced from water treatment processes could be a hazardous threat to human health and an environmental issue, the studies about TPs/DBPs determination are gaining importance as an interesting topic. In this thesis emphasis was put in the development of an improved methodology for the determination of N-nitrosamines and the identification of TPs from different CECs. Hence, the next two sections are devoted to those aspects.

I.3.3.1. Disinfection by-products (DBPs)

DBPs are actually a kind of TPs, however, DBPs normally refers to smaller molecules that are typically produced from natural organic matter (though they can also be produced from micropollutants). Besides, several DBPs are regulated due to the fact that they can be formed in higher amounts (as originating from natural compounds present at higher concentrations) and due to their well-studied toxicity. Some of the most relevant DBPs are THMs, HAAs, haloacetonitriles (HANs), and N-nitrosamines[19,102].

Among the halogenated DBPs, THMs are those formed in higher concentrations during chlorination (at similar levels than HAAs) and those that have been considered more

extensively in the legislation[103]. Thus, the US Environmental Protection Agency (US EPA) stablished a maximum of 80 µg L^{-1} of THMs in finished drinking water and included in this regulation 5 HAAs and some inorganic DBPs as chlorite or bromate, all of them shown in **Table I.4**[15]. Similarly, as shown in the Table, the EU set a 100 µg L^{-1} of THMs already in its 90s drinking water regulation, still in place. Yet, a revision of the drinking water directive is currently being undertaken and will include also HAAs and other inorganic DBPs, besides THMs.

Table I.4. Summary of DBPs regulation in the EU and USA

DBP	Current Europe Maximum Regulation Level[a]	Proposal Europe Maximum Regulation Level[b]	US EPA Maximum Regulation Level[c]
Bromate	10 µg L^{-1}	10 µg L^{-1}	10 µg L^{-1}
Chlorite	No value	0.25 mg L^{-1}	1 mg L^{-1}
Chlorate	No value	0.25 mg L^{-1}	No value
THMs[d]	100 µg L^{-1}	100 µg L^{-1}	80 µg L^{-1}
HAAs[e]	No value	80 µg L^{-1}	60 µg L^{-1}

[a] Europe Regulation (98/83/EC, November 1998)[104]
[b] Incoming Europe Regulation (new proposal) (2017/0332, February 2018)[105]
[c] US EPA Regulation from 1998[15]
[d] Sum of 4 compounds: chloroform, bromoform, dibromochloromethane, bromodichloromethane
[e] Sum of 9 compounds: monochloroacetic acid, dichloroacetic acid, trichloroacetic acid, monobromacetic acid, dibromoacetic acid, bromodichloroacetic acid, dibromochloroacetic acid, tribomoacetic acid

Considering that THMs are small and volatile molecules, they are determined by gas chromatography (GC) with an electron capture detector (ECD)[17,21,106,107]. As an example, the US EPA reported a method extraction and determination of halogenated DBPs based on liquid-1iquid extraction with GC-ECD detection, named US EPA 551.1 method[108].

I.3.3.1.1. N-nitrosamines

N-nitrosamines are compounds whose structures contain a tertiary amine coupled to a nitroso group (-NO), giving a general structure as shown in **Figure I.11**. They are typically formed by chloramination but could be also formed by chlorination of organic matter during water treatments[52] or by reaction of several oxidants with chemicals containing nitrogen[109].

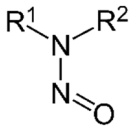

Figure I.11. General structure of N-nitrosamines

N-nitrosamines are reported to be carcinogenic and could induce tumours in several organs being a serious human health threat, but also an environmental issue because they could be formed during water treatment and then discharged into surface waters[110,111]. Besides water treatment they could also be formed e.g. during food cooking steps and food production[112–115]. First reports about N-nitrosamines dated from 1970s, when NDMA, the most widely known one, was detected in water samples[55]. Due to the high carcinogenic activity of some nitrosamines, the World Health Organization (WHO) has included NDMA in its guidelines for drinking water quality, with a guideline value of 100 ng L^{-1} [116]. N-Nitrosamines are on the chemical contaminants candidate list of the US EPA, however to date, major regulations are still at a regional scale. For instance, the government of California set a notification level of 10 ng L^{-1} and response level of 100 ng L^{-1} for NDMA, N-nitrosodiethylamine (NDEA), and N-nitrosodipropylamine (NDPA), on the basis of the 10^{-6} risk level estimates, which ranges from 1 to 15 ng L^{-1} for seven nitrosamines [117].

Research on N-nitrosamines occurrence in waters would not be possible without the development of sensitive methods and analytical procedures, particularly considering the low concentration levels that need to be determined. The methods currently used for the determination of N-nitrosamines are mostly based on enrichment by solid-phase extraction (SPE)[118,119], solid-phase microextraction (SPME)[120], or dispersive SPE[110] and chromatographic analysis with mass spectrometry (MS) detection, either GC[119,121] or liquid chromatography (LC)[122]. One of the reference methods is the US EPA-521 method[118] for the determination of seven nitrosamines in drinking water. This method proposes an SPE using coconut charcoal as the sorbent, dichloromethane (DCM) as the elution solvent, concentration of the extract to less than 1 mL, and GC coupled to tandem MS (GC-MS/MS) detection by employing a chemical ionization source operating in positive (PCI) mode and using an ion trap (IT) mass analyzer for MS/MS (GC-PCI–MS/MS). Electron impact (EI) sources could also be used, however N-nitrosamine fragmentation in EI sources provides smaller ions that could be interfered with by background ions, misleading the identification[119]. This is why, a softer ionization source such as PCI is recommended in the literature[110,118–120,123–127] where fragmentation would be lower. However, even without fragmentation, due to the low molecular weight of N-nitrosamines, background ions can interfere with their determination. Such ion interference could theoretically be solved by using high-resolution mass spectrometry (HRMS), as it is explored in this thesis.

I.3.3.2. Role of high-resolution mass spectrometry in the investigation of transformation products

Depending on the water treatment methods employed, different TPs could be expected. For instance, when water is treated by chlorination, contaminants are transformed due to cleavage of some bonds, but also chlorinated (and brominated) TPs are easily produced. Such halogenated TPs can be hazardous because of their carcinogenicity or mutagenicity related effects, potentially constituting a human health threat, if present in drinking water[17,128,129]. Compared to the precursor contaminants, there are relatively few studies that have investigated TPs of CECs in the aqueous environment. Thus, most TPs are still unknown, so studies where their structures are elucidated are necessary, being a topic of intense research during the last years[130,131].

TPs structural elucidation is intimately linked with the development of HRMS in the last decades, particularly when combined with LC, because many TPs are the result of the introduction of polar groups in the structure of their precursor compounds[132]. LC-HRMS systems are perfect for the detection of thousands of compounds from a sample, by measuring accurate masses of compounds unknown a priori[131,133].

HRMS systems offer high acquisition speed and resolving powers above 20,000 by working under high vacuum conditions (ca. 10^{-7} Torr). The most popular HRMS analysers include Orbitraps and quadrupole-time of flight (QTOF) hybrid analzers[134]. While Orbitrap instruments offer a superior resolution, QTOF systems offer the advantage of a faster scanning speed without sacrificing resolution[135]. Furthermore, ultrahigh-resolution (>1,000,000 resolution) Fourier transform ion cyclotron resonance (FT-ICR) MS instruments have also be employed for the non-target detection of DBPs and TPs in general[136].

Although “unit resolution” instruments were used in the past, HRMS instruments can deliver mass accuracy typically with less than 1-2 mDa or 5 ppm mass error, besides preserving isotopic patterns. Since TPs investigations are made most of the times under lab-controlled conditions, this gives little gap for error in the assignation of molecular formulas, since electrospray ionization (ESI) gives raise in most cases to the protonated or deprotonated analyte. Once the molecular formula is known, then elucidation of the structure is performed by MS/MS experiments, where fragment ions have also a good mass accuracy, so that formulas of such fragments and neutral losses can be clearly identified most of the times. MS/MS spectra need then to be interpreted, expect in some cases, where TPs have already been described in the literature, are present in commercial or open-source libraries (e.g. some TPs are also human metabolites) or pure standards of some potential structures can be purchased[25,137].

Even so, in some cases, MS/MS data is not sufficient to assign a clear structure. For instance, it is quite common that the exact position of some functional groups cannot be assigned, and a full identification of TPs structure is not possible. To overcome such limitations, some authors have performed preparative LC separation for isolating such TPs, followed by nuclear magnetic resonance (NMR) experiments[138,139]. However, such experiments are very time consuming and cannot always be performed.

Furthermore, besides the limitations in interpreting the spectra, another difficulty arises from the fact that some peaks of the TPs may have low intensities and not identifiable in total ion chromatograms. This issue is overcome by modern software that can perform peak-picking, peak alignment and a statistical comparison among untreated samples and samples treated with an oxidant or with radiation. An example is the Mass Hunter software from the vendor Agilent, used along this thesis, but other vendors have their own alternatives, while open-source tools exist, e.g. XCMS (https://metlin.scripps.edu/xcms)[138,139].

Besides LC-QTOF instruments, GC-TOF and GC-QTOF have also entered the market, and more recently GC-Orbitraps, showing their potential for improving screening results as compared to low-resolution systems relying on electron impact ionization. In this sense, both classical GC-sourced instruments (i.e. EI and chemical ionization - CI) and alternative instruments based on atmospheric pressure chemical ionization (APCI) instruments are available. The advantage of the first ones is that they can still make use of well-known low-resolution libraries (e.g. the National Institute of Standards and Technology - NIST library), whereas the second ones can provide the (pseudo)molecular ion, very similarly to LC-ESI-MS[140,141].

Although QTOF instruments are mostly applied in screening and structural elucidation, their high-resolution and mass accuracy can also be exploited in quantitative methods because of their selectivity, in a similar way that was used in the past with magnetic sector instruments[142,143]. This potential application of GC-QTOF is explored in **Chapter IV.1** of this thesis for the determination on N-nitrosamines, given the fact that their low masses can be easily interfered by matrix constituents. On the other hand, LC-QTOF was the system of choice for the investigation of TPs structures and occurrence during different disinfection treatments, as presented in **Chapters IV.2-5**.

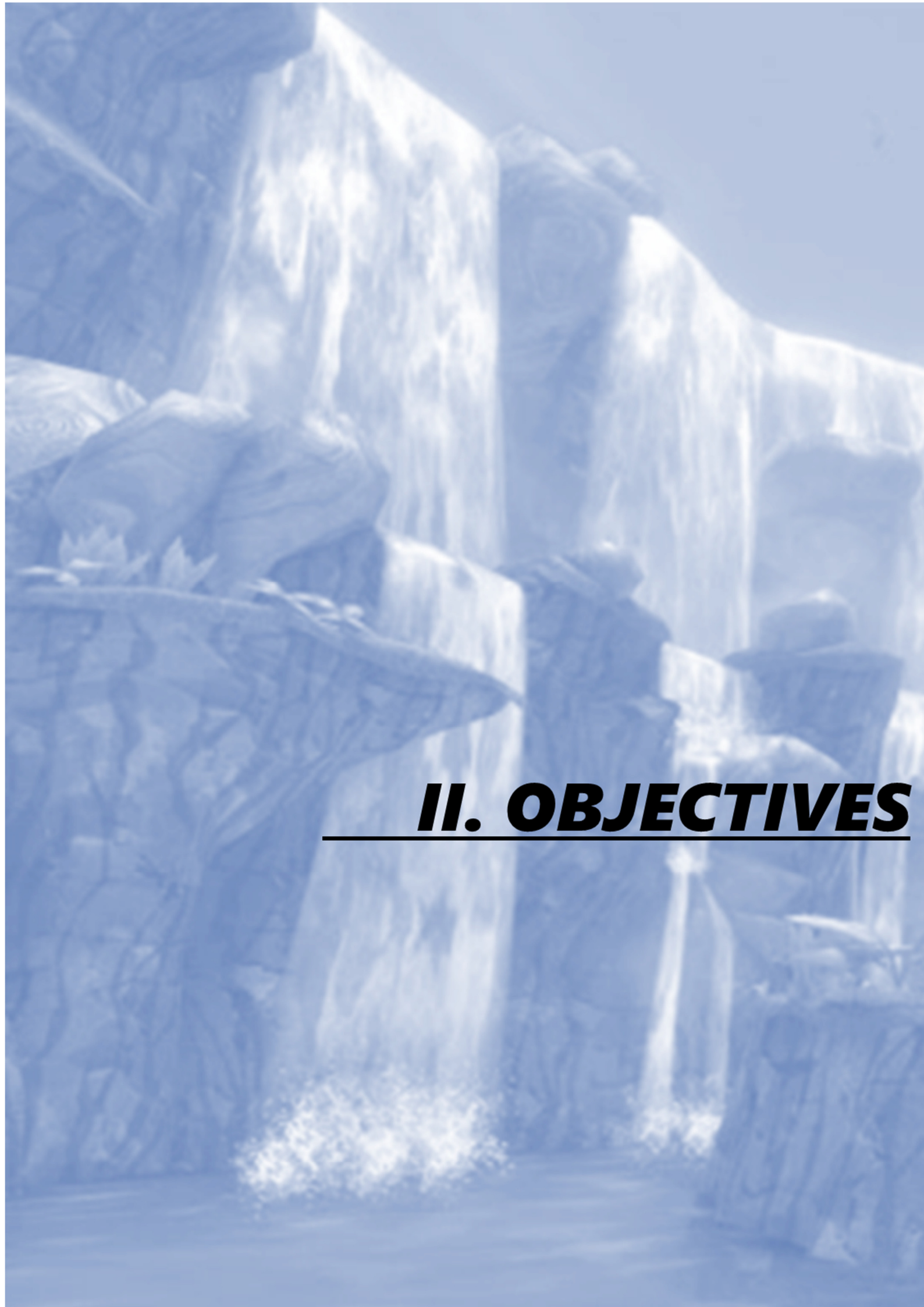

II. OBJECTIVES

USC
UNIVERSIDADE
DE SANTIAGO
DE COMPOSTELA

II. OBJECTIVES

Several CECs are present in the water cycle as a consequence of the anthropogenic impact. These CECs comprise a wide variety of chemicals and include, among some of the most relevant classes pharmaceuticals and industrial chemicals. These chemicals can eventually be removed during water treatment at WWTPs and/or DWTPs because they may react with chemical disinfecting agents, such as chlorine or chloramine, or UV light used for the same purposes.

However, it is nowadays known that reaction of CECs with UV or chlorinated agents (among others) can actually lead to the formation of TPs, including in some cases also well-known regulated DBPs. Knowledge is however still limited, and hence, this thesis aims at contributing to improve our understanding of the reactions, TPs formed and consequences of that, that take place at DWTPs and WWTPs.

Focus is put into, on the one hand: industrial chemicals which have a high production volume and could be expected to be mobile in the water cycle and persistent (named as persistent mobile organic chemicals, PMOCs), as prioritized withing the European Water JPI project PROMOTE; and on the other hand: on analgesic drugs and their metabolites, given the high concentrations that can reach water resources. As regards treatments covered, these are UV photolysis and chlorine-based disinfection.

To reach that goal, five smaller objectives were considered, where the use of either GC or LC coupled to MS (GC-MS or LC-MS) with QTOF analyzers plays a central role. These five subobjectives are covered in the five research chapters that constitute this thesis, viz.:

- Developing an alternative GC-MS method based on the use of a QTOF instrument for the trace determination of N-nitrosamines, a relevant class of DBPs, that could overperform or at least compete with already stablished methodologies (**Chapter IV.1**)
- Investigate the reaction of chlorine and monochloramine with phenazone-type drugs and their metabolites, characterizing their kinetics, TPs and predicting ecotoxicological implications (**Chapter IV.2**)
- Characterize the reaction of chlorine and bromine with two PMOCs employed by the rubber industry, 1,3-diphenylguanidine and 1,3-di-o-tolylguanidine, considering a full kinetic modelling, TPs identification, potential formation of DBPs and ecotoxicological assessment (**Chapter IV.3**)
- Explore the potential of pulsed UV-C laser sources as an alternative to other UV sources for the removal of ibuprofen from water, including the potential formation of TPs (**Chapter IV.4**)
- Asses the reactivity of 12 prioritized PMOCs upon UV treatment and investigating the TPs formed from 2 of them (1-vinylpyrrolidin-2-one and 2-piperazin-1-ylethanamine) and the predicted ecotoxicological impact (**Chapter IV.5**)

USC
UNIVERSIDADE
DE SANTIAGO
DE COMPOSTELA

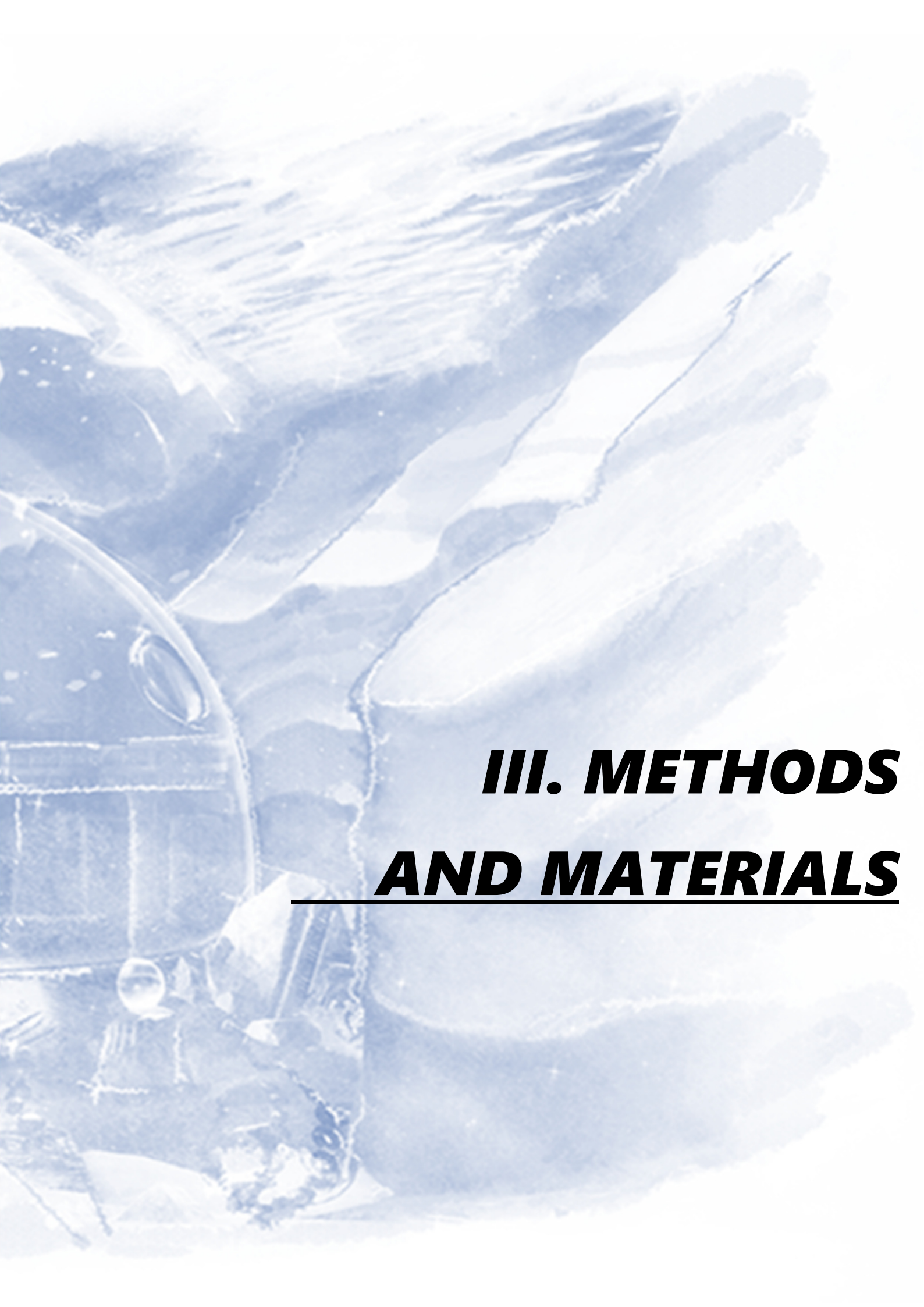

III. METHODS AND MATERIALS

USC
UNIVERSIDADE
DE SANTIAGO
DE COMPOSTELA

III. METHODS AND MATERIALS

III.1. Chemicals

III.1.1. Solvents, reagents, and sorbents

Solvents and reagents, as well as the different suppliers, used to perform the experimental work of this thesis are listed in **Table III.1**.

Table III.1. Solvents and reagents

Solvent	Supplier
Acetone	VWR Prolabo
Acetonitrile (ACN)	Merck
Dichloromethane (DCM)	VWR Prolabo
Ethanol	Merck
Ethyl acetate (AcOEt)	Merck
Isopropanol	Scharlab
Isooctane	Merck
n-Hexane	VWR Prolabo
Methanol (MeOH)	Merck
Reagent	**Supplier**
Ammonium chloride	Merck; Sigma-Aldrich
Ammonia for LC-MS	Sigma-Aldrich
Ascorbic acid	Merck
Dipotassium hydrogen phosphate	Sigma-Aldrich; Panreac
Formic Acid for LC-MS	Sigma-Aldrich
Glacial Acetic acid	Merck
Potassium bromide	Sigma-Aldrich
Potassium dihydrogen phosphate	Sigma-Aldrich
Sodium hydroxide	Sigma-Aldrich
Sodium hypochlorite (6-14%)	Sigma-Aldrich
Sodium thiosulfate	ACS Acros Organics

Ultrapure deionized water was obtained from a Milli-Q Gradient A-10 system (Milipore).

Coconut charcoal SPE cartridges (2 g) were supplied from Supelco (Sigma-Aldrich).

The exact nominal free chlorine content of the sodium hypochlorite solution was regularly determined in the laboratory using a spectrophotometric method based on the hypochlorite ion absorbance at $\lambda = 292$ nm ($\varepsilon = 350$ L mol^{-1} cm^{-1}) after pH > 8 adjustment

with sodium hydroxide, to ensure all the chlorine will be present in the solution as OCl^- ion ($pK_{a\,[HOCl]} = 7.2$)[144].

III.1.2. Standards

A list of the chemicals, including isotopically labelled internal standards used in this thesis is compiled in **Table III.2**.

Table III.2. Standards

Compound	Abbreviation	CAS Nº	Supplier
1,3,5,7-Tetraazatricyclo[3.3.1.1(3,7)]decane	-	100-97-0	Sigma-Aldrich
1,3,5-tris(2-hydroxyethyl)-1,3,5-triazinane-2,4,6-trione	-	839-90-7	Sigma-Aldrich
1,3-di-o-tolylguanidine	DTG	97-39-2	Sigma-Aldrich
1,3-diphenylguanidine	DPG	102-06-7	Sigma-Aldrich
1,4-bis[(2-ethylhexyl)oxy]-1,4-dioxobutane-2-sulfonate	-	577-11-7	Sigma-Aldrich
1-vinyl-pyrrolidone	VP	88-12-0	Sigma-Aldrich
2,4,6-Tribromophenol	TBP	118-79-6	Sigma-Aldrich
2-piperazin-1-ylethanamine	PPE	140-31-8	Sigma-Aldrich
3-Amino-3,5,5-trimethylcyclohexanamine	-	2855-13-2	Sigma-Aldrich
4-Acetamidoantipyrine	AAA	83-15-8	Sigma-Aldrich
4-Aminoantipyrine	AA	83-07-8	Sigma-Aldrich
4-Bromophenol	BP	106-41-2	Sigma-Aldrich
4-Formylantipyrine	FAA	1672-58-8	Sigma-Aldrich
4-hydroxy-2,2,6,6-tetramethylpiperidine-1-ethanol	-	52722-86-8	Sigma-Aldrich
6-phenyl-1,3,5-triazine-2,4-diamine	-	91-76-9	Sigma-Aldrich
Chloroform	-	67-63-3	Supelco
Diclofenac	DCF	15307-86-5	Sigma-Aldrich
Ibuprofen	IBU	15687-27-1	Sigma-Aldrich
Monophenylguanidine	-	14018-90-7	Sigma-Aldrich
N',N'''-methylenebis{1-[3-(hydroxymethyl)-2,5-dioxoimidazolidin-4-yl]urea}	-	39236-46-9	Sigma-Aldrich
N-methylhydrazinecarbothioamide	-	6610-29-3	Sigma-Aldrich
N-Nitrosodibutylamine[a]	NDBA	924-16-3	Sigma-Aldrich
N-Nitrosodiethylamine[a]	NDEA	55-18-5	Sigma-Aldrich
N-Nitrosodimethylamine[a]	NDMA	62-75-9	Sigma-Aldrich
N-Nitrosodipropylamine[a]	NDPA	621-64-7	Sigma-Aldrich
N-Nitrosomethylethylamine[a]	NMEA	109-83-1	Sigma-Aldrich

Compound	Abbreviation	CAS Nº	Supplier
N-Nitrosomorpholine[b]	NMOR	59-89-2	Sigma-Aldrich
N-Nitrosopiperidine[a]	NPIP	100-75-4	Sigma-Aldrich
N-Nitrosopyrrolidine[a]	NPYR	930-55-2	Sigma-Aldrich
N-Nitrosodiethylamine-d10[c]	NDEA-d10	1219794-54-3	Cambridge Isotope Laboratories
N-Nitrosopyrrolidine-d8[c]	NPYR-d8	1219802-09-1	Cambridge Isotope Laboratories
EPA 551B Halogenated Volatiles Mix[d]	-		Supelco
Phenazone	Phe	60-80-0	Sigma-Aldrich
Propyphenazone	PrPhe	479-92-5	LGC Promochem
Tartrazin *(disodium salt)*	-	1934-21-0	Sigma-Aldrich

[a] Purchased as a mixed (US EPA-521 Mix) 2000 µg mL^{-1} solution in DCM.
[b] Individually purchased as 5000 µg mL^{-1} solutions in MeOH.
[c] Individually purchased as 1000 µg mL^{-1} solutions in deuterated DCM.
[d] Mixture containing 2000 µg mL^{-1} each of the following components in acetone: Bromochloroacetonitrile, Dibromoacetonitrile, Dichloroacetonitrile, 1,1-Dichloro-2-propanone, 1,1,1-Trichloroacetone, Trichloroacetonitrile, Trichloronitromethane

III.1.3. Preparation of standards

Stock solutions (ca. 1000 mg L^{-1}) from solid standards were prepared by weight in MeOH or ultrapure water and diluted, as necessary.

In the case of the N-nitrosamines, the standards were purchased as 1000 – 5000 µg mL^{-1} solutions in DCM or MeOH. Mixed stock solutions of 100 µg mL^{-1} were prepared in MeOH and diluted as necessary in MeOH for water fortification or in AcOEt for injection in the GC-MS system.

All standards solutions were kept at -20ºC.

III.1.4. Preparation of monochloramine

Monochloramine (NH_2Cl) solution (2 mM) was produced daily in the laboratory by addition of NaOCl drop by drop to a NH_4Cl solution, previously adjusted to a pH above 8.5[19,145,146], with vigorous magnetic agitation. The concentration of the generated chloramines (NH_2Cl and $NHCl_2$) was determined by a spectrophotometric method using their molar extinction coefficients at two wavelength [19,147]: λ = 255 nm (ε NH_2Cl = 369 mol L^{-1} cm^{-1}; ε $NHCl_2$= 136 mol L^{-1} cm^{-1}) and λ = 295 nm (ε NH_2Cl =15 mol L^{-1} cm^{-1}; ε $NHCl_2$= 289 mol L^{-1} cm^{-1}).

III.2. Material and instrumentation

III.2.1. Laboratory material

- 2, 4, 16 and 22 mL glass vials
- 30 mm o.d. diameter quartz tubes (Afora)

- 1 cm^2 base UV fused quartz cuvettes (CV10Q3500S, Thorlabs Inc.)
- Common use glass material: beakers, volumetric flasks, pipettes, watch glasses
- Precision micropipettes with variable volume: 2-20 µL, 20-200 µL, 100-1000 µL, 1-5 mL
- 0.22 µm PVDF syringe filters (Merck-Millipore)

III.2.2. Auxiliary instrumentation

- 15-Positions magnetic stirrer (Thermo-Scientific)
- Analytical Balance (VWR model VWR 1611-3542)
- MiniVap Nitrogen system
- Syncore vacuum concentrator system (Büchi Labortechnik AG)
- Ultrasonic water bath (Ultrasons Medi-II)
- UV Photoreactor equipped with two 8-W low-pressure Hg lamps (Philips reference G8 T5) emitting at 254 nm, a fan to dissipate the heat and an orifice to introduce the quartz tube perpendicularly to the lamps
- UV-Vis Spectrophotometer (Thermo-Scientific)
- UV–Vis Lambda Spectrometer (Perkin-Elmer)
- VisiPrep vacuum manifold for SPE (Supelco)
- Vortex stirrer (RS Lab model RSLAB-6PRO)
- 5000A TOC analyzer (Shimadzu)
- Shimadzu TOC-L instrument (Shimadzu)
- 850 Professional Ion Chromatograph (Metrohm)
- Pulsed solid-state laser (Quanta Ray)
- pH-meter 654 (Metrohm)

III.2.3. Analytical instrumentation

Determination of N-nitrosamines was carried out using two GC-MS instruments (**Figure III.1**):

- GC-QTOF-MS: An Agilent 7890A gas chromatograph with an Agilent 7693 automatic sampler combined with an Agilent 7200 QTOF MS instrument (Agilent Technologies)
- GC-IT-MS: A Varian 450 GC system coupled to an ion trap Varian 240 mass spectrometer (Varian)

In experiments devoted to follow the reaction kinetics and identification of TPs and DBPs, the instrumentation used is described below:

- HPLC-QTOF-MS: An Agilent 1200 Series LC system equipped with a membrane degasser, a binary high-pressure gradient pump, a thermostat LC column compartment and an autosampler interfaced to an Agilent 6520 Series Accurate Mass Q-TOF-MS equipped with a Dual Electrospray ion source
- UHPLC-QTOF-MS: An Agilent 1290 UHPLC system coupled to an Agilent 6550 iFunnel QTOF mass spectrometer

- HPLC-PDA: Waters 2695 LC equipped with a degasser, binary high-pressure pump, LC column oven and an autosampler. The photodiode array detector (PDA) was a Waters 2996 equipped with a deuterium lamp. Instrument control and data treatment were done with Empower software (Waters)
- GC-Q-MS: a CTC Analytics Combi Pal autosampler with an Agilent 7890 GC and an Agilent 5975C mass spectrometer

Figure III.1. GC-MS systems: GC-IT-MS (left) and GC-QTOF-MS (right)

III.3. Samples

During the development of this work different types of water samples, with different complexity and organic matter content, were sampled: tap, river, and wastewater.

For the analysis of N-nitrosamines, tap water was obtained from the laboratory at three different times and analyzed immediately after collection. Grab samples were obtained from the influent and effluent of an urban WWTP in Galicia (Spain) equipped with a primary and secondary conventional-activated sludge treatment.

During the study of phenazone-type drugs degradation with chlorine and monochloramine, surface water samples were collected from a small creek (pH 6.5, dissolved organic carbon (DOC): 8.7 mg L^{-1}, bromide: 0.035 mg L^{-1}) not affected by urban activities, and from a river (pH 5.8, DOC: 22 mg L^{-1}, bromide: 0.045 mg L^{-1}) after receiving the discharge of a WWTP, ca. 5 Km downstream.

In the case of DPG and DTG, two samples were used to study the extent of the chlorination reaction in real matrix: a surface water sample collected from the River Sarela in Santiago de Compostela (pH 6.8, DOC: 2.42 mg L^{-1}, chloride: 7.98 mg L^{-1}, bromide: 0.043 mg L^{-1}) and a wastewater effluent collected from a WWTP comprising a primary and a secondary conventional sludge treatment (pH: 7.5, DOC: 14.1 mg L^{-1}, chloride: 23.1 mg L^{-1}, bromide: 0.075 mg L^{-1}). The same river water sample was used for the study of the UV degradation of VP and PPE.

In order to test the reaction of IBU irradiated with UV-laser radiation in real samples, effluent water (pH: 7.1, DOC: 3.5 mg L^{-1}, total suspended solids: 6 mg L^{-1}, nitrate: 26 mg L^{-1}, nitrite: 0.25 mg L^{-1}, chloride: 20 mg L^{-1}, bromide: 0.14 mg L^{-1}, sulfate:

22 mg L^{-1}, fluoride < 0.05 mg L^{-1}, phosphate < 0.04 mg L^{-1}) was collected from a wastewater treatment plant located in the NW of Spain, which processes the sewage of ca. 100,000 inhabitants and is equipped with primary and conventional activated sludge treatments.

All samples were collected in amber bottles and stored at 4 ºC until used. All samples were filtered before analysis through 0.45 µm nitrocellulose filters (Millipore) to remove particulate matter.

DOC was determined on a Shimadzu TOC-L or a Shimadzu 5000A instruments, according to the 5310-B Std. Meth. Ed.20 (APHA-AWWA-WPCF) method for water and wastewater examination[148]. DOC was calculated from the difference between the total carbon (TC) and inorganic carbon measurements. Bromide and chloride were determined with a Metrohm 850 Professional Ion Chromatograph.

III.4. Methodology

III.4.1. Determination of N-nitrosamines

III.4.1.1. Sample preparation

Extraction of N-nitrosamines from water samples was carried out according to the US EPA-521 method[118]. Briefly (**Figure III.2**), 500 mL of filtered water was taken and then 20 ng of NDEA-d10 (as surrogate standards for NDMA, NMEA, and NDEA) and 20 ng of NPYR-d8 (surrogate for the remaining nitrosamines) were added. Samples were percolated through the coconut charcoal (2 g) SPE cartridges at a flow rate of 10 mL min^{-1}. SPE cartridges were dried under a nitrogen stream for 45 min. After drying, compounds were eluted by gravity using 15 mL of DCM, and the resultant extract was concentrated in the Syncore system (water bath at 50 ºC, kept at 175 r.p.m. and 50,000 Pa pressure) down to approximately 0.3 mL. AcOEt was added to the extract and transferred to graduated glass tubes for further concentration to 100 µL by a gentle nitrogen stream, with the precaution of avoiding dryness of the extract in order to minimize the loss of N-nitrosamines by volatilization. Therefore, the solvent of the extract was changed to AcOEt thanks to the higher volatility of DCM. Finally, this extract was injected in the GC-MS system.

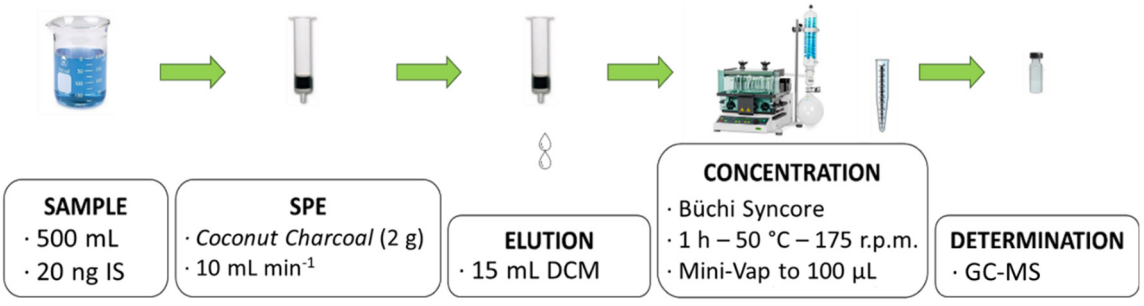

Figure III.2. Scheme of N-nitrosamines analysis

III.4.1.2. Determination conditions

Determination of N-nitrosamines was carried out using two GC-MS instruments: GC-QTOF-MS and GC-IT-MS. In both instruments, the volume injected was 2 µL in the splitless mode of operation, with an injector temperature established at 250 ºC with a splitless time of 1 min. Three GC capillary columns were tested: an HP-5MS (5% phenyl-methylpolysiloxane, 30 m x 0.25 mm x 0.25 µm film thickness, Agilent Technologies), a DB-WAXetr (extended temperature range high polarity polyethylene glycol, 30 m x 0.25 mm, 0.50 µm film thickness, Agilent Technologies), and an HP-35MS (35% phenyl-methylpolysiloxane, 30 m x 0.25 mm, 0.25 µm film thickness, Agilent Technologies). Under final conditions, the DB-WAXetr column was used for sample analysis. The solvent delay was set at 6 min. The oven temperature program was as follows: 60 ºC kept for 1 min; then ramped to 100 ºC at 10 ºC min^{-1} and kept for 1 min; and a final ramp to 245 ºC at 15 ºC min^{-1} and held for 2 min. Helium (99.9999%, Praxair, Spain) was used as carrier gas at a constant flow rate of 1 mL min^{-1}.

The GC-QTOF-MS was operated in the 2 GHz extended dynamic range mode, which provides a full width half maximum (FWHM) resolution of ca. 4000 at m/z 75 and ca. 6000 at m/z 187. The MS spectra were acquired and stored in the profile mode. MS sources conditions were: PCI using methane (99.95%) as ionization gas (20% pressure) at 150 µA of filament emission current and EI working at 70 eV with the filament emission set at 30 µA. The transfer line, PCI source, EI source, and MS quadrupole temperatures were set at 245 ºC, 300 ºC, 230 ºC, and 150 ºC, respectively. Full-scan acquisition mode was set in the range of 40–650 m/z with an acquisition rate of 5 spectrum s^{-1}. For the HRMS calibration to be maintained during the analysis sequence, perfluorotributylamine (PFTBA) was infused in the MS every 4 injections, according to the manufacturer specifications.

In the GC-IT-MS instrument, an external ionization configuration of the MS source was used. The transfer line, MS source, manifold, and IT temperatures were 280 ºC, 200 ºC, 50 ºC, and 150 ºC, respectively. Full-scan mode of acquisition was set in the range of 40–230 m/z, with an acquisition rate of 2 spectrum s^{-1}, average scans of 3 µScans, and target total ion chromatogram (TIC) of 20,000 counts. For EI, the filament emission current was set at 30 µA, while in PCI, using methane as an ionization gas, it was set at 100 µA. The damping gas was set at 2.5 mL min^{-1}. MS/MS experiments were also tested with spectra acquired in the GC-(PCI)-IT-MS system at 3 spectra s^{-1}.

III.4.1.3. Method validation

Analytes were quantified using NDEA-d10 as surrogate internal standards (IS) for NDMA, NMEA, and NDEA; and NPYR-d8 for the rest of the N-nitrosamines.

Linearity was assessed by a 9-point calibration curve ranging from the instrumental quantification limits (IQL) to 500 ng mL^{-1} (IS concentration: 200 ng mL^{-1}). Instrumental detection limits (IDL) and IQL were estimated from the lowest calibration standards as the concentrations providing a signal to noise ratio (S/N) of 3 and 10, respectively. Intra-day and inter-day instrumental precision were assessed from the relative standard deviation

(%RSD) of six injections of a standard of 50 ng mL^{-1} performed over 24 h (intra-day precision) or over three weeks (inter-day precision).

Validation of the SPE-GC-MS method was performed with wastewater samples spiked at two levels with 5 ng and 100 ng of all the analytes (10 and 200 ng L^{-1} referred to the sample, respectively) and 20 ng of IS before extraction. Additional aliquots were spiked only with IS and processed simultaneously in order to account for the background levels. Method detection and quantification limits (MDL and MQL) were estimated from the measured concentrations in spiked wastewater samples (n = 3), downscaling the levels for which the S/N values are 3 (MDL) and 10 (MQL). Accuracy determined for the wastewater samples spiked with 5 ng and 100 ng of all the analytes was expressed as the average recovery, calculated from calibrations performed with standards in AcOEt by the internal standard method from the nominal spiking value. Precision was expressed as the %RSD from the average concentration measured (n = 3).

III.4.2. Determination of DBPs

Chloroform was analysed by headspace injection using the GC-Q-MS. 10 mL of sample were poured in 20 mL headspace vials containing 10 µL of 1M ascorbic acid to quench residual chlorine. Vials were heated at 50 °C and stirred at 500 rpm for 10 min before 2.5 mL gas phase was injected into the GC system in pulsed split mode (ratio 1:10). The analytical column was an Agilent HP-5MS column (30m x 0.25 mm; film thickness 1 µm). The retention time of chloroform was 3.8 min for a temperature program starting at 40 °C and ending at 55 °C in 8 min.

HANs were analysed by the US EPA 551.1 extraction method followed by GC-MS determination as described elsewhere[19]. Detection limits for DBPs were 0.1 µg L^{-1}.

III.4.3. Experiments performed to study aqueous oxidation

III.4.3.1. Chlorination and chloramination of phenazone-type drugs and metabolites

Experiments were performed in 16 mL amber closed vials at room temperature (20 ± 2 ºC). The reaction kinetics were evaluated in ultrapure water at three different pH values (5.7, 7.0 and 8.3) buffered with a KH_2PO_4/K_2HPO_4 0.03 M solution, spiked with the target analytes at 1 µg mL^{-1} (4-5 µM) (**Figure III.3**). After the addition of chlorine or chloramine, aliquots of 1 mL were taken at different reaction times and the reaction was stopped with 0.6 mg mL^{-1} of ascorbic acid. In chlorination experiments, free chlorine concentration was set to 10 µg mL^{-1} (0.141 mM). Such pH values and chlorination dosages represent typical values for drinking water[116,149].

Additionally, KBr was added at 100 ng mL^{-1} (0.84 µM) in some experiments, which reacts with HOCl to produce hypobromous acid, to consider bromination in bromide-containing surface water[150].

Chloramination experiments were performed with 4 μg mL^{-1} (0.0777 mM) of monochloramine, which is the maximum residual disinfectant concentration allowed by the US EPA[151]. Finally, experiments without chlorine nor chloramine were prepared as a control.

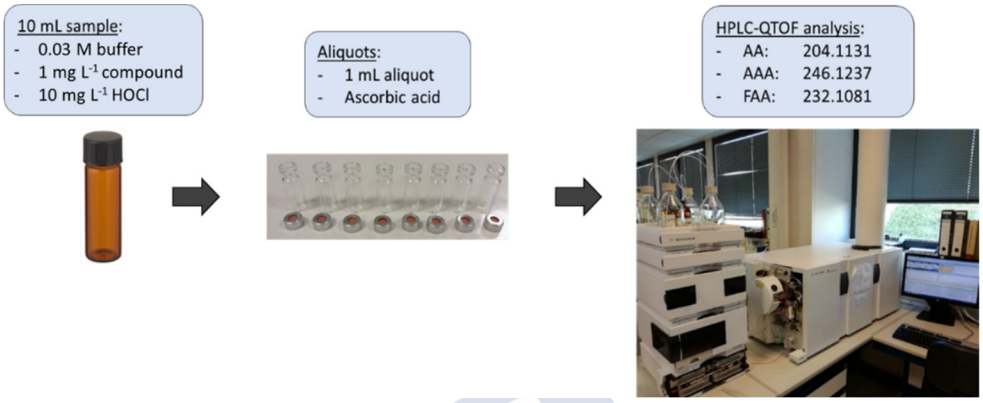

Figure III.3. Schematic representation of phenazone-type drugs chlorination experiments

III.4.3.2. Chlorination of DPG and DTG

Chlorination of DTG and DPG were performed individually in 100 mL amber closed vials at room temperature. Also, experiments without chlorine were prepared as a control.

Experiments to study chlorination kinetics were performed with 1 μM compound concentration, an excess of chlorine (10 μM, 20 μM or 50 μM) and different pH of sample (5–12) being considered in 10 mM phosphate buffer and NaOH for very basic pHs. Aliquots of 1 mL were taken at different reaction times and the reaction stopped with 20 μL of 0.01 M sodium thiosulfate before residual concentration of guanidine was analysed by HPLC-PDA. Ammonium chloride (1 mM) was used in some experiments as "soft" quenching method as being selective to free chlorine and as to avoid any $Na_2S_2O_3$-induced back reaction that could interfere with determination of rate constant[152]. An experiment was also performed without stopping the reaction and aliquots were manually injected at different reaction times using a Rheodyne valve in the HPLC-PDA system.

Experiments were performed at room temperature (22 ± 1 °C). The pH was measured before and after the experiment, and variation was less than 0.1 unit. Free active chlorine was analysed by the DPD colorimetric method[148] at the end of reaction time. Chlorine consumption was usually below 10% and pseudo-first-order plots were always linear.

Additional experiments for the identification of TPs (performed in triplicate) were carried out with a similar procedure. For these experiments, ultrapure water adjusted at pH 7.0 was used, spiked with the compound at 10 μM, and initial chlorine dose set to 100 μM.

TPs were identified after reduction by ascorbic acid for reaction times of 30 s, 1 min, 2 min, 5 min, 10 min and 30 min.

DBPs formation potentials (chloroform and HANs) were determined for a reaction time of 2 days at pH 7.0 in ultrapure water with an initial concentration (of either DPG or DTG) of 10 μM and molar chlorine to guanidine ratios of 1, 10 and 100 in headspace-free conditions.

III.4.3.3. Bromination of DPG and DTG

Bromination experiments were performed under the same conditions as chlorination, in order to determine apparent rate constants and detect TPs that can be produced in bromide containing waters. Bromine was generated in the lab according to the procedure described by Benitez et al.[153] . Briefly, bromine was produced from the reaction between 9 mM HOCl and 10 mM potassium bromide. The yield of this reaction was followed spectrophotometrically (hypobromite anion maximum absorption wavelength at 329 nm with an ε=332 M^{-1} cm^{-1} at pH above 11.5)[153].

Kinetics of bromination were studied as for chlorination for pH values ranging from 5 to 9 using the direct method in batch reactor with an excess of bromine (10–100 μM) compared to 1 μM DPG or DTG solution. Apparent rate constants were also determined by using the competition kinetics method[150] with 4-bromophenol (BP) in the pH 8–11 range or 2,4,6-tribromophenol (TBP) at pH 7.0 and 8.0 as reference compounds. In this method, different concentrations of bromine from 0 to 10 μM were introduced in 25 mL of a 10 mM phosphate buffer solution containing 5 μM DPG or DTG and 5 μM of reference compound (either BP or TBP). Residual concentrations of organic compounds were determined by HPLC-PDA.

III.4.3.4. Laser irradiation of ibuprofen

Laser experiments were performed on 4 mL aliquots of IBU spiked (10 mg L^{-1}), double distilled water or filtered effluent wastewater. Samples were placed inside 1 cm^2 base UV fused quartz cuvettes (CV10Q3500S) and irradiated with the pulsed solid-state laser. The laser emission was set at its fourth harmonic (λ = 266 nm) with a pulse width of 4–5 ns and a pulse repetition frequency of 50 Hz. The nominal laser emission power was set at 0.9 W and the area covered by the beam was set at ca. 1 cm^2. In consequence, the pulse fluence is ca. 18 mJ cm^{-2} and the pulse irradiance ca. 4 MW cm^{-2}. The laser beam was reflected on a narrowband laser line mirror (Y4-1025-45-UNP, CVI Laser Optics) mounted onto a 45° round mount (Thorlabs Inc.), in order to vertically irradiate the cuvette contents from its top entry (**Figure III.4**). The laser power was measured employing a FieldMax II TO (Coherent Inc) power meter equipped with a PowerMax PM150 sensor and placed at the same geometrical point as the quartz cuvettes. It was observed during the treatment that the laser beam irradiated a complete, vertical liquid column, from the upper liquid meniscus to the bottom, inner base surface of the cuvette.

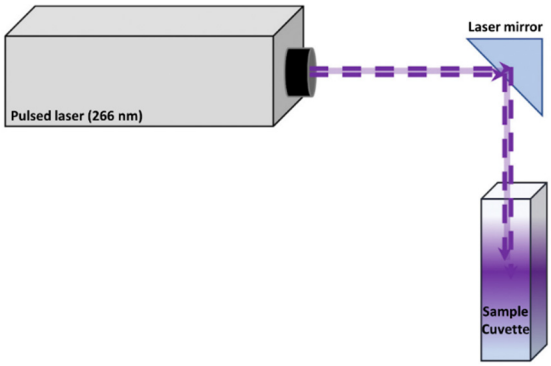

Figure III.4. Experimental set-up configuration employed to carry out Laser irradiation of IBU solutions.

III.4.3.5. UV-Photolysis of REACH-prioritized chemicals

Photodegradation experiments were performed in 30 mm o.d. diameter quartz tubes containing 25 mL of ultrapure water or river water. UV photodegradation was carried out using a homemade photoreactor equipped with two 8 W low-pressure Hg lamps emitting at 254 nm, a fan to dissipate the heat and an orifice to introduce the quartz tube perpendicularly to the lamps. Further details on its design can be found elsewhere [154,155]. The flux density of radiation was measured using potassium iodide as actinometer. The measured value was 7.2 mW cm^{-2} [155]. Lamps were equilibrated for 30 min before starting any test.

A preliminary study to determine the stability of the 12 chemicals was done in 25 mL of ultrapure water by using 2 mg L^{-1} of each chemical (**Figure III.5**). Different aliquots of 1 mL were taken at different times between 0 and 60 min. Further experiments were performed in ultrapure and river water by using 2 mg L^{-1} of either VP, or PPE or DCF in order to estimate the photochemical degradation kinetic and rate constant in both kind of samples. River water samples were filtered through a 0.22 µm PVDF syringe filters before LC analysis.

Experiments for TPs identification were performed in ultrapure water at higher concentrations (20 mg L^{-1}) in order to improve the detectability of such TPs. In some experiments, ethanol (50 µM) was also added as an ·OH radicals scavenger[156].

Figure III.5. Photolysis experimental set-up

III.4.4. Liquid chromatography – photodiode array detection (HPLC-PDA) of DPG and DTG

The chlorination kinetic study of DPG and DTG was followed by analysing the samples in the HPLC-PDA system. DPG was monitored at 235 nm, whereas DTG, BP and TBP were measured at 225 nm.

The LC column used was a 250 mm x 4.6 mm; 5 μm Kinetex EVO C18 (Phenomenex) at a flow rate of 1 mL min^{-1}. Mobile phases consisted in Milli-Q water (eluent A) and acetonitrile (eluent B), both acidified with 0.1 % formic acid. Gradient was as follows: 0 min, 5% B; 10 min, 100% B; 12 min, 100% B; 12.10 min, 5% B; 20 min, 5% B. The injection volume was set to 50 μL.

III.4.5. Analysis performed with the HPLC-QTOF-MS system

For the Q-TOF, nitrogen (99.9%), used for nebulising and drying gas, was provided by a nitrogen generator (Erre Due Srl). Nitrogen (99.9995%) used for collision-induced dissociation was supplied by Praxair Spain. The electrospray ion source was operated in positive (no TPs were detected in negative) mode with the following parameters being applied: gas temperature: 350 °C; drying gas: 5 L min^{-1}; nebulizer: 42 psig, capillary: 4000 V; fragmentor: 120 V; skimmer voltage: 65 V; and octapole RF peak: 750 V. Instrument was operated in the 2 GHz (extended-dynamic range) mode, which provides a Full Width at Half Maximum (FWHM) resolution of ca. 4,500 at m/z 121 and ca. 11,000 at 922, scan range: 70-1000 m/z. A reference solution was also continuously infused using a second nebulizer of the Dual- Electrospray ion source (5 psig), to recalibrate the QTOF using two masses (m/z 121.0509 and 922.0098) and maintain the mass accuracy.

Separation of phenazone-type drugs and their TPs was carried out on a 100 mm x 2 mm (particle size: 3 μm) Synergi Fusion RP (Phenomenex) at a flow rate of at 0.2 mL min^{-1} at 35 °C. Mobile phase consisted of Milli-Q water (A) and MeOH (B) both containing 5 mM of ammonium acetate. The gradient was as follows: 0 min, 5% B; 10-12 min, 100% B; 12.10 min -25 min, 5% B. Injection volume was set to 10 μL.

In the case of DPG, DTG, VP and PPE, the LC column was a Luna 150 mm x 2 mm; 3 μm C18 (2) (Phenomenex) at a flow of mobile phase of 0.2 mL min^{-1}, and column temperature established at 35 °C. Mobile phases consisted in Milli-Q water (eluent A) and acetonitrile (eluent B), both acidified with 0.1 % formic acid. Gradient was as follows: 0 min, 5% B; 10 min, 100% B; 12 min, 100% B; 12.10 min, 5% B; 20 min, 5% B. The injection volume was set at 10 μL.

Instrument control, data acquisition and evaluation were performed with the MassHunter software (Agilent Technologies). Quantification was carried out in single MS mode from the accurate mass extracted chromatogram by integrating the area of the peaks on the narrow-window (20 ppm) extracted ion chromatograms of the $[M+H]^+$ ion.

III.4.6. Analysis performed with the UHPLC-QTOF-MS system

Chromatographic separation was achieved using a 150 x 2mm, 3 µm Luna C18 column (Phenomenex) using ultrapure water and acetonitrile, both containing 0.1% formic acid, as eluents A and B, respectively. The LC gradient was as follows: initially 5% B, ramped to 100% B in 10 min (held for 2 min), then back conditioned for 9 min. Injection volume was 5 µL and flow rate to 0.2 mL min^{-1}. The LC-HRMS system was operated in negative ionization mode, with nitrogen being used as nebulizing gas. Spectra registration was performed in the 2 GHz extended dynamic range mode which provides a resolution of ca. 10,000 at m/z 121 in the 40–1000 m/z range. The mass accuracy was maintained by infusing a reference solution with a secondary electrospray according to manufacturer's specifications. IBU was determined by integration of the 205.1234 m/z (± 20 ppm) extracted ion chromatogram. TPs were screened for by extracting the m/z value of TPs described in the literature[157,158] at different irradiation times.

III.4.7. Identification of TPs

Determination of TPs was performed using the algorithm "Find by molecular feature" from the MassHunter software[159], which generates a list of possible entities (chromatographic peaks and m/z values) with a response higher than 1000 counts for each chromatogram, which were exported as CEF files. Such files were then transferred to the MassProfiler Professional software (Agilent Technologies) which compares the control group (aliquots at time 0 s) and aliquots collected at different treatment times, excluding those entities which were not observed at least in the three replicates of any reaction time. Then, empiric formulae were produced for the TPs using the "generate formula" tool of the MassHunter software, which considers the accurate mass and isotopic distribution, providing a score (100 is a perfect match). Cut-off values were set at mass error <5 ppm and score > 80. Finally, MS/MS analysis were acquired, using different collision energies (10, 20 and 40 V), and interpreted in order to tentatively elucidate the structure of the TPs.

III.4.8. Toxicity assessment

III.4.8.1. *In-silico* estimation

An *in-silico* preliminary estimation of the ecotoxicity of the investigated substance and its TPs was performed by two Quantitative Structure-Activity Relationship (QSAR) software, viz the US EPA Toxicity Estimation Software Tool (T.E.S.T.) version 4.1 and ECOSAR version 1.11.

In T.E.S.T., toxicity values can be estimated with different QSAR methodologies and a large number of molecular descriptors such as structural or electronic parameters. Endpoints were estimated by the consensus method, which uses an average value of the calculated toxicities by five different QSAR methodologies[159]. Toxicity values that can be estimated are: 96-h *fathead minnow* LC_{50}, 48-hour *daphnia magna* LC_{50}, 48-hour *tetrahymena pyriformis* growth inhibition concentration (IGC_{50}), oral rat LC_{50},

developmental toxicity (whether or not a chemical causes developmental toxicity effects to human or animals) and Ames mutagenicity (if a chemical induces revertant colony growth in any strain of *Salmonella typhimurium*).

In ECOSAR, toxicity values were estimated using different linear regression models for each chemical class. The 48-hour *daphnia magna* LC_{50}, 96-hour fish LC_{50}, 96-hour green algae EC_{50} and chronic toxicity values were estimated[159].

III.4.8.2. Experimental toxicity assessment

III.4.8.2.1. Vibrio Fisheri test

Besides the QSAR prediction, a bioluminescent *Vibrio Fisheri* test evaluation of the toxicity of DPG and DTG and different chlorination mixtures was performed according to the standard method NF EN ISO 11348-3 (2009) by using a LumisTox® 300. Details of the procedure are described elsewhere[160].

The inhibition of the luminescence was calculated according to the following equation:

$$H_t = \frac{I_{ct} - I_t}{I_{ct}} \times 100$$

Where:

- H_t is the inhibition percentage of the luminescence after the incubation period t,
- I_t is the luminescence of the test solutions after the 30 min incubation period (i.e. the final luminescence after addition of the sample),
- I_{ct} the corrected initial luminescence for the tested solution with $I_{ct} = f_k \times I_o$, and I_o was the initial luminescence of the bacteria suspensions before the sample was added, f_K the correction factor $f_K = \frac{I_{tK}}{I_{oK}}$ with I_{oK} is the initial luminescence of the control solution (2% NaCl) and I_{tK} is the luminescence of the control solution (2% NaCl) after the 30 min incubation period.

The EC_{50} and EC_{20} values were calculated from the linear representation of $\log(c_t)$ versus $\log(H_t/(100 - H_t))$, where $c_t = 100 \times (1/\text{dilution factor})$. The EC_{50} value was given by the point of intersection with the X-axis at $\log(H_t/(100 - H_t)) = 0$. The EC_{20} value was determined for $\log(H_t/(100 - H_t)) = -0.60$.

The EC_{50} and EC_{20} values of *Vibrio fisheri* test were estimated from a series of geometrical dilutions with dilution factors from 1 to 256 and initial DPG/DTG concentration of 100 mg L^{-1}.

III.4.8.2.2. Zebrafish embryo assays

The bioassays for the evaluation of the toxicity of IBU and different UV exposed solutions were carried out based on the OECD Fish Embryo Acute Toxicity (FET) Test 236. It consisted of eight treatments (one per plate): a negative control (dechlorinated

water), a positive control (4 mg L^{-1} of 3,4–dichloroaniline), and solutions of IBU before and after treatment with UV-C laser pulsed irradiation. Clean fertilized eggs were randomly placed in previously incubated, during 24h at 26ºC ± 0.5, 24-well plates (one per well) with 1 mL of each test solution. Plates with the embryos were maintained at 26ºC ± 0.5 for 96h under the same photoperiod of the adults. Solutions were renovated daily in order to maintain oxygen and solution concentrations, and to avoid medium degradation. Embryos were checked for mortality and morphological abnormalities on head, tail, eyes, yolk-sac, oedemas, abnormal cell growth, and developmental arrest were recorded as present or absent at 8, 24, 48, 72, and 96[161,162]. Additionally, 75% epiboly state was observed at 8 hours post-fertilization (hpf), somit formation and tail detachment was verified at 24 hpf, cardiac frequency at 48 and 72 hpf, and sensorimotor reflexes, larvae length, and yolk sac area were measured at 96 hpf. Embryo development and larvae measurements were checked under an inverted microscope (Nikon Eclipse 5100T) coupled with a digital camera Nikon D5 – Fi2. Sensorimotor reflexes were checked in 96 hpf larvae using an adaptation of the method described in Cunha et al.[163].

Data obtained during the embryo bioassays was computed using the Software Statistica 12.5 (Statsoft). Data were tested for normality and homogeneity of variances using the Kolmogorov – Smirnov test and Levene's test, respectively. Given that data met the criteria, a two-way ANOVA test was performed to evaluate differences with the negative control, as well as differences between before and after 15 min treatment with UV-C laser pulsed irradiation. *Post-hoc* comparisons were carried out using Fisher's least significant difference (LSD) test. Significant differences were set to $p<0.05$.

USC
UNIVERSIDADE
DE SANTIAGO
DE COMPOSTELA

IV. RESULTS AND DISCUSSION

USC
UNIVERSIDADE
DE SANTIAGO
DE COMPOSTELA

IV. RESULTS AND DISCUSSION

IV.1. Determination of N-nitrosamines by Gas Chromatography Coupled to Quadrupole-Time-of-Flight Mass Spectrometry in Water Samples

The results collected in this chapter have been published in:

Benigno José Sieira, Inmaculada Carpinteiro, Rosario Rodil, José Benito Quintana and Rafael Cela,

Determination of N-Nitrosamines by Gas Chromatography Coupled to Quadrupole–Time-of-Flight Mass Spectrometry in Water Samples.

Separations 7 (2020) 3

DOI: 10.3390/separations7010003

USC
UNIVERSIDADE
DE SANTIAGO
DE COMPOSTELA

The aim of this work is to develop an alternative to low-resolution IT mass analyzers for the determination of N-nitrosamines by GC.

Table IV.1.1. Structure and properties of the *N*-nitrosamines considered in this work

Abbr.	Compound Name	CAS Number	Molecular Formula	Structure	Molecular Weight (g/mol)	Boiling Point (ºC) [a]	pK_a [a]	log K_{ow} [a]
NDMA	*N*-Nitrosodimehylamine	62-75-9	$C_2H_6N_2O$		74.08	152	-3.63	-0.496
NMEA	*N*-Nitrosomethylethylamine	624-78-2	$C_3H_8N_2O$		88.11	163	-3.39	-0.014
NDEA	*N*-Nitrosodiethylamine	55-18-5	$C_4H_{10}N_2O$		102.14	176	-3.14	0.523
NDPA	*N*-Nitrosodipropylamine	621-64-7	$C_6H_{14}N_2O$		130.19	206	-3.18	1.542
NDBA	*N*-Nitrosodibutylamine	914-16-3	$C_8H_{18}N_2O$		158.24	116	-3.14	2.561
NPIP	*N*-Nitrosopiperidine	68374-62-9	$C_5H_{10}N_2O$		114.15	219	-3.18	0.438
NPYR	*N*-Nitrosopyrrolidine	930-55-2	$C_4H_8N_2O$		100.12	214	-3.14	-0.089
NMOR	*N*-Nitrosomorpholine	59-89-2	$C_4H_8N_2O_2$		116.12	224	-5.72	-0.594

[a] Data calculated using Advanced Chemistry Development (ACD/Labs) Software V11.02 (© 1994-2018 ACD/Labs)

The hypothesis to be tested is whether a HRMS QTOF instrument can lead to better performance due to its selectivity and overcome the low molecular weight ion interferences problems of low-resolution MS. Although a methodology based on magnetic sector HRMS was already published some years ago[164], we herein would like to demonstrate that GC-QTOF instruments, often used for qualitative purpose[165–167], can compete with such older technologies also for quantitative applications. Therefore, a comparison between IT and QTOF analyzers and both EI and PCI MS ionization sources was performed. Finally, real water samples, including wastewater and tap water, were analyzed to determine the considered compounds with GC-PCI-QTOF after SPE following the US EPA-521 method. The N-nitrosamines considered were those amenable by GC-MS, reported previously in drinking, surface, and wastewater[124,168,169] and included in the US EPA-521 method, i.e., NDMA, NMEA, NDEA, NDPA, NDBA, NPIP, NPYR, and NMOR (**Table IV.1.1**).

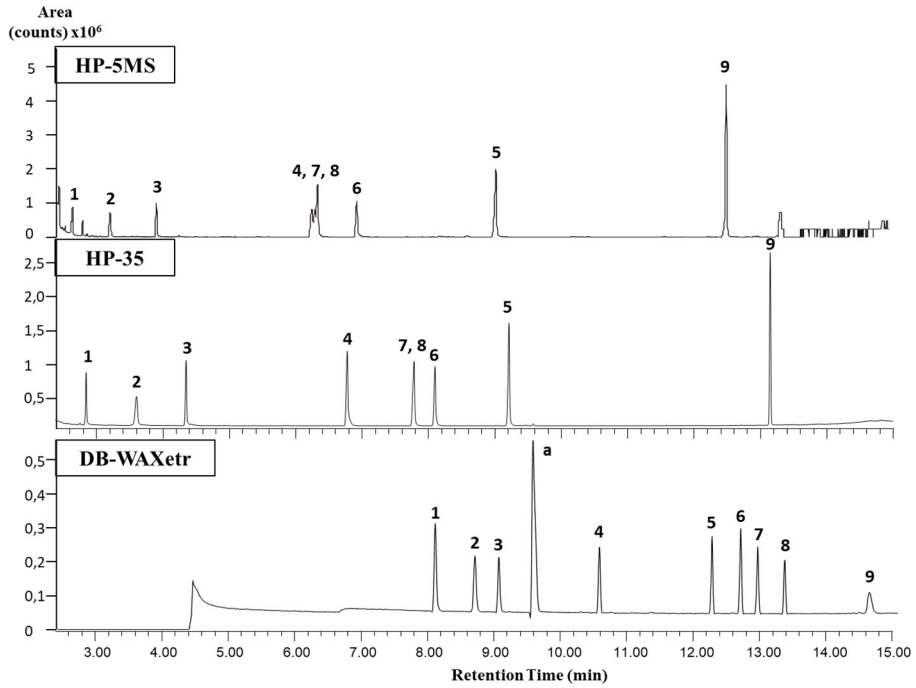

Figure IV.1.1. Total ion chromatograms obtained for the 3 tested capillary columns: (1) NDMA, (2) NMEA, (3) NDEA, (4) NDPA, (5) NDBA, (6) NPIP, (7) NPYR, (8) NMOR, (9) NDPhA, (a) Column bleed

IV.1.1. Capillary column selection

Three different capillary columns were tested using the temperature program described in **Section III.4.1.2** to obtain the best chromatographic separation. In order from less to more polar, the columns were: HP-5MS, HP-35MS, and DB-WAXetr. A 10 µg mL^{-1} mix standard was injected in all three cases. The compounds were identified based on their EI spectra using the NIST library. As shown in **Figure IV.1.1**., by using the HP-5MS capillary column, all compounds eluted before 13 min, with a co-elution of NPYR, NMOR, and NDPA at 6.5 min. Jurado-Sánchez et al. obtained a separation at baseline for seven common N-nitrosamines using the same HP-5MS capillary column, but a longer oven program was used, with a total runtime of 22 min and without the inclusion of NDPA[170].

With the HP-35MS capillary column, a better separation was observed, although NMOR and NPYR co-eluted at 8 min. The DB-WAXetr, which was the most polar and with higher film thickness column, was able to separate all N-nitrosamines at baseline with good peak shapes, without compromising the analysis time and with suitable retention of the most polar and volatile compounds, such as NDMA.

Table IV.1.2. Retention time and quantification (first m/z value) and qualifier ions (subsequent m/z values) used in each system. Relative intensities normalized to the higher m/z value are given in parenthesis.

		GC-IT-MS		GC-QTOF-MS	
Compound	Retention time (min)	EI	PCI	EI	PCI
NDMA	7.6	74 (100) 42 (229) 44 (85)	75 (100) 43 (10) 115 (3)	74.0475 (100) 44.0495 (24)	75.0553 (100) 115.0866 (2)
NMEA	8.3	88 (100) 42 (400) 71 (105)	89 (100) 61 (35) 117 (15)	88.0631 (100) 71.0604 (65)	89.0709 (100) 129.1022 (3)
NDEA	8.7	102 (100) 42 (280) 56 (90)	103 (100) 131 (28) 75 (5)	102.0788 (100) 85.0760 (32)	103.0866 (100) 143.1179 (5)
NDPA	10.2	113 (100) 70 (430) 41 (250)	131 (100) 159 (30) 89 (4)	113.1073 (100) 70.0655 (380)	131.1179 (100) 159.1492 (10)
NDBA	11.9	99 (100) 84 (240) 41 (180)	159 (100) 187 (28) 103 (2)	99.0920 (100) 84.0812 (240)	159.1492 (100) 187.1805 (15)
NPIP	12.3	114 (100) 42 (97) 84 (40)	115 (100) 143 (26) 84 (3)	114.0788 (100) 84.0808 (35)	115.0866 (100) 155.1179 (4)
NPYR	12.5	100 (100) 41 (92) 68 (37)	101 (100) 129 (19) 70 (5)	100.0631 (100) 68.0493 (16)	101.0709 (100) 141.1022 (4)
NMOR	12.9	86 (100) 56 (155) 116 (6)	117 (100) 145 (24) 86 (11)	86.0600 (100) 116.0580 (15)	117.0659 (100) 87.0679 (12)
NDEA-d10	8.7	112	113	112.1415	113.1494
NPYR-d8	12.5	108	109	108.1133	109.1212

IV.1.2. Mass spectrometry

A mix of eight nitrosamines (10 μg mL^{-1} each) was injected in both GC-MS systems with both ionization sources. Selected quantifier and qualifier ions are shown in **Table IV.1.2**. The MS/MS spectra were also recorded using a PCI source and IT analyzer as recommended the US EPA methods[118], but using methane as ionization gas, as the option available in the lab. However, the IDL achieved were far higher (between 4 and 29 times higher) than in single-stage MS mode, so this option was not considered further. In fact, the US EPA method 521 already reports on lower IDL using MS/MS vs. MS, but

recommends its use due to the lower selectivity of the IT-MS being operated in single-stage MS.

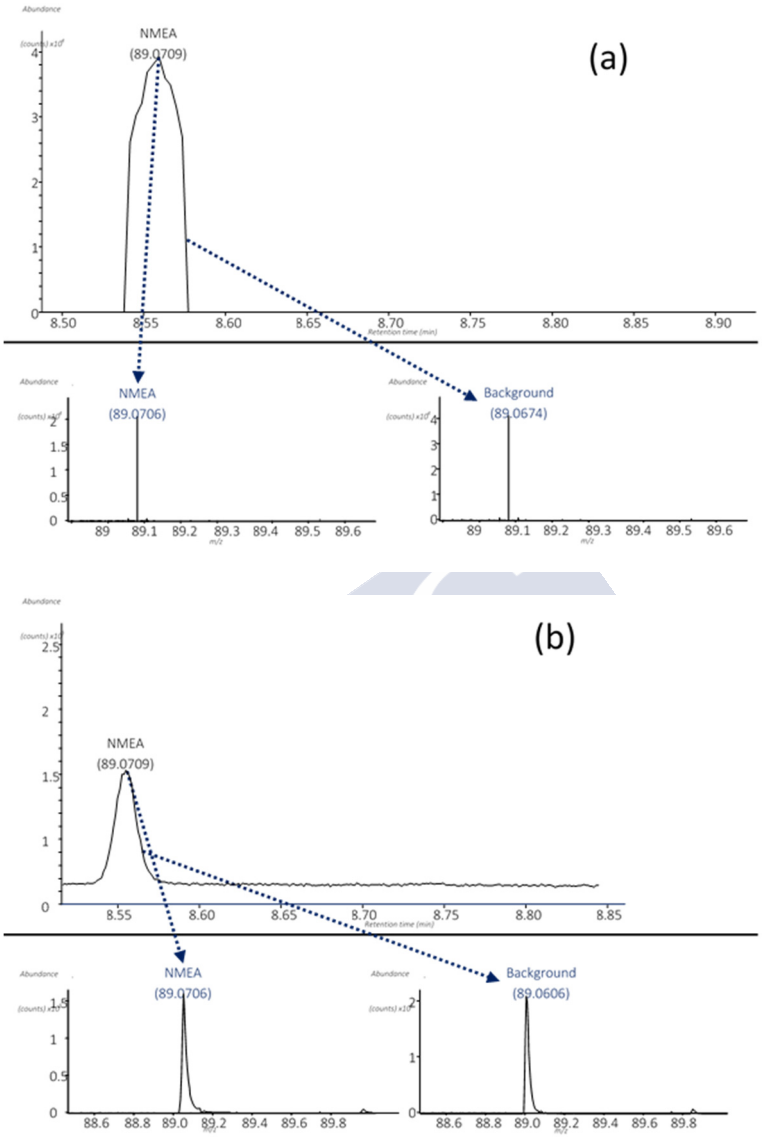

Figure IV.1.2. Isobaric interference for NMEA in PCI acquiring in centroid (a) and profile (b) modes. Extracted ion chromatograms (EIC) with ±50 ppm.

A relevant issue in the GC-TOF-MS system with the PCI source was that a Gaussian profile for the NMEA peak was not observed when the spectra was acquired in centroid mode (**Figure IV.1.2a**), due to an isobaric interference between a background ion at m/z 89.0674 and NMEA with m/z 89.0709. In order to solve this problem, the acquisition mode was switched from centroid to profile mode. Thus, a better peak shape for NMEA was obtained, as shown in **Figure IV.1.2b**. Furthermore, the use of the profile mode of acquisition results in a realistic baseline that can be used to estimate IDLs, since the centroid mode has a cut-off value that results in a flat baseline (there is actually no visible baseline).

IV.1.3. Instrumental performance

The performance for the two GC-MS systems (IT and QTOF analysers) operating with the two different ionization modes (EI and PCI) was evaluated using the following criteria: linearity, repeatability, IDLs, and IQLs. The results are presented in **Table IV.1.3**. The linearity was evaluated with standards at 7–9 different concentration levels (depending on the compound) in the range of IQL-500 ng mL^{-1}, with the IS level remaining at 200 ng mL^{-1}. The peak area divided by the IS peak area was plotted versus concentrations, fitting a linear model with determination coefficients (R^2) higher than 0.991 in both instrument and ionization modes (**Table IV.1.3**). Moreover, the Durbin–Watson statistic tests provided a p-value greater than 0.05 for all N-nitrosamines, indicating no significant correlation in the residuals at the 95% confidence level. The intra-day and inter-day precision were evaluated as IS corrected peak area by injections of a 50 ng mL^{-1} standard mixture, obtaining RSD values below 15% and 16% in all systems, respectively. As shown in the **Table IV.1.3**, GC-IT-MS with EI source provided the highest average intra-day RSD (7%), while the lowest average intra-day RSD was obtained with GC-QTOF-MS with the PCI source (1.6%), with a maximum individual value of 2.2% for NMOR. IDLs and IQLs were estimated as the lowest concentration providing a S/N ratio of 3 and 10, respectively, by direct injection of the lower levels standards of the calibration curve, obtaining the lowest IDLs when the QTOF system with PCI was used (0.2–4 ng mL^{-1}).

IV.1.4. Performance with real samples after SPE

The different GC-MS systems were also compared in terms of overall method LODs (MDLs) and LOQs (MQL) using 500 mL of effluent wastewater as real matrix after the SPE following the US EPA 521 method. As presented in **Table IV.1.4**, GC-PCI-QTOF-MS clearly provided the lowest average MDLs (0.5 ng L^{-1}) and MQLs (1.6 ng L^{-1}), being approximately 1 order of magnitude better than those obtained with the other 3 approaches.

The estimated MDLs obtained by GC-PCI-QTOF were in the range of 0.2 ng L^{-1} (NDEA) - 1.3 ng L^{-1} (NMEA). These values are comparable to those reported in the literature (**Table IV.1.5**). Cheng et al. have reported MDLs, using 500 mL of sample, in the range of 0.3-1.8 ng L^{-1} using SPE and a GC-PCI-MS/MS system using a protocol slightly different from the US EPA-521 method[123]. The US EPA method 521 reported MDLs in the range of 0.3–0.7 ng L^{-1}, also considering a volume of 500 mL and exactly the same SPE protocol but by large-volume injection of 20 µL of extract, then GC-PCI-IT-MS/MS[118]. The proposed GC-PCI-QTOF-MS method can provide MDLs at the same order of magnitude as the US EPA method, by injecting 10 times less extract, thus being a good alternative to that method, particularly considering that IT instruments are losing popularity and using methanol or acetonitrile as reaction gas is not feasible with all instruments. Furthermore, the method proposed here was validated with a more complex matrix than the EPA method (effluent wastewater, see below, Vs. tap water), demonstrating its high selectivity.

Table IV.1.3. GC-MS performance for both instruments using EI and PCI sources

	GC-IT-MS								GC-QTOF-MS							
	EI				PCI				EI				PCI			
	R^2 [a]	%RSD[b]	IDL[c] (ng mL^{-1})	IQL[c] (ng mL^{-1})	R^2 [a]	%RSD[b]	IDL[c] (ng mL^{-1})	IQL[c] (ng mL^{-1})	R^2 [a]	%RSD[b]	IDL[c] (ng mL^{-1})	IQL[c] (ng mL^{-1})	R^2 [a]	%RSD[b]	IDL[c] (ng mL^{-1})	IQL[c] (ng mL^{-1})
NDMA	1.0000	4/6	3	10	0.9997	3/5	3	8	1	2/10	1.3	4	0.9997	1.6/6	1.6	4.9
NMEA	0.9835	15/15	15	50	0.9984	8/11	15	50	0.999	11/13	5.6	19	0.9993	1.8/10	4	11
NDEA	1.0000	5/4	3	8	0.9998	7/4	5	17	0.999	1/2	2	5.9	0.9997	1.5/10	0.3	0.9
NDPA	1.0000	5/5	2	7	0.9986	4/2	3	8	1	4/2	4.8	16	0.9998	1.7/10	0.2	0.6
NDBA	0.9997	5/11	1	9	0.9997	8/5	15	50	0.999	5/8	8.8	29	0.9992	1.4/7	1	2
NPIP	0.9995	4/5	1	3	0.9991	6/3	1	3	0.999	4/1	1.1	3.4	0.9993	1.7/12	1	1.2
NPYR	0.9998	7/5	1	4	0.9986	8/3	1	3	0.999	5/10	1.3	4	0.9993	1.1/6	0.3	0.8
NMOR	0.9994	9/16	3	8	0.9992	3/3	2	6	0.998	3/6	19	63	0.9998	2.2/8	1	2.8
average	0.9978	7/8	3.6	12.4	0.9991	6/5	5.6	18.1	0.999	4/7	5.4	17.5	0.9995	1.6/9	1.2	3

[a] R^2, Linearity is expressed by the determination coefficient in the range of IQL-500 ng mL^{-1}

[b] %RSD, intra-day / inter-day (over a three-weeks period) precision expressed as the RSD (%) (n=6) at the 50 ng mL^{-1} level

[c] IDLs and IQLs were estimated at a S/N of 3 and 10, respectively

Table IV.1.4. MDLs, MQLs , accuracy, expressed as recoveries (R %), intra-day precision, expressed as RSD, and mass accuracy (average error in mDa), obtained from a spiked (10 ng L^{-1} and 200 ng L^{-1}) wastewater effluent sample.

	MDLs (ng L^{-1})				MQLs (ng L^{-1})				R %		RSD %		Mass accuracy (mDa)	
									10 ng L^{-1}	200 ng L^{-1}	10 ng L^{-1}	200 ng L^{-1}	10 ng L^{-1}	200 ng L^{-1}
	GC-IT-MS		GC-QTOF-MS		GC-IT-MS		GC-QTOF-MS		GC-QTOF-MS					
	EI	PCI	EI	PCI	EI	PCI	EI	PCI	PCI					
NDMA	7.2	1.3	1.7	0.4	22	3.9	5.1	1.2	119	62	3.2	5.2	0.2	0.15
NMEA	20	24	2.2	1.3	60	72	6.6	3.9	65	66	0.75	6.5	0.35	0.9
NDEA	2	1.8	1.2	0.2	6	5.4	3.6	0.6	119	89	2.1	5.2	0.2	0.1
NDPA	5.8	7.6	3.9	0.4	17	23	11.7	1.2	101	109	5.6	4.2	0.32	0.13
NDBA	12	6.7	5.4	0.6	36	20	16.2	1.8	107	113	5.1	4.6	0.35	0.35
NPIP	3.6	1.2	1	0.4	11	3.6	3	1.2	117	106	2.1	2.5	0.2	0.55
NPYR	4.8	1.2	3.9	0.4	14	3.6	11.7	1.2	118	105	4.5	6.7	0.65	0.45
NMOR	10	3.9	22	0.6	30	12	66	1.8	92	106	0.97	5	0.52	0.7
average	8.2	6	5.2	0.5	25	18	15.5	1.6	105	95	3	5	0.35	0.42

Table IV.1.5. Compilation of MDLs reported in the literature for the determination of N-nitrosamines in water

Reference	164	121	118	172	123	171	122	170	119	124	120
Sample Preparation	SPE	SPE		SPE	SPE	SPE	SPE	SPE	SPE	SPME	SPME
Detection Techniques	GC-EI-Magnetic Sector	GC-EI-MS/MS (TQ)	GC-PCI-MS/MS (IT)	GC-EI-MS/MS (TQ)	GC-PCI-MS/MS (IT)	LC-ESI-MS/MS (Orbitrap)	LC-ESI-MS/MS (QTRAP)	GC-EI-MS (Q)	GC-PCI-MS/MS (IT)	GC-PCI-MS/MS (IT)	GC-PCI-MS/MS (TQ)
NDMA	0.8	1.1	0.3	0.5	0.8	0.4	3.1	10	1	5	30
NMEA	0.6	1.8	0.3	0.6	1.4	0.9	2.4	Not avail.	1.9	4	90
NDEA	0.1	1.6	0.3	0.9	1.8	0.7	10.6	3	1.4	3	64
NDPA	0.2	2.3	0.3	0.8	1.6	0.8	0.2	Not avail.	1.4	2	59
NDBA	0.1	3.1	0.4	1.7	1.6	3.3	3.1	13	2.7	1	79
NPIP	0.1	2.2	0.7	0.9	1.4	0.1	0.9	4	1.1	5	59
NPYR	0.2	1.7	0.4	1.2	0.8	1	2.1	12	1.5	1	Not avail.
NMOR	1.7	1.9	Not avail.	0.7	1.4	0.2	0.2	7	0.8	4	138

LC: liquid chromatography; QTRAP: Linear Ion Trap; Q: quadrupole; TQ: Triple quadrupole

Accuracy and precision of the overall method were assessed using effluent water, spiked at 10 ng L^{-1} and 200 ng L^{-1} only with the GC-PCI-QTOF system, as to verify its performance before its application to real samples. A chromatogram of an effluent water sample spiked at 10 ng L^{-1} is shown in **Figure IV.1.3**. Results are shown in **Table IV.1.4**, in which all compounds show recoveries in the range of 90 - 120%, except for NDMA and NMEA, with relative standard deviations below 7% and mass accuracies exhibiting an error below 1 mDa.

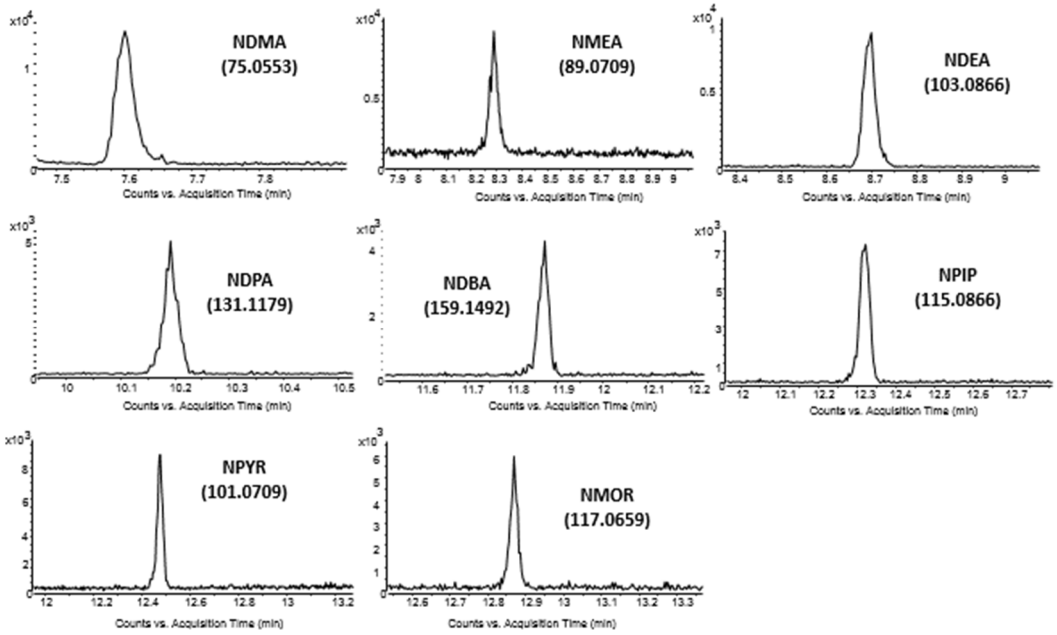

Figure IV.1.3. Extracted ion chromatogram (±50 ppm) for an effluent water sample spiked at 10 ng L^{-1}

IV.1.5. Analysis of real samples

Finally, the GC-PCI-QTOF method was used for the analysis of real samples after SPE. The samples considered were 2 wastewater effluent (n=3) and 2 wastewater influent (n=3), both of them collected as grab samples in two different days; and 3 tap water (n=3) collected at three different times of the same day. Samples were analyzed as explained in **section III.4.1** and the levels detected are presented in **Table IV.1.6**, with RSD values below 20%.

In drinking water, three nitrosamines (NDMA, NMOR and NDBA) were found in all analyzed samples, while NPIP and NDEA were found in two of them, at concentrations ranging between 1.5 and 9 ng L^{-1}. These levels are in agreement with those found in the literature in tap and treated drinking water, usually less than 10 ng L^{-1} [168,173,174]. These levels would be below the 10 ng L^{-1} reporting level set by the authorities of California[117] and far below the 100 ng L^{-1} level considered as guideline value by the WHO for NDMA in drinking water[116].

NDMA, NDEA, NMOR and NDBA were the compounds found in the wastewater samples analyzed with concentrations ranging from 2.6 to 27 ng L^{-1}. The levels found were lower than those reported in the literature by Llop et al. i.e. levels ranging from 11 ng L^{-1} (NDPA) to 139718 ng L^{-1} (NMOR)[124], or those high (up to 5000 ng L^{-1}) and variable concentrations of NDMA reported in effluents of three WWTPs by Zhou et al.[175]. However, they are similar to those reported by Krauss et al. in WWTPs from Switzerland, where in primary effluents, NDMA, NMOR, NDBA, NPIP and NDEA were found at concentrations typically in the range 5–25 ng L^{-1} while in the secondary effluent NDMA concentrations were usually lower than 10 ng L^{-1} [169].

Table IV.1.6. Concentrations (ng L^{-1}) ± standard deviation found in real samples collected during two different days (1 and 2). Sampling times are indicated between parentheses for tap water samples collected in the same day. NMEA, NPYR and NDPA were <MDL in all samples.

	NDMA	NDEA	NPIP	NMOR	NDBA
Influent wastewater (1)	4.6 ± 0.5	< MDL	< MDL	< MDL	< MDL
Influent wastewater (2)	27 ± 2	15.1 ± 0.6	< MDL	< MDL	< MDL
Effluent wastewater (1)	4.4 ± 0.1	2.8 ± 0.2	< MDL	2.7 ± 0.5	3.1 ± 0.4
Effluent wastewater (2)	2.6 ± 0.3	3.35 ± 0.05	< MDL	3.0 ± 0.2	8 ± 1
Tap water (8:45 h)	2.2 ± 0.2	2.8 ± 0.1	< MDL	1.72 ± 0.01	7.1 ± 0.2
Tap water (12:30 h)	5 ± 1	4.5 ± 0.7	2.7 ± 0.3	2.4 ± 0.3	9 ± 1
Tap water (15:45 h)	1.5 ± 0.2	< MDL	1.8 ± 0.1	1.8 ± 0.3	4.3 ± 0.7

IV.2. Reaction of Phenazone-type drugs and metabolites with chlorine and monochloramine

USC
UNIVERSIDADE
DE SANTIAGO
DE COMPOSTELA

The aim of this work was to investigate the reaction of aminopyrine and metamizole metabolites (AA, FAA and AAA) with chlorine and the reaction of Phe, PrPhe and metamizole metabolites with monochloramine (**Table IV.2.1**).

Although in some countries the use of metamizole has been banned (eg. USA or UK) or regulated (e.g. Belgium)[176], in other countries it is still available by prescription and available over the counter in yet others. In Spain, the sales of metamizole during the last 10 years have been increased a 67% in the last decade (from 3.28 in 2010 to 5.48 in 2019 DDD per 1000 inhabitants per day)[177]. Several investigations have shown some evidence that these substances are not completely eliminated during wastewater treatment[81,85,178]. Hence, they may also reach groundwater aquifers or surface water[76] which are finally a source of drinking water[179,180]. In the case of phenazone-type drugs, photodegradation[181], ozonation[182,183], UV/chloramine treatment[184] and mainly chlorination[128,185,186] have been previously reported while for the metabolites few studied have been published dealing with ozonation[182] and photochemical treatment[181]. However, metabolites reaction with chlorine has not been studied so far.

Table IV.2.1. Physico-chemical properties of phenazone-type drugs and metabolites considered in this work

Structure	Compounds (abbreviation)	R	log P[a]	pK$_a$[a]
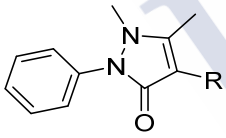	Phenazone (Phe)	H	0.44	0.65 (basic)
	Propyphenazone (PrPhe)	$CH(CH_3)_2$	1.72	1.46 (basic)
	4-Aminoantipyrine (AA)	NH_2	-0.26	4.07 (basic)
	4- Formylaminoantipyrine (FAA)	NHCHO	-0.06	1.07 (basic) 12.72 (acid)
	4-Acetoamidoantipyrine (AAA)	$NHCOCH_3$	-0.89	1.07 (basic) 12.84 (acid)

[a] Data calculated using Advanced Chemistry Development (ACD/Labs) Software V11.02 (© 1994-2018 ACD/Labs)

For those compounds reacting to a significant degree, the pH and, also bromide content in the case of chlorination, were also considered. Further, TPs were tentatively identified by LC-HRMS. Finally, a preliminary ecotoxicity estimation of the TPs was performed by QSAR using both the T.E.S.T. and ECOSAR software from the US EPA as detailed in **III.4.8.1**.

IV.2.1. Preliminary experiments

Preliminary chlorination and chloramination tests were performed in order to assess the reactivity of the selected compounds in presence of chlorine and monochloramine.

Table IV.2.2: Pseudo-first order rate constants (k') (s^{-1}) obtained during chlorination and chloramination experiments.

	10 µg mL^{-1} Cl_2				4 µg mL^{-1} NH_2Cl		
	0 ng mL^{-1} Br^-			100 ng mL^{-1} Br^-			
pH	**5.7**	**7**	**8.3**	**7**	**5.7**	**7**	**8.3**
Phe	0.77[a]	0.39 [a]	0.17 [a]	0.69 [a]	$9.97x10^{-5} \pm 6x10^{-6}$	$1.31x10^{-5} \pm 3x10^{-7}$	$3.06x10^{-6} \pm 1x10^{-7}$
PrPhe	1.73 [a]	1.39 [a]	0.77 [a]	0.63 [a]	$3.09x10^{-4} \pm 2x10^{-5}$	$3.25x10^{-5} \pm 3x10^{-7}$	$6.67x10^{-6} \pm 4x10^{-7}$
AA	0.18 ± 0.06	0.19 ± 0.06	0.20 ± 0.07	0.14 ± 0.05	$1.05x10^{-3} \pm 1x10^{-4}$	$1.64x10^{-4} \pm 2x10^{-5}$	$4.86x10^{-5} \pm 3x10^{-6}$
FAA	$1.36x10^{-2} \pm 5x10^{-4}$	$1.32x10^{-2} \pm 1x10^{-4}$	$1.17x10^{-2} \pm 1x10^{-4}$	$5.78x10^{-2} \pm 5x10^{-3}$	-	-	-
AAA	$2.75x10^{-2} \pm 2x10^{-3}$	$1.60x10^{-2} \pm 8x10^{-4}$	$4.16x10^{-3} \pm 4x10^{-5}$	$6.93x10^{-2} \pm 7x10^{-3}$	-	-	-

[a] Values from.Rodil et. al[185]

Since Phe and PrPhe chlorination had been previously investigated in our lab[185], and considering the similarity in terms of structure of AA, FAA and AAA, chlorination was performed under similar conditions, with 10 µg mL^{-1} of free chlorine in 10 mL of ultrapure water at neutral pH (7) containing 1 µg mL^{-1} of compound (AA, FAA or AAA). After 30 min, AA, AAA and FAA were completely removed.

Chloramination reactions for Phe, PrPhe, AA, AAA and FAA were performed by using 1 µg mL^{-1} of each compound in 10 mL of ultrapure water at neutral pH with 4 µg mL^{-1} of NH_2Cl. After 72 h, Phe, PrPhe and AA were completely removed, while for AAA and FAA signal decrease was below 10%. So, AAA and FAA were deemed stable and their chloramination was no further studied.

IV.2.2. Reaction kinetics

The influence of the pH over the reaction kinetics was studied considering three levels, i.e. pH 5.7, 7 and 8.3. Aliquots were taken at different reaction times from 0 to 5 min for chlorination and up to 72 h for chloramination. The ratio of the area obtained at a certain time divided by those obtained at time 0, against the reaction time were fitted to an exponential model, where the exponent is the pseudo-first order velocity constant (k') (values compiled in **Table IV.2.2**, examples of the fittings presented in **Figure IV.2.1**), from which the second order constant (k) was also determined (**Table IV.2.3**). Then, half-lives were calculated as $t_{1/2} = \ln 2/k'$ (**Table IV.2.4**).

Table IV.2.3. Second-order rate constants (k) (M^{-1} s^{-1}) obtained during chlorination and chloramination experiments.

	10 µg mL^{-1} Cl_2				4 µg mL^{-1} NH_2Cl		
	0 ng mL^{-1} Br^-			100 ng mL^{-1} Br^-			
pH	**5.7**	**7.0**	**8.3**	**7.0**	**5.7**	**7.0**	**8.3**
Phe	$5.47x10^3$ [a]	$2.73x10^3$ [a]	$1.20x10^3$ [a]	$4.92x10^3$ [a]	1.3	0.17	0.04
PrPhe	$1.23x10^4$ [a]	$9.85x10^3$ [a]	$5.47x10^3$ [a]	$4.48x10^3$ [a]	4.1	0.42	0.09
AA	$1.31x10^3$	$1.37x10^3$	$1.41x10^3$	$9.85x10^2$	14	2.11	0.63
FAA	97	94	83	410	-	-	-
AAA	195	114	30	492	-	-	-

[a] Values from Rodil et al.[185]

Table IV.2.4. Chlorination and chloramination half-lives (compounds concentration: 1 µg mL^{-1}), calculated from k' values presented in Table IV.2.2.

	10 µg $mL^{-1}Cl_2$ ($t_{1/2}$ in s)				4 µg mL^{-1} NH_2Cl ($t_{1/2}$ in h)		
	0 ng mL^{-1} Br^-			100 ng mL^{-1} Br^-			
pH	**5.7**	**7.0**	**8.3**	**7.0**	**5.7**	**7.0**	**8.3**
Phe	0.9[a]	1.8 [a]	4.1 [a]	1 [a]	1.9 ± 0.1	14.7 ± 0.3	63.9 ± 2
PrPhe	0.4 [a]	0.5 [a]	0.9 [a]	1.1 [a]	0.6 ± 0.04	5.9 ± 0.05	29.3 ± 1.8
AA	3.7 ± 1.2	3.6 ± 1.1	3.5 ± 1.2	5 ± 1.8	0.2 ± 0.02	1.2 ± 0.1	3.9 ± 0.2
FAA	50 ± 2	52 ± 0.4	59 ± 0.5	12 ± 1	-	-	-
AAA	25 ± 2	43 ± 2	163 ± 2	10 ± 1	-	-	-

[a] Values from Rodil et al.[185]

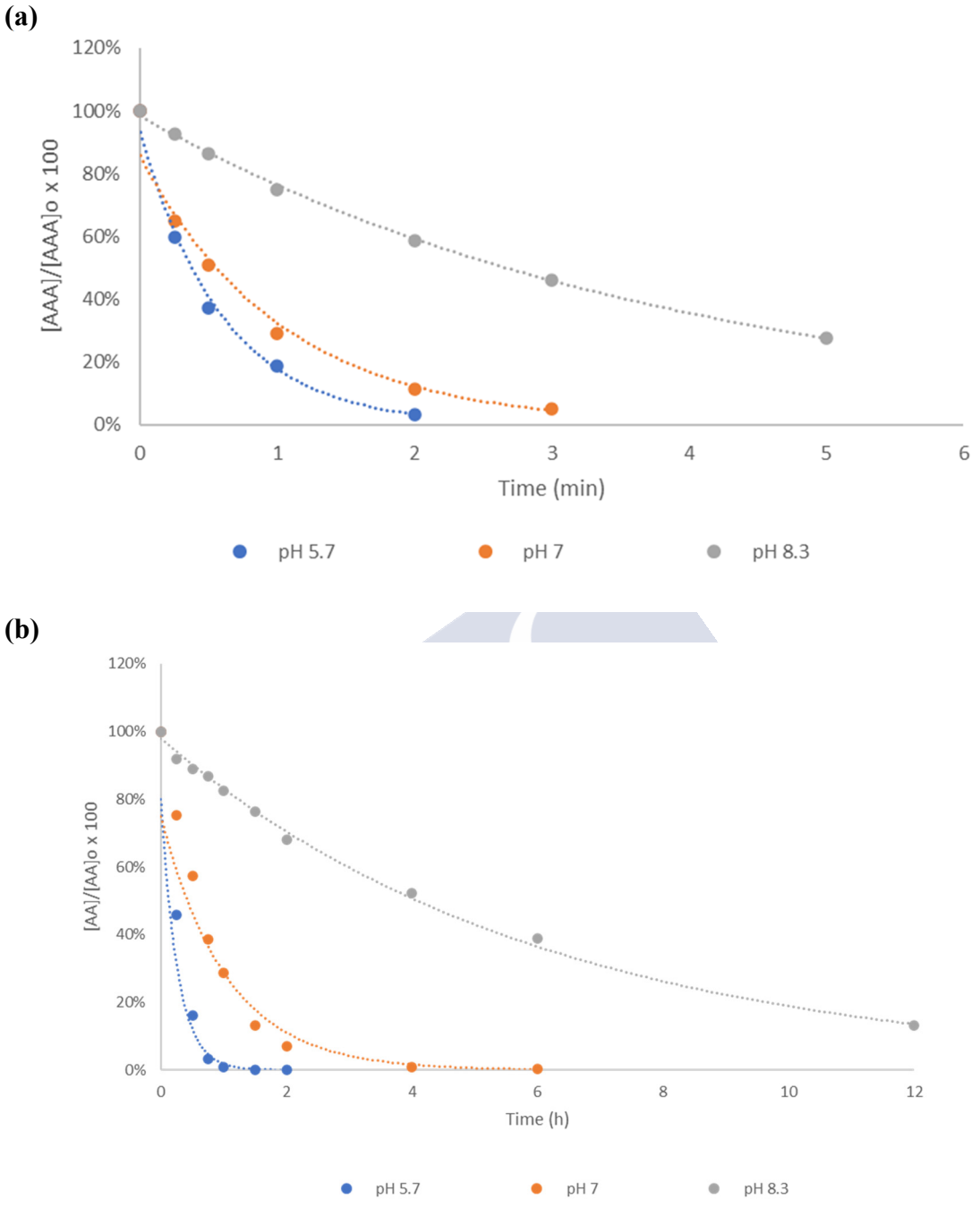

Figure IV.2.1. Reaction kinetics plots at different pH values, for (a) AAA with chlorine and (b) AA with monochloramine.

Phe, PrPhe and AA reaction with chlorine is faster than in the case of AAA and FAA (**Table IV.2.3**), which may explain why these last two chemicals did not significantly react with monochloramine. Furthermore, as shown in **Table IV.2.3**, reaction kinetics are significantly faster with HClO than NH_2Cl, e.g. k at pH 7 with HClO were between 97 and 63,000 times higher than with NH_2Cl. When bromide was added in chlorination experiments, a Student's t test showed no statistically significantly different half-lives as

compared to samples that did not contain such anion for AA (p-value 0.3144) (**Table IV.2.4**), similarly to what has been previously observed for Phe and PrPhe[185]. On the other hand, AAA and FAA showed statistically faster reactions with bromide (Student's t test p-values $1.4x10^5$ and $3.5x10^7$, respectively). This may be due to the fact that Phe, PrPhe and AA kinetics are comparatively faster, not allowing time for HBrO being formed.

As regards the pH (**Table IV.2.4**), its effect on the $t_{1/2}$ on the reaction of AA with HClO was not statistically significant (ANOVA p-value 0.9783), whereas statistically significant differences were observed over the reaction of AAA and FAA (ANOVA p-values <0.0001), as for Phe and PrPhe[185], being the reaction faster at lower pH values (**Figure IV.2.1a**). This could be explained by the speciation of HOCl/ClO^-, considering that HOCl is a much more electrophilic than ClO^-, which could be counterbalanced by the speciation of the primary amine moiety only present in AA structure. On the other hand, chloramination of Phe, PrPhe and AA was affected by the pH (ANOVA p-values < 0.0001), being faster at lower pH values (**Figure IV.2.1b**). This could be attributed, as mentioned in the literature[187,188], to monochloramine auto-decomposition at lower pH values leading to the formation of dichloramine and HOCl.

IV.2.3. Transformation products

A summary of the detected TPs (proposed formulas, mass errors and scores) is shown in **Table IV.2.5** (Phe and PrPhe) and **Table IV.2.6** (AA, AAA and FAA).

Table IV.2.5. LC-QTOF data on TPs identification in Phe and PrPhe chloramination experiments.

Experimental m/z	t_R (min)	Proposed formula	Difference (ppm / mDa)	Score (%)	TPs identification[a]
189.1023	10.07	$C_{11}H_{12}N_2O$	0.32 / 0.06	99.98	Phe
223.0634	10.76	$C_{11}H_{11}N_2OCl$	1.95 / 0.43	99.16	Cl-Phe
209.0486	8.82	$C_{10}H_9N_2OCl$	4.72 / 0.98	95.62	Cl-Phe-Me
239.0589	7.99	$C_{11}H_{11}N_2O_2Cl$	3.02 / 0.72	97.84	Cl, OH-Phe
225.0432	10.05	$C_{10}H_9N_2O_2Cl$	3.11 / 0.71	95.23	Cl, OH-Phe-Me
261.0192	10.45	$C_{10}H_{10}N_2O_2Cl_2$	-0.04 / -0.01	100.00	Cl_2, OH-Phe-Me
275.0349	11.99	$C_{11}H_{12}N_2O_2Cl_2$	-2.77 / -0.76	97.85	Cl_2, OH-Phe
231.1497	12.43	$C_{14}H_{18}N_2O$	2.22 / 0.51	98.97	PrPhe
247.1447	10.82	$C_{14}H_{18}N_2O_2$	2.42 / 0.60	98.54	OH-PrPhe
265.1548	12.24	$C_{14}H_{21}N_2O_3$	0.50 / 0.13	99.93	$(OH)_2$-PrPhe
281.1500	11.60	$C_{14}H_{20}N_2O_4$	1.49 / 0.42	99.36	$(OH)_3$-PrPhe
265.1111	12.62	$C_{14}H_{17}N_2OCl$	-0.40/-1.50	99.39	Cl-PrPhe
299.0736	13.59	$C_{14}H_{16}N_2OCl_2$	7.90 / 2.35	83.92	Cl_2-PrPhe

[a] Previously reported and identified in chlorination experiments by Rodil et al.[185] except Cl-PrPhe

Table IV.2.6. List of AA, FAA and AAA TPs detected during chlorination experiments and LC-QTOF identification data.

TPs	Precursor	t_R (min)	Experimental m/z	Proposed formula	Calculated m/z	Error (mDa)	Mass error (ppm)	DBE	Score
AAA	-	9.81	246.1229	$C_{13}H_{15}N_3O_2$	246.1237	0.8	3.28	8	97.4
FAA	-	9.49	232.108	$C_{12}H_{13}N_3O_2$	232.1081	0.05	0.23	8	100
AA	AAA, FAA	11.39	204.1131	$C_{11}H_{13}N_3O$	204.1131	0.04	0.19	7	100
TP-208	AA, AAA, FAA	10.89	208.1084	$C_{10}H_{13}N_3O_2$	208.1084	-0.35	-1.67	6	99.4
TP-194	AA, AAA, FAA	9.98	194.0922	$C_9H_{11}N_3O_2$	194.0921	0.3	1.57	6	99.5
TP-191	AA, AAA, FAA	10.17	191.0819	$C_{10}H_{10}N_2O_2$	191.0819	-0.4	-2.08	7	99.2
TP-166	AA, AAA, FAA	10.16	166.097	$C_8H_{11}N_3O$	166.0983	0.49	2.96	5	98.7
TP-165	AA, AAA, FAA	10.19	165.1023	$C_9H_{12}N_2O$	165.1022	-0.06	-0.37	5	100

Phe and PrPhe chlorination TPs have already been described by Rodil et al.[185], so only chloramination TPs were investigated here. Chloramination of Phe and PrPhe yielded six and five TPs, respectively (**Table IV.2.5**). All TPs were the same as those reported during chlorination[185], excepting Cl-PrPhe, which could not be detected in such former work. This could be due to the much faster chlorination kinetics, so that this TP undergoes a rapid reaction with chlorine to yield other TPs. The spectrum of Cl-PrPhe is presented in **Figure IV.2.2**, whereas for the remaining chloramination TPs, spectra have already been published[185]. Also, similarly to chlorination, Cl-Phe and OH-PrPhe are the main TPs produced by chloramination from Phe and PrPhe, respectively (**Figure IV.2.3a** and **IV.2.3b**)[185].

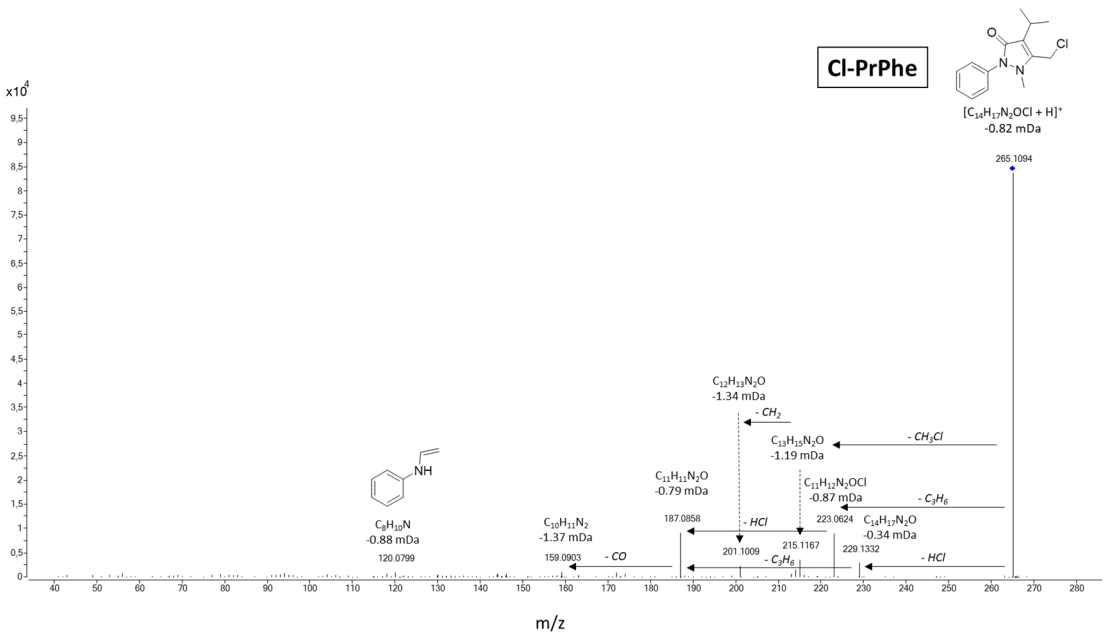

Figure IV.2.2: QTOF product ion spectrum of Cl-PrPhe

As regards AA, FAA and AAA, a summary of the TPs detected during chlorination is presented in **Table IV.2.6** (HRMS data) and **Figure IV.2.4** (proposed structures). Six TPs were identified, five of them being common for the 3 compounds and the remaining one being AA (TP-204), produced during AAA and FAA chlorination as an initial N-hydrolysis step (**Figure IV.2.4**). As it can be observed in **Table IV.2.6**, the empirical formula could be proposed with a high degree of certainty, with score values higher than 97% and mass errors lower than 5 ppm. The proposed structures shown in **Figure IV.2.4** are based on the interpretation of the MS/MS spectra which are presented in **Figure SIV.2.1** as an Annex section **(IV.2.6)**. Besides AA, one product (TP-191) presents a DBE (double-bond equivalents) of 7 (**Table IV.2.6**). This TP is produced by substitution of the primary amine by a hydroxy group and demethylation of AA (**Figure IV.2.4**). On the other hand, the remaining TPs present lower DBE values due to pyrazole ring opening. TP-166 and TP-208 showed similar MS/MS spectra (**Figure SIV.2.1g** and **SIV.2.1d**), with the only difference of the first loss of C_2H_2O in the case of TP-208, corresponding to a ketone group.

This loss is also observed for TP-165 (**Figure SIV.2.1h**), which also possess a ketone group. On the other hand, TP-194 spectrum (**Figure SIV.2.1e**) exhibits a loss of CO, typical of an aldehyde. Only one of these TPs, TP-165, has been reported previously in ozonation and photodegradation studies, for which two different structures were proposed: 2-methyl-1-phenylhydrazide acetic acid[189] and 1-methyl-2-phenylhydrazide acetic acid[179,181,182,190]. Unfortunately, its MS/MS spectrum was not reported in any of these publications. In this work, we propose the first one, 2-methyl-1-phenylhydrazide acetic acid, as the most probable structure, as it is more compatible with the precursor structure, though the MS/MS spectrum is not conclusive (**Figure SIV.2.1h**). The chlorination time-profile plot representing the formation of TPs is presented in **Figure IV.2.5**, where the most intense product for FAA and AAA is in fact AA, followed by TP-208 and TP-165 (being the most intense products observed during AA chlorination).

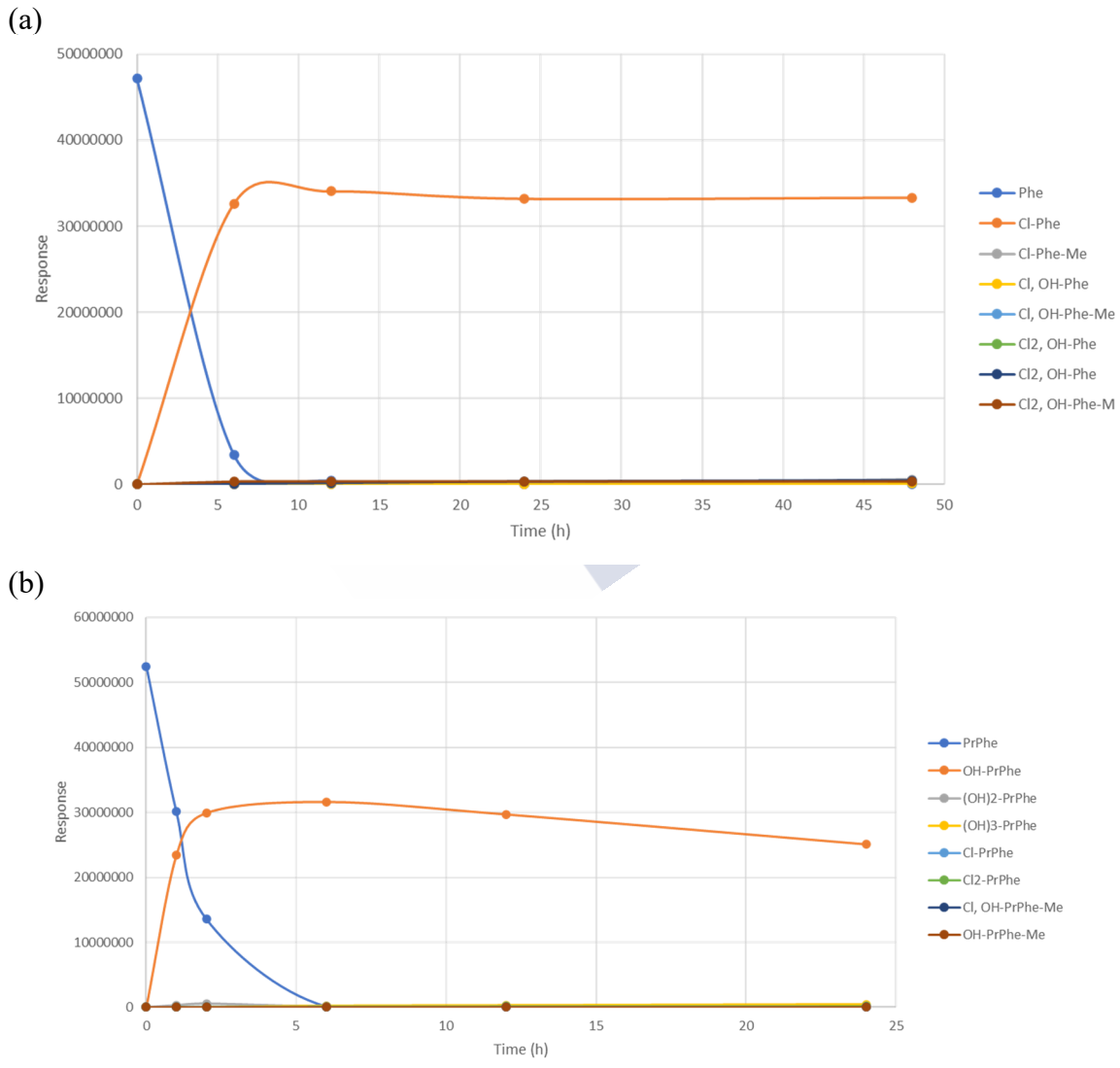

Figure IV.2.3: Time course of TPs formation (MS response) during chloramination of (a) Phe and (b) PrPhe. Conditions: 4 μg mL^{-1} (0.0777 mM) of monochloramine, 1 μg mL^{-1} (4-5 μM) of Phe/PrPhe, and pH 5.7.

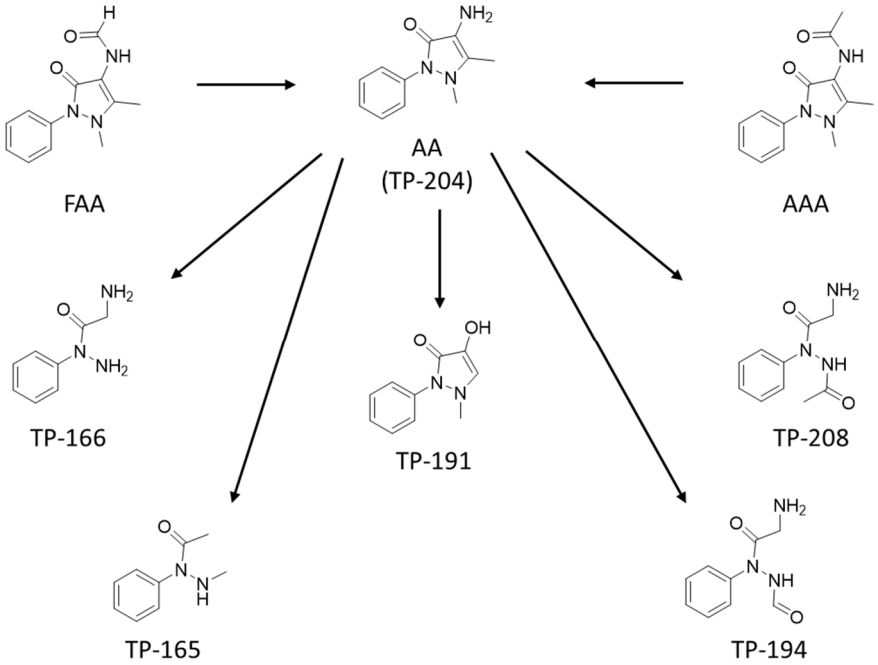

Figure IV.2.4: Proposed reaction pattern of metamizole metabolites during chlorination.

In the case of AA chloramination, the same 5 TPs obtained during chlorination were observed. However, the formation profile of the TPs along time is different, the main product being by far TP-165 (**Figure IV.2.6**).

IV.2.4. Reaction on real samples matrices

Chlorination and chloramination reactions were also studied with two real water samples, one with low anthropogenic impact (creek) and one impacted from a wastewater discharge (river). AA, AAA and FAA reaction with chlorine in creek (pH 6.5) and river (pH 5.8) water showed no statistically different half-lives (Student's t test p-values >0.1590) than in ultrapure water at pH 7 and 5.7 respectively, and the reaction was complete for the three compounds (**Table IV.2.7**). Furthermore, four of the six TPs were detected in the samples, and only TP-166 and TP-165 were not observed during chlorination in real samples.

Phe and PrPhe reaction with monochloramine was slower in real samples (Student's t-test p-values <0.0088), with apparent half-lives slightly higher in creek water (17.5 and 7.6 h, respectively) and significantly higher in river water (27 and 21 h, respectively, **Table IV.2.7**) than those obtained in ultrapure water at similar pH (7 and 5.7, respectively, **Table IV.2.4**). Moreover, even at longer times (up to 72 h) reaction was not complete and about 70% and 45% Phe and PrPhe remained in solution, respectively. Regarding TPs, only Cl-Phe and Cl-Phe-Me were detected for Phe, and OH-PrPhe and OH_2-PrPhe for PrPhe (**Table IV.2.7**).

(a)

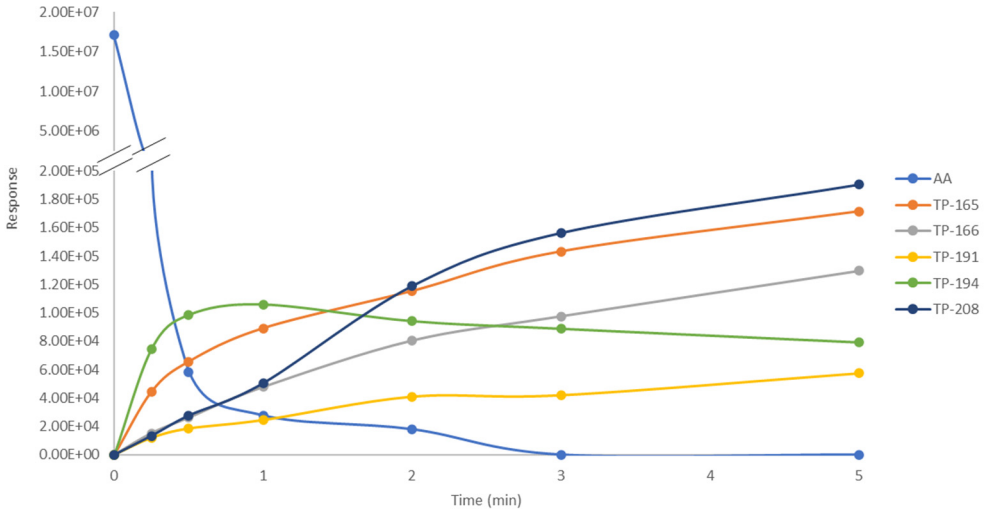

(b)

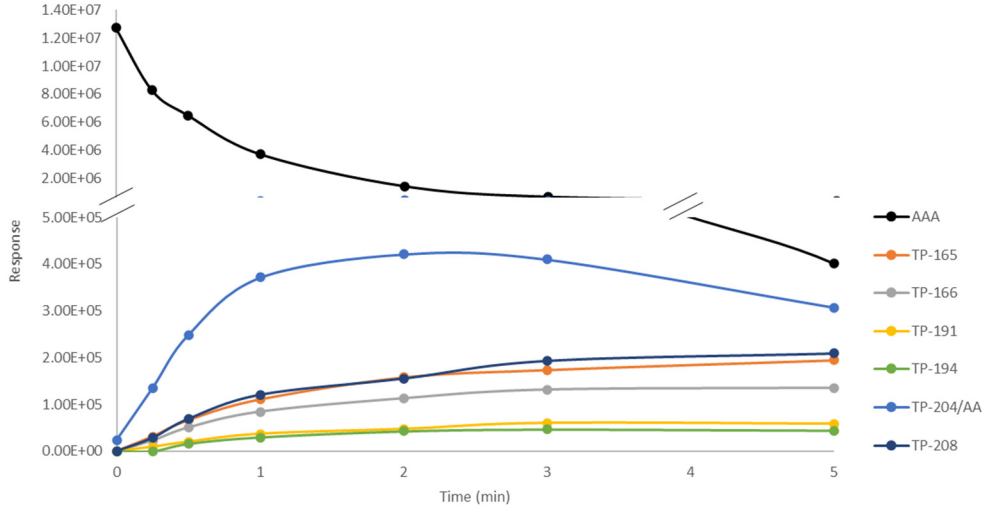

(c)

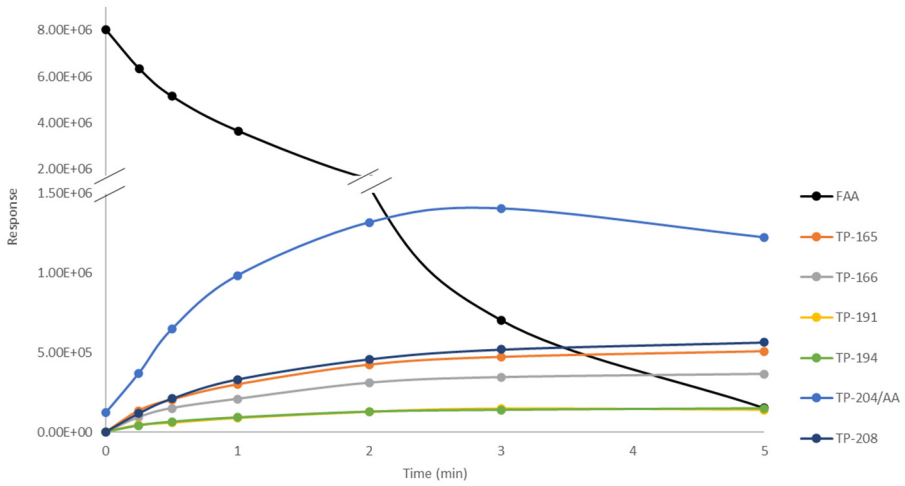

Figure IV.2.5 Time course of TPs formation during chlorination for (a) AA, (b) AAA and (c) FAA. Conditions: 10 µg mL^{-1} (0.141 mM) of free chlorine, 1 µg mL^{-1} (4-5 µM) of AA/AAA/FAA, and pH 7.

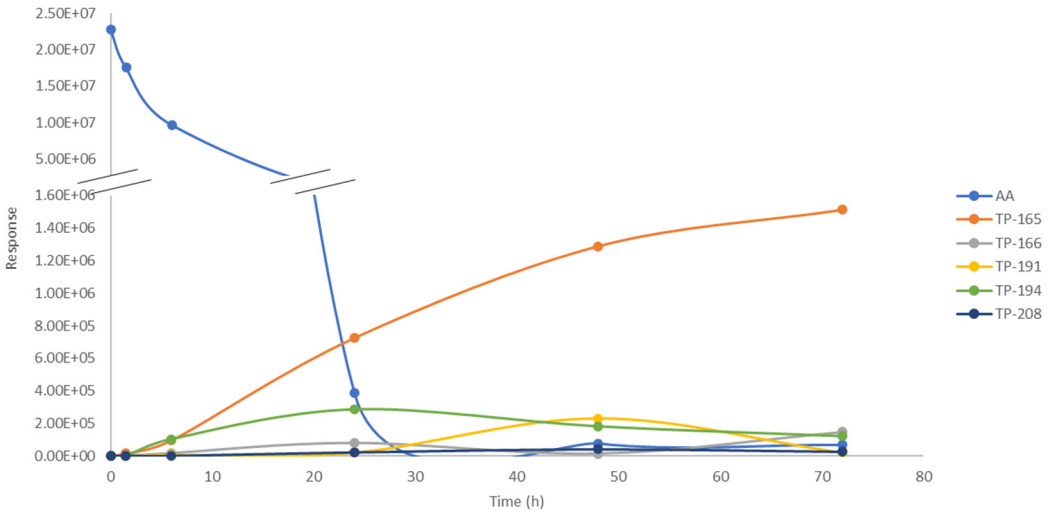

Figure IV.2.6: Time course of TPs formation during chloramination for AA. Conditions: 4 μg mL^{-1} (0.0777 mM) of monochloramine, 1 μg mL^{-1} (4-5 μM) of AA, and pH 5.7.

Table IV.2.7: Half-lives obtained in real water samples spiked with 1 μg mL^{-1} of the phenazone-type drugs and metabolites and 10 μg mL^{-1} of free chlorine or 4 μg mL^{-1} of monochloramine, and TPs observed.

		10 μg mL^{-1} Cl_2 ($t_{1/2}$ in s)		4 μg mL^{-1} NH_2Cl ($t_{1/2}$ in h)	
Precursor		**Creek**	**River**	**Creek**	**River**
Phe		-[a]	-[a]	17.5 ± 1	27 ± 5
PrPhe		-[a]	-[a]	7.6 ± 0.3	21 ± 7
AA		4.0 ± 0.4	6.3 ± 0.6	17 ±0.6	2.6 ± 0.3
FAA		58 ± 6	51 ± 5	-	-
AAA		47 ± 5	25 ± 1.6	-	-
		10 μg mL^{-1} Cl_2 TPs		4 μg mL^{-1} NH_2Cl TPs	
Precursor	**TP**	**Creek**	**River**	**Creek**	**River**
Phe	**Cl-Phe**	Yes[a]	Yes[a]	Yes	Yes
	Cl-Phe-Me	Yes[a]	No[a]	No	Yes
PrPhe	**OH-Prophe**	No[a]	Yes[a]	Yes	Yes
	$(OH)_2$-Prophe	Yes[a]	Yes[a]	Yes	Yes
AA	**TP-191**	Yes	Yes	No	No
	TP-194	No	No	Yes	Yes
	TP-166	No	No	Yes	No
	TP-165	No	No	Yes	Yes
FAA	**TP-204/AA**	Yes	Yes	-	-
	TP-208	Yes	Yes	-	-
	TP-194	Yes	Yes	-	-
AA	**TP-191**	Yes	Yes	-	-

[a] Previously reported in chlorination experiments [185]

Similarly, the half-lives of AA with monochloramine are significantly longer in both creek and river samples (Student's t-test p-values 0.0003 and 0.0004, respectively) (**Table IV.2.7**) than those obtained in ultrapure water at pH 7 and pH 5.7, respectively (**Table IV.2.4**). The reaction was complete at 72 h, remaining less than 1% of AA. Conversely to chlorination, TP-165 and TP-166 were found after the reaction of AA with monochloramine in real water samples.

Table IV.2.8. Ecotoxicological data of phenazone-type drugs and metabolites, and TPs, predicted by the US EPA T.E.S.T. and ECOSAR software.

Compound	ECOSAR							T.E.S.T.			
	Chemical class	Acute toxicity (mg L^{-1})			Chronic toxicity (mg L^{-1})			96h *Fathead Minnow* LC_{50} (mg L^{-1})	48 h *Daphnia magna* LC_{50} (mg L^{-1})	Oral rat LD_{50} (mg kg body $weight^{-1}$)	Toxicity/ Mutagenicity
		Fish (96h LC_{50})	*Daphnid* (48h LC_{50})	Algae (96h EC_{50})	Fish	*Daphnid*	Algae				
Phe	Hydrazine	2.32	3.47	1.31	4.85	1.06	0.14	36.82	24.7	819.5	Toxicant / Negative
PrPhe	Hydrazine	1.12	2.33	0.92	1.73	0.48	0.11	10.35	13.2	667.9	Toxicant / Negative
Cl-Phe	Hydrazine	1.72	3.07	1.18	3.05	0.76	0.14	10.67	24.5	870.3	Toxicant / Negative
Br-Phe	Hydrazine	2.26	3.9	1.5	4.15	1.01	0.17	9.64	17.3	1476	Toxicant / Negative
Cl-,OH-Phe	Hydrazine	7.48	7.79	2.82	21.5	3.62	0.29	18.34	50.8	1119	Toxicant / Negative
Cl_2,OH-Phe	Hydrazine	3.24	4.93	1.86	6.66	1.47	0.21	N/A	N/A	N/A	N/A
Cl-Phe-Me	Hydrazine	1.97	3.26	1.24	3.75	0.88	0.14	34.61	25	757.9	Toxicant / Negative
Cl,OH-Phe-Me	Hydrazine	8.61	8.3	2.97	26.5	4.22	0.29	53.71	132	461.8	Toxicant / Negative
OH-PrPhe	Hydrazine	3.07	4.56	1.72	6.42	1.4	0.19	7.26	27.8	841.6	Toxicant / Negative
OH_2-PrPhe	Hydrazine	5	6.33	2.34	12.1	2.34	0.25	N/A	N/A	N/A	N/A
OH_3-PrPhe	Hydrazine	21.5	15.9	5.51	84.1	11	0.52	N/A	N/A	N/A	N/A
OH-PrPhe-Me	Hydrazine	3.54	4.87	1.82	7.94	1.64	0.19	28.07	45.4	612.4	Toxicant / Negative

N/A: Not related to existent chemical class.

Table IV.2.8 (cont.): Ecotoxicological data of phenazone type drugs and metabolites, and TPs, predicted by the US EPA T.E.S.T. and ECOSAR software.

Compound	ECOSAR							T.E.S.T.			
	Chemical class	Acute toxicity (mg L^{-1})			Chronic toxicity (mg L^{-1})			96h *Fathead Minnow* LC_{50} (mg L^{-1})	48 h *Daphnia magna* LC_{50} (mg L^{-1})	Oral rat LD_{50} (mg kg body $weight^{-1}$)	Toxicity/ Mutagenicity
		Fish (96h LC_{50})	*Daphnid* (48h LC_{50})	Algae (96h EC_{50})	Fish	*Daphnid*	Algae				
Cl,OH-PrPhe-Me	Hydrazine	1.66	3.22	1.26	2.74	0.73	0.15	28.33	12.6	392.3	Toxicant / Negative
Cl-PrPhe	Hydrazine	0.636	1.78	0.725	0.758	0.262	0.092	5.18	3.03	807.9	Toxicant/Negative
Cl_2-PrPhe	Hydrazine	0.41	1.42	0.59	0.39	0.16	0.08	8.08	5.79	517.6	Toxicant / Negative
Cl,Br-PrPhe	Hydrazine	0.43	1.55	0.65	0.41	0.17	0.09	7.43	6.86	N/A	Toxicant / Negative
AA	Hydrazine	898	84.1	112	109	5.47	31.2	62.45	48.7	588.5	Toxicant / Negative
FAA	Hydrazine	3.13	4.51	1.69	6.74	1.44	0.19	108	146	699.4	Toxicant / Positive
AAA	Hydrazine	6.05	6.91	2.53	16	2.88	0.26	4.51	74.4	1123	Toxicant / Negative
TP-208	Hydrazine	$7.13x10^3$	575	$1.04x10^3$	$1.41x10^3$	32	260	373.4	131	637.6	Toxicant / Negative
TP-194	Hydrazine	$1.32x10^4$	$1.00x10^3$	$2.02x10^3$	$3.04x10^3$	53	484	292.2	66.8	843.2	Toxicant / Negative
TP-191	Hydrazine	6.71	6.68	2.4	20.1	3.27	0.24	82.83	17	447	Toxicant / Negative
TP-166	Hydrazine	$5.24x10^3$	422	757	$1.10x10^3$	23.7	189	227.9	29.1	229.5	Toxicant / Negative
TP-165	Hydrazine	3.06	3.9	1.44	7.57	1.43	0.15	220.7	59	156.7	Toxicant / Negative

N/A: Not related to existent chemical class.

IV.2.5. (Eco)toxicity estimation

In order to obtain a preliminary estimation of the (eco)toxicity of the TPs, the US EPA T.E.S.T. and ECOSAR software were used as described in **Section III.4.8.1**. The results obtained are compiled in **Table IV.2.8**. As already reported in the literature, significant differences were observed for toxicity prediction using both software[159], so these data shall be used only as a preliminary screening for toxicity.

According to the results (**Table IV.2.8**), Cl-Phe, Br-Phe and Cl-Phe-Me (Phe TPs) and Cl-PrPhe, Cl_2-PrPhe and Cl,Br-PrPhe (PrPhe TPs) would present higher acute (lower LC_{50} or EC_{50}) and chronic (lower chronic value - ChV) toxicities for the three considered trophic levels (fish, *daphnid* and algae) than their precursor compounds. In the case of AA and according to ECOSAR data, FAA, AAA, TP-191 and TP-165 would also exhibit higher toxicity than AA, while the T.E.S.T. software results estimated that AAA would be more toxic for *Fathead Minnow* and TP-191 and TP-166 for *Daphnia magna* than AA. According to the European Chemicals Agency (ECHA) guidance[191], precursors and TPs, which showed oral rat toxicities LD_{50} values in the 392-1476 mg kg body weight^{-1}, would be classified as Category 4, except TP-165 and TP-166 which would be classified as Category 3 (oral rat toxicities LD_{50} values of 157 and 229 mg kg body weight^{-1}, respectively).

IV.2.6. Annex

This annex contains:

Figure SIV.2.1: QTOF product ion spectra of AA, AAA and FAA and their TPs: (a) AA; (b) FAA, (c) AAA; (d) TP-208; (e) TP-194; (f) TP-191; (g) TP-166 and (h) TP-165.

(a)

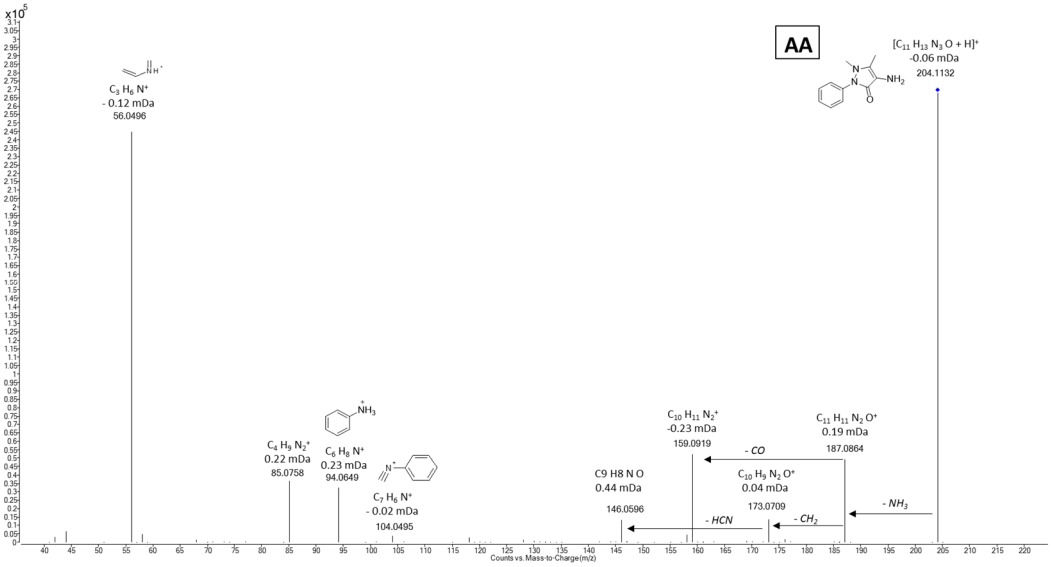

Figure SIV.2.1: QTOF product ion spectra of AA, AAA and FAA and their TPs: (a) AA

(b)

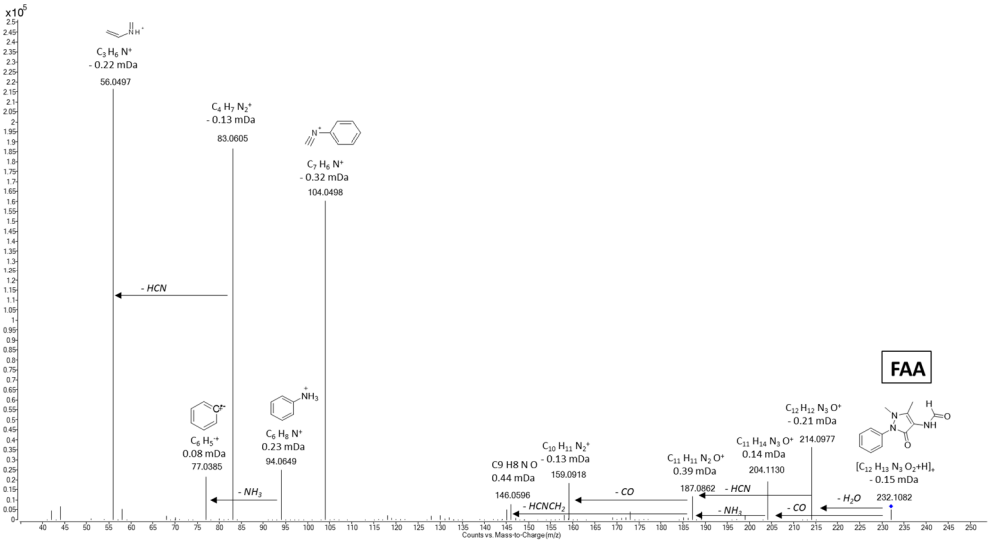

(c)

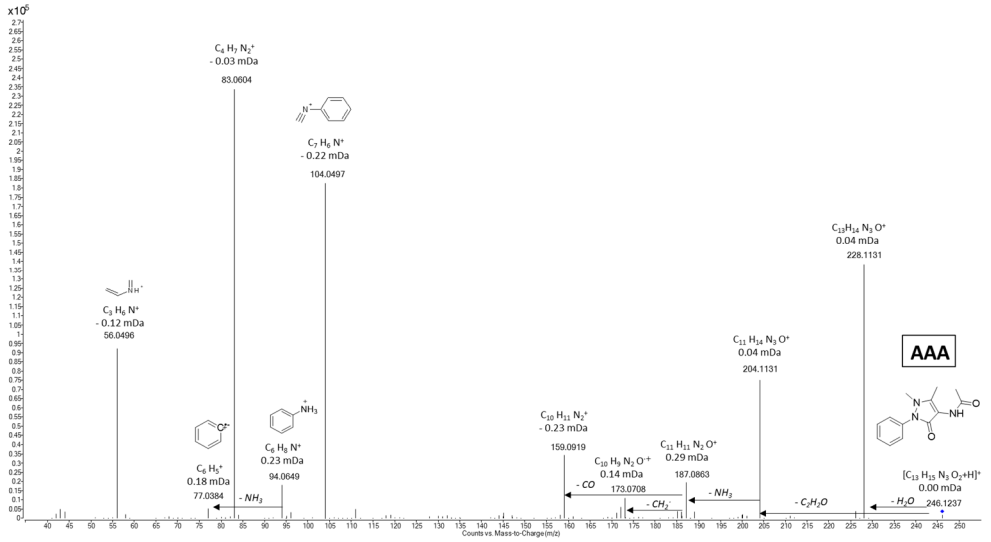

(d)

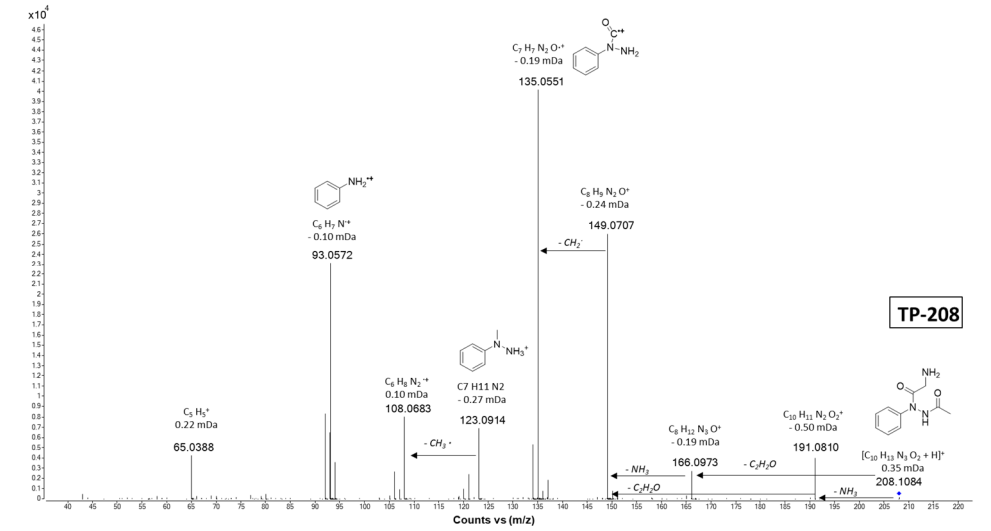

Figure SIV.2.1 (cont.): QTOF product ion spectra of AA, AAA and FAA and their TPs: (b) FAA, (c) AAA; (d) TP-208

(e)

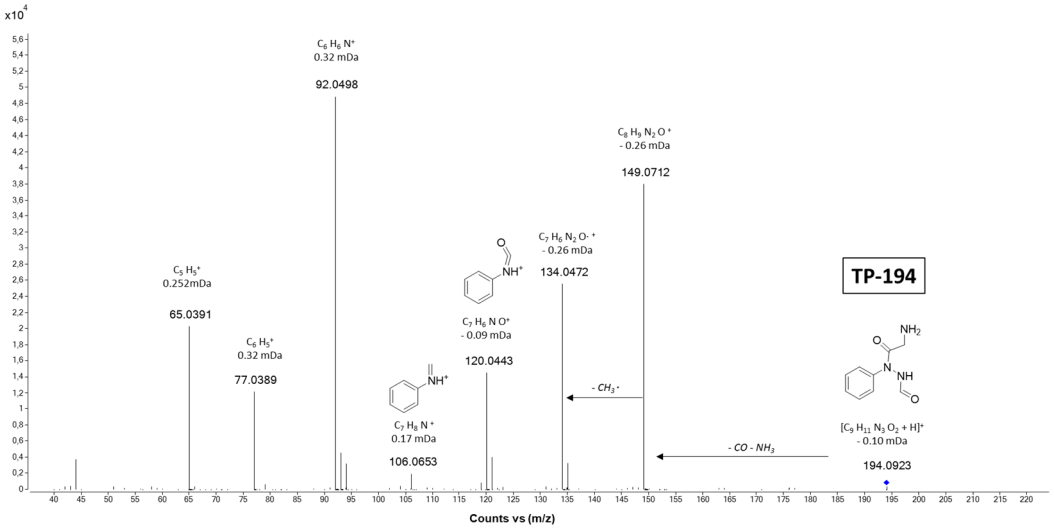

(f)

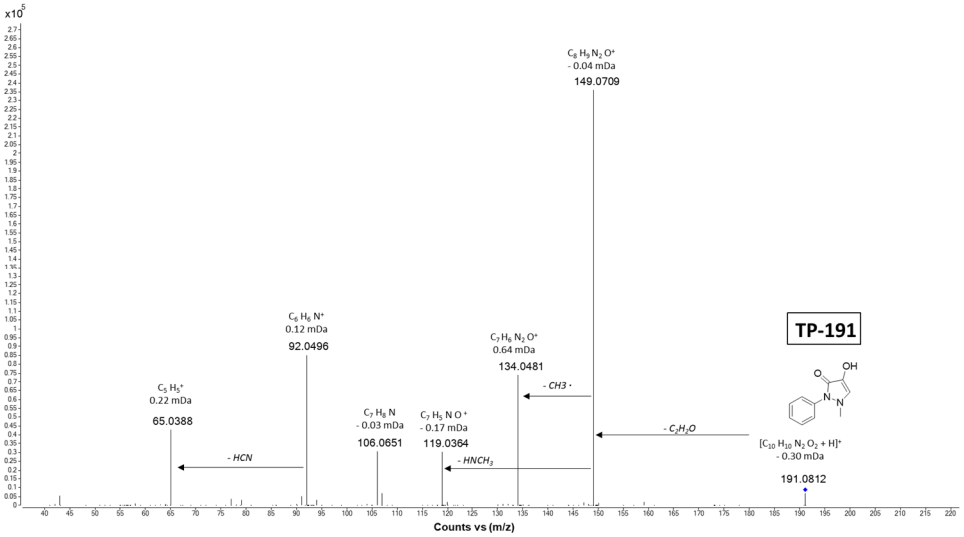

(g)

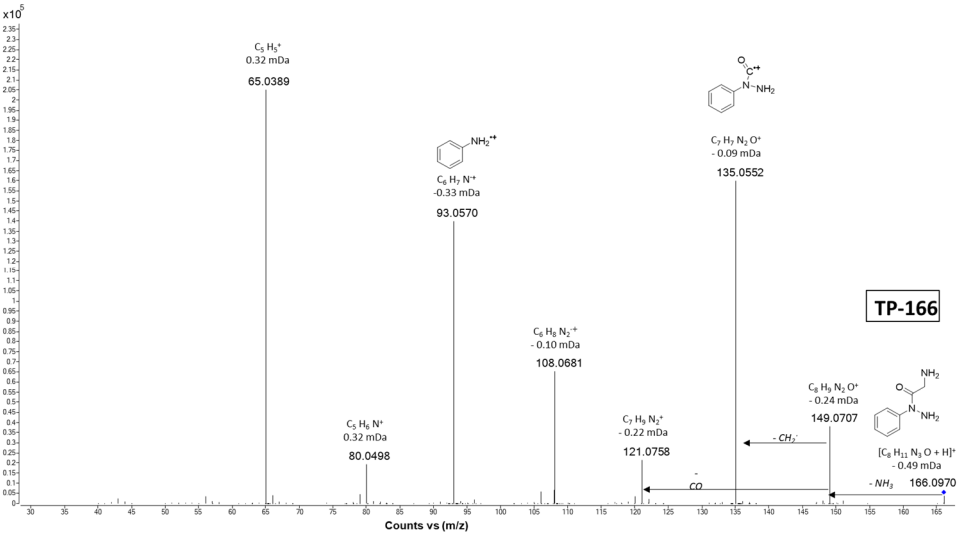

Figure SIV.2.1 (cont.): QTOF product ion spectra of AA, AAA and FAA and their TPs: (e) TP-194; (f) TP-191; (g) TP-166

(h)

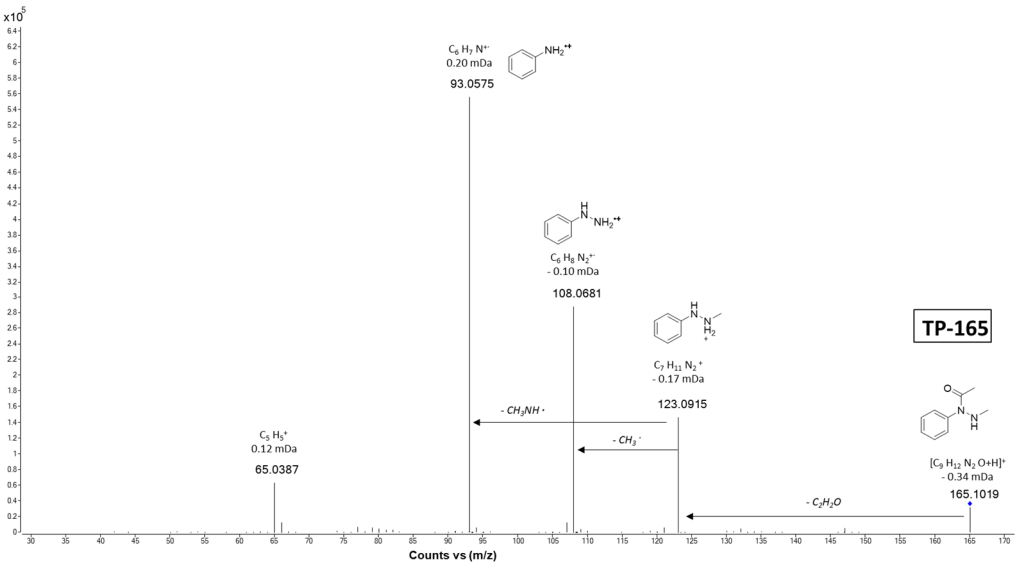

Figure SIV.2.1 (cont.): QTOF product ion spectra of AA, AAA and FAA and their TPs: (h) TP-165.

USC
UNIVERSIDADE
DE SANTIAGO
DE COMPOSTELA

IV.3. Chlorination and bromination of 1,3-diphenylguanidine and 1,3-di-o-tolylguanidine

The results collected in this chapter have been published in:

Benigno José Sieira, Rosa Montes, Arnaud Touffet, Rosario Rodil, Rafael Cela, Hervé Gallard, José Benito Quintana

Chlorination and bromination of 1,3-diphenylguanidine and 1,3-di-o-tolylguanidine: Kinetics, transformation products and toxicity assessment.

Journal of Hazardous Materials 385 (2020) 121590.

DOI: 10.1016/j.jhazmat.2019.121590

This work was performed in collaboration with Dr. Arnaud Touffet and Prof. Hervé Gallard from *Institute de Chimie des Milieux et des Matériaux de Poitiers (IC2MP), École Nationale Supérieure d'Ingénieurs de Poitiers (ENSIP)*, University of Poitiers (France).

I developed this work during a 3-month stay at the University of Poitiers under the suppervision of Prof. Hervé Gallard.

USC
UNIVERSIDADE
DE SANTIAGO
DE COMPOSTELA

The aim of this work was to perform a comprehensive study about the chlorination of DTG and DPG (**Figure IV.3.1**) in water. This includes a kinetic study and modelling, identification of TPs (including those formed by bromination, since hypobromite is rapidly formed from bromide into solution during chlorination[153] by LC-QTOF, quantification of the yield of known DBPs formed and preliminary (eco)toxicological assessment. These compounds are high production volume industrial chemicals[192] that have been found in different water compartments at the ng L^{-1} level[91,193] and, more recently, DPG has also been identified as being the major chemical leaching from tire wear particles[62,194]. Furthermore, there is some literature that describes DTG and DPG toxicity and pharmacological activity in mice and rats[195,196]. Nevertheless, the possible reaction of both chemicals with chemical oxidants used in DWTPs and WWTPs has not been studied so far.

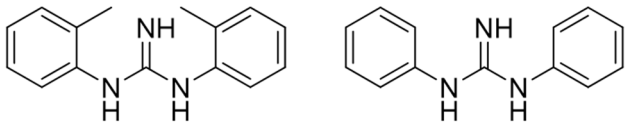

DTG DPG

Figure IV.3.1. DTG and DPG structures

IV.3.1. Chlorination kinetic study

A full kinetic study of DTG and DPG reaction with chlorine was performed considering a wide range of pH values, from 5 to 11-12. In excess of chlorine, results were adjusted to a pseudo-first order kinetic equation (**Figure IV.3.2a**) to obtain the observed rate constant k_{obs} in s^{-1} as the slope of the linear regression. The first order with respect to chlorine was verified by changing the initial concentration of chlorine (**Figure IV.3.2b**). In addition, it was verified that guanidine concentrations were similar when thiosulfate or ammonium chloride were used to stop the reaction or when manual injection was used without quenching the reaction (**Figure IV.3.2a**) suggesting that N-chlorinated guanidine compunds were not formed[152].

The apparent rate constant (k_{app} in M^{-1} s^{-1}) was determined for each experiment from the k_{obs} value and the initial concentration of chlorine. The values of k_{app} are compiled in **Tables IV.3.1** and **IV.3.2**. They range from 32 M^{-1} s^{-1} at pH 5 to a maximum of ca. 1.11×10^4 M^{-1} s^{-1} at pH 8.4 for DPG. In the case of DTG, reaction is even faster, with k_{app} ranging from 25 (at pH 4.9, the lowest pH tested in this case) to 1.83×10^4 M^{-1} s^{-1} at pH 9.9. At natural water pH values, this translates in very fast reactions, with half-lives of a few seconds to some minutes with typical chlorine doses (1−10 mg L^{-1}).

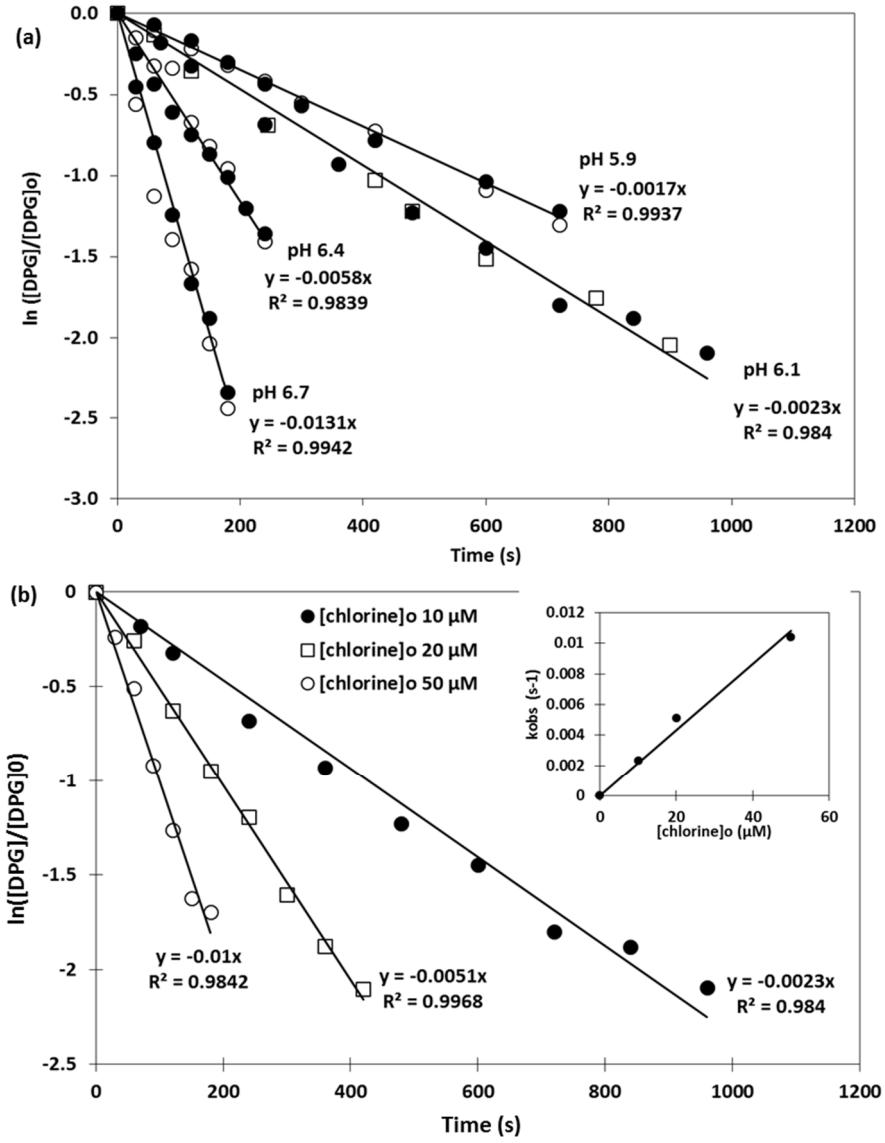

Figure IV.3.2: Examples of pseudo-fist-order kinetics plots obtained during the chlorination of DPG (phosphate buffer 10 mM). (a) Influence of pH and quenching methods ($[DPG]_0$ 1 µM, $[chlorine]_0$ 10 µM). The reaction was stopped by thiosulfate (full circle), ammonium (open circle) or manual direct injection was used (open square). Linear regressions are plotted for reduction by thiosulfate. (b) Influence of chlorine concentrations ($[DPG]_0$ 1 µM, pH 6.1). The reaction was stopped by thiosulfate

A theoretical model of the pH-dependent apparent rate constant (k_{app}) for the reaction between each guanidine and chlorine was described based on the speciation of $HOCl/ClO^-$ (pK_a=7.54, **Eq. IV.3.1**) and guanidines (pK_a = 10.67 for DTG, and pK_a = 10.12 for DPG, **Eq. IV.3.2**)[197] and considering HOCl as the only active electrophile[198]. The large increase in k_{app} when the pH increased from 5 to 9 suggests a greater contribution of the neutral guanidine to the protonated form. Thus, the resulting model for the DTG and DPG reaction mechanism is described as follows assuming that HOCl reacts only with neutral guanidine species in the first assumption (**Eq.IV.3.3**).

Table IV.3.1. Experimentally obtained k_{app} for DPG at the different pH values and corresponding half-lives calculated for 10 µM Cl_2 (i.e. 0.71 mg Cl_2 L^{-1}).

pH	k_{app} (M^{-1} s^{-1})	$t_{1/2}$ (s)
5.0	32	2203
5.6	73	950
5.9	170	408
6.0	194	357
6.1	230	301
6.4	580	120
6.5	670	104
6.7	1310	53
7.0	2400	29
7.5	3923	18
8.0	9760	7
8.4	11061	6
9.0	10776	6
9.5	4567	15
10.0	5999	12
11.0	1269	55
11.7	372	186

Table IV.3.2. Experimentally obtained k_{app} for DTG at the different pH values and corresponding half-lives calculated for 10 µM Cl_2 (i.e. 0.71 mg Cl_2 L^{-1}).

pH	k_{app} (M^{-1} s^{-1})	$t_{1/2}$ (s)
4.9	25	2803
5.5	148	469
6.0	364	190
6.5	1764	39
7.0	5599	12
7.5	7941	9
8.0	11327	6
9.9	18297	4
11.0	8205	9

Eq.IV.3.1 $HOCl \overset{K_a}{\rightleftharpoons} OCl^- + H^+$ *fast*

Eq.IV.3.2 $guanidine^+ \overset{K}{\rightleftharpoons} guanidine + H^+$ *fast*

Eq.IV.3.3 $guanidine + HOCl \xrightarrow{k} TPs$ *slow*

The general expression for the reaction of the guanidine compound (either DPG or DTG) with chlorine is described in **Eq.IV.3.4** and **Eq.IV.3.5**.:

$$\frac{d\,[\text{guanidine}]_T}{d\,t} = -k\,[\text{guanidine}][HOCl] = -k_{app}\,[\text{guanidine}]_T\,[HOCl]_T$$

Eq.IV.3.4

Eq.IV.3.5 $$k_{app} = k\,\alpha_{HOCl}\,\alpha_{guanidine}$$

where: k is the specific rate constant of HOCl with the neutral species of DTG/DPG, K_a is the acid-base equilibrium constant of HOCl, $[HOCl]_T$ is the total concentration of free chlorine ($HOCl + OCl^-$), $[guanidine]_T$ is the total concentration of DPG or DTG, and α_{HOCl} and $\alpha_{guanidine}$ are the molar fractions of HOCl and neutral guanidine species, respectively.

By introducing the expression of both, HOCl and guanidine molar fractions, the k_{app} value is given by the expression shown in **Eq. IV.3.6**.:

Eq.IV.3.6 $$k_{app} = \frac{k\,K[H^+]}{(K+[H^+])(Ka+[H^+])}$$

The value of the rate constant k was determined by a non-linear least-square regression of the experimental pH profile of the k_{app} values using Sigma Plot 11.0 (Systat Software Inc.).

The pH dependence of k_{app} is shown in **Figure IV.3.3.a** and **b** for DPG and DTG, respectively. For both compounds, the pH profile exhibits a maximum between pH 8 and pH 10. This maximum corresponds to the concomitant presence of both HOCl and neutral guanidine. The maximum pH value is equal to the average value of the pK_a of HOCl and guanidines i.e. 8.8 for DPG and 9.1 for DTG. As shown in **Figure IV.3.3**, the model fits well with the experimental data considering only the reaction of HOCl with neutral guanidine.

When a full kinetic model was evaluated for initial reaction of halogenation of guanidines, the model includes the reactions of hypohalous acid (HOCl or HOBr) with neutral or protonated guanidines and the reaction of hypohalite ion (ClO^- or BrO^-) with neutral guanidine (**Eq. IV.3.7-11**).

Eq.IV.3.7 $$HOX \underset{}{\overset{K_a}{\rightleftharpoons}} OX^- + H^+ \qquad fast$$

Eq.IV.3.8 $$guanidine^+ \overset{K}{\rightleftharpoons} guanidine + H^+ \qquad fast$$

Eq.IV.3.9 $$guanidine + HOX \xrightarrow{k_1} TPs \qquad slow$$

Eq.IV.3.10 $$guanidine^+ + HOX \xrightarrow{k_2} TPs \qquad slow$$

Eq.IV.3.11 $$guanidine + XO^- \xrightarrow{k_3} TPs \qquad slow$$

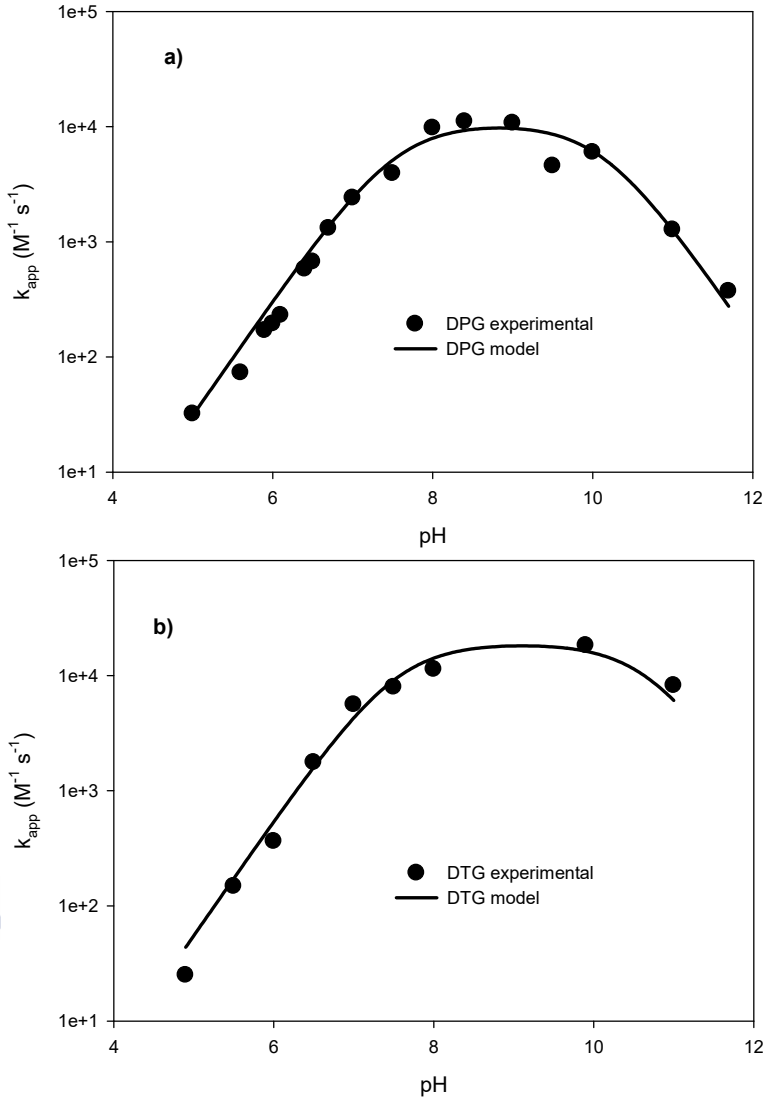

Figure IV.3.3. pH dependence of the experimental and modelled apparent rate constants of chlorination of (a) DPG and (b) DTG.

Then, the general expression for the rate of halogenation of guanidine is given by the expression **Eq.IV.3.12**.

$$\frac{d\,[\text{guanidine}]_T}{d\,t} = -k_1\,[\text{guanidine}][\text{HOX}] - k_2\,[\text{guanidine}^+][\text{HOX}] - k_3\,[\text{guanidine}][\text{XO}^-] = -k_{app}\,[\text{guanidine}]_T\,[\text{HOX}]_T$$

Eq.IV.3.12

The apparent rate constant depends on the intrinsic rate constants k_1, k_2, and k_3 and the molar fractions of guanidine and halogen species (**Eq. IV.3.13**).

Eq.IV.3.13 $$k_{app} = k_1\,\alpha_{HOX}\,\alpha_{guanidine} + k_2\,\alpha_{HOX}\,\alpha_{guanidine+} + k_3\,\alpha_{XO-}\,\alpha_{guanidine}$$

Replacing the molar fractions by their expressions in function of H^+ concentration and equilibrium rate constants give the following expression for k_{app} shown in **Eq. IV.3.14**.

Eq.IV.3.14 $$k_{app} = \frac{k_1 K[H^+] + k_2[H^+]^2 + k_3 K K_a}{(K_a + [H^+])(K + [H^+])}$$

Specific rate constants and coefficients of determination obtained by kinetic modelling by non-linear regression (Sigma Plot 11.0) of the experimental pH profile of apparent rate constants are given in **Table IV.3.3**. Values are compared with values obtained by the simple kinetic model considering only the reaction of HOX with neutral guanidine.

Table IV.3.3. Specific rate constants of halogenation of DPG and DTG determined by kinetic modelling considering simple or full kinetic model.

		Full model				Simple model	
		k_1	k_2	k_3	R^2	k	R^2
Chlorination	DPG	4.1×10^6	1.4×10^{-7}	2.4×10^{-6}	0.898	4.1×10^6	0.898
	DTG	2.4×10^7	2.5×10^{-8}	3.9×10^3	0.975	2.6×10^7	0.960
Bromination	DPG	8.3×10^6	2.2×10^{-8}	0	0.950	8.3×10^6	0.950
	DTG	5.5×10^6	1.2×10^{-6}	0	0.997	5.5×10^6	0.997

The results presented in **Table IV.3.3** show that, except for chlorination of DTG, values of k_2 and k_3 are very low or equal to zero and that determination coefficients are similar for the two models. The only significant k_3 value of 3.9×10^3 M^{-1} s^{-1} was generated for the chlorination of DTG with slightly higher R^2 for full kinetic model. Still k_3 is 4 orders of magnitude lower than k_1. This did not justify the use of the full kinetic model in place of the simple model because this result only depends on the unique value of k_{app} at pH 11.0 for DTG.

So, no improvement was obtained by including the reaction of ClO^- with neutral guanidine and the reaction of HOCl with protonated guanidine, which is in accordance with the literature[199].

The rate constants, k, of the reactions between HOCl and DPG and DTG neutral species determined from model fitting to the experimental values are 4.1 (±0.3) × 10^6 M^{-1} s^{-1} and 2.6 (±0.1) × 10^7 M^{-1} s^{-1} for DPG and DTG, respectively (**Table IV.3.3**). The apparent rate constants at neutral pH (~10^3 M^{-1} s^{-1}) and intrinsic rate constants (k) of neutral species (~10^6 - 10^7 M^{-1} s^{-1}) are in the range of rate constants of secondary amines with chlorine[199]. However, N-chloroamino compounds were not detected during kinetic experiments and identification of TPs would indicate that initial reactive site is the aromatic ring. Lower rate constant of 19 M^{-1} s^{-1} was obtained for ethyl guanidine at pH 7.2–7.4[200], which can be explained by the stronger basic character of alkyl guanidines.

IV.3.2. Bromination kinetic study

The apparent rate constants of bromination determined by using direct and competition kinetics methods are listed in **Tables IV.3.4** and **IV.3.5** for DPG and DTG, respectively and are plotted versus pH in **Figure IV.3.4**. Examples of pseudo-first order

and competition kinetics plots are given in **Figure IV.3.5** and **IV.3.6** for DPG. The apparent rate constants range from 76 to 2.89×10^5 M^{-1} s^{-1} for DPG and from 36 to 5.87×10^4 M^{-1} s^{-1} for DTG. In contrast to chlorine, lower rate constants were determined for DTG, which could be attributed to steric effects between the bulky bromine atoms and the methyl groups in DTG.

Table IV.3.4. Experimentally obtained k_{app}, kinetics methods for bromination of DPG at the different pH values and corresponding half-lives calculated for 10 µM Br_2 (i.e. 0.71 mg Br_2 L^{-1}). Values of k_{ref} are apparent rate constants of BP and TBP calculated from Heeb et al.[201].

pH	Kinetic method	k_{ref} (M^{-1} s^{-1})	k_{app} (M^{-1} s^{-1})	$t_{½}$ (s)
5.00	direct	-	76	916.9
5.18	direct	-	84	827.0
5.50	direct	-	314	220.7
5.63	direct	-	195	354.7
5.74	direct	-	334	207.5
6.00	direct	-	228	304.0
6.83	direct	-	344	201.6
7.00	competition with TBP	2112	311	222.9
7.08	direct	-	363	190.9
7.57	direct	-	460	150.7
8.00	direct	-	940	73.7
8.00	competition with TBP	2842	4276	16.2
8.05	competition with BP	26900	16829	4.1
8.50	direct	-	962	72.1
8.46	competition with BP	50700	61934	1.1
8.95	competition with BP	93300	158254	0.4
9.06	direct	-	2240	30.9
9.65	competition with BP	439000	289338	0.2
10.00	competition with BP	245910	246000	0.3
10.48	competition with BP	93300	96164	0.7
11.03	competition with BP	27700	37977	1.8
11.75	competition with BP	5360	8245	8.4

The experimental results fit well with the proposed model at pHs below 6 and above 9, while a strong deviation and even discrepancies were observed between rate constants determined by the direct kinetics method and the competition kinetics method using BP as reference compound in the pH 7–9 range.

Several experiments were conducted in order to further investigate the observed deviation from the model during the bromination of DPG and DTG. For DPG, apparent

rate constants determined at pH 8.5 and 9.0 by the direct kinetics method in batch reactor were about 70-fold lower than rate constants determined by the competition method using BP as reference compound. These rate constants are even 10-fold lower than rate constants obtained during chlorination for the same pH range. Competition kinetic method using TBP as reference compound (**Figure IV.3.6.b**) gave also low apparent constants at pH 7.0 and 8.0 and in the range of rate constants determined by the direct method. Such experimental pH profiles of k_{app} could not be explained by speciation of bromine nor guanidines.

Table IV.3.5. Experimentally obtained k_{app}, kinetics methods for bromination of DTG at the different pH values and corresponding half-lives calculated for 10 µM Br_2 (i.e. 0.71 mg Br_2 L^{-1}). Values of k_{ref} are apparent rate constants of BP and TBP calculated from Heeb et al.[201].

pH	Kinetic method	k_{ref} (M^{-1} s^{-1})	k_{app} (M^{-1} s^{-1})	$t_{½}$ (s)
5.22	direct	-	36	1918.4
5.55	direct	-	48	1438.6
6.04	direct	-	113	611.7
6.50	direct	-	277	250.3
6.85	direct	-	318	217.8
6.99	competition with TBP	2112	127	545.8
7.50	direct	-	417	166.2
8.02	competition with TBP	2842	797	86.9
9.15	competition with BP	698000	47857	1.4
9.90	competition with BP	294000	58707	1.2
10.55	competition with BP	80300	42185	1.6
10.94	competition with BP	33900	25430	2.7
11.80	competition with BP	4780	8355	8.3

A further experiment performed at pH 6.9 with an excess of DPG (50 µM) compared to bromine (5 µM) was performed. Residual oxidant was then analysed for different reaction times as triiodide at 351 nm (ε = 26 900 M^{-1} cm^{-1})[202] in a 5-cm quartz spectrophotometric cell after addition of 250 µL of 1 M KI phosphate buffer (pH 6.5) solution in 5 mL of sample. This experiment showed a strong deviation from the linear form of the pseudo-first-order kinetic model (**Figure IV.3.7**), which suggests that compound(s) with oxidant properties remained in solution and could interfere in rate constant determination.

Finally, when a higher concentration of 50 µM bromine was added in a 50 µM DPG solution at pH 6.9, the colourless solution turned pink progressively for 3 minutes and colour disappeared after addition of thiosulfate (see **Figure IV.3.8** for UV/visible spectra). In absence of thiosulfate, colour slowly disappeared for about 12 hours. The visible absorption band was centered at 520 nm. These observations are very similar to the formation of the highly coloured semiquinoid free radical formed during oxidation of N,N-

di-ethyl-p-phenylenediamine and commonly used for chlorine analysis[12]. Even though phenylguanidines differ from aromatic p-diamines and that the formation of a radical cation during the oxidation of phenylguanidines could not be confirmed in our study, a stable TP with oxidizing property likely affected the determination of rate constants with bromine at pH 7 – 8. Such TP existence could not be confirmed, however, by LC-HRMS, likely because it is reduced by the chromatographic eluents. Such deviations are attributed to a metastable TP with oxidizing properties which could not be identified by LC-HRMS in that pH range.

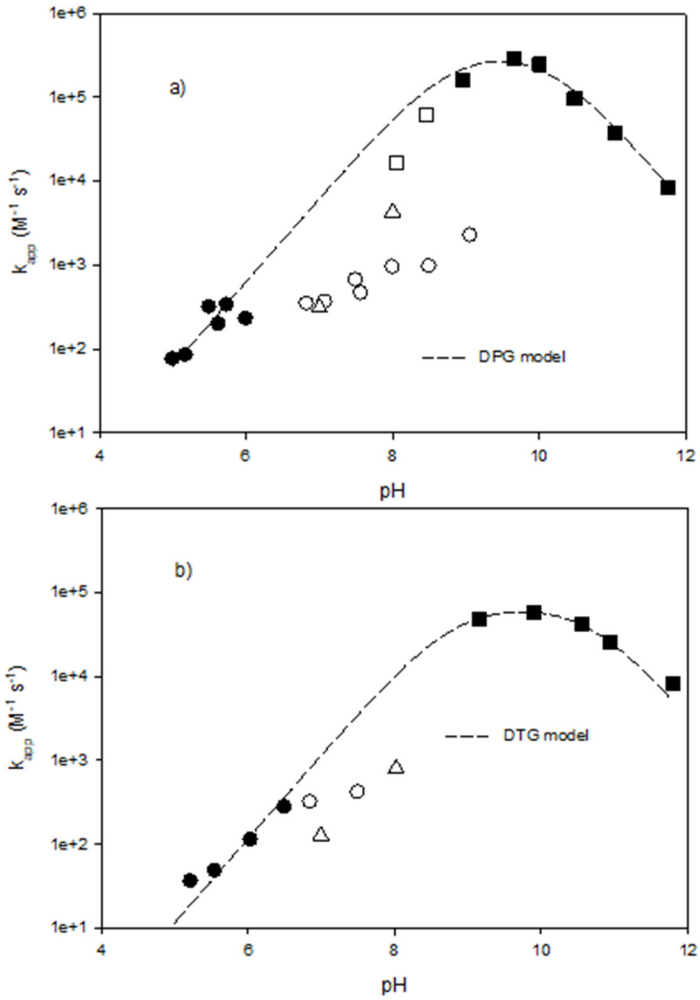

Figure IV.3.4. pH dependence of the experimental (symbols) and modelled apparent rate constants of bromination of (a) DPG and (b) DTG. Direct kinetic method (circle) and competitive kinetic method using BP (square) or TBP (triangle) as reference compounds were used for k_{app} determination. Only full symbols were used for model calculation.

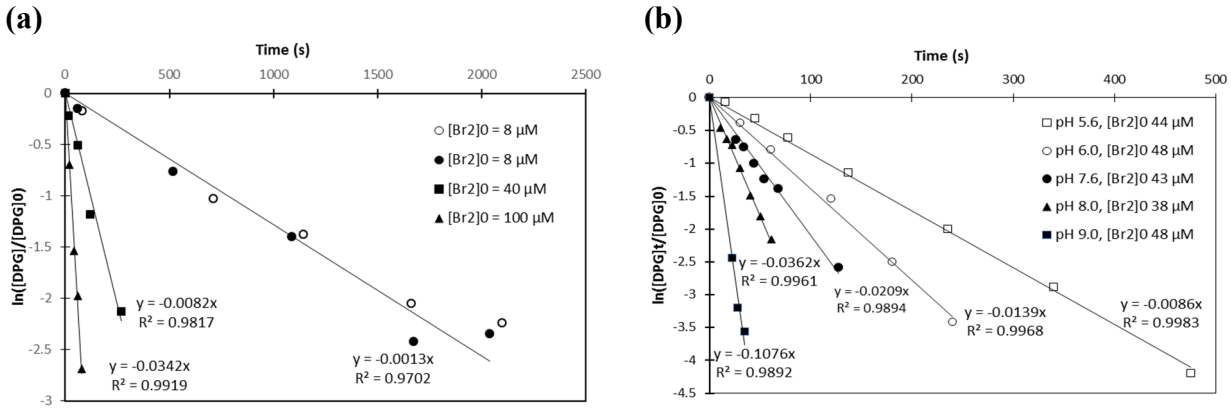

Figure IV.3.5. Examples of pseudo-fist order kinetics plots obtained for bromination of DPG (phosphate buffer 10 mM). (a) Influence of pH ([DPG]$_0$ 1 µM). The reaction was stopped by thiosulfate. (b) Influence of bromine concentration and quenching method ([DPG]$_0$ 1 µM, pH 5.6). The reaction was stopped by thiosulfate (full circle) or manual direct injection was used (open circle). Linear regression is plotted for reduction by thiosulfate.

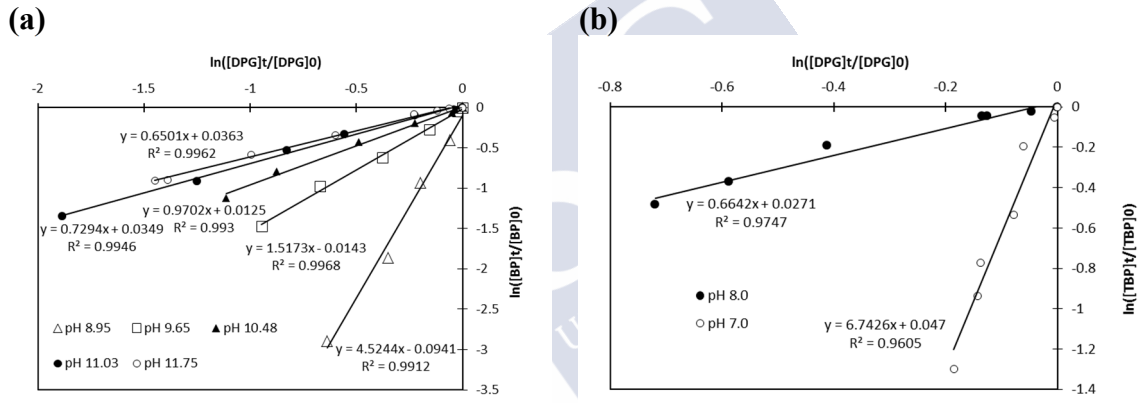

Figure IV.3.6. Determination of apparent second order rate constants for bromination of DPG by using the competition kinetics method with (a) BP and (b) TBP as reference compound ([DPG]$_0$ 5 µM, [BP]$_0$ or [TBP]$_0$ 5 µM, [bromine]$_0$ 0 to 10 µM, phosphate buffer 10 mM).

Excluding those pH values, and compared to chlorination, maximum k_{app} values are slightly shifted to higher pH values due to the higher pK_a of HOBr (pK_a=8.8). Calculated intrinsic rate constants for the reaction of HOBr with neutral DPG and DTG were 8.3 (±0.4) x 10^6 and 5.5 (±0.7) x 10^6, respectively. While HOBr reacts usually much faster than HOCl with organic compounds[201], the rate constant of HOBr with DPG was only twice as high as the reaction of HOCl with DPG and the rate constant for the reaction of HOBr with DTG was lower than that of HOCl. Steric hindrance (as mentioned), different reactive sites and type of reaction (oxidation vs substitution) might explain this unexpected result, which requires further investigation.

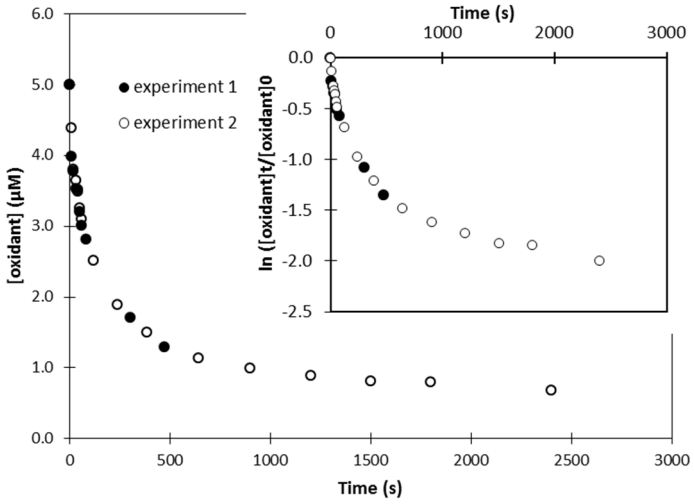

Figure IV.3.7. Decay of oxidant response during bromination of DPG (pH 6.9, $[DPG]_0$ 50 µM, $[bromine]_0$ 5 µM, phosphate buffer 10 mM)

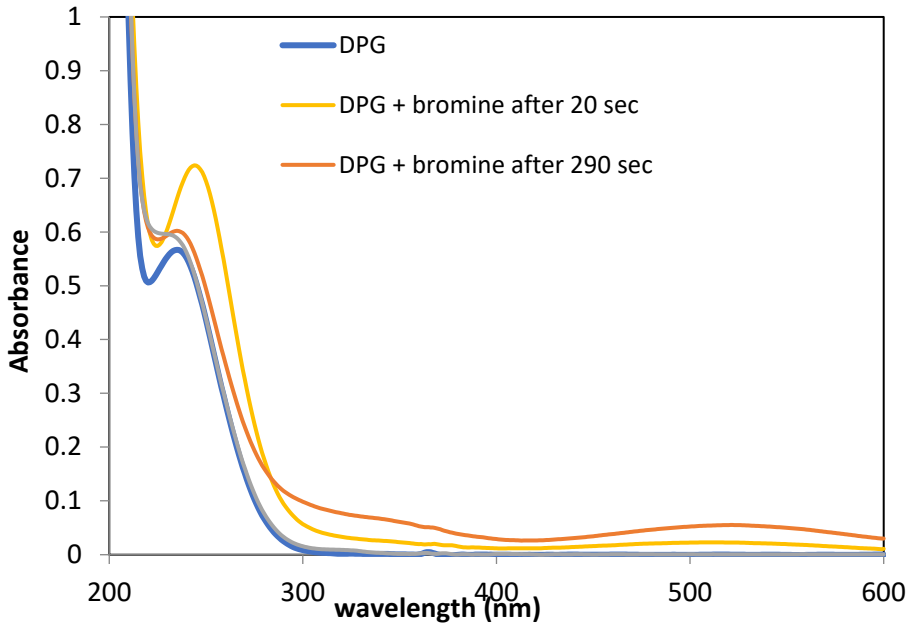

Figure IV.3.8. UV/Vis spectra of DPG solution before and after bromine addition (pH 6.9, 10 mM phosphate buffer, $[DPG]_0$ 50 µM, $[Br_2]_0$ 50 µM, reduction by an excess of thiosulfate)

IV.3.3. Transformation products

Identification of TPs was performed for both DTP and DPG considering chlorination and bromination. Experiments were carried out as described in **Sections III.4.3.2** and **III.4.3.3**. All samples were analysed in the HPLC-QTOF equipment as detailed in **III.4.5**. The proposed structures of the TPs are presented in **Figure IV.3.9** and **IV.3.10**. Further details on formulas, mass errors and scores of the TPs, as well as individual structures derived from the interpretation of MS/MS spectra are presented in

Tables IV.3.6 and **IV.3.7**. TPs were named with the precursor compound abbreviation followed by the nominal mass of its $[M+H]^+$ ion. As it can be observed the empirical formula could be proposed with a high degree of certainty, with score values higher than 95% and mass errors lower than 5 ppm, except for DTG-274, whose score was 79% and mass error was 9.7 ppm due to its low intensity.

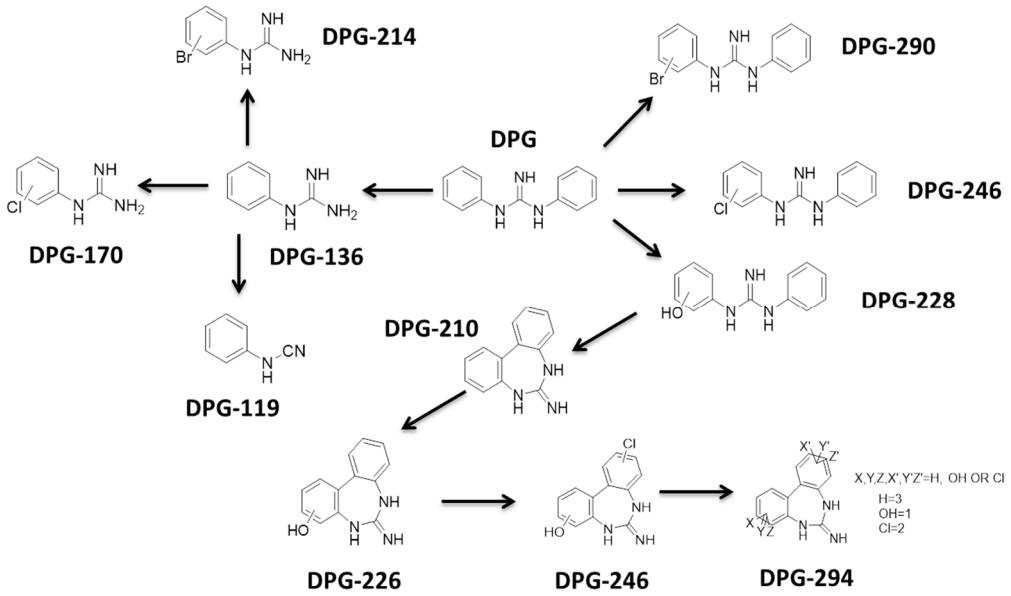

Figure IV.3.9. Schematic representation of DPG TPs

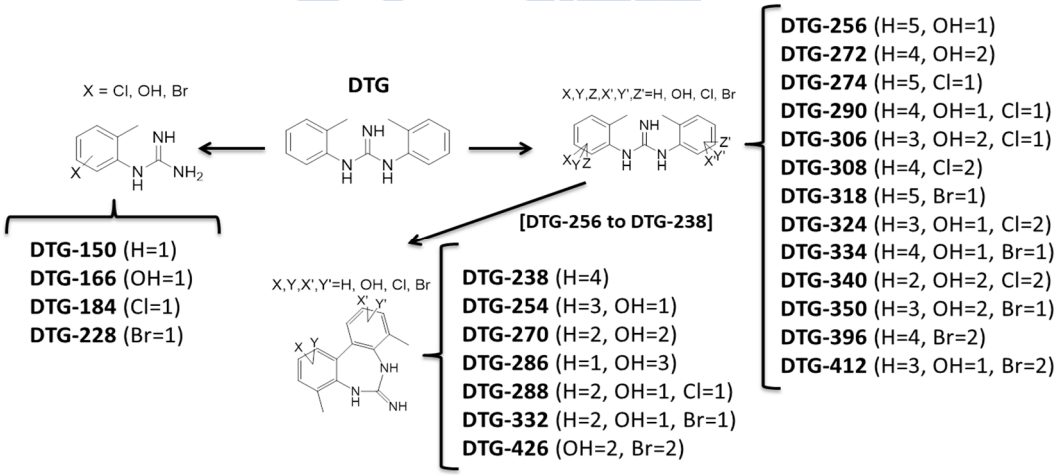

Figure IV.3.10. Schematic representation of DTG TPs

Table IV.3.6: List of chlorination and bromination DPG TPs.

Name	Experimental m/z	Molecular formula	Theoretical m/z	Error (ppm)	Error (mDa)	DBE	Score (%)	Structure
DPG	212.1182	$C_{13}H_{13}N_3$	-	-	-	9	-	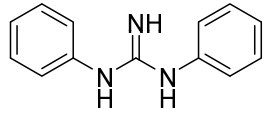
DPG-119	119.0604	$C_7H_6N_2$	119.0604	-0.21	-0.03	6	100	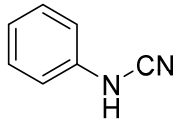
DPG-136	136.0867	$C_7H_9N_3$	136.0869	1.66	0.22	5	99.69	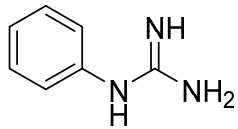
DPG-170	170.0475	$C_7H_8N_3Cl$	170.048	2.67	0.45	5	98.9	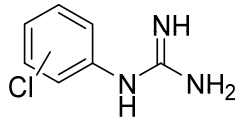
DPG-210	210.1025	$C_{13}H_{11}N_3$	210.1026	0.35	0.07	10	99.97	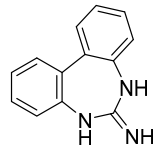
DPG-214	213.9968	$C_7H_8N_3Br$	213.9974	2.99	0.64	5	98.14	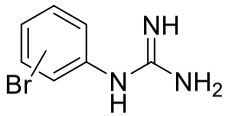
DPG-226	226.0975	$C_{13}H_{11}N_3O$	226.0975	-0.05	-0.01	10	100	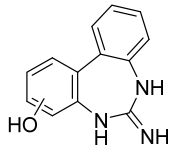

Table IV.3.6 (cont.): List of chlorination and bromination DPG TPs.

Name	Experimental m/z	Molecular formula	Theoretical m/z	Error (ppm)	Error (mDa)	DBE	Score (%)	Structure
DPG-228	228.1131	$C_{13}H_{13}N_3O$	228.1131	0.17	0.04	9	99.99	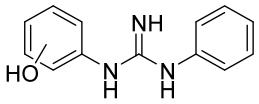
DPG-246	246.0795	$C_{13}H_{12}N_3Cl$	246.0793	-1.01	-0.25	9	99.74	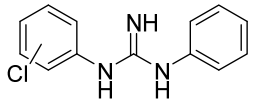
DPG-260	260.0579	$C_{13}H_{10}N_3OCl$	260.0585	2.38	0.62	10	98.51	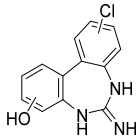
DPG-290	290.0287	$C_{13}H_{12}N_3Br$	290.0287	0.13	0.04	9	100	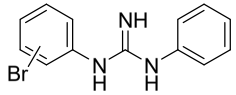
DPG-294	294.0186	$C_{13}H_9N_3OCl_2$	294.0195	3.22	0.94	10	96.91	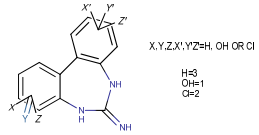

Table IV.3.7: List of chlorination and bromination DTG TPs.

Name	Experimental m/z	Molecular formula	Theoretical m/z	Error (ppm)	Error (mDa)	DBE	Score (%)	Structure
DTG	240.1495	$C_{15}H_{17}N_3$	-	-		9	-	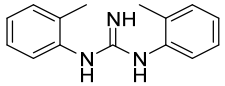
DTG-150	150.1026	$C_8H_{11}N_3$	150.1026	-0.18	-0.03	5	100	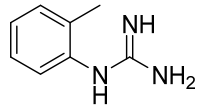
DTG-166	166.0971	$C_8H_{11}N_3O$	166.0975	2.35	0.39	5	99.17	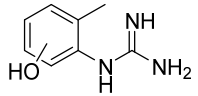
DTG-184	184.0632	$C_8H_{10}N_3Cl$	184.0636	2.19	0.4	5	99.17	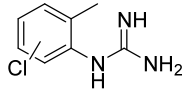
DTG-228	228.0131	$C_8H_{10}N_3Br$	228.0131	-0.06	-0.01	5	100	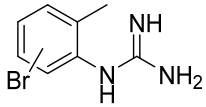
DTG-238	238.1336	$C_{15}H_{15}N_3$	238.1339	1.16	0.27	10	99.68	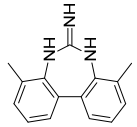
DTG-254	254.1285	$C_{15}H_{15}N_3O$	254.1288	1.14	0.29	10	99.66	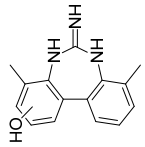

Table IV.3.7. (cont.): List of chlorination and bromination DTG TPs.

Name	Experimental m/z	Molecular formula	Theoretical m/z	Error (ppm)	Error (mDa)	DBE	Score (%)	Structure
DTG-256	256.1436	$C_{15}H_{17}N_3O$	256.1444	3.29	0.84	9	97.23	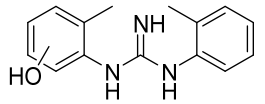
DTG-270*	270.1238	$C_{15}H_{15}N_3O_2$	270.1237	-0.36	-0.1	10	99.96	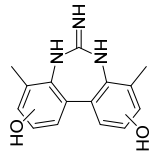
DTG-272	272.1391	$C_{15}H_{17}N_3O_2$	272.1394	0.93	0.25	9	99.75	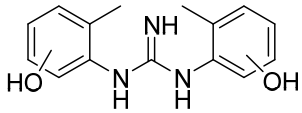
DTG-274*	274.1079	$C_{15}H_{16}N_3Cl$	274.1106	9.71	2.65	9	79.46	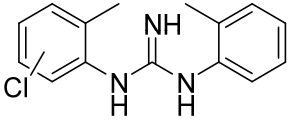
DTG-286*	286.1182	$C_{15}H_{15}N_3O_3$	286.1186	1.47	0.42	10	99.36	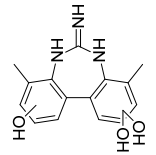
DTG-288*	288.0895	$C_{15}H_{14}N_3OCl$	288.0898	1.1	0.32	10	99.64	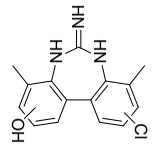

* TPs with low intensity, thus no MS/MS spectra could be recorded

Table IV.3.7. (cont.): List of chlorination and bromination DTG TPs.

Name	Experimental m/z	Molecular formula	Theoretical m/z	Error (ppm)	Error (mDa)	DBE	Score (%)	Structure
DTG-290	290.1042	$C_{15}H_{16}N_3OCl$	290.1055	4.38	1.27	9	95.41	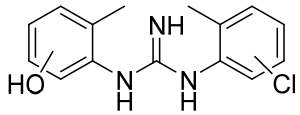
DTG-306*	306.0995	$C_{15}H_{16}N_3O_2Cl$	306.0931	2.89	0.88	9	97.39	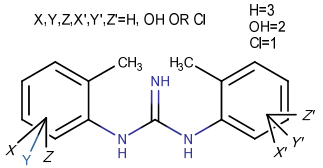
DTG-308	308.0706	$C_{15}H_{15}N_3Cl_2$	308.0716	3.19	0.98	9	96.81	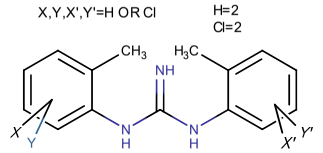
DTG-318	318.06	$C_{15}H_{16}N_3Br$	318.06	0.12	0.04	9	100	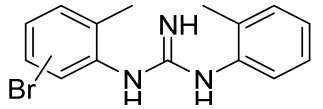
DTG-324	324.0657	$C_{15}H_{15}N_3Cl_2O$	324.0665	2.46	0.79	9	97.98	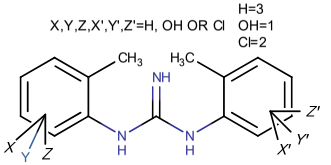
DTG-332*	332.0393	$C_{15}H_{14}N_3OBr$	332.0393	0	0	10	100	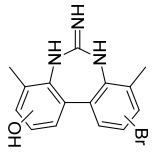

* TPs with low intensity, thus no MS/MS spectra could be recorded

Table IV.3.7. (cont.): List of chlorination and bromination DTG TPs.

Name	Experimental m/z	Molecular formula	Theoretical m/z	Error (ppm)	Error (mDa)	DBE	Score (%)	Structure
DTG-334	334.055	C_{15} H_{16} N_3 O Br	334.055	-0.15	-0.05	9	99.99	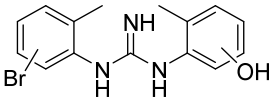
DTG-340*	340.0609	C_{15} H_{15} N_3 O_2 Cl_2	340.0614	1.5	0.51	9	99.2	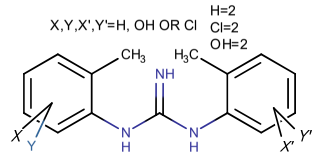
DTG-350*	350.0499	C_{15} H_{16} N_3 O_2 Br	350.0499	-0.1	-0.03	9	100	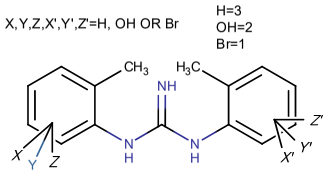
DTG-396*	395.9705	C_{15} H_{15} N_3 Br_2	395.9705	0.13	0.05	9	99.99	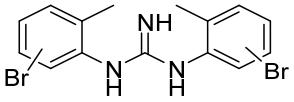
DTG-412	411.9655	C_{15} H_{15} N_3 O Br_2	411.9655	-0.09	-0.04	9	100	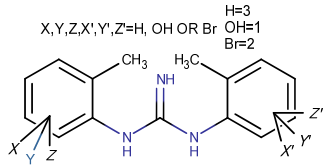
DTG-426*	425.9431	C_{15} H_{13} N_3 O_2 Br_2	425.9425	-1.53	1.63	10	98.97	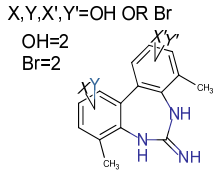

* TPs with low intensity, thus no MS/MS spectra could be recorded

The proposed structures are based on the interpretation of the MS/ MS spectra, which are presented into **Section IV.3.7, Annex Figure SIV.3.1** and **SIV.3.2**, for DPG and DTG TPs, respectively. Moreover, DPG-136 (i.e. monophenylguanidine) was unequivocally identified by purchasing its authentic standard.

There are four main types of reactions occurring during chlorination, i.e. ipso-chlorination to produce monoguanidine derivatives, introduction of chlorine atoms (bromine when samples are brominated) into an aromatic ring, hydroxylation and intramolecular cyclization. Thus, DPG-136 was easily identified by its spectrum (**Figure SIV.3.1c**), and because an authentic standard was available, as mentioned. This TP further reacts by halogenation to the corresponding chlorinated or brominated derivatives (DPG-170 and DPG-214), easily identified because their MS/MS spectra is similar to DPG-136 and exhibit the halogen isotopic pattern (**Figure SIV.3.1.d** and **f**). DPG-119 is also produced at long reaction times. Hydroxylation of DPG produces DPG-228, while halogenation produces DPG-246 (chlorination) and DPG-290 (bromination), all of them easily identified by their MS/MS spectra (**Figure SIV.3.1h**, **i** and **k**).

A key TP is DPG-210, with an empirical formula similar to DPG itself but with one further double-bond equivalent (i.e. 2 atoms of H less), **Table IV.3.6**. Its MS/MS spectrum exhibits first the loss of ammonia to m/z 192.0671 and also the elimination of CH_3N_2 to m/z 167.0720 from the protonated molecular ion (**Figure SIV.3.1.e**). This second ion would not be possible unless a cycle is formed. Because of this, we hypothesize here that DPG-210 corresponds to the structure shown in **Figure IV.3.9**, by formation of the 7-membering cycle from DPG-228 (hydroxylated DPG) by elimination of water. In fact, the maximum intensity of DPG-228 was observed at 0.5 min and then its intensity rapidly drops, while DPG-210 maximum is reached at 1 min and then drops more slowly (see **Figure IV.3.11a**). The fact that DPG-210 has also been observed as a photolysis TP by Zahn et al.[62], although no structure was proposed in that publication, further supports this hypothesis. Once DPG-210 is formed, this molecule further reacts to yield a mono-hydroxylated-TP (DPG-226), a hydroxychloro-TP (DPG-260) or a dichloro,hydroxy-TP (DPG-294).

In the case of DTG, the reaction was similar to DPG, as expected, but a larger number of TPs could be identified (23 vs. 11 TPs). In general, the main difference in the TPs produced is that a greater degree of hydroxylation and halogenation is observed, e.g. DTG-308 (a dichlorinated derivative of DTG), which can be explained by the electron donor effect of the methyl group on the aromatic ring. Although no MS/MS spectra (**Figure SIV.3.2**) was obtained for all TPs, due to the low intensity of some of them, structures compiled into **Figure IV.3.10** and **Table IV.3.7** (those TPs without MS/MS data are marked with a * symbol in the Table) were assigned on the basis of the MS/MS spectra (when available) and by analogy to DPG TPs.

As regards of the most relevant TPs, Figure **IV.3.11b** and **IV.3.12.b** present the normalized amount of each TP and their precursors for a reaction with 100 μM chlorine and up to 30 min of contact time. Normalization was performed by using the signal of the

original compound (DPG or DTG) as a surrogate to calculate an approximate yield, except for DPG-136, DPG-119, DPG-170, DTG-150, DTG-166, DTG-184 and DTG-228, where monophenyl-guanidine (DPG-136) was used instead, as being considered structurally closer. In the case of DPG (**Figure IV.3.11**), the most intense TP is DPG-136 with a yield of ca. 5% at 0.5−2 min, dropping down to 3% at 30 min. The second most relevant TP is DPG-246 (monochloro-DPG), with a yield of ca. 3% at 0.5−2 min, dropping down to ca. 0.2% at 30 min. It is noteworthy that at 30 min, there was no DPG detectable and the sum of all TPs intensities would approximately represent a 5% yield. This could likely be attributed to the formation of ring-opening products like chloroform with a relatively high yield (see **IV.3.4**) and the uncertainty of the semi-quantitative approach, due to the lack of authentic standards for most TPs.

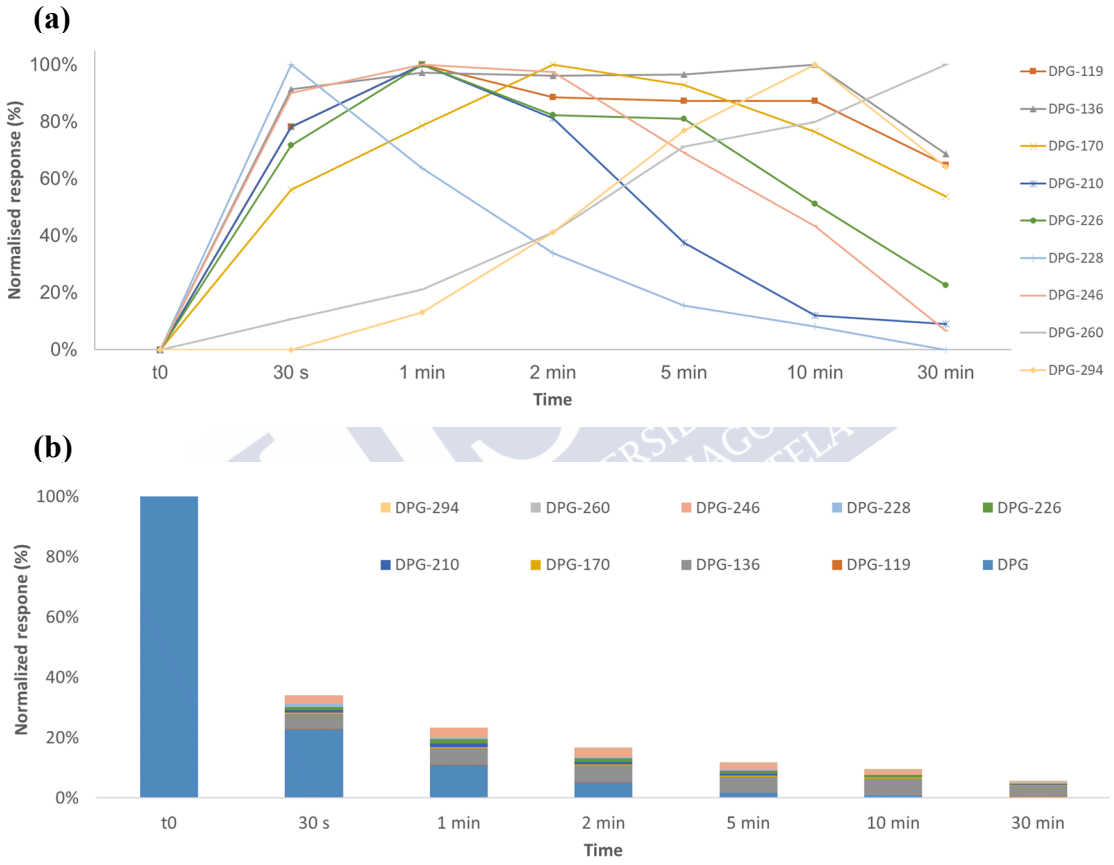

Figure IV.3.11. Plot summarizing the formation of TPs from DPG (10 µM DPG + 100 µM Cl_2) at different reaction times: (a) results normalized to the time when the TP reached its maximum; (b) results normalized by assuming that the response of the TPs was equal to DPG, except for DPG-136, DPG-119 and DPG-170 (where DPG-136 was used instead)

In the case of DTG (**Figure IV.3.12**), the most intense TP is DTG-254 (hydroxylated cyclic product) with a yield of ca. 30% at 0.5−2 min, followed by DTG-290 (hydroxy,chloro-DTG) with a yield of ca. 15% at 0.5−2 min. These two TPs are also the most relevant at 30 min, representing an estimated yield of 4 and 8% respectively. Also, in the case of DTG, the total yield of TPs at 30 min is ca. 20%.

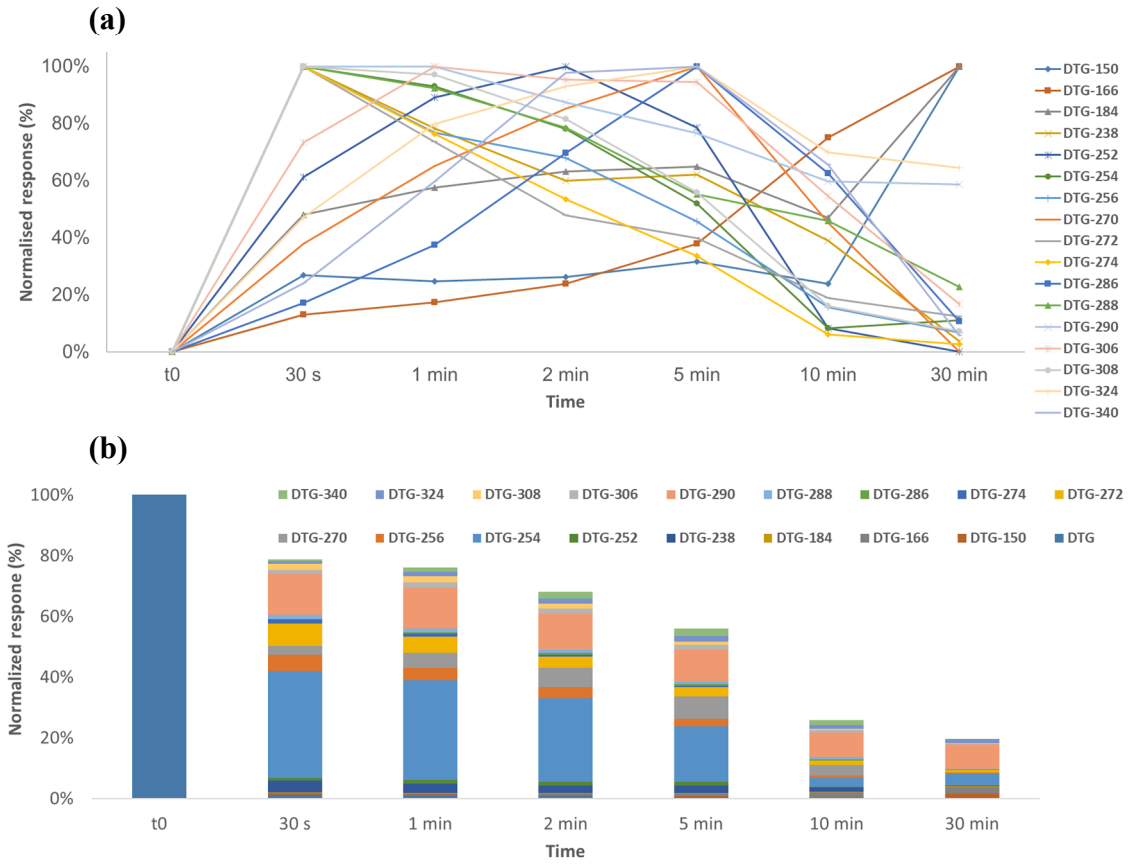

Figure IV.3.12. Plot summarizing the formation of TPs from DTG (10 μM DTG + 100 μM Cl_2) at different reaction times: (a) results normalized to the time when the TP reached its maximum; (b) results normalized by assuming that the response of the TPs was equal to DTG, except for DTG-150, DTG-166, DTG-184 and DTG-228 (where DPG-136 was used instead).

IV.3.4. Disinfection by-products

Subsequently to TPs identification, we investigated the formation potential of classical DBPs (chloroform and HANs). Chloroform was measured as the only THMs that can be formed without bromide and representing the most relevant group of DBPs, while HANs is another important group of DBPs which can be produced from N-containing chemicals, as it is the case of DPG and DTG. **Figure IV.3.13** shows the molar yields of $CHCl_3$ and dichloroacetonitrile (DCAN), the only HAN detected, produced from the chlorination of DPG and DTG after 2 day reaction time. Similar yields were obtained for both guanidines. For $CHCl_3$, the yield of ca. 25% for a molar guanidine/Cl_2 ratio of 1:100 is similar to $CHCl_3$ yields ranging from 10 to 32% already described for hydroxylated and chlorinated aromatic compounds[198]. This is consistent with the formation of chloro- or/and hydroxy- DPG and DTG that further react with chlorine leading to $CHCl_3$ as end-product after ring cleavage. Among HANs, only DCAN was detected at significant levels and with yields much lower than $CHCl_3$. For a ratio of 1:100, molar yields were 4.4% and 2.3% for DPG and DTG, respectively.

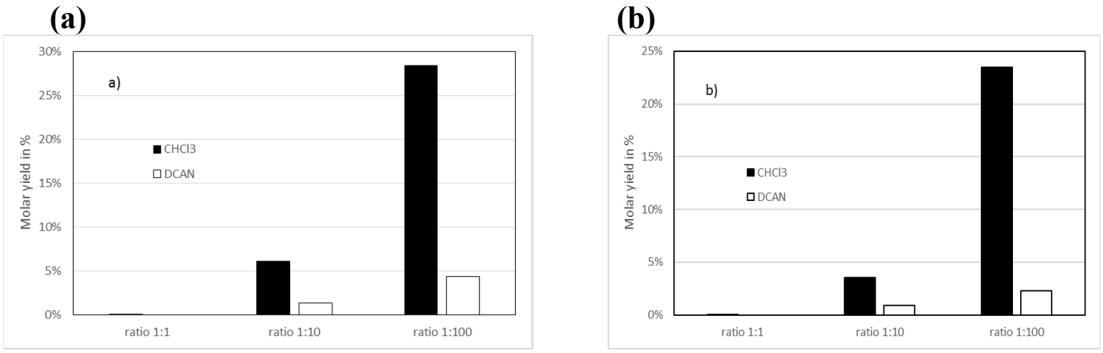

Figure IV.3.13. Molar yield of chloroform and DCAN obtained at different molar DPG/DTG:chlorine ratios: (a) DPG, (b) DTG. (pH 7.0, $[DPG]_o$ or $[DTG]_o$= 10 µM, reaction time 48 hours).

IV.3.5. Reaction in real sample matrices

The reactivity of both guanidine compounds was tested by spiking two real matrices (a surface water and a wastewater effluent) with 1 µM (i.e., ca. 200 µg L^{-1}) of either DPG or DTG and 10 µM chlorine and the reaction kinetics followed for 20 min (reaction quenched with ascorbic acid) by LC-HRMS.

In the case of the surface water, DPG and DTG reacted rapidly, being below 1% of their initial concentration after 2 min (**Figure IV.3.14a** and **b**). Conversely, with the effluent wastewater (with a higher TOC), still an 87% of DPG and 73% of DTG remained after 20 min (**Figure IV.3.14c** and **d**). Indeed, formation of TPs is easier to happen during drinking water production than by chlorination of wastewater (after secondary treatment). Even so, the chlorinated wastewater was analysed for the TPs previously identified in ultrapure water and several of them could be detected. The amount of bromide in those samples is very low (< 0.1 mg L^{-1}, see **III.3**), therefore no brominated TPs were detected. When excluding those brominated TPs, 6 out of 9 TPs where detected for DPG (DPG-136, DPG-228, DPG-210, DPG-226, DPG-260 and DPG- 294) and 7 out 16 where detected for DTG (DTG-150, DTG-256, DTG- 290, DTG-239, DTG-254, DTG-270 and DTG-288).

IV.3.6. (Eco)toxicity assessment

To obtain a preliminary estimation of the ecotoxicological implications of the chlorination reaction, the US EPA T.E.S.T. software was used in order to predict the toxicity of the two guanidines and their TPs. This prediction was performed only for *Daphnia Magna* LC_{50} (48 h), *Tetrahymena Pyriformis* LC_{50} (48 h) and oral rat LD_{50} (as a proxy of human toxicity), since the software was unable to produce an estimation for other endpoints. The results obtained are summarized in **Tables IV.3.8** and **IV.3.9**.

As it can be appreciated, oral rat toxicity LD_{50} values are in the 602−805 mg Kg^{-1} body weight for the two guanidines, which would classify them as Category 4 (i.e. the less toxic category) according to the ECHA Guidance[191]. The TPs would also be classified as Category 4. Hence human toxicological hazard is expected to be low.

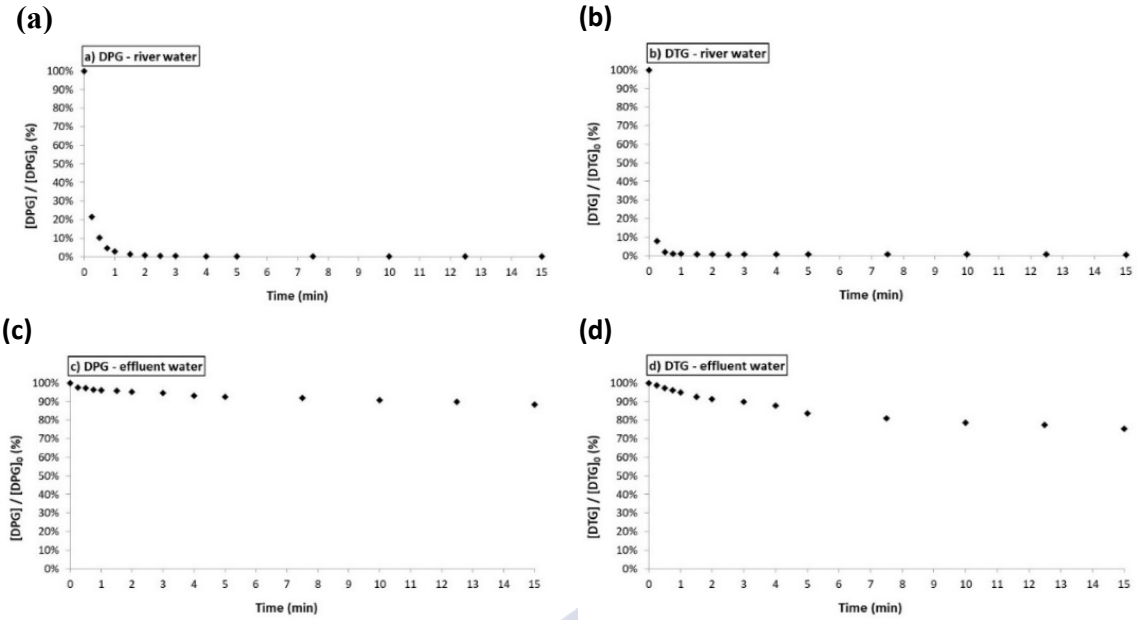

Figure IV.3.14. Dissipation plots during the chlorination of real water samples (1 µM DPG/DTG + 10 µM Cl_2): (a) DPG in river water, (b) DTG in river water, (c) DPG in effluent, (d) DTG in effluent.

Table IV.3.8. QSAR predicted toxicity values for DPG and its TPs.

	Daphnia magna	*T. pyriformis*	Oral rat
	LC_{50} (48 hr) (mg L^{-1})	IGC_{50} (48 hr) (mg L^{-1})	LD_{50} (mg kg^{-1})
DPG	5.09	28.5	805
DPG-119	16.4	np	493
DPG-136	30.6	np	500
DPG-170	11.5	np	455
DPG-210	5.29	11.4	908
DPG-214	1.14	9.53	1320
DPG-226	2.46	10.4	1143
DPG-228	5.24	21.1	2433
DPG-246	1.22	7.21	886
DPG-260	1.89	4.78	1241
DPG-290	1.14	9.53	1320
DPG-294	0.75	2.88	1019

np: no prediction possible

The predicted acute aquatic toxicity endpoint values lie in the 5−28 mg L^{-1} and 3−6 mg L^{-1} ranges, for DPG and DTG respectively (**Tables IV.3.8** and **IV.3.9**). Thus, they would not be classified as Category Acute 1 (the only acute aquatic toxicity category) according to the ECHA Guidance[191]. As regards the TPs, the predicted aquatic toxicity of the monoguanidine TPs is lower than the precursor guanidines for the crustacean *Daphnia Magna*, while it could not be predicted for the fish *T. pyriformis*. On the other hand,

particularly TPs which are halogenated are predicted to be more toxic. Thus, DPG-294 and 14 TPs from DTG (see **Table IV.3.8** and **IV.3.9**) would have a predicted toxicity endpoint< 1 mg L^{-1} and would thus be classified in the Category Acute 1 for aquatic organisms. Care must be taken with these data, since the third trophic level (algae) toxicity could not be predicted, and values obtained for algae can likely result into more ecotoxicity. In fact, DTG is classified in the REACH dossier as Aquatic Acute 1[192].

Table IV.3.9. QSAR Predicted toxicity values for DTG and its TPs.

	Daphnia magna LC_{50} (48 hr) (mg L^{-1})	*T. pyriformis* IGC_{50} (48 hr) (mg L^{-1})	Oral rat LD_{50} (mg kg^{-1})
DTG	2.92	5.53	602
DTG-150	27.5	np	498
DTG-166	23.5	np	993
DTG-184	22.7	np	429
DTG-228	5.00	np	519
DTG-238	3.14	6.35	553
DTG-254	1.68	8.26	1036
DTG-256	3.43	9.19	1259
DTG-270	2.16	6.52	1121
DTG-272	2.52	11.2	2352
DTG-274	0.70	2.29	1178
DTG-286	8.28	9.80	527
DTG-288	0.76	1.98	721
DTG-290	0.93	2.14	1014
DTG-306	0.95	2.06	1870
DTG-308	0.49	1.24	1109
DTG-318	0.39	4.35	1103
DTG-324	0.74	1.11	940
DTG-332	0.51	1.55	1627
DTG-334	0.87	3.21	927
DTG-340	0.31	1.11	1074
DTG-250	0.79	2.38	1485
DTG-396	0.19	1.46	563
DTG-412	0.28	1.21	823
DTG-426	0.03	0.55	384

np: no prediction possible

Furthermore, the acute toxicity of DPG and DTG was assessed using the bioluminescent *Vibrio fisheri* test. **Figure IV.3.15** shows two dose-response curves of DPG after an incubation time of 30 min at 15 °C.

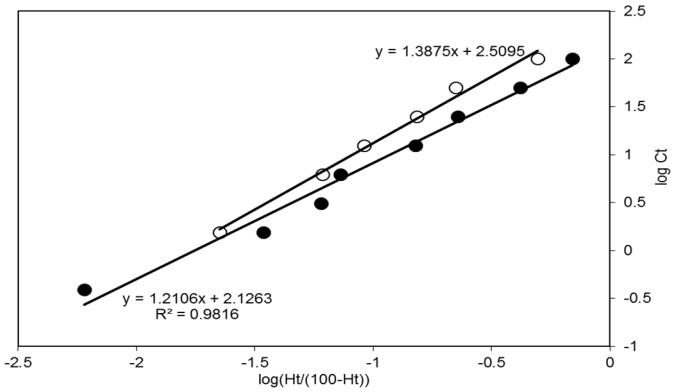

Figure IV.3.15. Dose-response curves log(Ct) versus log (Ht / (100 – Ht)) for EC_{50} and EC_{20} value calculations of DPG toxicity using Microtox® test. See III.4.8.2.1. for calculation details. The two different symbols correspond to two replicate experiments.

The initial EC_{20} of DPG was 40 ± 2 mg L^{-1} and the EC_{50} was estimated to be 245 ± 33 mg L^{-1} from extrapolation of the dose-response curves. The toxicity of DTG was lower and only an EC_{20} of 80 mg L^{-1} could be determined. These results confirm that both guanidines have a low acute aquatic toxicity. Due to solubility limitations, the effect of chlorination on acute toxicity was only tested with a DPG solution of 40 mg L^{-1} corresponding to the EC_{20}. Chlorination was performed with chlorine doses of 40 and 400 mg Cl_2 L^{-1} (i.e. molar Cl_2/DPG ratio of 3 and 30). Toxicity tests were conducted after the absence of chlorine residual was checked. Results in **Figure IV.3.16** shows that the bioluminescence inhibition strongly increases from 14% before chlorination to 45 and 99% for Cl_2/DPG ratios of 3 and 30, respectively. Similar results were generally observed in the literature after chlorination and were assigned to more toxic halogenated TPs[160,203]. Even though the increase of toxicity could not be assigned to specific TPs/DBPs, results of bioluminescent *Vibrio fisheri* test were in agreement with predicted aquatic toxicity endpoints obtained by QSAR.

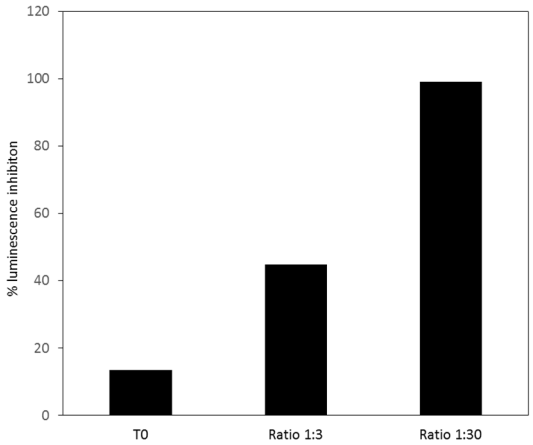

Figure IV.3.16. Evolution of bioluminescence inhibition measured using *Vibrio fisheri* Microtox® test during DPG chlorination. $[DPG]_o$ = 40 mg Cl_2 L^{-1}, molar DPG:Cl_2 ratios of 1:3 and 1:30, chlorination time of 4 days at pH 7.0

IV.3.7. Annex

This annex contains:

Figure SIV.3.1: Chromatograms and MS/MS spectra of DPG and its TPs: (a) DPG, (b) DPG-119, (c) DPG-136, (d) DPG-170, (e) DPG-210, (f) DPG-214, (g) DPG-226, (h) DPG-228, (i) DPG-246, (j) DPG-260, (k) DPG-290 and (l) DPG-294.

Figure SIV.3.2: Chromatograms and MS/MS spectra of DTG and its TPs: (a) DTG, (b) DTG-150, (c) DTG-166, (d) DTG-184, (e) DTG-228, (f) DTG-238, (g) DTG-254, (h) DTG-256, (i) DTG-272, (j) DTG-290, (k) DTG-308, (l) DTG-318, (m) DTG-324, (n) DTG-334 and (o) DTG-412.

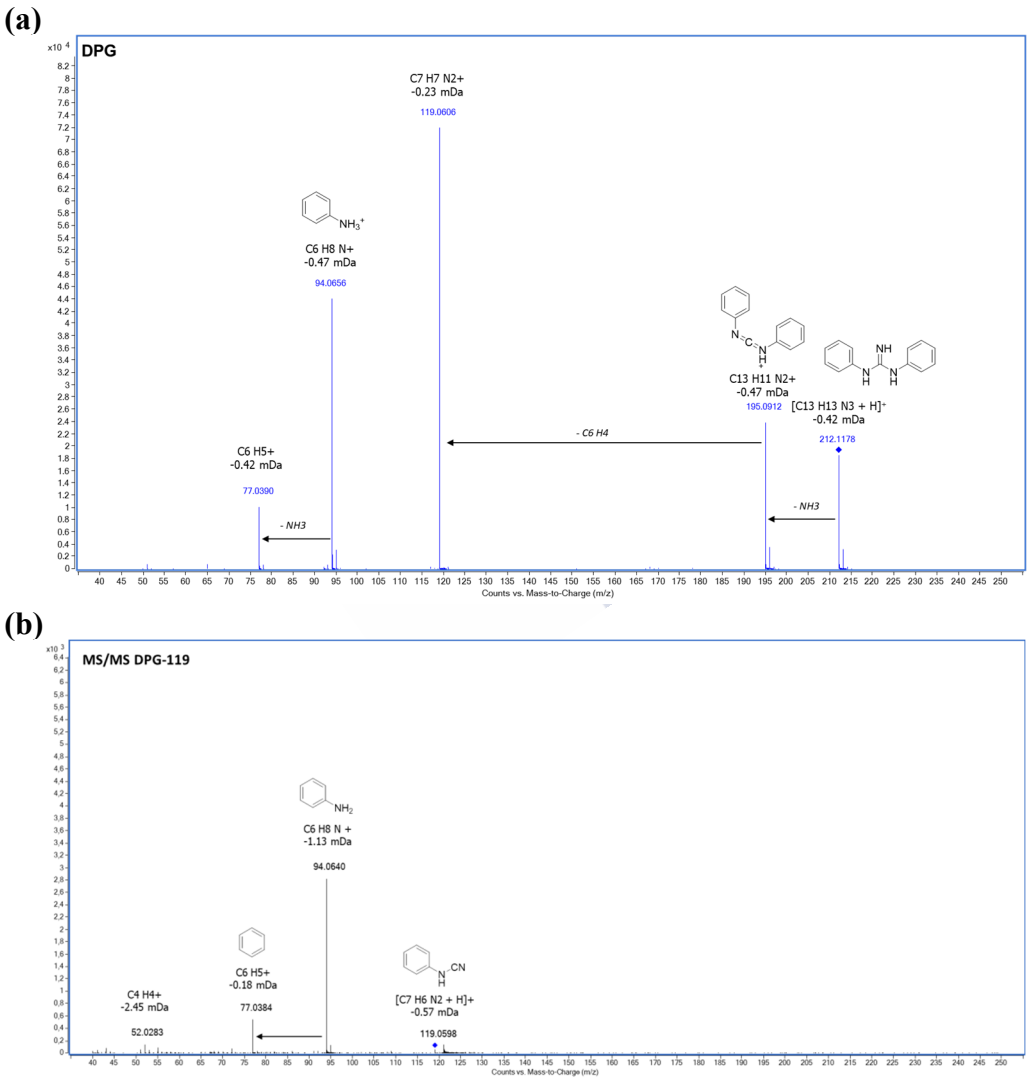

Figure SIV.3.1: Chromatograms and MS/MS spectra of DPG and its TPs: (a) DPG, (b) DPG-119

(c)

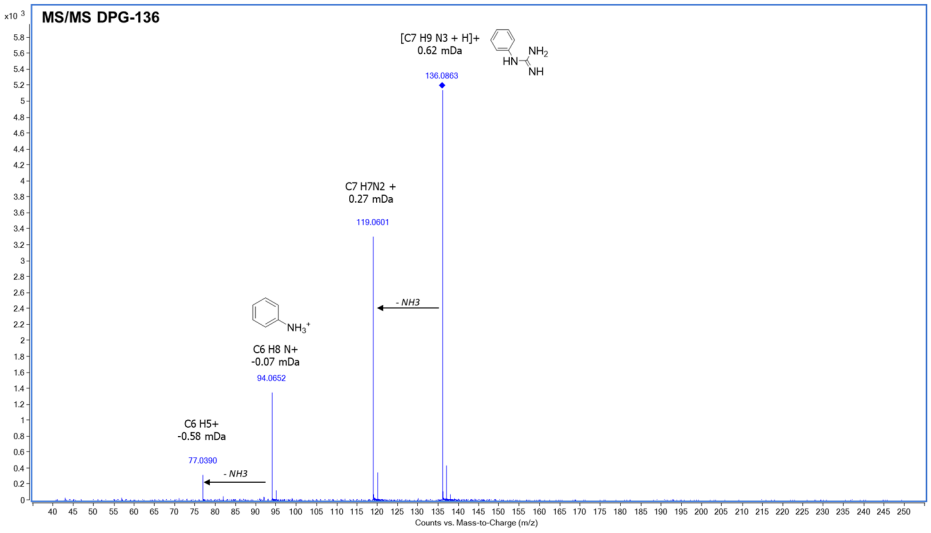

(d)

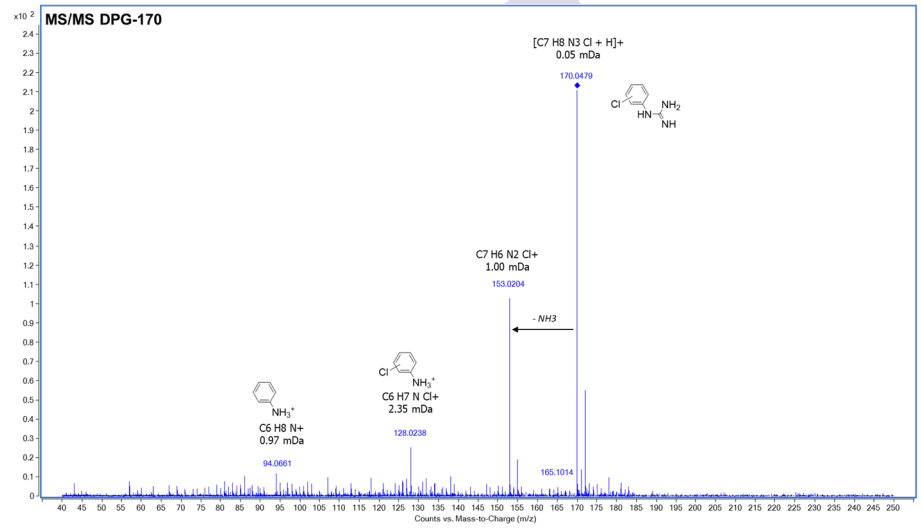

(e)

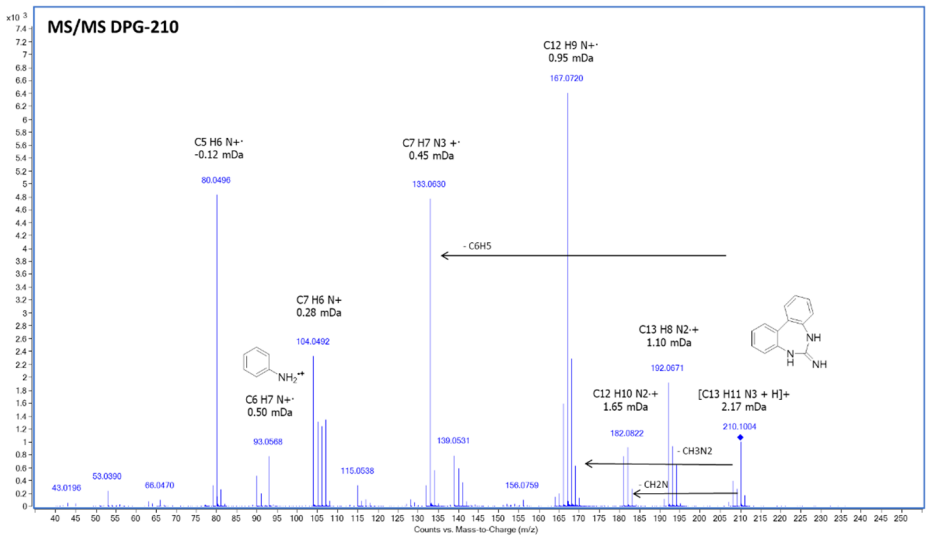

Figure SIV.3.1 (cont.): Chromatograms and MS/MS spectra of DPG and its TPs: (c) DPG-136, (d) DPG-170, (e) DPG-210

(f)

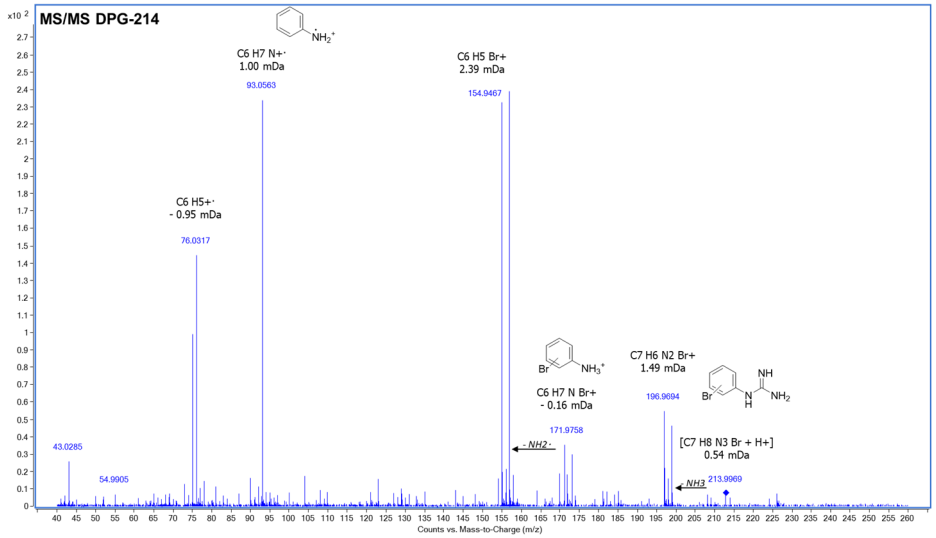

(g)

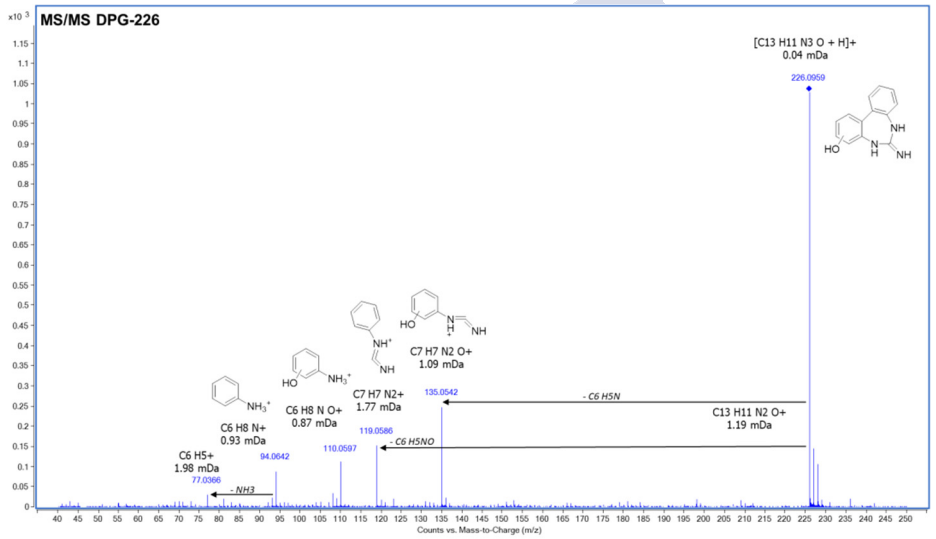

(h)

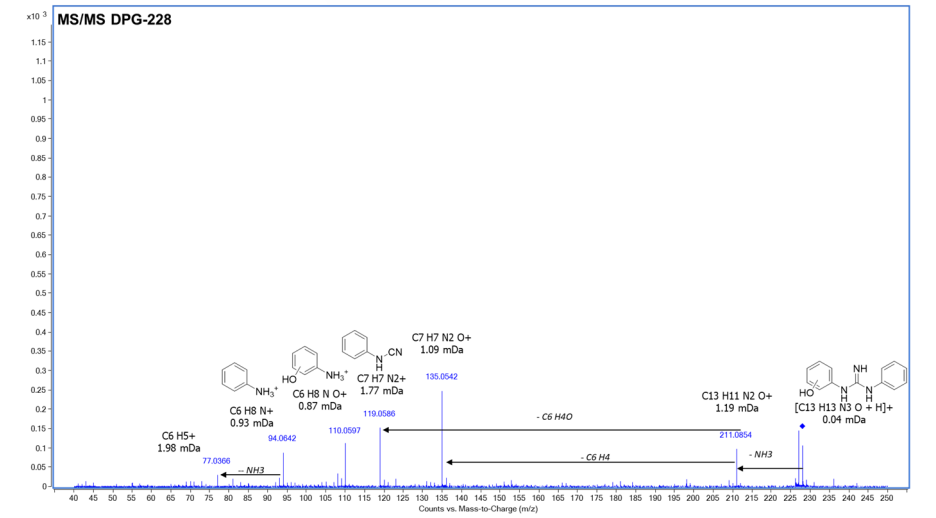

Figure SIV.3.1 (cont.): Chromatograms and MS/MS spectra of DPG and its TPs: (f) DPG-214, (g) DPG-226, (h) DPG-228

(i)

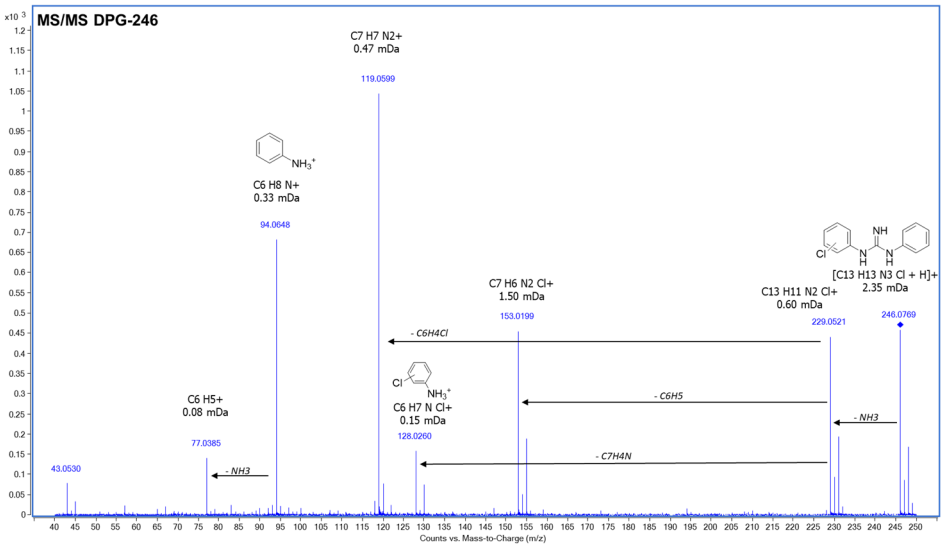

(j)

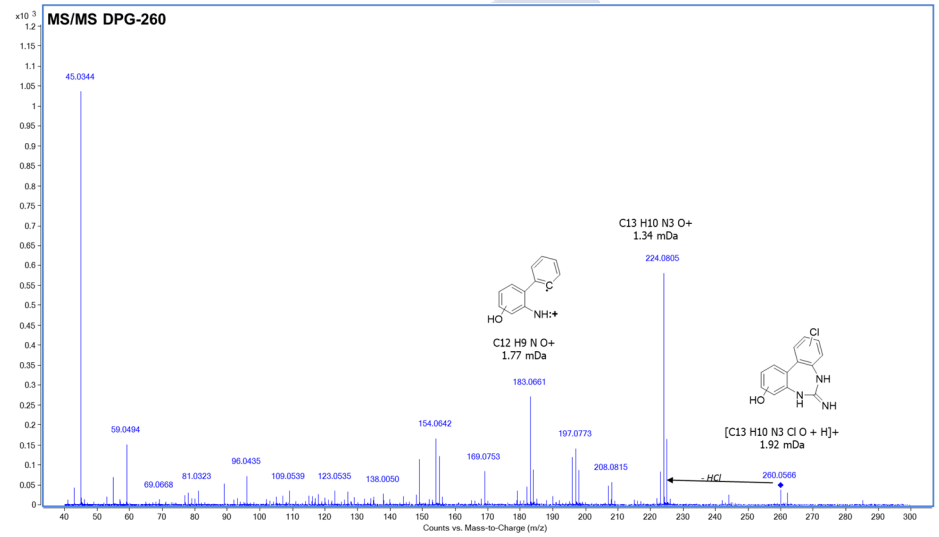

(k)

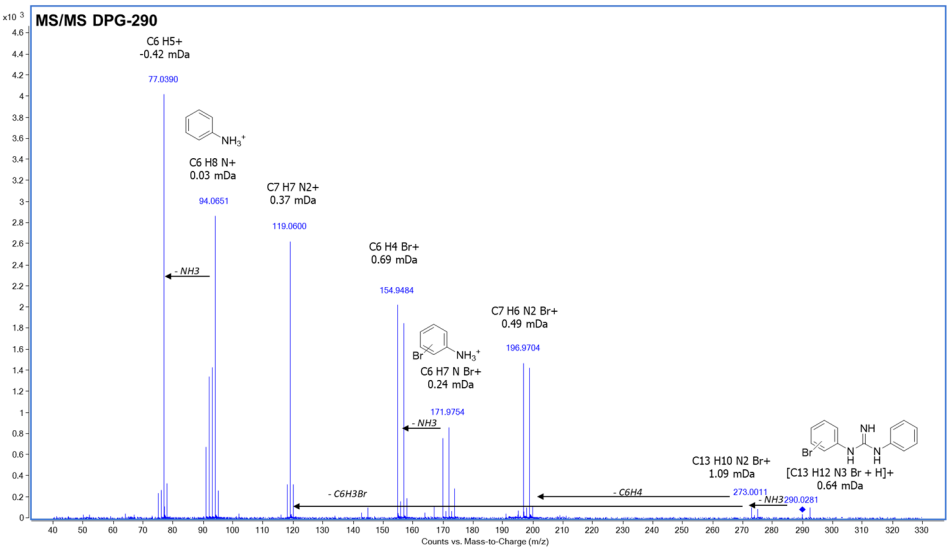

Figure SIV.3.1 (cont.): Chromatograms and MS/MS spectra of DPG and its TPs: (i) DPG-246, (j) DPG-260, (k) DPG-290

(l)

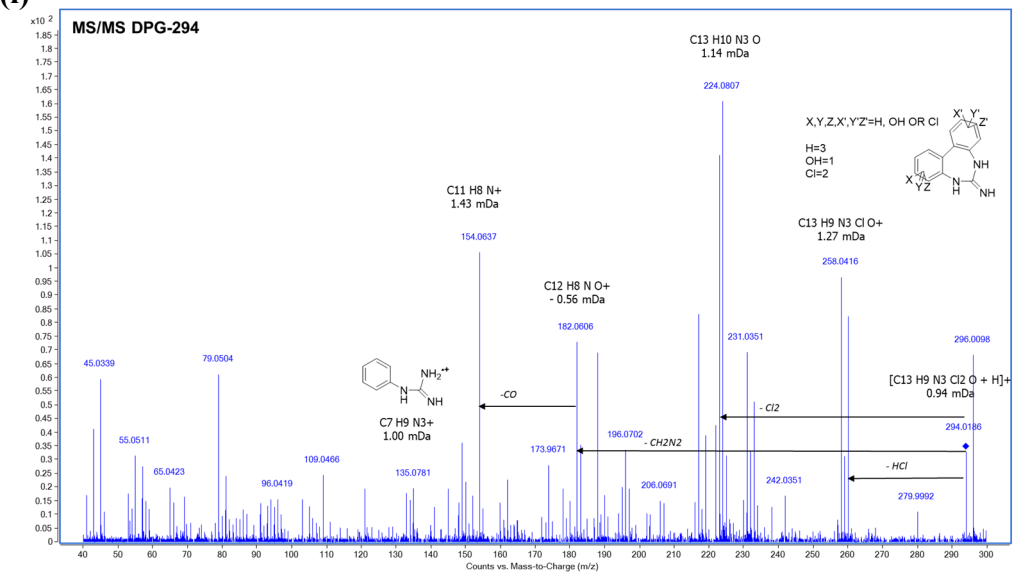

Figure SIV.3 (cont.): Chromatograms and MS/MS spectra of DPG and its TPs: (l) DPG-294.

(a)

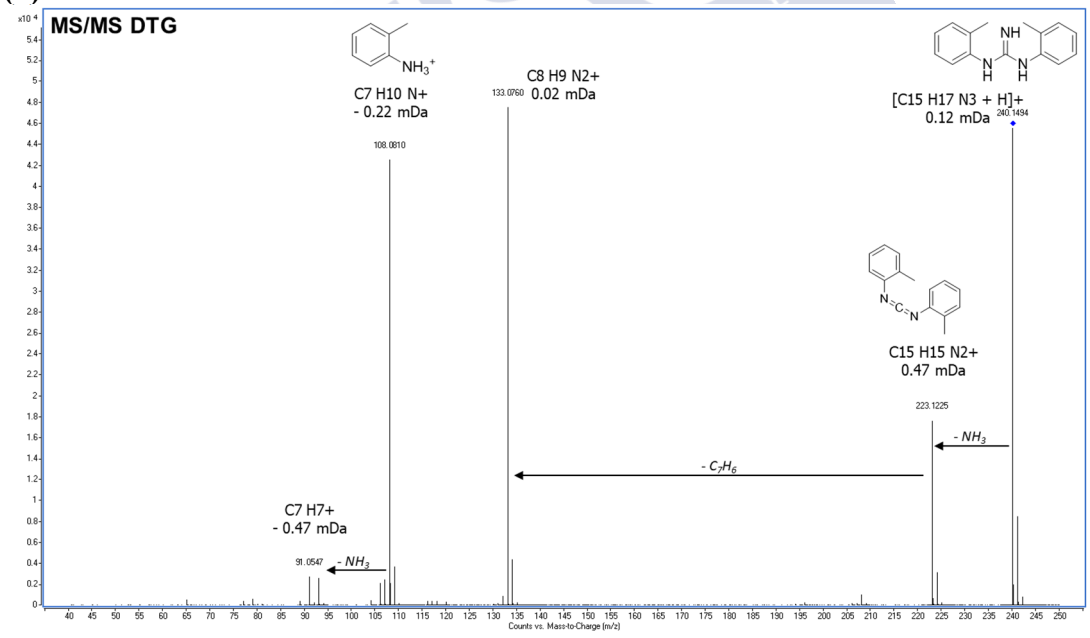

Figure SIV.3.2: Chromatograms and MS/MS spectra of DTG and its TPs: (a) DTG

(b)

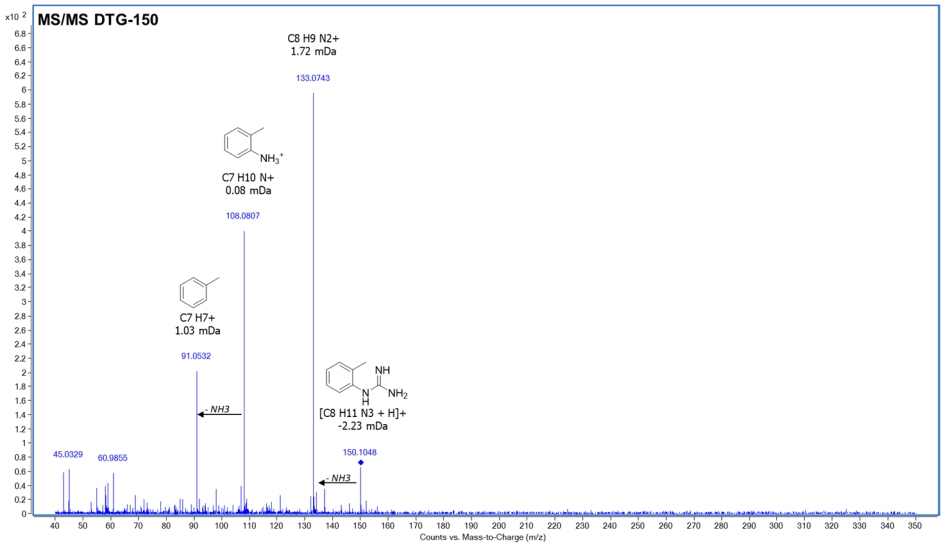

(c)

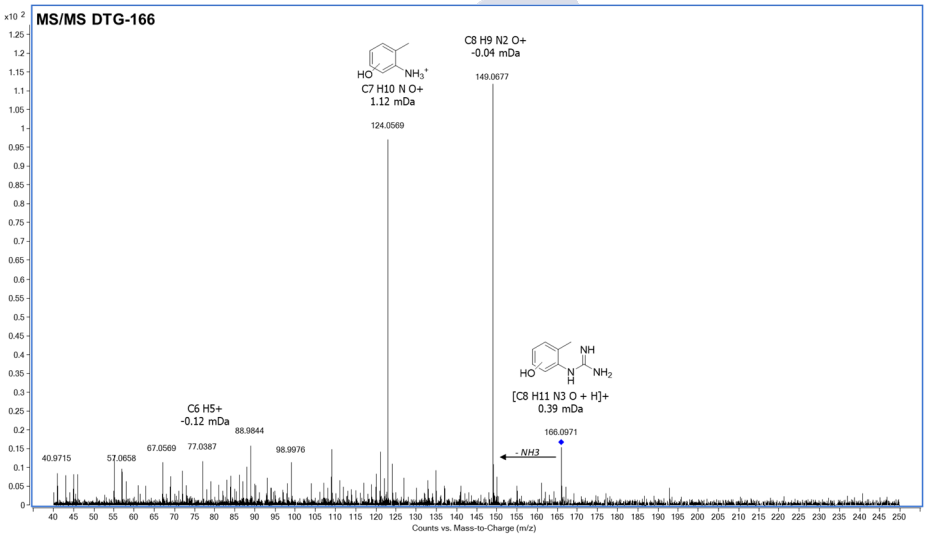

(d)

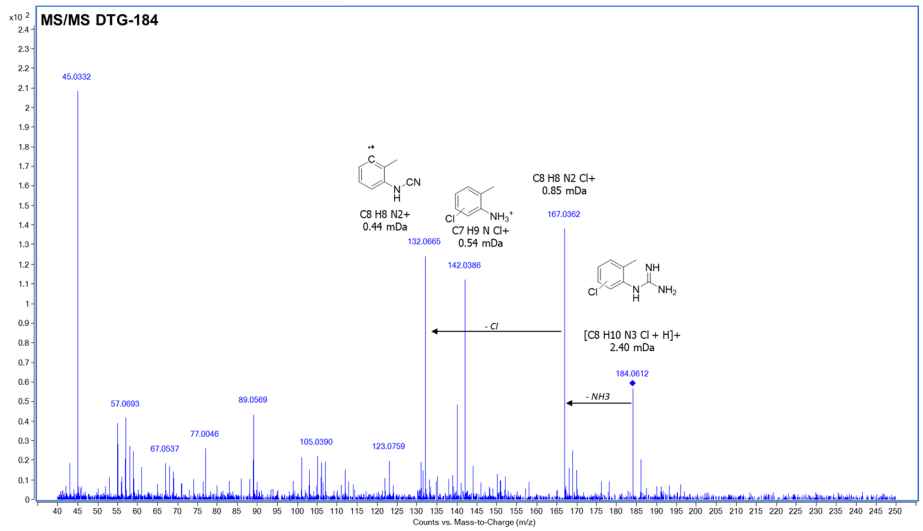

Figure SIV.3.2 (cont.): Chromatograms and MS/MS spectra of DTG and its TPs: (b) DTG-150, (c) DTG-166, (d) DTG-184

(e)

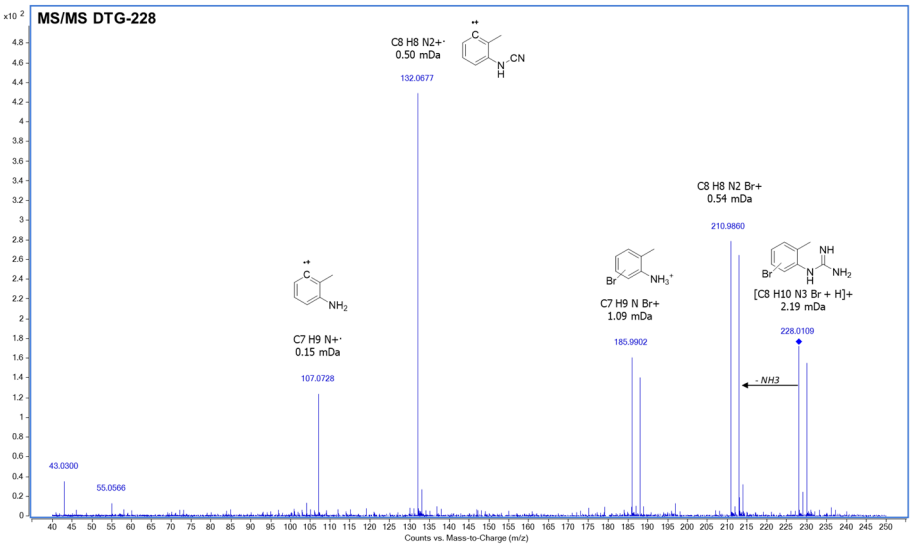

(f)

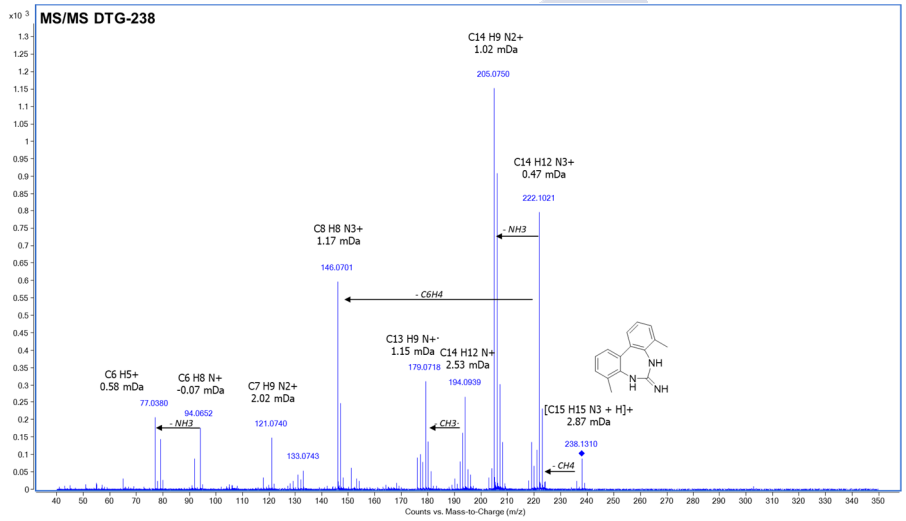

(g)

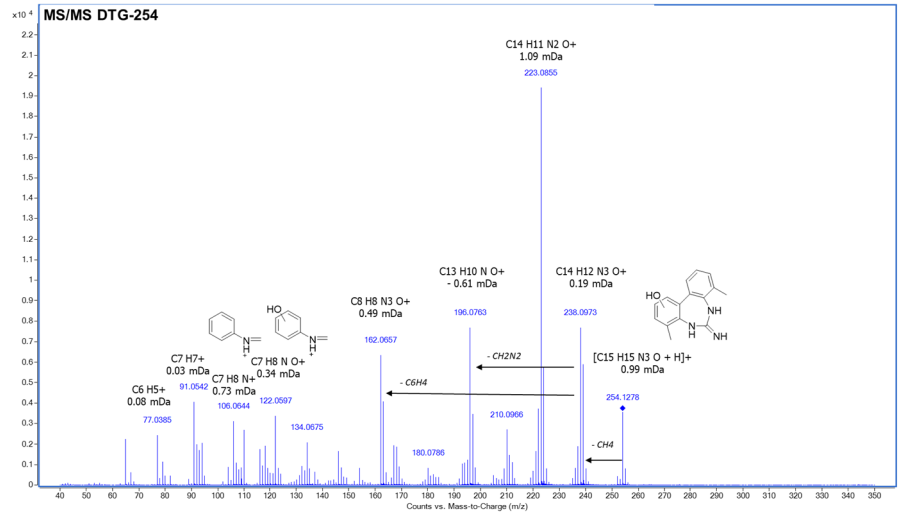

Figure SIV.3.2 (cont.): Chromatograms and MS/MS spectra of DTG and its TPs: (e) DTG-228, (f) DTG-238, (g) DTG-254

(h)

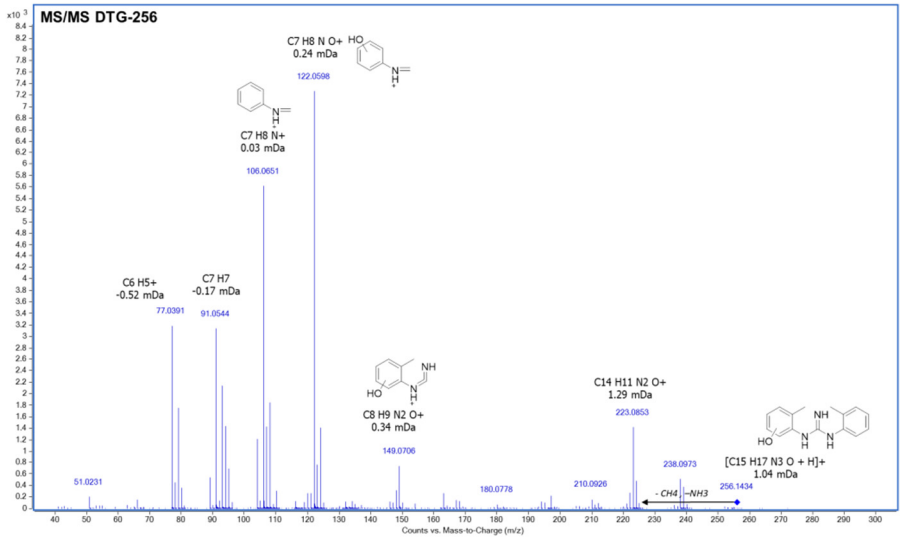

(i)

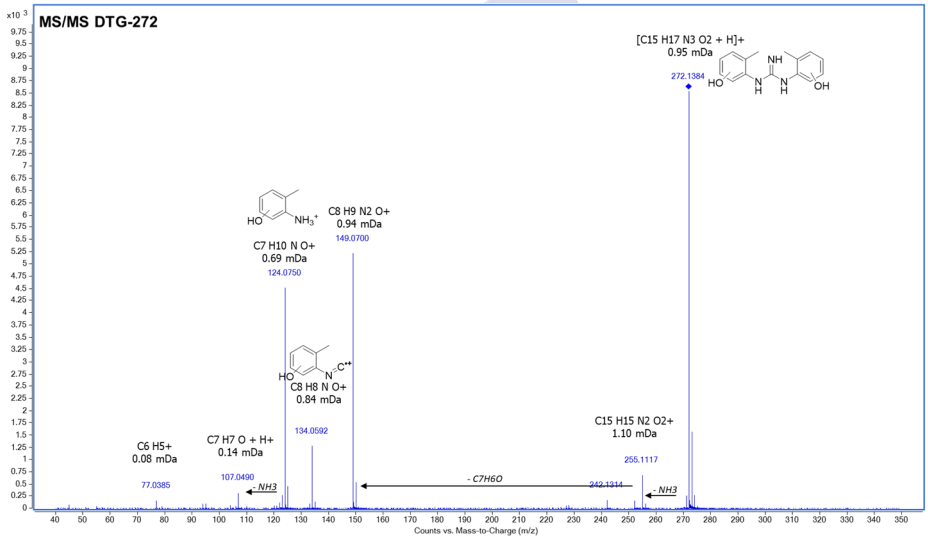

(j)

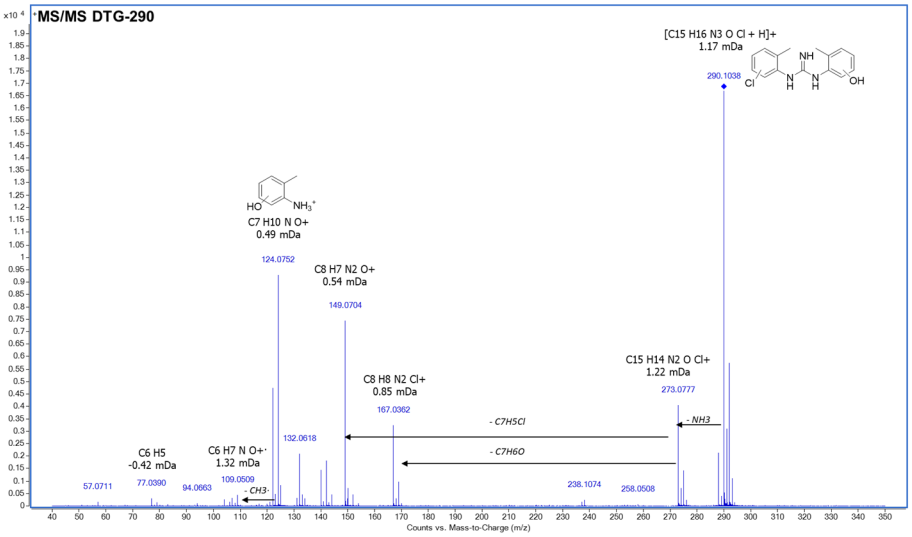

Figure SIV.3.2 (cont.): Chromatograms and MS/MS spectra of DTG and its TPs: (h) DTG-256, (i) DTG-272, (j) DTG-290

(k)

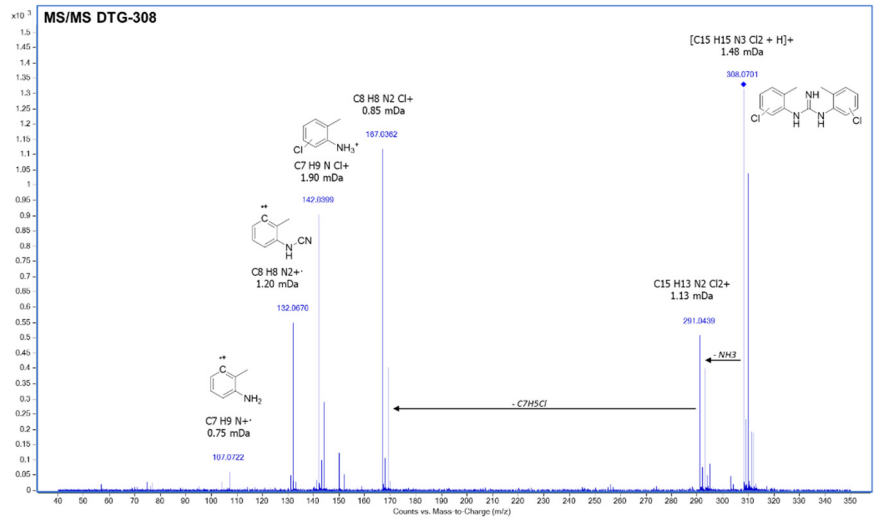

(l)

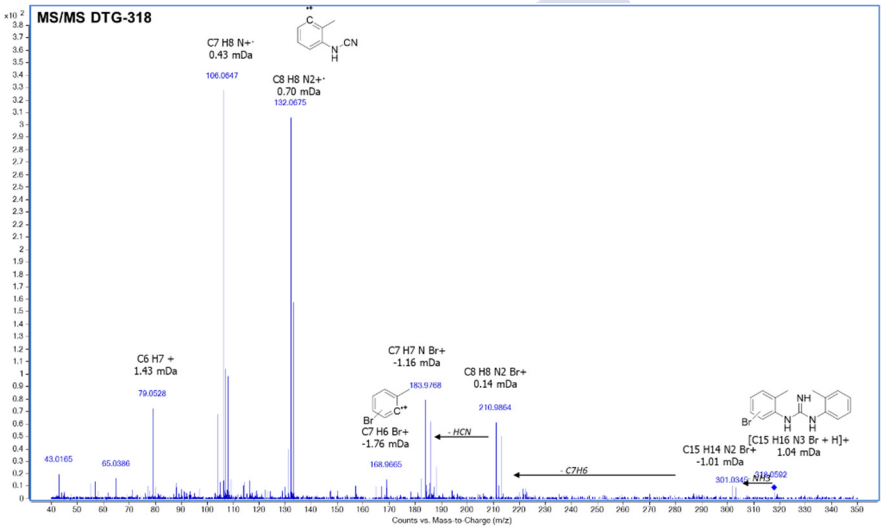

(m)

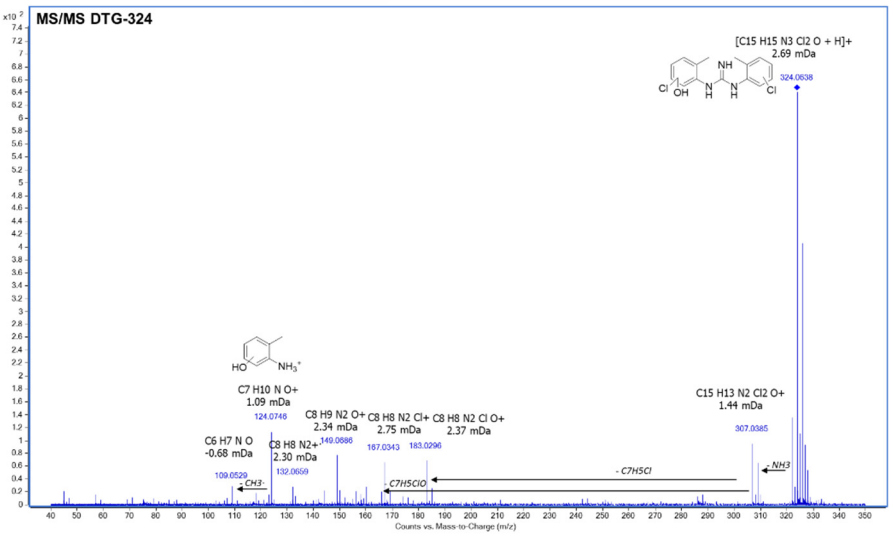

Figure SIV.3.2 (cont.): Chromatograms and MS/MS spectra of DTG and its TPs: (k) DTG-308, (l) DTG-318, (m) DTG-324

(n)

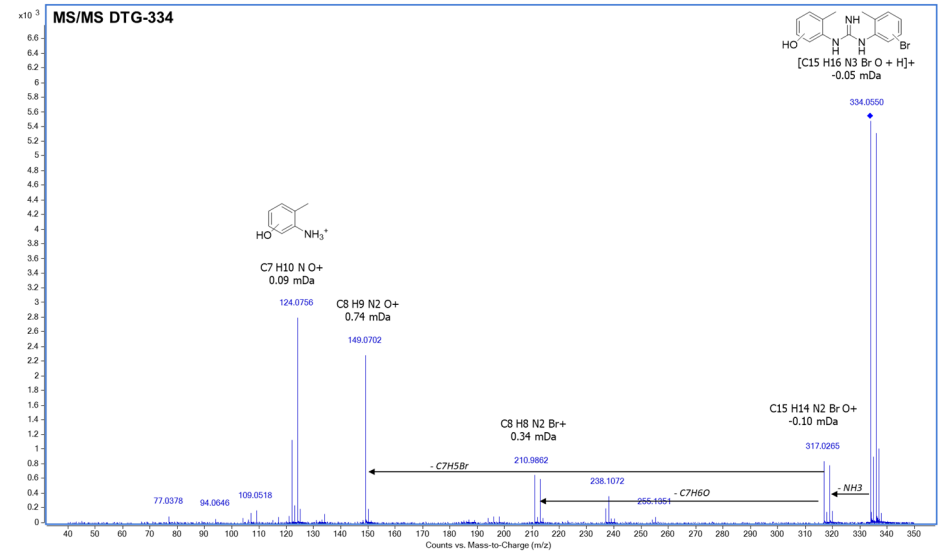

(o)

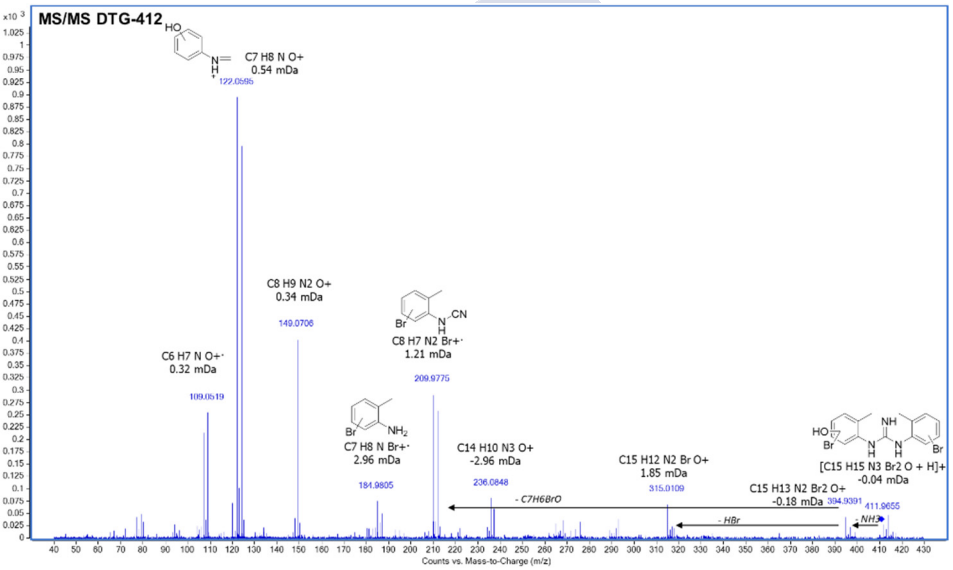

Figure SIV.3.2 (cont.): Chromatograms and MS/MS spectra of DTG and its TPs: (n) DTG-334 and (o) DTG-412.

USC
UNIVERSIDADE
DE SANTIAGO
DE COMPOSTELA

IV.4. Removal of Ibuprofen by UV-C laser pulsed irradiation

The results collected in this chapter have been partly published in:

Francisco Rey-García, Benigno José Sieira, Carmen Bao-Varela, José Ramón Leis, Luis Alberto Angurel, José Benito Quintana, Rosario Rodil, Germán Francisco de la Fuente

Can UV-C laser pulsed irradiation be used for the removal of organic micropollutants from water? Case study with ibuprofen.

Science of the Total Environment 742 (2020) 140507.

DOI: 10.1016/j.scitotenv.2020.140507.

This work was performed in collaboration with Francisco Rey-García, Carmen Bao-Varela and José Ramón Leis of the "Photonics4life" group from the Universidade de Santiago de Compostela and Germán Francisco de la Fuente and Luis Alberto Angurel of the Aragón Materials Science Institute (ICMA), a Joint Research Institute of the Spanish National Research Council (CSIC) and the University of Zaragoza (UZ).

Toxicity assessment was performed in collaboration with Susana Barros, Miguel Santos and Teresa Neuparth of the Endocrine Disrupters and Emerging Contaminants Group from the Interdisciplinary Centre of Marine and Environmental Research (CIIMAR) and the University of Porto (Portugal).

USC
UNIVERSIDADE
DE SANTIAGO
DE COMPOSTELA

The objective of this work is to explore the potential of ns pulsed UV lasers, for direct photochemical removal of micropollutants present in water. For this purpose, IBU (**Figure IV.4.1**) was selected as a proof of principle, model compound, and 266 nm as the emission wavelength of the laser. This wavelength is as the absorbance bands found in aromatic rings and poly-unsaturated groups, present in most NSAIDs compounds. Particular consideration was given to the presence of reported photochemical TPs, since they can be in some cases more toxic than the original organic contaminant compounds themselves[25].

IBU is one the pharmaceuticals detected at higher concentrations in water [204,205]. For these reasons, removal technologies, such as biodegradation during wastewater treatment[206], UV disinfection[207] and other AOPs have been tested with IBU and other NSAIDs, with the objective of improving their removal efficiency during wastewater treatment[208–210].

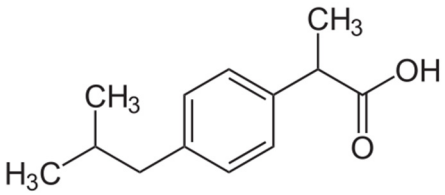

Figure IV.4.1. Structure of ibuprofen

IV.4.1. Laser irradiation of ultrapure water samples

Initial irradiation experiments were performed with double distilled water spiked with IBU, for maximum periods of 15 min. The UV–vis spectrum of IBU in ultrapure water presents two maxima around 221 and 193 nm, with the latter contributed by two bands at 191.7 and 193.4 nm. These maxima can be ascribed to conjugated pi-electrons of the aromatic ring. Additionally, the C=O double bond also promotes signals between 170 and 200 and, moreover, around 270 nm due to n➔π* and π➔π* transitions. When the sample is irradiated, a weak broad band centred at 260 nm is observed in the spectra (**Figure IV.4.2**). This band's intensity increases up until 2 min of irradiation time, while those with maxima at 221 and 193 nm decrease as the solution is irradiated, suggesting that IBU has been transformed by pulsed laser irradiation. This transformation takes place during the first 12 min of irradiation; the spectrum remains unchanged thereafter (**Figure IV.4.2**).

Moreover, the formation of a clear isosbestic point (i.e. wavelength at which the absorbance of a sample does not change) at 233.5 nm is observed in early stages of the reaction, disappearing after 3 min irradiation. This behavior is consistent with the occurrence of a typical consecutive transformation process (such as A➔B➔C; where A represents IBU, B intermediate TPs, and C the final products).

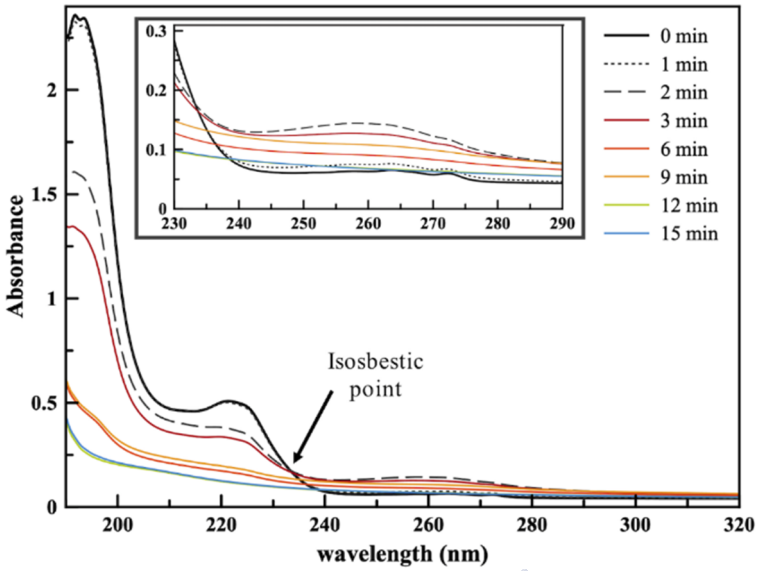

Figure IV.4.2. UV absorption spectra of irradiated IBU 10 mg L^{-1} solutions noting the isosbestic point. Inset: detail of absorption spectra around band at 260 nm.

Aiming to corroborate and quantify the above results, i.e. measure the dissipation of IBU and screen for possible TPs being produced, samples were measured in the UHPLC-QTOF-MS system (see **Section III.4.6**) at different irradiation times. As presented in **Table IV.4.1**, 5 TPs (out of the 19 TPs screened for) could be tentatively identified. The tentatively identified TPs arose from hydroxylation and decarboxylation routes, suggesting a free radical transformation mechanism, as observed by Adityosulindro et al.[211].

Figure IV.4.3 represents the amount of IBU and TPs in ultrapure water at different irradiation times (**Table IV.4.2**), and, also confirms the observations by direct UV–vis spectroscopy (**Figure IV.4.2**), as IBU decreases rapidly until its complete elimination with an irradiation treatment of 15 min. On the other hand, the TPs intensity is higher during the first few minutes of irradiation, thus only the monohydroxylated and dihydroxylated TPs (TP-177, TP-221 and TP-237) remain at the end of the experiment, summing an apparent yield (calculated assuming an LC-HRMS response equivalent to IBU) <10%. Since no pure standards are available for the TPs identified, their yield was calculated considering that their response is the same as that of IBU.

Initial and final (15 min) samples were also analyzed for DOC and a DOC removal of 25% (from 8.5 to 6.4 mg L^{-1}) was measured. This, together with what is observed in **Figure IV.4.3** (**Table IV.4.2**), would indicate that IBU is mostly transformed to low molecular weight chemicals and volatile compounds.

Table IV.4.1: LC-HRMS data on IBU and the detected TPs. TPs were screened for as detailed on Section III.4.6

Compound	Molecular formula	$[M-H]^-$ (m/z)	Error (ppm)	Score (%)[a]	Structure[b]	Reference
IBU	$C_{13}H_{18}O_2$	205.1234	-1.96	99.23	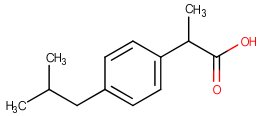	--
TP-237	$C_{13}H_{18}O_3$	237.1132	3.28	97.36	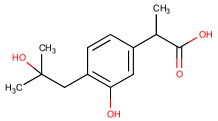	157
TP-221	$C_{13}H_{18}O_3$	221.1183	-2.33	98.8	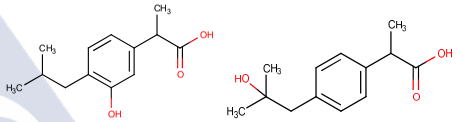	157
TP-191	$C_{12}H_{16}O_2$	191.1078	-1.84	99.38	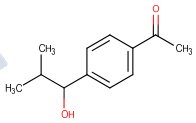	158
TP-177	$C_{12}H_{18}O$	177.1285	-2.18	99.21	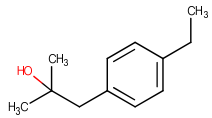	158
TP-175	$C_{12}H_{16}O$	175.1128	5.33	95.52	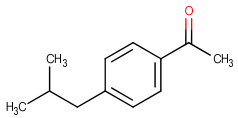	157

[a] The score (in percentage) represents how well molecular formula and HRMS data match, considering mass error and isotopic profile

[b] Structures proposed based on the referenced published literature

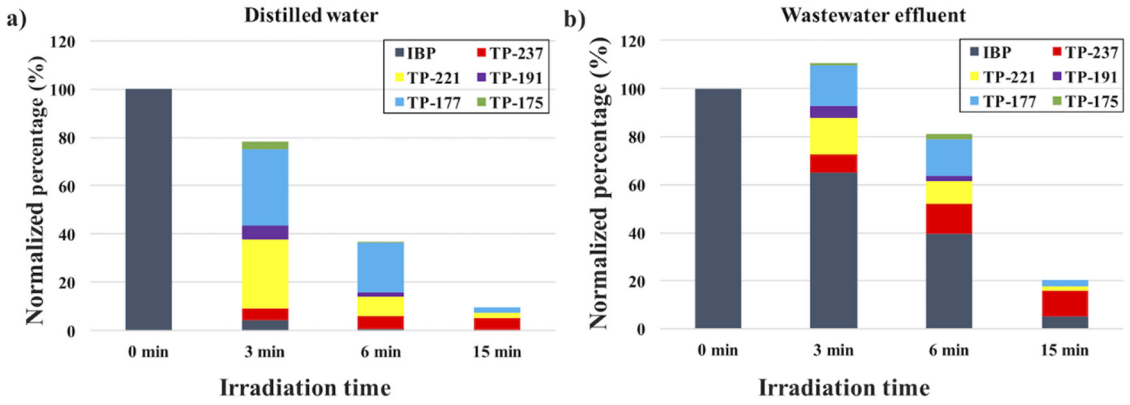

Figure IV.4.3. Graphics representing the percentage of IBU remaining and TPs formed at different irradiation times in a) ultrapure, and b) effluent water. N.B.: the yield of the TPs formed was calculated (Tables IV.4.2 and IV.4.4) considering that their response is the same as that of IBU, since no pure standards were available.

Table IV.4.2: Percentage of IBU remaining, and TPs formed at different irradiation times in ultrapure water. N.B.: the yield of the TPs formed was calculated considering that their response is the same as that of IBU, since no pure standards were available.

Time (min)	IBU	TP-237	TP-221	TP-191	TP-177	TP-175
0	100	0.0	0.0	0.0	0.0	0.0
3	4.1	5.1	28.6	5.6	31.9	2.9
6	0.7	5.3	8.2	1.6	20.4	0.4
15	0.0	5.2	2.3	0.0	2.3	0.0

Table IV.4.3: Comparison of different approaches for IBU removal in ultrapure water.

Process	Conc. (mg L^{-1})	Volume (mL)	Time (min)	Power density (Mj cm^{-2})	IBU removal	TOC removal	Reference
UV-vis/H_2O_2/Fe(II)	179	1500	60	-	100%	~40%	158
UVA/TiO_2	5	2000	120	-	98.9%	-	212
UVA/TiO_2	10	500	18	0.06	100%	-	213
UVA/ZnO	10	500	18	0.06	100%	-	213
UVC	46	20	60	0.04	70%	-	207
H_2O_2/Fe	20	9	120	-	88%	27%	211
UV-vis/TiO_2nano	5	50	180	-	100%	-	214
UVC (LASER)	10	4	12	18	100%	25%	This work

Table IV.4.3 compares the results obtained in this work with the literature on IBU photochemical studies, including photocatalysis and AOPs. As can be appreciated, direct laser pulsed irradiation can provide removal efficiencies similar to those obtained by

methods which include a catalyst, and H_2O_2 in some cases, without requiring additional reagents. Indeed, this data was obtained from a batch scale and would need to be confirmed at a larger scale. In addition, the efficiency of the laser source is higher than that of conventional lamps, as demonstrated comparing the power density of the different sources included in **Table IV.4.3**.

IV.4.2. Mechanistic considerations

No changes were detected in the temperature of the solutions during the irradiation experiments. However, a local significant temperature increase could have taken place since the laser pulse duration (nanoseconds) is faster than the molecule or solvent thermal relaxation time. On the other hand, remarkable changes in the pH of the solution were observed along the time length of the experiment. The pH decreases from 5.25 to 4.52 when IBU has been completely degraded, as observed in **Figure IV.4.2** and corroborated in **Figure IV.4.3** (**Table IV.4.2**). This effect was attributed to the extraction of hydroxyl groups associated to the formation of hydroxylated TPs (**Table IV.4.1**).

Thermal pulsed laser cumulative effect (also known as incubation) was also tested as a first assay on the possible production of radicals. Thus, **Figure IV.4.4** represents the spectra of a solution irradiated consecutively in sets of 1 min intervals (with 2 min rest periods between each irradiation), up to a total cumulative irradiation time of 12 min. Intervals of 1 min were selected here considering the results presented in **Figure IV.4.2**. These suggest that, within the 1–2 min interval, there is a significant change in the effect of laser irradiation. During the first minute a low amount of IBU has been removed while, after 2 min irradiation, peak intensity maxima decrease considerably, evidencing an important IBU loss. Following this methodology, the degradation process of IBU takes place slowly since the peak maxima slightly decrease in their intensity and the isosbestic point is observed even after 12 min of consecutive irradiation. This fact suggested that the process is stopped in reaction A➔B, evidencing that the following consecutive step, namely B➔C, has not taken place and supposing that radicals are not formed, or that their concentration after 1 min irradiation is not sufficient to promote the consecutive reaction. Considering that in previous experiments ~96% IBU is degraded (**Table IV.4.2**) and, concomitantly, achieving a maximum amount of 28.6% for TP-221 after 3 min irradiation, it is reasonable to ascertain that a minimum threshold irradiation time above 1 min is needed to achieve the consecutive process A➔B➔C. Thus, a minimum of incubation energy in the form of light quanta, would be needed to ensure complete degradation of IBU and, therefore, to ensure a consecutive process. Likewise, it was verified that the spectra of the 3 and 6 min irradiated solutions were maintained after 4 days, demonstrating altogether the irreversibility of the reaction.

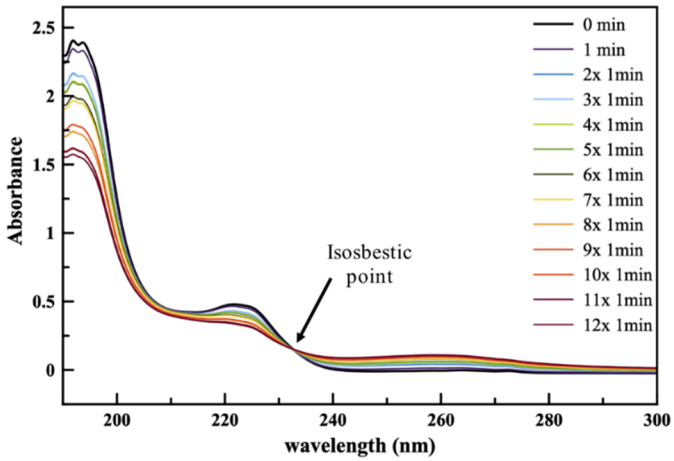

Figure IV.4.4. UV/Vis absorption spectra of a 10 mg L^{-1} IBU solution irradiated during consecutive 1 min intervals, with 2 min rest in between each irradiation

The probed stability, together with that observed in cumulative studies suggest that a radical reaction mechanism should not be contemplated here. Indeed, standard analysis with Rhodamine-6G (Rho6G) was also performed by mixing the radical trap with IBU in stoichiometric ratio (1:1), followed by irradiating this solution during 3 min while monitoring absorbance[215]. Since no colour change in the solution associated to variation of the spectrum profile was observed, there is no evidence for the presence of radicals. It could be, nevertheless, a competitive process between IBU and Rho6G in which the pharmaceutical degradation is preferent.

IV.4.3. Laser irradiation of effluent wastewater samples

In order to test the reaction in real wastewater, a secondary effluent was considered, spiked with IBU (10 mg L^{-1}) and irradiated at 3, 6 and 15 min. This IBU spiked effluent was analyzed by LC-HRMS for IBU itself and the TPs previously identified in ultrapure water. As presented in **Figure IV.4.3b** (and **Table IV.4.4**), IBU was not completely degraded since still a 5.7% of IBU remained at 15 min and ca. another 15% was simply transformed into TP-237, TP-177 and TP-221. Quintana et al. achieved, after microbial biodegradation, IBU degradation values above 90% in 22 days on effluent waters, also identifying the TPs just mentioned above[206]. As a recent comparison, de Wilt et al. achieved complete IBU removal from effluent water by a recent optimized AOP within a short time[216]. They combined ozonation and biological reactors, however, while the approach presented here makes use of direct pulsed laser light. On the other hand, although a significant depletion of IBU and TPs was, nevertheless, achieved in 15 min, the remaining quantities probably appear due to the competition of other chemicals[204,205] present in the wastewater effluent. Indeed, the reaction mechanism in effluent samples may differ from that in pure water, due to the presence of nitrates, nitrites, dissolved organic matter and other water constituents, and to indirect photolytic mechanisms. Such processes are normally associated to accelerated kinetics[217–219], but decelerative effects can also occur[220]. However, they were not observed in this case, and only the same 5 TPs identified in ultrapure water could be detected (from the 19 TPs that were screened). Such accelerated

kinetics could, however, be more relevant at lower (closer to environmentally expected) concentrations.

Considering that Baranda et al. employed low fluences of pulsed light from a Xe lamp to remove some pesticides containing aromatic rings[32], C=O double bonds and hydroxyl groups like ibuprofen, it must be assumed that other NSAIDs present could be degraded reducing the IBU removal rate. In addition, their influence would be masked in the UV spectra due to variations that are also associated to bands around 170–200 nm (assigned to C=O double bond) and/or 270 nm (assigned to the n➔π* and π➔π* transitions). On the other hand, TPs formation yields are calculated assuming the IBU response, as pure standards were not available, as commented before (**Table IV.4.4**). Thus, such yield is just a qualitative estimation (that is why the sum of IBU and TPs is over 100% after 3 min irradiation).

Table IV.4.4: Percentage of IBU remaining, and TPs formed at different irradiation times in spiked effluent water. N.B.: the yield of the TPs formed was calculated considering that their response is the same as that of IBU, since no pure standards were available.

Time (min)	IBU	TP-237	TP-221	TP-191	TP-177	TP-175
0	100	0.0	0.0	0.0	0.0	0.0
3	64.8	7.6	15.6	4.5	17.0	1.2
6	39.5	12.5	9.5	2.2	15.3	2.1
15	5.3	10.4	1.9	0.0	2.9	0.0

Finally, a discrete DOC removal of 3.5% was measured for initial (3 min) and final (15 min) samples. This value is close to that registered by Adityosulindro et al. using a heterogeneous Fenton process with Fe-catalyst for effluent solutions spiked with IBU (20 mg L^{-1}) and treated during 3 h[211]. Removals of 23% and 3% for IBU and DOC, respectively, were achieved without pH modification. In addition, their effluent comes from a small village wastewater treatment plant, while our work concerns wastewater from a plant treating the sewage of ca. 100,000 inhabitants.

Concerning the energy efficiency for contaminant removal from water for this pulsed laser technique, the Electrical Energy per Order (EEO) was estimated using the method published by Bolton et al. and an equivalent, commercially available pulsed laser with emission at 266 nm and 1 kHz pulse repetition rate[221]. Considering the IBU degradation rate (**Table IV.4.4**), EEO values approaching 23.3 kWh m^{-3} per order would be achieved in wastewater. Although these values are not yet competitive, recent advances on 266 nm solid state laser technology suggest that these efficiency levels may be increased significantly with state-of-the-art lasers[222,223]. In addition, new industrial laser integration devices enable the use of fast large area beam scanning, which opens the way to use recent advances in high efficiency continuous processing, as demonstrated in other areas of technology[224,225].

IV.4.4. Toxicity assessment

The toxicity of IBU and IBU water samples treated with UV-C laser pulsed radiation (referred as IBU-hν) was assessed using the zebrafish embryo assay, as explained in **Section III.4.8.2.2**.

The bioassays performed met the OECD FET test 236 criteria, with an average for negative control mortality of 8%, and 98% for embryo hatching rate at 96 hpf. The positive control registered a 45% mortality after 96h of exposure.

The results of exposure to 1 mg L^{-1} of IBU show significant differences from the negative control as soon as 8 h after the beginning of exposure, time at which 27 exposed embryos did not reach 75% epiboly state (**Table IV.4.5**). Moreover, embryos exposed to IBU reached 100% mortality after 72 h of exposure, even though no significant anomalies have occurred prior to this time-point (**Table IV.4.5**). So, at 1 mg L^{-1} concentration level IBU was able to induce severe toxicity in exposed zebrafish embryos.

Table IV.4.5: Abnormalities observed in *Danio rerio* embryos exposed to IBU before and after 15 min treatment with UV-C laser pulsed irradiation.

		Mortality (%)	75% Epiboly (%)	Somit formation (%)	Abnormalities (%)	Hatching (%)
8 hpf	**CTRL**	0% ± 0	98% ± 2	N.A.	0% ± 0	N.A.
	IBU	3% ± 3	**73% ± 6*** #**	N.A.	0% ± 0	N.A.
	IBU-hν	3% ± 2	**100% ± 0 #**	N.A.	0% ± 0	N.A.
24 hpf	**CTRL**	7% ± 3	N.A.	100% ± 0	0% ± 0	N.A.
	IBU	8% ± 4	N.A.	95% ± 3	0% ± 0	N.A.
	IBU-hν	5% ± 3	N.A.	100% ± 0	0% ± 0	N.A.
48 hpf	**CTRL**	8% ± 3	N.A.	100% ± 0	0% ± 0	0% ± 0
	IBU	13% ± 4	N.A.	100% ± 0	0% ± 0	0% ± 0
	IBU-hν	5% ± 3	N.A.	100% ± 0	0% ± 0	0% ± 0
72 hpf	**CTRL**	8% ± 3	N.A.	100% ± 0	0% ± 0	1% ± 1
	IBU	**100% ± 0*** #**	N.A.	N.A.	N.A.	N.A.
	IBU-hν	**5% ± 3 #**	N.A.	100% ± 0	0% ± 0	58% ± 11***
96 hpf	**CTRL**	8% ± 3	N.A.	100% ± 0	2% ± 1	98% ± 1
	IBU	100% ± 0	N.A.	N.A.	N.A.	N.A.
	IBU-hν	5% ± 3	N.A.	100% ± 0	3% ± 3	100% ± 0

Note: Significant differences from control are marked with asterisks ($p<0.05$ - *; $p<0.01$ - **; $p<0.001$ - ***) and differences between treated and non-treated groups are highlighted in bold and marked with cardinals (#). Data are expressed as mean ± standard error (SE) (N=16 for control; N=8 for IBU treatments).

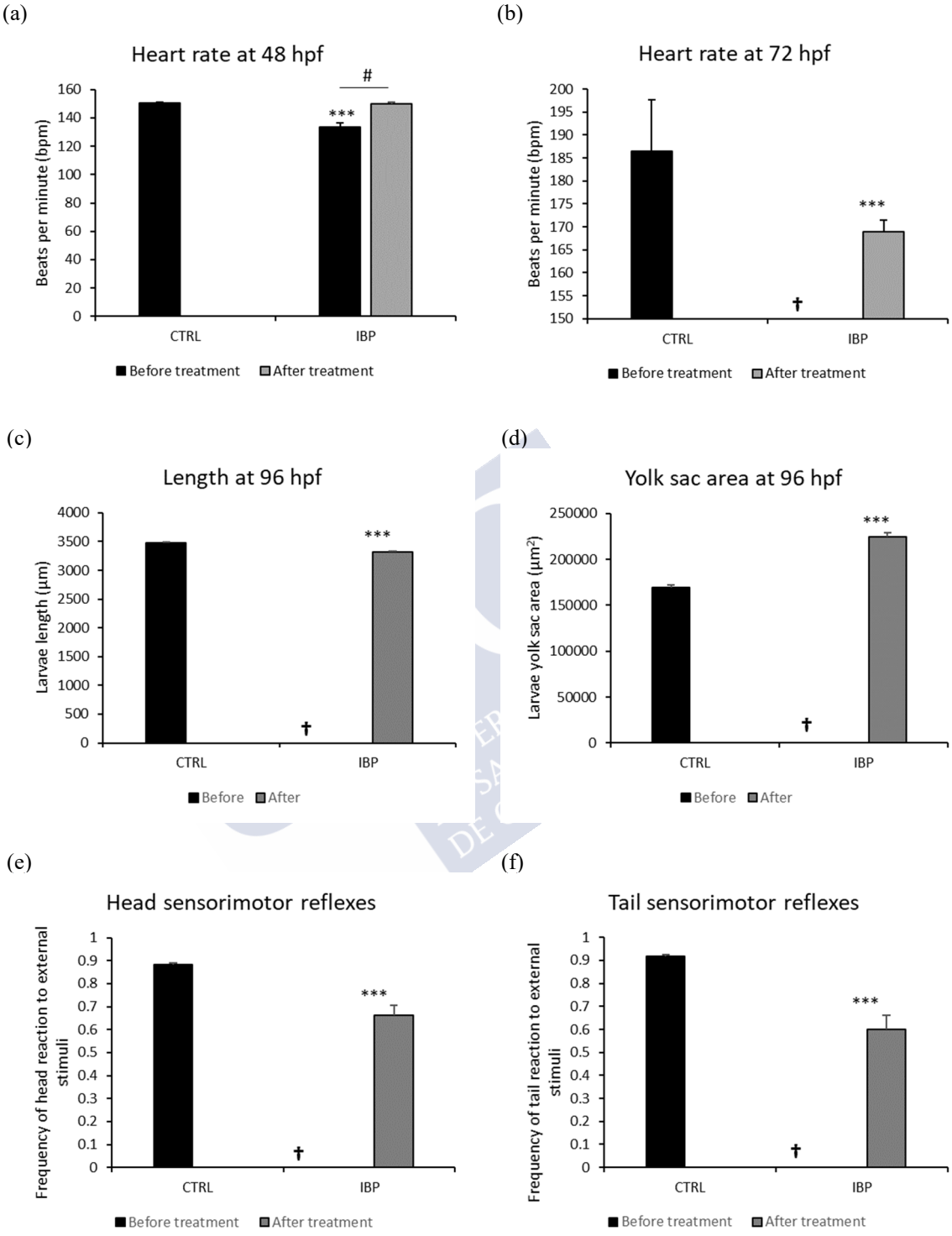

Figure IV.4.5: *D. rerio* cardiac frequency at 48 hpf (a) and 72 hpf (b), and larvae length in µm (c), yolk-sac area in µm² (d), and sensorimotor reflexes of head (e) and tail (f) after the exposure to IBU, IBU-hv. Significant differences from control are marked with asterisks (p<0.05 - *; p<0.01 - **; p<0.001 - *) and differences between parental and hv treated groups are marked with cardinals (#). 100% mortality of is marked by †. Data are expressed as mean ± SE (N=16 for a and b; N=35 for c and d; N=20 for e and f).**

The data regarding embryo exposure to water samples treated with UV-C laser pulsed irradiation (IBU-hν), revealed a significant increase in the water quality of the samples IBU-hν, reducing the embryo mortality at 96 hpf, from 100% to 5%. Heartbeat rates were returned to the control levels at 48 hpf, showing significant differences between IBU and IBU-hν. However, exposure to IBU-hν induced significantly different heartbeat when compared with the negative control (**Figure IV.4.5**). All endpoints still showed significant differences from the negative control group (**Figure IV.4.5**).

IV.5. Transformation of 1-vinylpyrrolidin-2-one and 2-piperazin-1-ylethanamine upon UV irradiation

USC
UNIVERSIDADE
DE SANTIAGO
DE COMPOSTELA

The aim of the work presented in this section was to investigate the potential reaction of 12 different chemicals prioritized because of their potential persistence and mobility with UV radiation (**Table IV.5.1**), given the fact that this is a disinfection methodology commonly applied in many WWTPs and DWTPs. Chemicals were prioritized within the Water JPI project PROMOTE, as detailed in **section I.3.2**. Then those which substantially reacted were further investigated in order to characterize their TPs and finally a toxicity screening was performed by means of two QSAR software.

IV.5.1. Photochemical reactivity

From the 12 chemicals (**Table IV.5.1**) irradiated for up to 60 min, only 2 of them reacted significantly, i.e. VP and PPE, with half-lives of 1.9 and 40 min, respectively. Similar kinetic constants to those in ultrapure water were obtained in river water samples spiked with these two chemicals (**Figure IV.5.1** and **Table IV.5.2**).

Table IV.5.1. List of chemicals tested for UV photolysis.

Compound Name	CAS Number	Structure
3-Amino-3,5,5-trimethylcyclohexanamine	2855-13-2	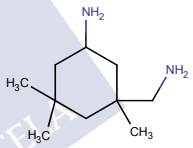
1,3,5,7-Tetraazatricyclo[3.3.1.1(3,7)]decane	100-97-0	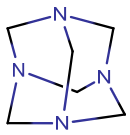
1-vinylpyrrolidin-2-one (VP)	88-12-0	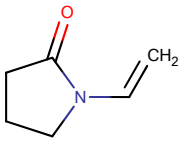
2-piperazin-1-ylethanamine (PPE)	140-31-8	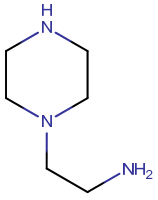
1,4-bis[(2-ethylhexyl)oxy]-1,4-dioxobutane-2-sulfonate	577-11-7	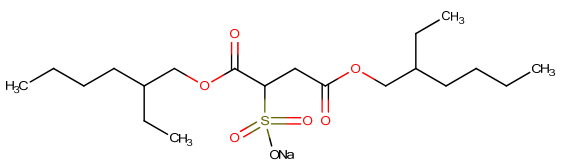

Compound Name	CAS Number	Structure
1,3,5-tris(2-hydroxyethyl)-1,3,5-triazinane-2,4,6-trione	839-90-7	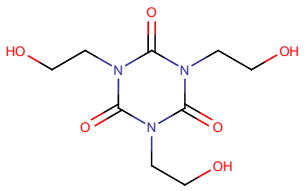
1,3-diphenylguanidine	102-06-7	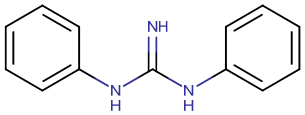
6-phenyl-1,3,5-triazine-2,4-diamine	91-76-9	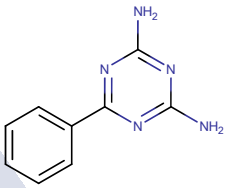
N-methylhydrazinecarbothioamide	6610-29-3	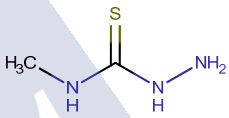
N',N'''-methylenebis{1-[3-(hydroxymethyl)-2,5-dioxoimidazolidin-4-yl]urea}	39236-46-9	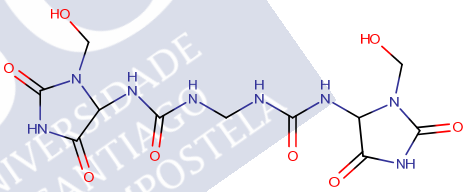
4-hydroxy-2,2,6,6-tetramethylpiperidine-1-ethanol	52722-86-8	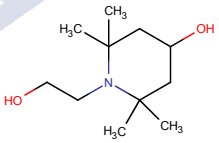
Tartrazin	1934-21-0	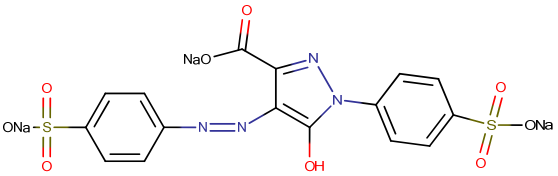

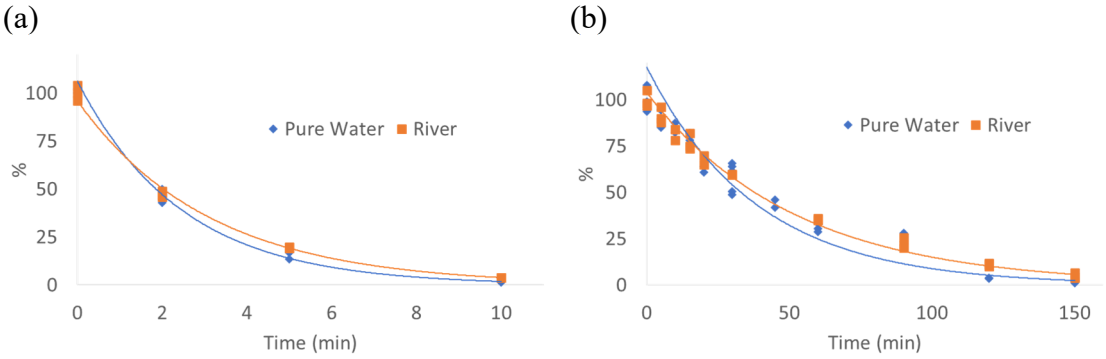

Figure IV.5.1. UV photolysis kinetic plots in ultrapure and river water of (a) VP and (b) PPE. Data normalized to time 0 (untreated samples).

Table IV.5.2. Photochemical kinetic parameters obtained from non-linear fitting to an exponential decay and calculation of quantum yields (UPW: ultrapure water; SW: surface water).

	k (min^{-1}) [a]	$t_{1/2}$ (min) [a]	R^2	ε (M^{-1} cm^{-1})	Φ (mol $einstein^{-1}$) [a]
VP (UPW)	0.36 ± 0.03	1.9 ± 0.2	0.9989	$4.38x10^3$	0.28± 0.03
VP (SW)	0.33 ± 0.01	1.7 ± 0.1	0.9999	-	-
PPE (UPW)	0.017 ± 0.001	40 ± 3	0.9728	3.66	16 ± 1
PPE (SW)	0.019 ± 0.002	36 ± 3	0.9908	-	-
DCF (UPW)	0.50 ± 0.06	1.4 ± 0.2	0.996	$5.76x10^3$	0.292 [b]

[a] Mean ± 95% confidence interval
[b] Value from Wols et al[226]

DCF, a pharmaceutical with several studies on their photochemical kinetics, produced a half-life of 1.4 min (**Table IV.5.2**). Since data on the quantum yield (Φ) of DCF at 254 nm has already been published[226], it could be employed as a chemical actinometer, in order to calculate the value of Φ for VP and PPE, according to **Equation IV.5.1**[155,227].

Eq. IV.5.1
$$\Phi_{chem} = \Phi_{DCF} \times \frac{k_{d(chem)}}{k_{d(DCF)}} \times \frac{\varepsilon_{254(DCF)}\, I_{0,254}}{\varepsilon_{254(chem)} I_{0,254}}$$

Where Φ_{chem} and Φ_{DCF} are the quantum yields, $k_{d(chem)}$ and $k_{d(DCF)}$ are the direct photolysis rate constants (min^{-1}), $\varepsilon_{254(chem)}$ and $\varepsilon_{254(DCF)}$ the molar absorption coefficients at 254 nm and $I_{0,254}$ is the intensity of the lamp, which emits almost exclusively at 254 nm; *chem* and *DCF* subindexes referring to the chemical whose quantum yield is to be calculated and DCF (used as chemical actinometer), respectively. The values of ε were determined experimentally using 1 cm path-length quartz cuvettes and are compiled in **Table IV.5.1**. VP quantum yield was 0.28 mol $einstein^{-1}$, whereas PPE had a quantum yield notably higher than 1 (16 mol $einstein^{-1}$). Such a high UV reactivity was unexpected in the case PPE given its weak absorption in the UV region. However, PPE has been proven also

to be reactive to solar radiation[62], which is also not expectable given its UV-visible spectrum (**Figure IV.5.2b**). In the publication of Zahn et al.[62] this solar photochemical activity was ascribed to the formation of singlet oxygen since the reaction did not take place in absence of oxygen or presence of furfuryl alcohol. When we performed the photochemical reaction in the presence of ethanol, an ·OH radicals scavenger[156], the reaction was partially quenched: 32 ± 3% Vs. 56 ± 4% PPE remaining after 1 h irradiation in absence or presence of ethanol, respectively. Thus, generation of ·OH radicals and other species from oxygen may be related to such photochemical reactivity[62,228].

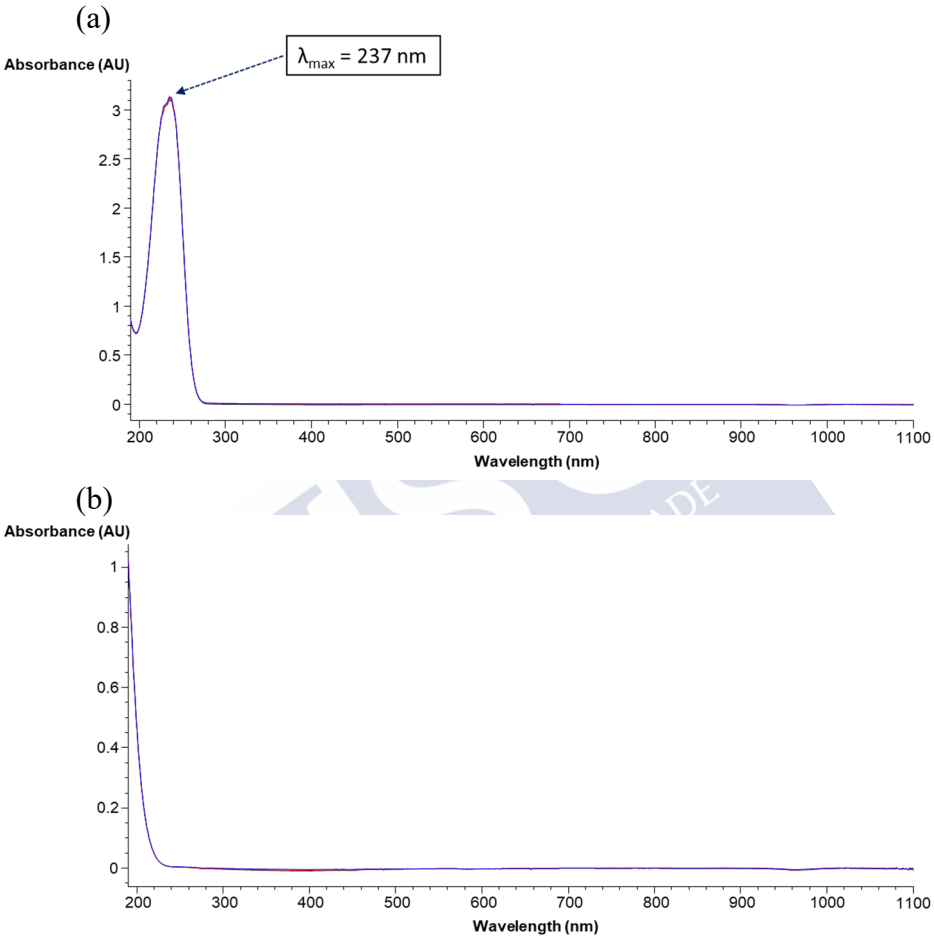

Figure IV.5.2. UV/Vis absorption spectrum of (a) VP and (b) PPE

IV.5.2. TPs identification

TPs identification was performed as described in **III.4.3.5**, **III.4.5** and **III.4.7**, by batch experiments where single-stage HRMS data was used to propose molecular formulas of the TPs on the basis of mass accuracy and isotopic profile. As compiled in **Tables IV.5.3** and **IV.5.4**, up to 5 and 7 TPs were detected for VP and PPE, respectively, and their empirical formula could be assigned with a high level of certainty (mass error below ±0.6 mDa and scores higher than 98%). TPs are named with the abbreviation of their precursor compound and the nominal masses of the observed $[M+H]^+$ ion. Then, structures (compiled

in **Figures IV.5.3** and **IV.5.4**) were proposed on the basis of MS/MS experiments, which are discussed below.

IV.5.2.1. VP

Five TPs were detected for VP, of which 2 of them are proposed to be formed by oxidation of the vinylic side chain (i.e. VP-116 and VP-132), one by hydrolysis (VP-86) and the two remaining by dimerization reactions (VP-219 and VP-227), as presented in **Figure IV.5.3**.

Table IV.5.3. Summary of LC-QTOF formula assignment for VP TPs

Compound	Experimental m/z	Molecular formulae	Error (mDa)	DBE	Score (%)
VP	112.0759	C6 H9 N O	0.21	3	99.70
VP-86	86.0605	C4 H7 N O	0.46	2	99.98
VP-116	116.0706	C5 H9 N O2	<0.01	2	99.99
VP-132	132.0661	C5 H9 N O3	0.58	2	99.98
VP-219	219.1602	C12 H18 N4	-0.22	6	99.77
VP-227	227.1391	C11 H18 N2 O3	0.08	4	99.97

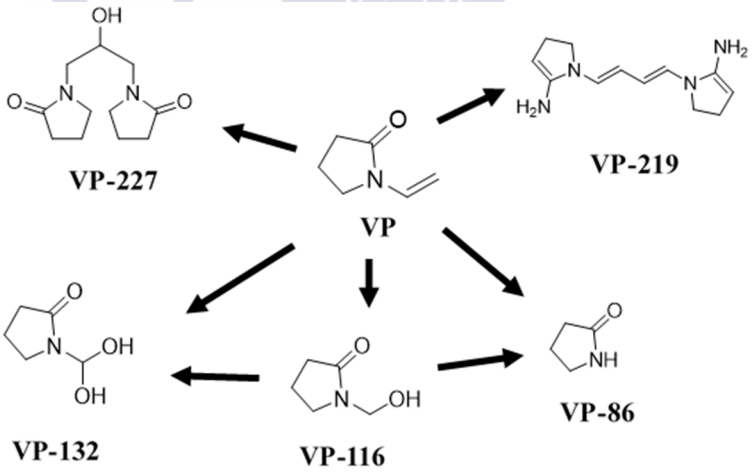

Figure IV.5.3. Summary of VP TPs

VP-86, i.e. 2-pyrrolidone, was also observed as the only detectable TP during hydrolysis experiments of VP by Zahn et al[62]. Obviously, this TP was thus easy to identify as being expectable and because of the MS/MS spectrum (**Figure SIV.5.1b**), that exhibits the loss of ammonia (in agreement with the observations of Zahn et al.) and other smaller

product ions, consistent with that structure. Also, the spectrum matched well with that available in the METLIN library (MID 6452).

VP-116 and VP-132 are proposed to be formed as a result of the oxidation of the vinyl moiety, leading to mono- or di-hydroxylated species (**Figure IV.5.3**). VP-116 spectrum shows only the loss of water and CO to yield m/z 70 (nominal masses are presented for conciseness), **Figure SIV.5.1c**. Similarly, VP-132 spectrum (**Figure IV.5.5a**) also shows the same loss to yield m/z 86 in this case. Then, a loss of ammonia to produce m/z 69 or C_2H_4O to yield m/z 42. Both m/z 86 and m/z 69 are also present in VP spectrum (**Figure SIV.5.1a**), which would confirm that the reaction takes place in the vinylic chain.

Table IV.5.4. Summary of LC-QTOF formula assignment for PPE TPs

Compound	Experimental m/z	Molecular formulae	Error (mDa)	DBE	Score (%)
PPE	130.1336	C6 H15 N3	-0.27	1	100.00
PPE-87	87.0913	C4 H10 N2	-0.37	1	98.93
PPE-111	111.0917	C6 H10 N2	0.03	3	100.00
PPE-115	115.0867	C5 H10 N2 O	0.11	2	99.92
PPE-126	126.1023	C6 H11 N3	-0.27	3	99.51
PPE-144	144.1127	C6 H13 N3 O	-0.44	2	98.85
PPE-146	146.1286	C6 H15 N3 O	-0.19	1	99.79
PPE-160	160.1076	C6H15N3O2	0.45	2	98.84

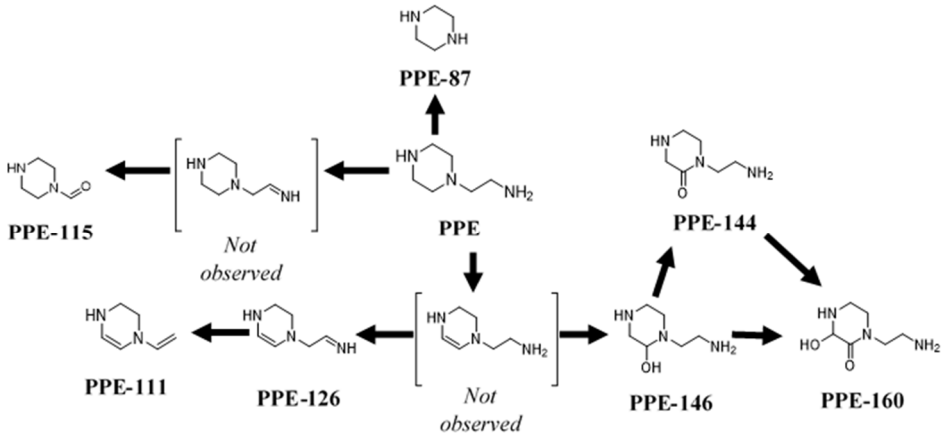

Figure IV.5.4. Summary of PPE TPs

VP-219 would be produced as a result of the dimerization of VP and substitution of the two CO groups by amino groups. Dimerization is a reaction expectable for VP, given than such compound is used as monomer in the production of VP-polymers. Although the introduction of N in the structure is not very intuitive, its spectrum (**Figure IV.5.4b**) clearly shows a first loss of one 2-iminopyrrolidine group, followed by loss of ammonia (m/z 135 and m/z 118 respectively), while m/z 85, corresponding to 2-iminopyrrolidine is also observed, which then losses ammonia to yield m/z 68.

Finally, VP-227 would result from the dimerization of VP and either VP-116 or VP-132. Its spectrum (**Figure SIV.5.1d**) exhibits mainly two peaks, m/z 124, which would be formed as a result of the loss of a pyrrolidone moiety and water or m/z 104 related to the central alkyl group.

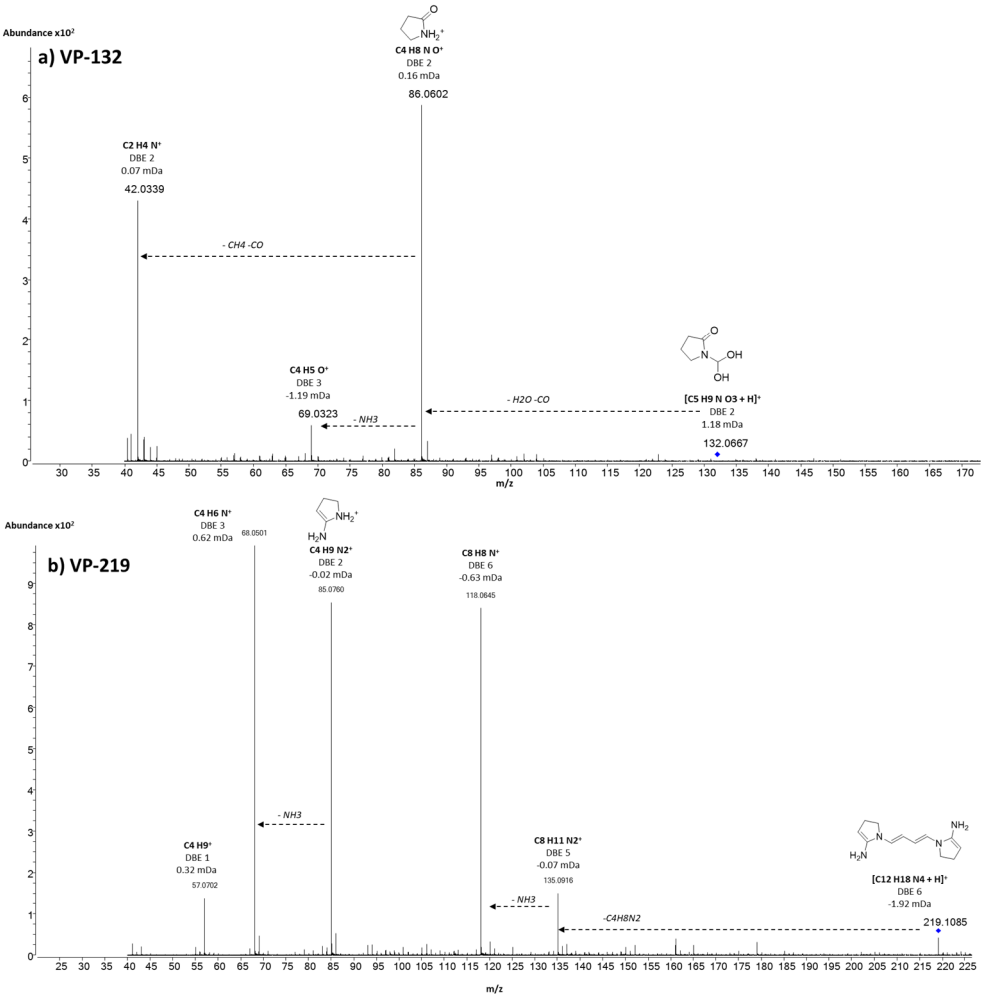

Figure IV.5.5. MS/MS spectra of (a) VP-132 and (b) VP-219

From **Figure IV.5.6**, which summarizes the evolution of these TPs along time up to 1 h of irradiation, it is evident that dimeric TPs (particularly VP-219) are formed initially and then are further degraded. Furthermore, at longer times, VP-116 is by far the most intense TP. Assuming its LC-MS response would be equal to that of VP, it would represent about a 50% yield. Indeed, this is only a surmise and actual yields could be calculated only

if standards would be available, but can help in understanding the relative relevance of each TP.

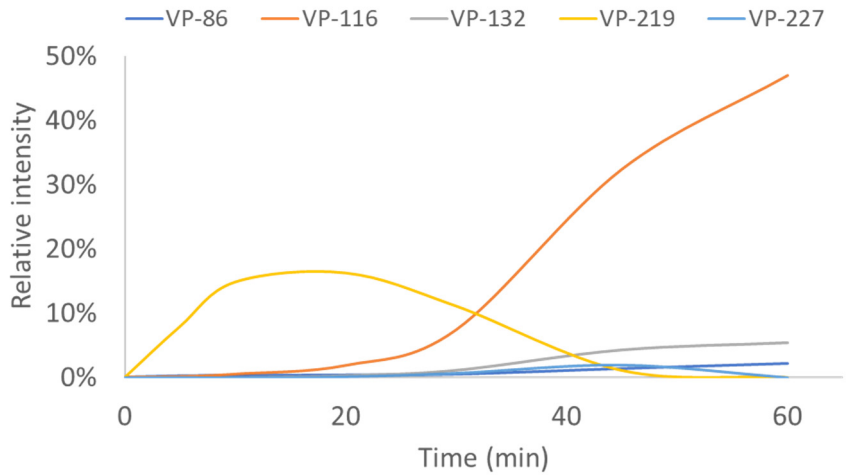

Figure IV.5.6. TPs formation profiles for VP. Signal of TPs normalized to the signal of their parent chemical at time 0.

IV.5.2.2. PPE

As presented in **Table IV.5.4** and **Figure IV.5.4**, a total of 7 TPs were detected in the case of PPE, from which, one is a hydrolytic product (PPE-87) and the remaining are proposed to be formed by a dehydrogenation mechanism (PPE-126), which is then followed by either oxidative cleavage of the ethenamine group (PPE-111 and PPE-115) or oxidation of the piperazine cycle (PPE-144, PPE-146 and PPE-160).

PPE-87, i.e. piperazine, was easily identified as the most logical structure and on the basis of its MS/MS spectrum (**Figure SIV.5.2b**), which also matches quite well the triple-quadrupole spectra available in MassBank (e.g. records KO003735 and KO003736).

From the remaining TPs, PPE-160 was also observed as the only sunlight photolytic product of PPE by Zahn et al, who also detected this same chemical and PPE-126 as MnO_2 TPs[62]. The MS/MS spectra obtained in our work (**Figure SIV.5.2d** and **SIV.5.2f**) fit well with that described in such publication, so the same structures are proposed. Zahn et al. also detected a TP with nominal m/z 142 as a result of MnO_2 reaction. Such TP was not observed in UV photolysis, but in turn we observed PPE-144 and PPE-146. The spectrum of PPE-144 (**Figure IV.5.7b**) shows different pathways involving either a loss of water or either CH_3O, which could be compatible with a keto group, due to keto-enolic equilibrium. Thus, the structure shown in **Figure IV.5.4** is proposed, which would be similar to the TP with m/z 142 detected by Zahn et al., but without posing an unsaturation in the ethenamine group. Similarly, PPE-146 is proposed as hydroxylated PPE, given the fact that the first product ion (m/z 103, **Figure SIV.5.2e**) would correspond to the loss of the ethenamine group.

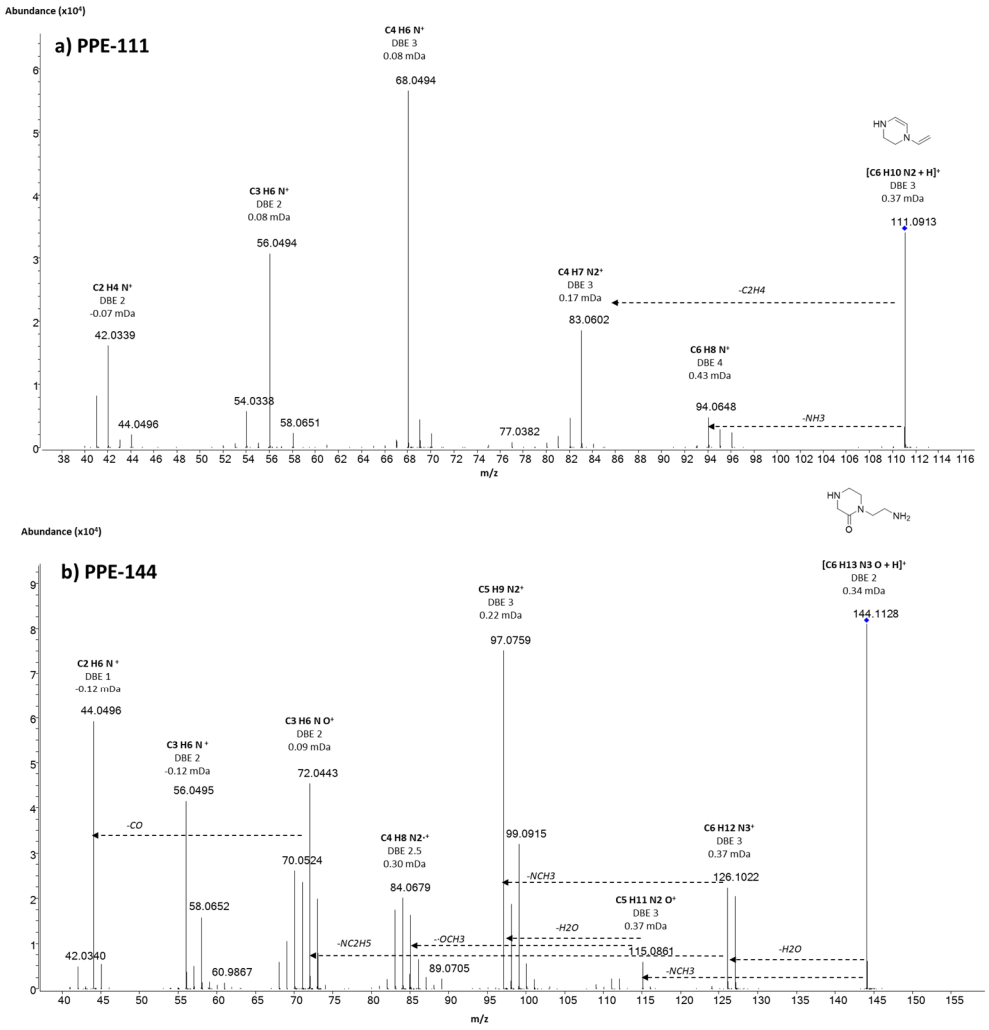

Figure IV.5.7. MS/MS spectra of (a) PPE-111 and (b) PPE-144

PPE-111 and PPE-115 are proposed to be oxidative cleavage products (**Figure IV.5.4**). PPE-111 was assigned to the structure suggested in **Figure IV.5.4**, given the loss of C_2H_4 observed in the spectrum (**Figure IV.5.7a**), which would be related to the ethene group in the structure. In the case of PPE-115, its spectrum (**Figure SIV.5.2c**) exhibits the loss of either CO or water, related again to a keto group. Thus, this keto group could be also present in the ring, but it is believed to be most likely to happen in the alkyl chain through an oxidative mechanism, also related to PPE-111 structure. The transformation pathway presented in **Figure IV.5.4** assumes the formation of 2 further dehydration TPs, which were not detected, by analogy with PPE-126 and the reaction mechanism proposed by Zahn et al. for MnO_2[62].

As shown if **Figure IV.5.8**, all TPs are being formed in a similar way and continue stable up to 2.5 hours of irradiation. Among them the most relevant TP in terms of intensity is PPE-126, followed by PPE-87 and PPE-144.

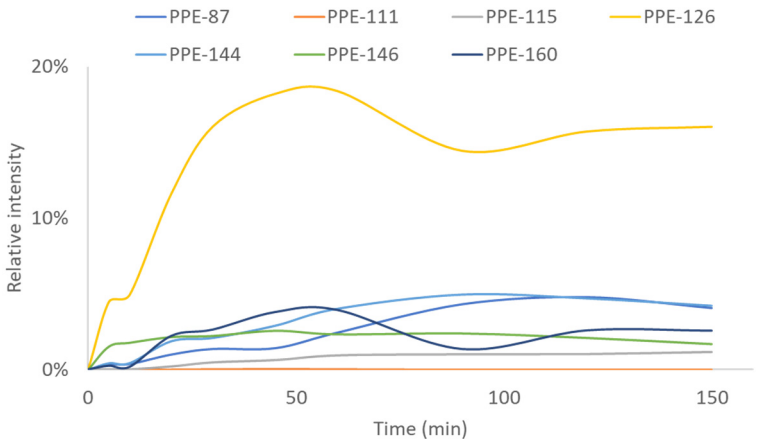

Figure IV.5.8. TPs formation profiles for PPE. Signal of TPs normalized to the signal of their parent chemical at time 0.

IV.5.3. Predicted toxicity

The prediction of VP, PPE and their TPs (eco)toxicity was performed both with US EPA T.E.S.T. and ECOSAR software, as detailed in **section III.4.8.1**. Data is compiled into **Table IV.5.5** (T.E.S.T.) and **Table IV.5.6** (ECOSAR; note that two toxicity values are predicted for some TPs depending on the functional groups class used to generate them). Furthermore, these data are also depicted in **Figure IV.5.9**, where toxicological endpoints for TPs were compared to that of their parent chemicals, so that red colors indicate a lower predictable effect concentration (i.e. higher toxicity). It is evident from that data that each software leads to different results, as observed previously, and this data should be taken with caution[159].

Table IV.5.5. Summary of EPA T.E.S.T. predicted toxicity endpoints. Note: n.a. means that no prediction was possible.

Compound	*Fathead minnow* LC_{50} 96 h (mg L^{-1})	*Daphnia magna* LC_{50} 48 h (mg L^{-1})	*T.pyrifromis* IGC_{50} 48 h (mg L^{-1})	Oral rat LD_{50} (mg kg^{-1})
VP	$1.73x10^{2}$	$1.36 x10^{1}$	$1.62 x10^{3}$	$1.36 x10^{3}$
VP-86	$4.86 x10^{2}$	$4.17 x10^{1}$	$3.14 x10^{3}$	$1.11 x10^{3}$
VP-116	$1.39 x10^{3}$	$1.15 x10^{2}$	$7.42 x10^{3}$	$1.16 x10^{3}$
VP-132	$2.49 x10^{3}$	$3.61 x10^{2}$	$8.92 x10^{3}$	$8.92 x10^{3}$
VP-219	$1.09 x10^{2}$	2.83	n.a.	$7.37 x10^{2}$
VP-227	$1.91 x10^{2}$	$4.32 x10^{2}$	$1.53 x10^{3}$	$4.71 x10^{3}$
PPE	$2.55 x10^{3}$	$6.07 x10^{1}$	$1.59 x10^{3}$	$1.78 x10^{3}$
PPE-87	$1.37 x10^{3}$	$1.31 x10^{2}$	$2.02 x10^{3}$	$2.09 x10^{3}$
PPE-111	$9.06 x10^{2}$	$4.43 x10^{1}$	$4.27 x10^{2}$	$1.29 x10^{3}$
PPE-115	$1.07 x10^{3}$	$2.15 x10^{3}$	n.a.	$1.80 x10^{3}$
PPE-126	n.a.	n.a.	n.a.	n.a.
PPE-144	$2.91 x10^{3}$	$6.96 x10^{1}$	$1.30 x10^{3}$	$2.75 x10^{3}$
PPE-146	$3.38 x10^{3}$	$2.11 x10^{2}$	$2.07 x10^{3}$	$3.37 x10^{3}$
PPE-160	$3.81 x10^{3}$	$4.10 x10^{2}$	$3.88 x10^{3}$	$3.23 x10^{3}$

Table IV.5.6. Summary of ECOSAR predicted toxicity endpoints. Note: in some cases, two values were obtained, the * symbol denoting that the amide class was used, while those without * was from aliphatic amines.

	Acute toxicty (mg L^{-1})			Chronic toxicity (mg L^{-1})		
Compound	Fish 96h LC_{50}	Daphnid 48 h LC_{50}	Green Algae 96 h EC_{50}	Fish ChV	Daphnid ChV	Green Algae ChV
VP*	$7.23x10^{2}$	$9.16 x10^{2}$	$4.63 x10^{1}$	4.38	$7.96 x10^{1}$	$1.36 x10^{1}$
VP-86	$1.53 x10^{3}$	$2.11 x10^{3}$	$7.98 x10^{1}$	7.22	$1.49 x10^{2}$	$1.83 x10^{1}$
VP-116	$1.97 x10^{4}$	$3.29 x10^{4}$	$6.50 x10^{2}$	$5.36 x10^{1}$	$1.46 x10^{3}$	$8.57 x10^{1}$
VP-132	$3.40 x10^{4}$	$5.88 x10^{4}$	$1.03 x10^{3}$	$8.37 x10^{1}$	$2.40 x10^{3}$	$1.23 x10^{2}$
VP-219	$8.50 x10^{1}$	9.60	8.82	5.84	$7.48 x10^{-1}$	2.82
VP-227	$4.08 x10^{4}$	$6.85 x10^{4}$	$1.33 x10^{3}$	$1.10 x10^{2}$	$3.01 x10^{3}$	$1.73 x10^{2}$
PPE	$5.48 x10^{3}$	$4.31 x10^{2}$	$8.09 x10^{2}$	$1.13 x10^{3}$	$2.37 x10^{1}$	$1.99 x10^{2}$
PPE-87	$1.14 x10^{3}$	$9.83 x10^{1}$	$1.54 x10^{2}$	$1.79 x10^{2}$	5.89	$4.05 x10^{1}$
PPE-111	$2.63x10^{2}$	$2.58 x10^{1}$	$3.13 x10^{1}$	$2.76 x10^{1}$	1.76	9.03
PPE-115	$4.79 x10^{3}$	$3.77 x10^{2}$	$7.06 x10^{2}$	$9.84 x10^{2}$	$2.07 x10^{1}$	$1.74 x10^{2}$
PPE-115*	$1.91 x10^{4}$	$3.19 x10^{4}$	$6.34 x10^{2}$	$5.24 x10^{1}$	$1.43 x10^{3}$	$8.40 x10^{1}$
PPE-126	$1.05 x10^{3}$	$9.39 x10^{1}$	$1.38 x10^{2}$	$1.49 x10^{2}$	5.82	$3.71 x10^{1}$
PPE-144	$1.54 x10^{4}$	$1.13 x10^{3}$	$2.44 x10^{3}$	$3.94 x10^{3}$	$5.78 x10^{1}$	$5.70 x10^{2}$
PPE-144*	$7.34 x10^{4}$	$1.35 x10^{5}$	$1.94 x10^{3}$	$1.53 x10^{2}$	$4.78 x10^{3}$	$1.95 x10^{2}$
PPE-146	$6.31 x10^{4}$	$4.16 x10^{3}$	$1.11 x10^{4}$	$2.24 x10^{4}$	$1.92 x10^{2}$	$2.40 x10^{3}$
PPE-160	$1.75 x10^{5}$	$1.07 x10^{4}$	$3.31 x10^{4}$	$7.75 x10^{4}$	$4.62 x10^{2}$	$6.79 x10^{3}$
PPE-160*	$1.30 x10^{6}$	$2.99 x10^{6}$	$1.95 x10^{4}$	$1.37 x10^{3}$	$6.04 x10^{4}$	$9.96 x10^{2}$

Yet, as regards VP, both software agree that among its TPs, VP-219 is the only one that would result into a higher ecotoxicological concern, since it could be up to 100 times more toxic to daphnid species in chronic exposure (**Figure IV.5.9**). However, as mentioned above, such compound appears to be an intermediate TP, whereas the most intense, VP-116 would be less ecotoxic than VP itself. Also, from the oral rat predicted toxicity, that would be similar to VP, so, human risk seems to be maintained at a similar level. In all cases, predicted oral rat acute toxicity values fall in the 300-2000 mg Kg^{-1} body weight range or higher, so they would classify in Category 4 or non-toxic according to the ECHA Guidance[191], thus human risk can be expected to be low. Applying the same guidance document, none of the TPs would classify as non-acute toxic (all acute toxicity endpoints are >1 mg L^{-1}), while chronic toxicity evaluation would require more robust data, even for screening purposes.

In the case of PPE, most TPs are not expected to be more toxic to rat than PPE (**Figure IV.5.9**) and according to their predicted values they would also classify in Category 4 or non-toxic, therefore likely not being hazardous for human health. PPE-111 seems to be the most concerning one in terms of toxicity, although predicted values differ among both QSAR tools and the yield of formation of this TP is very low (**Figure IV.5.9**).

(a)

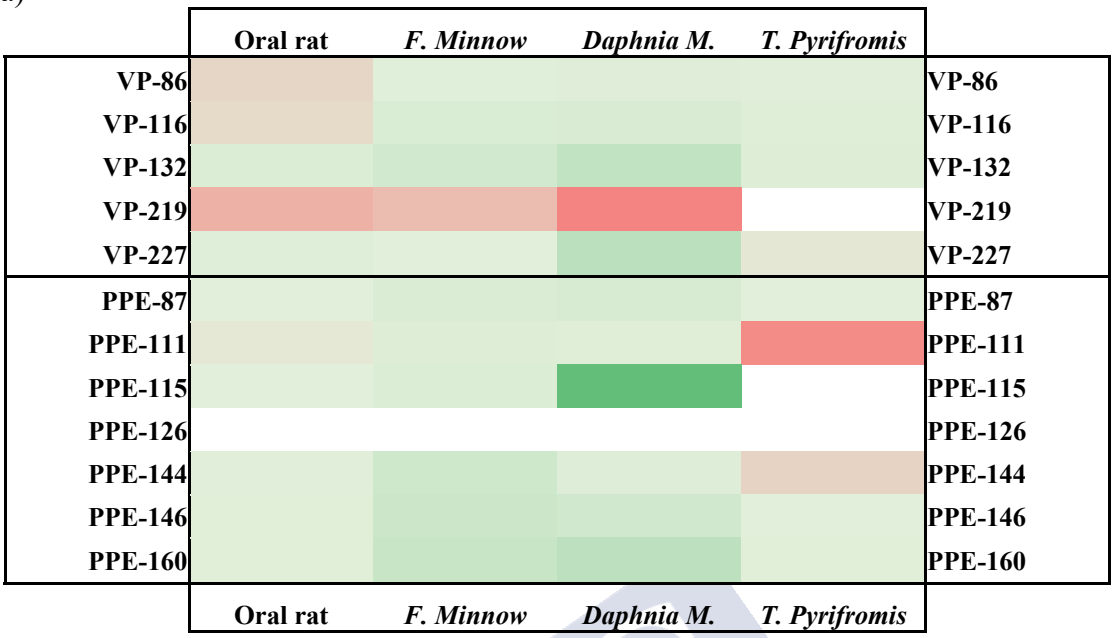

(b)

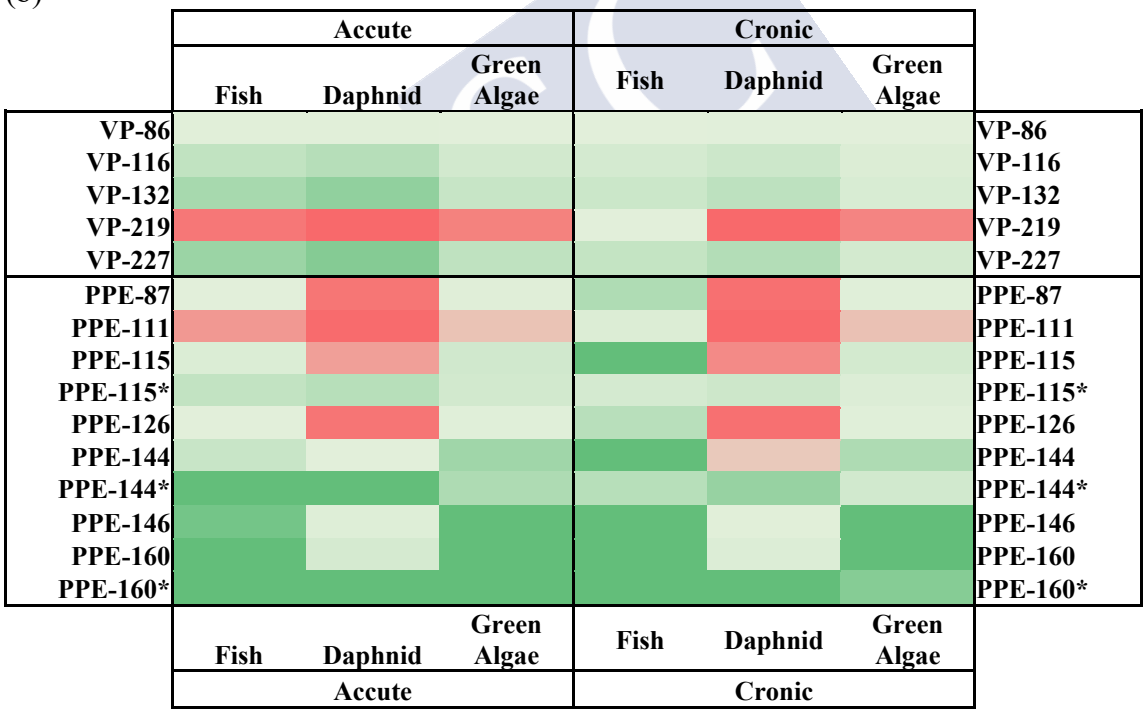

Figure IV.5.9. Summary of (eco)toxicological predicted data respective to the parent chemical. (a): T.E.S.T. prediction. (b): ECOSAR prediction. Color code: From dark green (less toxic than parent chemical) to dark red (more toxic than parent chemical); White color refers to values that could not be predicted by T.E.S.T. Detailed predicted toxicity values are compiled in Tables IV.5.5 and IV.5.6. When two ECOSAR values were predicted, those TPs marked with * corresponded to prediction by using the class amide, while the other one refers to aliphatic amine class.

On the other hand, the most intense TP is PPE-126 (**Figure IV.5.8**), but its toxicity could not be predicted by T.E.S.T., while ECOSAR foreseen values are more relevant in the case of daphnid species. Even so, the predicted acute toxicological endpoints are >1 mg

L^{-1}, thus acute ecotoxic effects would not be expected. Thus far, an experimental ecotoxicological evaluation would be required to confirm these findings.

IV.5.4. Annex

This annex contains:

Figure SIV.5.1: QTOF product ion spectra of VP and its TPs: (a) VP; (b) VP-86, (c) VP-116 and (d) VP-227.

Figure SIV.5.2: QTOF product ion spectra of PPE and its TPs: (a) PPE; (b) PPE-87, (c) PPE-115, (d) PPE-116, (e) PPE-146 and (f) PPE-160.

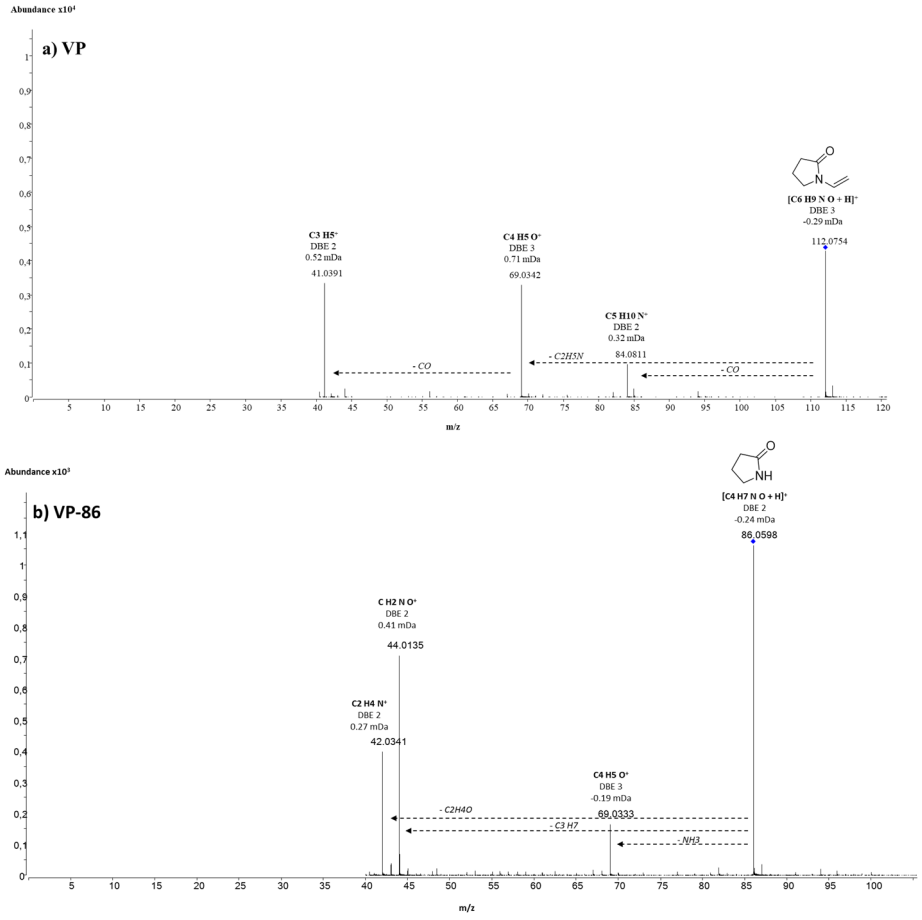

Figure SIV.5.1: QTOF product ion spectra of VP and its TPs: (a) VP; (b) VP-86

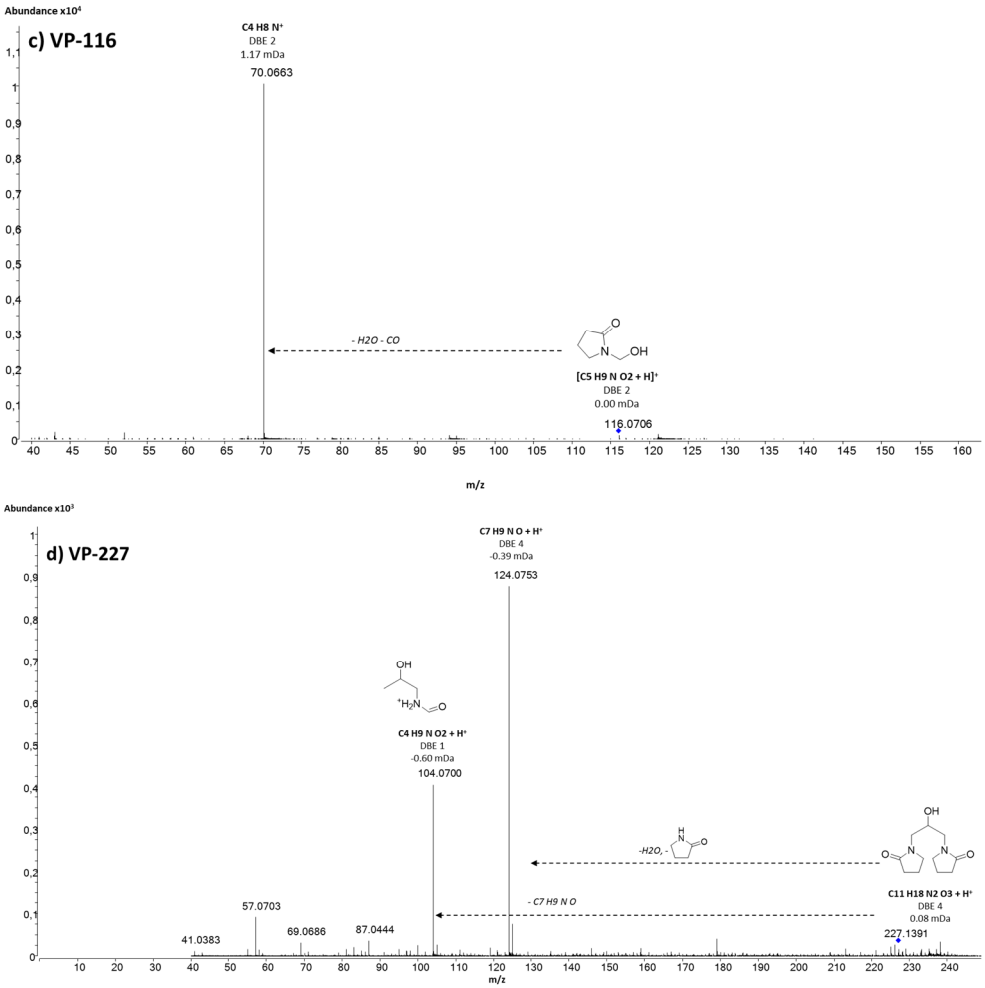

Figure SIV.5.1 (cont.): QTOF product ion spectra of VP and its TPs: (c) VP-116 and (d) VP-227.

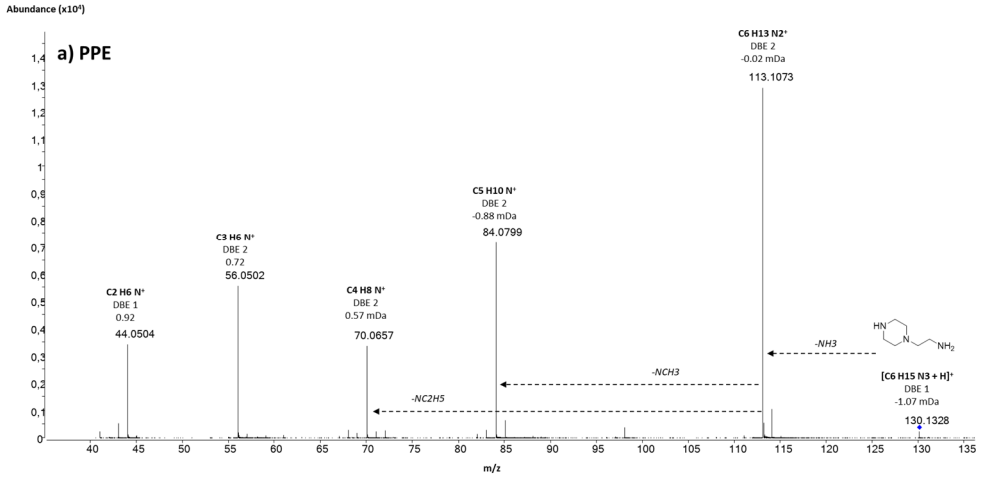

Figure SIV.5.2: QTOF product ion spectra of VP and its TPs: (a) PPE

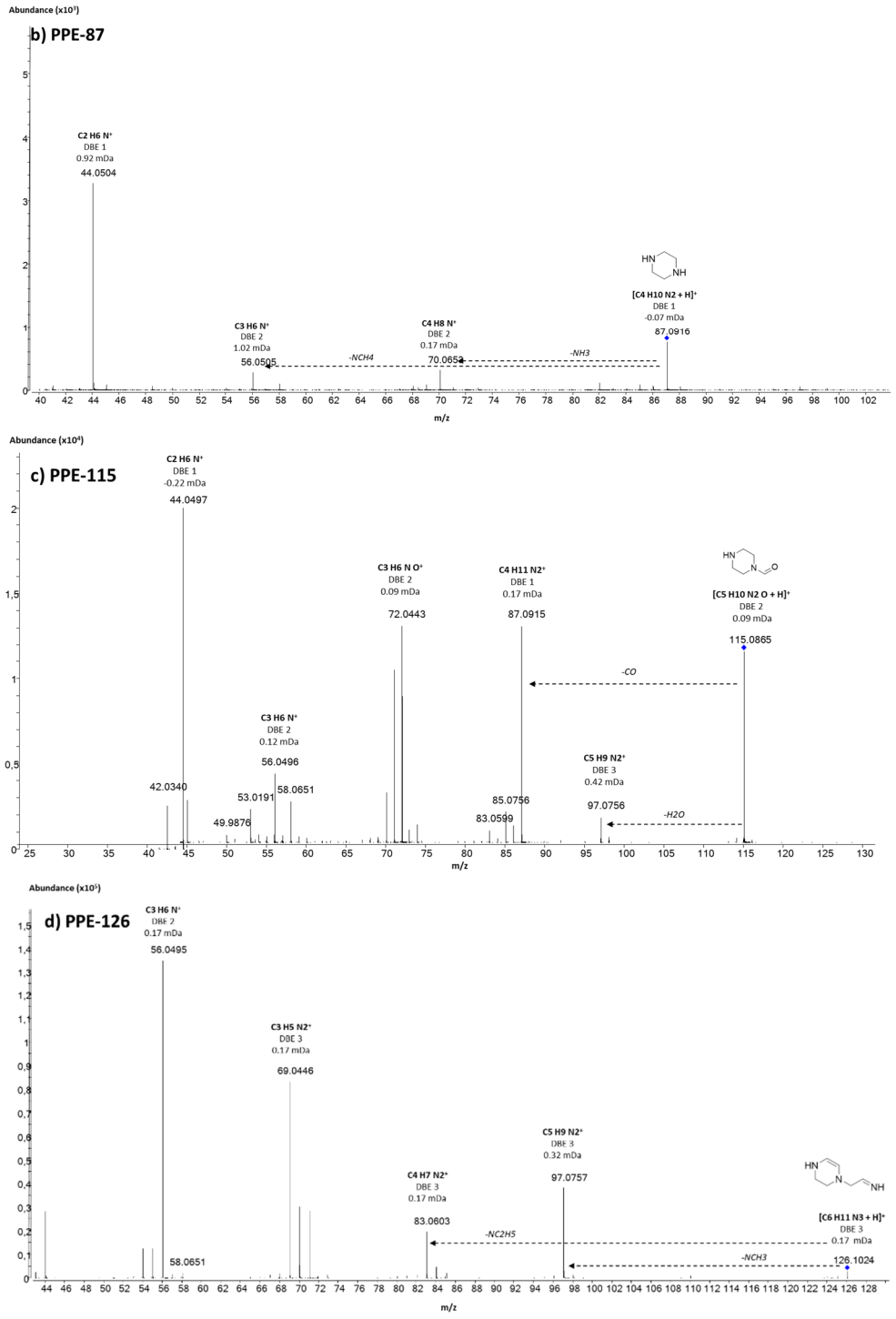

Figure SIV.5.2 (cont.): QTOF product ion spectra of VP and its TPs: (b) PPE-87, (c) PPE-115, (d) PPE-116.

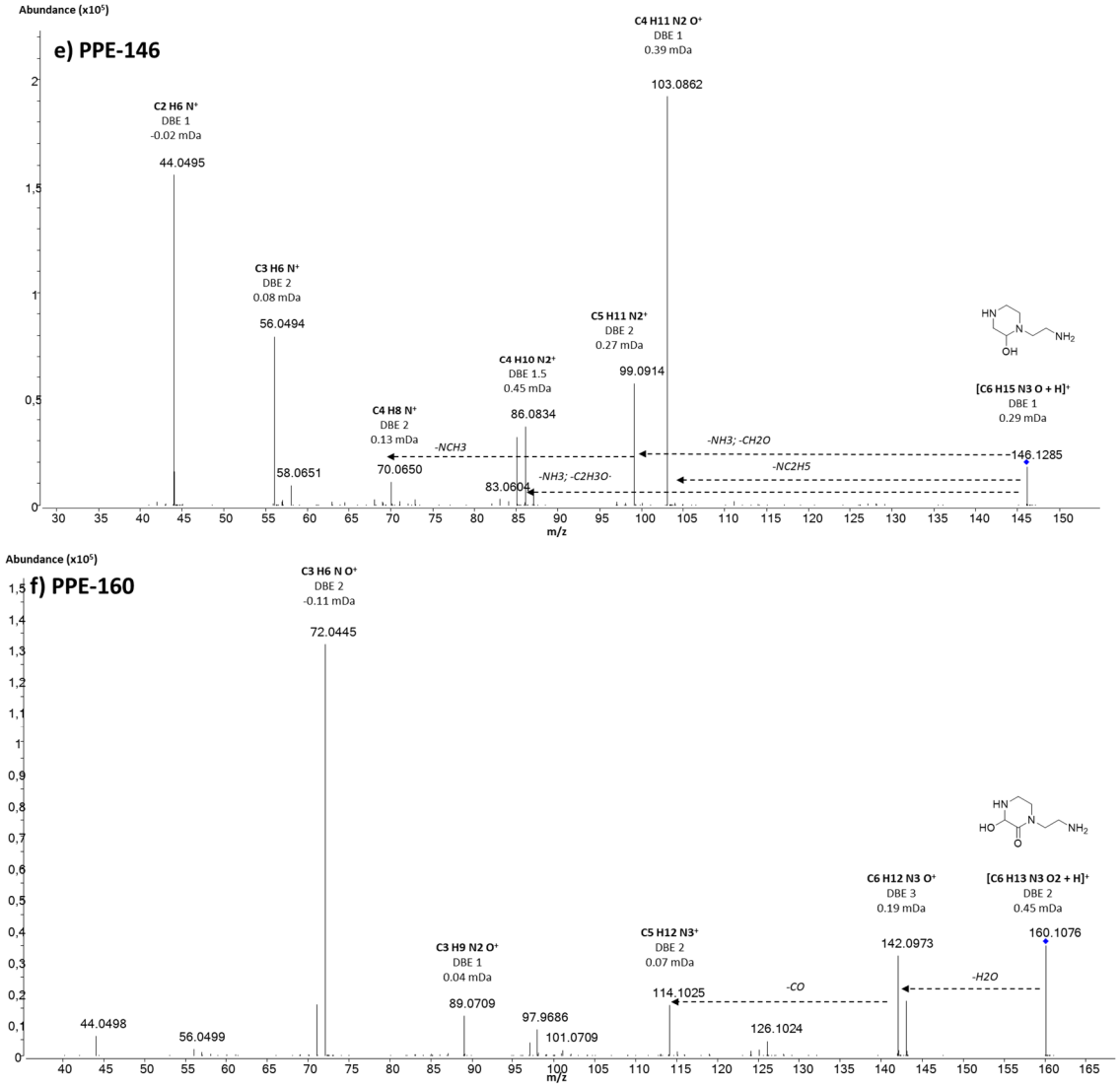

Figure SIV.5.2 (cont.): QTOF product ion spectra of VP and its TPs: (e) PPE-146 and (f) PPE-160

V. CONCLUSIONS

USC
UNIVERSIDADE
DE SANTIAGO
DE COMPOSTELA

CONCLUSIONS

This thesis has contributed to expand the knowledge in the field of disinfection by-products (DBPs) and transformation products (TPs) associated to water disinfection by chlorine-based or UV-based treatments. This was possible by exploiting the analytical capabilities of gas chromatography and liquid chromatography hyphenated to quadrupole-time of flight mass spectrometry (GC-QTOF-MS and LC-QTOF-MS) and performing experiments with different contaminants of emerging concern (CECs) upon different treatments. Also, both *in-silico* tools combined, in some cases, with real ecotoxicological tests in collaboration with other research teams were performed, to obtain a preliminary assessment of the expected consequences due to the formation of TPs and DBPs.

The main conclusions from this thesis are:

- LC-QTOF-MS instruments provide the required level of mass-resolving power and mass-accuracy necessary to being able to tentatively identify a wide set of TPs.
- Besides those qualitative features, the selectivity of QTOF analyzers can also be exploited for quantitative purposes. In that context, GC-QTOF-MS was proven to provide sufficiently low limits of detection (LODs) for the determination of N-nitrosamines in water samples, with excellent selectivity as compared to existing methods, particularly when combined to positive chemical ionization (PCI).
- 1,3-Diphenylguanidine (DPG) and 1,3-di-o-tolylguanidine (DTG) rapidly react with chlorine and bromine at natural water pH values and their reaction leads to the formation of several TPs (up to 35 proposed structures), via ipso-halogenation, hydroxylation, halogenation, and cyclization, and traditional/regulated DBPs such as chloroform and, to a minor extent, dichloroacetonitrile, when the molar ratio of chlorine to DPG/DTG is high.. Several of these TPs are *in-silico* predicted and confirmed by measuring the *Vibrio Fisheri* acute toxicity assay to be more toxic than the original guanidine compounds.
- In the case of phenazone-type drugs, all five chemicals tested (phenazone, propyphenazone and the metamizole metabolites 4-formylaminoantipyrine (FAA), 4-acetoamidoantipyrine (AAA) and 4-aminoantiyprine (AA)) undergo rapid reaction with chlorine, while chloramination is much slower and only three compounds (phenazone, propyphenazone and AA) reacted to a significant extension.
- The same TPs were observed during chlorination and chloramination. In the case of metamizole metabolites, the reaction pathway is common for all three, as FAA and AAA are first transformed into AA, which then further reacts to produce 5 other different non-halogenated TPs that could be identified by LC-QTOF. In the case of phenazone and propyphenazone, the formation of halogenated and hydroxylated derivatives is observed. Some of these TPs are *in-silico* predicted to be more toxic than the original compounds.
- The use of a laser with a 0.9 W nominal power, ns pulsed laser emitting at a wavelength of 266 nm was able to efficiently degrade, or significantly reduce the presence of ibuprofen (IBU) from water. IBU TPs detected after 15 min of treatment of ultrapure water and wastewater represent a very small signal. Given the dissolved organic carbon

balance, IBU might have partly been transformed into small molecules, not detectable by LC-QTOF, from which some are volatile and were removed from water.

- From the results of the zebrafish embryo bioassays, it seems clear that such TPs (even those unidentified) pose little toxicity and that laser treatment is a field requiring further research.
- Since lasers enable miniaturization and achievement of directional beam delivery, they bring about new opportunities for scale up geometries which are not reasonably achievable with more conventional sources.
- From 12 prioritized persistent and mobile high-production volume chemicals, only 2 of them (1-vinylpyrrolidin-2-one and 2-piperazin-1-ylethanamine, VP and PPE) significantly reacted with UV radiation.
- VP and PPE lead to the formation of up to 12 TPs, which were tentatively identified by LC-QTOF, and could eventually be formed during water treatment. A preliminary QSAR screening of the potential toxicological implications of those VP and PPE TPs seems to point to a low environmental and human hazard.
- *In-silico* toxicity prediction seems to have a large uncertainty and shall be used only as a preliminary screening. So, experimental ecotoxicological experiments should be conducted to confirm the results.

In view of the above-mentioned conclusions, the following research needs could be stablished:

- The development of newest generation GC-QTOF instruments with enhanced sensitivity and resolving power, together with the development of a softer ionization source may bring about even better quantitative performance, and this could be further exploited in the future, particularly for chemicals of low molecular weight.
- Also, since in some cases low molecular weight and volatile TPs and DBPs can be produced from the reaction of CECs with disinfectant agents, the combination of both GC-QTOF and LC-QTOF would help to achieve a more comprehensive understanding of those TPs/DBPs and the reaction mechanisms.
- It is essential in future studies to combine experimental ecotoxicological tests with those provided by QSAR tools in order to achieve a more reliable assessment of the risk posed by TPs, as in some cases the different predictive tools lead to a strong disagreement.
- Similarly, it is necessary to screen and eventually quantify the large number of TPs that have been identified in lab-scale experiments in real samples, in order to better understand their relevance.
- Lasers have shown to be a promising alternative to classical continuous sources for UV water treatment of IBU. However, this needs to be confirmed with more CECs and scaled up, in order to investigate their potential for future development.

REFERENCES

USC
UNIVERSIDADE
DE SANTIAGO
DE COMPOSTELA

REFERENCES

1. Abu Shmeis, R. M. Water Chemistry and Microbiology. In: Chormey, D. S., Bakırdere, S., Turan, N. B. & Engin, G. O. (Eds.) *Fundamentals of Quorum Sensing, Analytical Methods and Applications in Membrane Bioreactors*. *Comprehensive Analytical Chemistry* vol. 81, pp. 1-56. Elsevier (2018).

2. Stasinakis, A. S. *et al.* Contribution of primary and secondary treatment on the removal of benzothiazoles, benzotriazoles, endocrine disruptors, pharmaceuticals and perfluorinated compounds in a sewage treatment plant. *Sci. Total Environ.* **463–464**, 1067–1075 (2013).

3. Odlare, M. Introductory Chapter for Water Resources. *Reference Module in Earth Systems and Environmental Sciences* Series. Elsevier (2014). doi:10.1016/b978-0-12-409548-9.09035-7.

4. Gerba, C. P. & Pepper, I. L. Drinking Water Treatment and Distribution. In: Pepper, I. L., Gerba, C. P. & Gentri, T. J. (Eds). *Environmental Microbiology: Third Edition, pp. 633-643.* Elsevier (2015).

5. Quach-Cu, J. *et al.* The effect of primary, secondary, and tertiary wastewater treatment processes on antibiotic resistance gene (ARG) concentrations in solid and dissolved wastewater fractions. *Water (Switzerland)* **10**, 13–18 (2018).

6. Arashiro, L. T., Ferrer, I., Rousseau, D. P. L., Van Hulle, S. W. H. & Garfí, M. The effect of primary treatment of wastewater in high rate algal pond systems: Biomass and bioenergy recovery. *Bioresour. Technol.* **280**, 27–36 (2019).

7. Dargnat, C., Teil, M. J., Chevreuil, M. & Blanchard, M. Phthalate removal throughout wastewater treatment plant. Case study of Marne Aval station (France). *Sci. Total Environ.* **407**, 1235–1244 (2009).

8. Samer, M. Biological and Chemical Wastewater Treatment Processes. *INTECH Open* (2015) doi: 10.5772/61250.

9. Jing, Z. & Cao, S. Combined application of UV photolysis and ozonation with biological aerating filter in tertiary wastewater treatment. *Int. J. Photoenergy* **2012**, 140605 (2012).

10. Gerba, C. P. & Pepper, I. L. Municipal Wastewater Treatment. In: Pepper, I. L., Gerba, C. P. & Gentri, T. J. (Eds). *Environmental Microbiology: Third Edition, pp. 583-603.* Elsevier (2015).

11. The history of drinking water treatment. Document US EPA-816-F-00-006. US EPA (2000).

12. Harp, D. L. Current technology of chlorine analysis for water and wastewater. *Hach Co.* (2002).

13. Abou Mehrez, O., Dossier-Berne, F. & Legube, B. Chlorination and chloramination of aminophenols in aqueous solution: oxidant demand and by-product formation. *Environ. Technol.* **36**, 310–316 (2014).

14. Quintana, J. B., Rodil, R., López-Mahía, P., Muniategui-Lorenzo, S. & Prada-Rodríguez, D. Investigating the chlorination of acidic pharmaceuticals and by-product formation aided by an experimental design methodology. *Water Res.* **44**, 243–255 (2010).

15. Richardson, S. D. Disinfection by-products and other emerging contaminants in drinking water. *Trends Anal. Chem.* **22**, 666–684 (2003).

16. Benitez, F. J., Acero, J. L., Real, F. J., Roldan, G. & Casas, F. Bromination of selected pharmaceuticals in water matrices. *Chemosphere* **85**, 1430–1437 (2011).

17. Tian, C., Liu, R., Liu, H. & Qu, J. Disinfection by-products formation and precursors transformation during chlorination and chloramination of highly-polluted source water: Significance of ammonia. *Water Res.* **47**, 5901–5910 (2013).

18. Audrieth, L. F.; Rowe, R. A. The Stability of Aqueous Chloramine Solutions. *Chem. Eng. Univ. Illinois* **I**, 4726–4728 (1955).

19. Le Roux, J., Gallard, H. & Croue, J. Chloramination of nitrogenous contaminants (pharmaceuticals and pesticides): NDMA and halogenated DBPs formation. *Water Res.* **45**, 3164-3174 (2011).

20. Shen, R. & Andrews, S. A. Demonstration of 20 pharmaceuticals and personal care products (PPCPs) as nitrosamine precursors during chloramine disinfection. *Water Res.* **45**, 944–952 (2010).

21. Yang, X., Guo, W. & Lee, W. Formation of disinfection byproducts upon chlorine dioxide preoxidation followed by chlorination or chloramination of natural organic matter. *Chemosphere* **91**, 1477–1485 (2013).

22. Azzouz, A. & Ballesteros, E. Influence of seasonal climate differences on the pharmaceutical, hormone and personal care product removal efficiency of a drinking water treatment plant. *Chemosphere* **93**, 2046–2054 (2013).

23. Pinkernell, U., Nowack, B., Gallard, H. & Von Gunten, U. Methods for the photometric determination of reactive bromine and chlorine species with ABTS. *Water Res.* **34**, 4343–4350 (2000).

24. Rodríguez-Álvarez, T., Rodil, R., Quintana, J. B., Triñanes, S. & Cela, R. Oxidation of non-steroidal anti-inflammatory drugs with aqueous permanganate. *Water Res.* **47**, 3220–3230 (2013).

25. Quintana, J. B., Rodil, R. & Rodríguez, I. Transformation products of emerging contaminants upon reaction with conventional disinfection oxidants. In: Nollet, L. & Lambropoulou, D. (Eds) *Transformation products of emerging contaminants in the environment*, pp. 150–154. Wiley (2014).

26. Yang, W., Zhou, H. & Cicek, N. Treatment of Organic Micropollutants in Water and Wastewater by UV-based Processes : A Literature Review. *Critical Rev. Environ. Sci. Technol.* **44**, 1443–1476 (2014).

27. Kovacic, M. *et al.* UV photolysis of diclofenac in water ; kinetics , degradation pathway and environmental aspects. *Environ. Sci. Pollut. Res.* **23**, 14908–14917 (2016).

28. Rering, C., Williams, K., Hengel, M. & Tjeerdema, R. Comparison of Direct and Indirect Photolysis in Imazosulfuron Photodegradation. *J. Agric. Food Chem.* **65**, 3103–3108 (2017).

29. Benitez, F. J., Acero, J. L., Real, F. J., Roldan, G. & Rodriguez, E. Photolysis of model emerging contaminants in ultra-pure water: Kinetics, by-products formation and degradation pathways. *Water Res.* **47**, 870–880 (2013).

30. Attri, P. *et al.* Generation mechanism of hydroxyl radical species and its lifetime prediction during the plasma-initiated ultraviolet (UV) photolysis. *Sci. Rep.* **5**, 9332 (2015).

31. Yu, Y., Zhou, D. & Wu, F. Mechanism and products of the photolysis of hexabromocyclododecane in acetonitrile-water solutions under a UV-C lamp. *Chem. Eng. J.* **281**, 892–899 (2015).

32. Baranda, A. B., Lasagabaster, A. & de Marañón, I. M. Static and Continuous flow-through pulsed light technology for pesticide abatement in water. *J. Hazard. Mater.* **340**, 140–151 (2017).

33. Unkroth, A., Wagner, V. & Sauerbrey, R. Laser-assisted photochemical wastewater treatment. *Water Sci. Technol.* **35**, 181–188 (1997).

34. Pascu, M.-L. *et al.* Direct Modification of Bioactive Phenothiazines by Exposure to Laser Radiation. *Recent Pat. Antiinfect. Drug Discov.* **6**, 147–157 (2011).

35. Smarandache, A. Laser beams interaction with polidocanol foam: Molecular background. *Photomed. Laser Surg.* **30**, 262–267 (2012).

36. Chu, W.-S. Patent Application Publication (10) Pub . No .: US 2002 / 0124603 A1. vol. 1 1–33 (2002).

37. Kanakaraju, D., Glass, B. D. & Oelgemöller, M. Advanced oxidation process-mediated removal of pharmaceuticals from water: A review. *J. Environ. Manage.* **219**, 189–207 (2018).

38. Ribeiro, A. R., Nunes, O. C., Pereira, M. F. R. & Silva, A. M. T. An overview on the advanced oxidation processes applied for the treatment of water pollutants defined in the recently launched Directive 2013/39/EU. *Environ. Int.* **75**, 33–51 (2015).

39. Szabó, R. K. *et al.* Phototransformation of ibuprofen and ketoprofen in aqueous solutions. *Chemosphere* **84**, 1658–1663 (2011).

40. Litter, M. I. Introduction to Photochemical Advanced Oxidation Processes for Water Treatment. *Environ. Photochem. Part II* **2**, 325–366 (2005).

41. Bes Monge, S., Silva, A. M. T. & Bengoa, C. *Manual técnico sobre procesos de oxidación avanzada aplicados al tratamiento de aguas residuales industriales*. RED TRITÓN 316RT0508 (2016).

42. Li, K. Y., Kuo, C. H. & Weeks Jr., J. L. A kinetic study of ozone-phenol reaction in aqueous solutions. *AIChE J* **25**, 583−591 (2004).

43. Poznyak, T., Tapia, R., Vivero, J. & Chairez, I. Effect of pH to the decomposition of aqueous phenols mixture by ozone. *J. Mex. Chem. Soc.* **50**, 28−35 (2006).

44. J. Hoigné, H. B. Rate constants of reactions of ozone with organic and inorganic compounds in water (II). *Water Res.* **17**, 185–194 (1983).

45. Turhan, K. & Uzman, S. Removal of phenol from water using ozone. *Desalination* **229**, 257–263 (2008).

46. Mo, W., Cornejo, P. K., Malley, J. P., Kane, T. E. & Collins, M. R. Life cycle environmental and economic implications of small drinking water system upgrades to reduce disinfection byproducts. *Water Res.* **143**, 155–164 (2018).

47. Scheurer, M., Michel, A., Brauch, H. J., Ruck, W. & Sacher, F. Occurrence and fate of the antidiabetic drug metformin and its metabolite guanylurea in the environment and during drinking water treatment. *Water Res.* **46**, 4790–4802 (2012).

48. Hollender, J. *et al.* Elimination of organic micropollutants in a municipal wastewater treatment plant upgraded with a full-scale post-ozonation followed by sand filtration. *Environ. Sci. Technol.* **43**, 7862–7869 (2009).

49. Augugliaro, V. & Rizzuti, L. The pH dependence of the ozone absorption kinetics in aqueous phenol solutions. *Chem. Eng. Sci.* **33**, 1441–1447 (1978).

50. Piechowski, M., Thelen, M., Hoigné, J. & Buhler, R. E. Tert-butanol as an OH scavenger in the Pulse Radiolysis of Oxygenated Aqueous Systems. *Ber. Bunsenge. Phys. Chem.* **96**, 1448–1454 (1992).

51. Suárez, S., Carballa, M., Omil, F. & Lema, J. M. How are pharmaceutical and personal care products (PPCPs) removed from urban wastewaters? *Rev. Environ. Sci. Biotechnol.* **7**, 125–138 (2008).

52. Plumlee, M. H., López-Mesas, M., Heidlberger, A., Ishida, K. P. & Reinhard, M. N-nitrosodimethylamine (NDMA) removal by reverse osmosis and UV treatment and analysis via LC-MS/MS. *Water Res.* **42**, 347–355 (2008).

53. Richardson, S. D. & Kimura, S. Y. Water Analysis: Emerging Contaminants and Current Issues. *Anal. Chem.* **77**, 3807–3838 (2019).

54. Mitch, W. A. & Sedlak, D. L. Characterization and Fate of N-Nitrosodimethylamine Precursors in Municipal Wastewater Treatment Plants. *Environ. Sci. Technol.* **38**, 1445–1454 (2004).

55. Nawrocki, J. & Andrzejewski, P. Nitrosamines and water. *J. Hazard. Mater.* **189**, 1–18 (2011).

56. Acero, J. L., Benitez, F. J., Teva, F. & Leal, A. I. Retention of emerging micropollutants from UP water and a municipal secondary effluent by ultrafiltration and nanofiltration. *Chem. Eng. J.* **163**, 264–272 (2010).

57. Acero, J. L., Javier Benitez, F., Real, F. J. & Teva, F. Coupling of adsorption, coagulation, and ultrafiltration processes for the removal of emerging contaminants in a secondary effluent. *Chem. Eng. J.* **210**, 1–8 (2012).

58. Krzeminski, P. *et al.* Performance of secondary wastewater treatment methods for the removal of contaminants of emerging concern implicated in crop uptake and antibiotic resistance spread: A review. *Sci. Total Environ.* **648**, 1052–1081 (2019).

59. Contaminants of Emerging Concern in Urban Wastewater. Joint NORMAN and Water Europe Position Paper. NORMAN noetwork (2019).

60. Sauvé, S. & Desrosiers, M. A review of what is an emerging contaminant. *Chem. Cent. J.* **8**, 1–7 (2014).

61. Directive 2000/60/EC of the European Parliament and of the Council of 23 October 2000 establishing a framework for Community action in the field of water policy. *Off. J. Eur. Communities* **L327**/1-71 (2000).

62. Zahn, D. *et al.* Identification of potentially mobile and persistent transformation products of REACH-registered chemicals and their occurrence in surface waters. *Water Res.* **150**, 86–96 (2019).

63. Kümmerer, K. *Pharmaceuticals in the environment*. *Ann. Rev. Env. Res.* **35**, 57-75 (2010).

64. Informe de utilización de medicamentos U/AIN/V1/11/09/2017. Utilización de medicamentos antiinflamatorios no esteroideos en España durante el periodo 2013-2016. Agencia Española del Medicamento y Productos Saniatarios (2017).

65. Marchlewicz, A., Guzik, U. & Wojcieszyńska, D. Over-the-Counter Monocyclic Non-Steroidal

Anti-Inflammatory Drugs in Environment - Sources, Risks, Biodegradation. *Water. Air. Soil Pollut.* **226**, 355 (2015).

66. Santos, J. L., Aparicio, I., Callejón, M. & Alonso, E. Occurrence of pharmaceutically active compounds during 1-year period in wastewaters from four wastewater treatment plants in Seville (Spain). *J. Hazard. Mater.* **164**, 1509–1516 (2009).

67. Luo, Y. *et al.* A review on the occurrence of micropollutants in the aquatic environment and their fate and removal during wastewater treatment. *Sci. Total Environ.* **473–474**, 619–641 (2014).

68. Kruglova, A. *et al.* Comparative study of emerging micropollutants removal by aerobic activated sludge of large laboratory-scale membrane bioreactors and sequencing batch reactors under low-temperature conditions. *Bioresour. Technol.* **214**, 81–88 (2016).

69. Wang, J. & Wang, S. Removal of pharmaceuticals and personal care products (PPCPs) from wastewater: A review. *J. Environ. Manage.* **182**, 620–640 (2016).

70. Behera, S. K., Kim, H. W., Oh, J. E. & Park, H. S. Occurrence and removal of antibiotics, hormones and several other pharmaceuticals in wastewater treatment plants of the largest industrial city of Korea. *Sci. Total Environ.* **409**, 4351–4360 (2011).

71. Gracia-Lor, E., Sancho, J. V., Serrano, R. & Hernández, F. Occurrence and removal of pharmaceuticals in wastewater treatment plants at the Spanish Mediterranean area of Valencia. *Chemosphere* **87**, 453–462 (2012).

72. Loos, R. *et al.* EU-wide monitoring survey on emerging polar organic contaminants in wastewater treatment plant effluents. *Water Res.* **47**, 6475–6487 (2013).

73. Terzić, S. *et al.* Occurrence and fate of emerging wastewater contaminants in Western Balkan Region. *Sci. Total Environ.* **399**, 66–77 (2008).

74. Kim, J. W. *et al.* Occurrence of Pharmaceutical and Personal Care Products (PPCPs) in Surface Water from Mankyung River, South Korea. *J. Heal. Sci.* **55**, 249–258 (2009).

75. Stasinakis, A. S., Mermigka, S., Samaras, V. G., Farmaki, E. & Thomaidis, N. S. Occurrence of endocrine disrupters and selected pharmaceuticals in Aisonas River (Greece) and environmental risk assessment using hazard indexes. *Environ. Sci. Pollut. Res.* **19**, 1574–1583 (2012).

76. Wiegel, S. *et al.* Pharmaceuticals in the river Elbe and its tributaries. *Chemosphere* **57**, 107–126 (2004).

77. Fonseca, E. *et al.* Occurrence and ecological risks of pharmaceuticals in a Mediterranean river in Eastern Spain. *Environ. Int.* **144**, 106004 (2020).

78. Kosma, C. I., Lambropoulou, D. A. & Albanis, T. A. Investigation of PPCPs in wastewater treatment plants in Greece: Occurrence, removal and environmental risk assessment. *Sci. Total Environ.* **466–467**, 421–438 (2014).

79. Ternes, T., Bonerz, M. & Schmidt, T. Determination of neutral pharmaceuticals in wastewater and rivers by liquid chromatography-electrospray tandem mass spectrometry. *J. Chromatogr. A* **938**, 175–185 (2001).

80. Gyenge-Szabó, Z., Szoboszlai, N., Frigyes, D., Záray, G. & Mihucz, V. G. Monitoring of four dipyrone metabolites in communal wastewater by solid phase extraction liquid

chromatography electrospray ionization quadrupole time-of-flight mass spectrometry. *J. Pharm. Biomed. Anal.* **90**, 58–63 (2014).

81. Martínez Bueno, M. J. *et al.* Application of Liquid Chromatography / Quadrupole-Linear Ion Trap Mass Spectrometry and Time-of-Flight Mass Spectrometry to the Determination of Pharmaceuticals and Related Contaminants in Wastewater. *Anal. Chem* **79**, 2918–2926 (2007).

82. Agundez, J. A. G., Martinez, C. & Benitez, J. Metabolism of aminopyrine and derivatives in man: in vivo study of monomorphic and polymorphic metabolic pathways. *Xenobiotica* **25**, 417–427 (1995).

83. Agundez, J. A. G., Martinez, C., Martín, R. & Benitez, J. Determination of Aminopyrine, Dipyrone and Its Metabolites in Urine by High-Performance Liquid Chromatography. *Ther. Drug Monit.* **16**, 316-322 (1994).

84. Levy, M., Zylber-Katz, E. & Rosenkranz, B. Clinical Pharmacokinetics of Dipyrone and its Metabolites. *Clin. Pharmacokinet.* **28**, 216–234 (1995).

85. Feldmann, D. F., Zuehlke, S. & Heberer, T. Occurrence, fate and assessment of polar metamizole (dipyrone) residues in hospital and municipal wastewater. *Chemosphere* **71**, 1754–1764 (2008).

86. Vlahov, V., Badian, M., Verho, M. & Bacracheva, N. Pharmacokinetics of metamizol metabolites in healthy subjects after a single oral dose of metamizol sodium. *Eur. J. Clin. Pharmacol.* **38**, 61–65 (1990).

87. Volz, M. & Kellner, H. Kinetics and metabolism of pyrazolones (propyphenazone, aminopyrine and dipyrone). *Braz. J. Clin. Pharmacol.* **10**, 299S-308S (1980).

88. Bachmann, F., Duthaler, U., Rudin, D., Krähenbühl, S. & Haschke, M. N-demethylation of N-methyl-4-aminoantipyrine, the main metabolite of metamizole. *Eur. J. Pharm. Sci.* **120**, 172–180 (2018).

89. Zuehlke, S., Duennbier, U., Lesjean, B., Gnirss, R. & Buisson, H. Long-Term Comparison of Trace Organics Removal Performances Between Conventional and Membrane Activated Sludge Processes. *Water Environ. Res.* **78**, 2480–2486 (2006).

90. Reemtsma, T. *et al.* Mind the Gap: Persistent and Mobile Organic Compounds—Water Contaminants That Slip Through. *Environ. Sci. Technol.* **50**, 10308–10315 (2016).

91. Schulze, S. *et al.* Occurrence of emerging persistent and mobile organic contaminants in European water samples. *Water Res.* **153**, 80–90 (2019).

92. Gago-Ferrero, P. *et al.* Extended Suspect and Non-Target Strategies to Characterize Emerging Polar Organic Contaminants in Raw Wastewater with LC-HRMS/MS. *Environ. Sci. Technol.* **49**, 12333–12341 (2015).

93. Montes, R. *et al.* Screening for Polar Chemicals in Water by Trifunctional Mixed-Mode Liquid Chromatography–High Resolution Mass Spectrometry. *Environ. Sci. Technol.* **51**, 6250–6259 (2017).

94. Neumann, M. & Schliebner, I. Protecting the sources of our drinking water. A revised proposal for implementing criteria and an assessment procedure to identify Persistent, Mobile and Toxic (PMT) and very Persistent, very Mobile (vPvM) substances registered under REACH. German Environmentl Agency (2017).

95. Schulze, S. *et al.* Using REACH registration data to rank the environmental emission potential of

persistent and mobile organic chemicals. *Sci. Total Environ.* **625**, 1122–1128 (2018).

96. Tang, J. *et al.* Different senescent HDPE pipe-risk: brief field investigation from source water to tap water in China (Changsha City). *Environ. Sci. Pollut. Res.* **22**, 16210–16214 (2015).

97. PROMOTE JPI Water project Website: https://www.ufz.de/promote/ (acccesed on September 2020)

98. Fatta-Kassinos, D., Vasquez, M. I. & Kümmerer, K. Transformation products of pharmaceuticals in surface waters and wastewater formed during photolysis and advanced oxidation processes - Degradation, elucidation of byproducts and assessment of their biological potency. *Chemosphere* **85**, 693–709 (2011).

99. Somasundaram, L. & Coats, J. R. Pesticide Transformation Products Research: A future perspective. *ACS Symposium Series* **489**, 285–288 (1991).

100. Picó, Y. & Barceló, D. Transformation products of emerging contaminants in the environment and high-resolution mass spectrometry: A new horizon. *Anal. Bioanal. Chem.* **407**, 6257–6273 (2015).

101. Michael, I. et al. Metabolites and transformation products of pharmaceuticals in the aquatic environment as contaminants of emerging concern. In: Nollet, L. & Lambropoulou, D. (Eds) *Transformation products of emerging contaminants in the environment*, pp. 413–458. Wiley (2014).

102. Dong, H., Qiang, Z., Lian, J. & Qu, J. Degradation of nitro-based pharmaceuticals by UV photolysis : Kinetics and simultaneous reduction on halonitromethanes formation potential. *Water Res.* **119**, 83–90 (2017).

103. Zwiener, C. Trihalomethanes (THMs), Haloacetic Acids (HAAs), and Emerging Disinfection By-products in Drinking Water. In: Reemtsma, T. & Jekel, M. Organic Pollutants in the Water Cycle: Properties, Occurrence, Analysis and Environmental Relevance of Polar Compounds, pp. 251–268. Wiley (2006).

104. Council Directive 98/83/EC of 3 November 1998 on the quality of water intended for human consumption. *Off. J. Eur. Communities* **L330**/32-54 (1998).

105. Proposal for a Directive of the European Parliament and of the Council on the quality of water intended for human consumption (recast) COM/2017/0753 final - 2017/0332 (COD).

106. Liu, R. *et al.* Effects of bromide on the formation and transformation of disinfection by-products during chlorination and chloramination. *Sci. Total Environ.* **625**, 252–261 (2018).

107. Acero, J. L., Benitez, F. J., Real, F. J., Roldan, G. & Rodriguez, E. Chlorination and bromination kinetics of emerging contaminants in aqueous systems. *Chem. Eng. J.* **219**, 43–50 (2013).

108. Method 551.1: Determination of chlorination disinfection byproducts, chlorinated solvents , and halogenated pesticides/ herbicides in drinking water by liquid-liquid extraction and gas chromatography with electron-capture detection. Revision 1.0. US EPA (1995).

109. Wang, W. *et al.* Formation of Multiple Nitrosamines from the Ozonation of Corresponding Precursor Secondary Amines: Influencing Factors and Transformation Mechanisms. *Water. Air. Soil Pollut.* **230**, 41 (2019).

110. Fu, S. C., Tzing, S. H., Chen, H. C., Wang, Y. C. & Ding, W. H. Dispersive micro-solid phase extraction combined with gas chromatography-chemical ionization mass spectrometry for the

determination of N-nitrosamines in swimming pool water samples. *Anal. Bioanal. Chem.* **402**, 2209–2216 (2012).

111. Al-kaseem, M., Al-assaf, Z. & Karabet, F. Rapid and Simple Extraction Method for Volatile N-Nitrosamines in Meat Products. *Pharmacol. Pharm.* **4**, 611–618 (2013).

112. Al-Kaseem, M., Al-Assaf, Z. & Karabeet, F. Determination of Seven Volatile N-Nitrosamines in Fast Food. *Pharmacol. Pharm.* **2014**, 195–203 (2014).

113. D. Wiltschko, M. Lipp & Anklam, E. A Review on Analytical Methods to Determine Nitrosamines in Food. Joint Research Center (1998).

114. Andrade, R., Reyes, F. G. & Rath, S. A method for the determination of volatile N-nitrosamines in food by HS-SPME-GC-TEA. *Food Chem.* **91**, 173–179 (2005).

115. Gremaud, E., Biaudet, H. & Turesky, R. J. Rapid Solid-Phase Extraction Method for the Detection of Volatile Nitrosamines in Food. *J. Agric. Food Chem.* **45**, 4706–4713 (1997).

116. WHO Guidelines for Drinking Water Quality. Fourth Edition. World Health Organization (2017).

117. Boards, C.W. NDMA and Other Nitrosamines—Drinking Water Issues. Available online: https://www.waterboards.ca.gov/drinking_water/certlic/drinkingwater/NDMA.html (accessed on September 2020).

118. Munch, J. & Bassett, M. Solid Phase Extraction and Capillary Column Gas Chromatography with Large Volume Injection and Chemical Ionization Tandem Mass Spectrometry (MS/MS). US *EPA Report. 182,* 1–47 (2004).

119. Pozzi, R., Bocchini, P., Pinelli, F. & Galletti, G. C. Determination of nitrosamines in water by gas chromatography/chemical ionization/selective ion trapping mass spectrometry. *J. Chromatogr. A* **1218**, 1808–1814 (2011).

120. Grebel, J. E., Young, C. C. & Suffet, I. H. Solid-phase microextraction of N-nitrosamines. *J. Chromatogr. A* **1117**, 11–18 (2006).

121. Chen, W. *et al.* Comparison of gas chromatography-mass spectrometry and gas chromatography-tandem mass spectrometry with electron ionization for determination of N-nitrosamines in environmental water. *Chemosphere* **168**, 1400–1410 (2017).

122. Zhao, Y., Boyd, J., Hrudey, S. E. & Li, X. Characterization of New Nitrosamines in Drinking Water Using Liquid Chromatography Tandem Mass Spectrometry. *Environ. Sci. Technol.* **40**, 7636–7641 (2006).

123. Cheng, R. C. *et al.* Alternative methods for the analysis of NDMA and other nitrosamines in water. J. *Am. Water Work. Assoc.* **98**, 82–96 (2006).

124. Llop, A., Borrull, F. & Pocurull, E. Fully automated determination of N-nitrosamines in environmental waters by headspace solid-phase microextraction followed by GC-MS-MS. *J. Sep. Sci.* **33**, 3692–3700 (2010).

125. Yurchenko, S. & Mölder, U. N-nitrosodimethylamine analysis in Estonian beer using positive-ion chemical ionization with gas chromatography mass spectrometry. *Food Chem.* **89**, 455–463 (2005).

126. Yurchenko, S. & Mölder, U. Volatile N-nitrosamines in various fish products. *Food Chem.* **96**, 325–333 (2006).

127. Yurchenko, S. & Mölder, U. The occurrence of volatile N-nitrosamines in Estonian meat products. *Food Chem.* **100**, 1713–1721 (2007).

128. Cai, M.-Q., Feng, L. & Zhang, L.-Q. Transformation of aminopyrine in the presence of free available chlorine: Kinetics, products, and reaction pathways. *Chemosphere* **171**, 625–634 (2017).

129. Quintana, J. B., Rodil, R. & Cela, R. Reaction of β-blockers and β-agonist pharmaceuticals with aqueous chlorine. Investigation of kinetics and by-products by liquid chromatography quadrupole time-of-flight mass spectrometry. *Anal. Bioanal. Chem.* **403**, 2385–2395 (2012).

130. Hollender, J. *et al.* High resolution mass spectrometry-based non-target screening can support regulatory environmental monitoring and chemicals management. *Environ. Sci. Eur.* **31**, 42 (2019).

131. Schymanski, E. L. *et al.* Non-target screening with high-resolution mass spectrometry: Critical review using a collaborative trial on water analysis. *Anal. Bioanal. Chem.* **407**, 6237–6255 (2015).

132. Postigo, C. & Richardson, S. D. Transformation of pharmaceuticals during oxidation/disinfection processes in drinking water treatment. *J. Hazard. Mater.* **279**, 461–475 (2014).

133. Kern, S., Fenner, K., Singer, H. P., Schwarzenbach, R. P. & Hollender, J. Identification of transformation products of organic contaminants in natural waters by computer-aided prediction and high-resolution mass spectrometry. *Environ. Sci. Technol.* **43**, 7039–7046 (2009).

134. Menger, F., Gago-Ferrero, P. Wiberg, K., Ahrens, L. Wide-scope screening of polar contaminants of concern in water: A critical review of liquid chromatography-high resolution mass spectrometry-based strategies. *Trends Environ. Anal. Chem*. **28**, e00102 (2020).

135. Krauss, M., Singer, H. & Hollender, J. LC – high resolution MS in environmental analysis : from target screening to the identification of unknowns. *Anal. Bioanal. Chem.* **397**, 943–951 (2010).

136. Richardson, S. D. & Postigo, C. *Discovery of New Emerging DBPs by High-Resolution Mass Spectrometry*. *Comprehensive Analytical Chemistry* vol. 71. Elsevier (2016).

137. González-Mariño, I., Carpinteiro, I., Rodil, R., Rodríguez, I. & Quintana, J. B. High-Resolution Mass Spectrometry Identification of Micropollutants Transformation Products Produced During Water Disinfection With Chlorine and Related Chemicals. In: Pérez, S., Eichhorn, P. & Barceló, D. (Eds.), *Applications of time-of-flight and orbitrap mass spectrometry in environmental, food, doping, and forensic analysis*. Comprehensive Analytical Chemistry Vol. 71, pp. 283-334. Elsevier (2016).

138. Preiss, A. & Godejohann, M. Applications of NMR Techniques for the Identification and Structure Elucidation of Emerging Organic and Other Xenobiotic Organic Contaminants. In: Nollet, L. & Lambropoulou, D. (Eds) *Transformation products of emerging contaminants in the environment*, pp. 351–384. Wiley (2014).

139. Kormos, J. L., Schulz, M., Wagner, M. & Ternes, T. A. Multistep approach for the structural identification of biotransformation products of iodinated X-ray contrast media by liquid chromatography/hybrid triple quadrupole linear ion trap mass spectrometry and 1H and 13C nuclear magnetic resonance. *Anal. Chem.* **81**, 9216–9224 (2009).

140. Raro, M. *et al.* Potential of atmospheric pressure chemical ionization source in gas chromatography tandem mass spectrometry for the screening of urinary exogenous androgenic

anabolic steroids. *Anal. Chim. Acta* **906**, 128–138 (2016).

141. Hernández, F., Sancho, J. V, Ibáñez, M. & Abad, E. Current use of high-resolution mass spectrometry in the environmental sciences. *Anal. Bional. Chem.* **403**, 1251–1264 (2012).

142. Van Bavel, B. *et al.* Atmospheric-Pressure Chemical Ionization Tandem Mass Spectrometry (APGC/MS/MS) an Alternative to High-Resolution Mass Spectrometry (HRGC/HRMS) for the Determination of Dioxins. *Anal. Chem.* **87**, 9047–9053 (2015).

143. González-Mariño, I., Quintana, J. B., Rodríguez, I., González-Díez, M. & Cela, R. Screening and selective quantification of illicit drugs in wastewater by mixed-mode solid-phase extraction and quadrupole-time-of-flight liquid chromatography-mass spectrometry. *Anal. Chem.* **84**, 1708–1717 (2012).

144. Johnson, M. & Melbourne, P. Photolytic spectroscopic quantification of residual chlorine in potable waters. *Analyst* **121**, 1075–1078 (1996).

145. Lane, R. F., Adams, C. D., Randtke, S. J. & Carter, R. E. Chlorination and chloramination of bisphenol A, bisphenol F, and bisphenol A diglycidyl ether in drinking water. *Water Res.* **79**, 68–78 (2015).

146. Mitch, W. A. & Sedlak, D. L. Formation of N -Nitrosodimethylamine (NDMA) from Dimethylamine during Chlorination. *Environ. Sci. Technol.* **36**, 588–595 (2002).

147. Schreiber, I. M. & Mitch, W. A. Influence of the method of reagent addition on NDMA formation during chloramination. *Environ. Sci. Technol.* **39**, 3811-3818 (2005).

148. Clesceri, L., Eaton, A., Greenberg, A. & Franson, M. A. *Standard Methods for the Examination of Water and Wastewater*. American Public Health Association (1998).

149. Pescod, M. *Wastewater treatment and use in agriculture*.FAO Irrigation and drainage paper 47. Food and Agriculture Organization of the United Nations (1992).

150. Acero, J. L., Benitez, F. J., Real, F. J., Roldan, G. & Rodriguez, E. Chlorination and bromination kinetics of emerging contaminants in aqueous systems. *Chem. Eng. J.* **219**, 43–50 (2013).

151. US-EPA. Drinking Water requirements for States and Public health water systems: https://www.epa.gov/dwreginfo (Accessed on September 2020).

152. Dodd, M. C. & Huang, C. H. Transformation of the antibacterial agent sulfamethoxazole in reactions with chlorine: Kinetics, mechanisms, and pathways. *Environ. Sci. Technol.* **38**, 5607–5615 (2004).

153. Benitez, F. J., Acero, J. L., Real, F. J., Roldan, G. & Casas, F. Bromination of selected pharmaceuticals in water matrices. *Chemosphere* **85**, 1430–1437 (2011).

154. Castro, G. *et al.* Time-of-flight mass spectrometry assessment of fluconazole and climbazole UV and UV/H2O2 degradability: Kinetics study and transformation products elucidation. *Water Res.* **88**, 681–690 (2016).

155. González-Mariño, I., Rodríguez, I., Rojo, L. & Cela, R. Photodegradation of nitenpyram under UV and solar radiation: Kinetics, transformation products identification and toxicity prediction. *Sci. Total Environ.* **644**, 995–1005 (2018).

156. Hu, X., Ji, H. & Wu, L. Singlet oxygen photogeneration and 2,4,6-TCP photodegradation at Pt/TiO2 under visible light illumination. *RSC Adv.* **2**, 12378–12383 (2012).

157. Illés, E. *et al.* Hydroxyl radical induced degradation of ibuprofen. *Sci. Total Environ.* **447**, 286–292 (2013).

158. Méndez-Arriaga, F., Esplugas, S. & Giménez, J. Degradation of the emerging contaminant ibuprofen in water by photo-Fenton. *Water Res.* **44**, 589–595 (2010).

159. Carpinteiro, I., Rodil, R., Quintana, J. B. & Cela, R. Reaction of diazepam and related benzodiazepines with chlorine. Kinetics, transformation products and in-silico toxicological assessment. *Water Res.* **120**, 280–289 (2017).

160. Tawk, A., Deborde, M., Labanowski, J. & Gallard, H. Chlorination of the β-triketone herbicides tembotrione and sulcotrione: Kinetic and mechanistic study, transformation products identification and toxicity. *Water Res.* **76**, 132–142 (2015).

161. Barros, S. *et al.* Chronic environmentally relevant levels of simvastatin disrupt embryonic development, biochemical and molecular responses in zebrafish (Danio rerio). *Aquat. Toxicol.* **201**, 47–57 (2018).

162. Torres, T., Cunha, I., Martins, R. & Santos, M. M. Screening the toxicity of selected personal care products using embryo bioassays: 4-MBC, propylparaben and triclocarban. *Int. J. Mol. Sci.* **17**, 1762 (2016).

163. Cunha, V., Rodrigues, P., Santos, M. M., Moradas-Ferreira, P. & Ferreira, M. Fluoxetine modulates the transcription of genes involved in serotonin, dopamine and adrenergic signalling in zebrafish embryos. *Chemosphere* **191**, 954–961 (2018).

164. Planas, C., Palacios, Ó., Ventura, F., Rivera, J. & Caixach, J. Analysis of nitrosamines in water by automated SPE and isotope dilution GC/HRMS. Occurrence in the different steps of a drinking water treatment plant, and in chlorinated samples from a reservoir and a sewage treatment plant effluent. *Talanta* **76**, 906–913 (2008).

165. Moschet, C., Lew, B. M., Hasenbein, S., Anumol, T. & Young, T. M. LC- and GC-QTOF-MS as Complementary Tools for a Comprehensive Micropollutant Analysis in Aquatic Systems. *Environ. Sci. Technol.* **51**, 1553–1561 (2017).

166. Wang, Y., Gao, W., Wang, Y. & Jiang, G. Suspect screening analysis of the occurrence and removal of micropollutants by GC-QTOF MS during wastewater treatment processes. *J. Hazard. Mater.* **376**, 153–159 (2019).

167. Abushareeda, W. *et al.* Gas chromatographic quadrupole time-of-flight full scan high resolution mass spectrometric screening of human urine in antidoping analysis. *J. Chromatogr. B.* **1063**, 74–83 (2017).

168. Charrois, J. W. A., Boyd, J. M., Froese, K. L. & Hrudey, S. E. Occurrence of *N* -nitrosamines in Alberta public drinking-water distribution systems. *J. Environ. Eng. Sci.* **6**, 103–114 (2007).

169. Krauss, M., Longrée, P., Dorusch, F., Ort, C. & Hollender, J. Occurrence and removal of N-nitrosamines in wastewater treatment plants. *Water Res.* **43**, 4381–4391 (2009).

170. Jurado-Sánchez, B., Ballesteros, E. & Gallego, M. Comparison of the sensitivities of seven N-nitrosamines in pre-screened waters using an automated preconcentration system and gas chromatography with different detectors. *J. Chromatogr. A* **1154**, 66–73 (2007).

171. Krauss, M. & Hollender, J. Analysis of nitrosamines in wastewater: Exploring the trace level quantification capabilities of a hybrid linear ion trap/orbitrap mass spectrometer. *Anal. Chem.*

80, 834–842 (2008).

172. McDonald, J. A., Harden, N. B., Nghiem, L. D. & Khan, S. J. Analysis of N-nitrosamines in water by isotope dilution gas chromatography-electron ionisation tandem mass spectrometry. *Talanta* **99**, 146–154 (2012).

173. Krasner, S. W., Mitch, W. A., Mccurry, D. L., Hanigan, D. & Westerhoff, P. Formation , precursors , control , and occurrence of nitrosamines in drinking water: A review. *Water Res.* **47**, 4433–4450 (2013).

174. Luo, Q., Wang, D. & Wang, Z. Occurrences of nitrosamines in chlorinated and chloraminated drinking water in three representative cities, China. *Sci. Total Environ.* **437**, 219–225 (2012).

175. Zhou, Q. *et al.* Field evidence of biodegradation of N-Nitrosodimethylamine (NDMA) in groundwater with incidental and active recycled water recharge. *Water Res.* **43**, 793–805 (2009).

176. Consolidated List of Products Whose Consumption and/or Sale Have Been Banned, Withdrawn, Severely Restricted or not Approved by Governments. UN. Department of Economic and Social Affairs (2009).

177. Utilización de medicamentos analgésicos no opioides en España durante el periodo 2010-2018. Agencia Española de Medicamentos y Productos Sanitarios. Available: https://www.aemps.gob.es/medicamentos-de-uso-humano/observatorio-de-uso-de-medicamentos/utilizacion-de-medicamentos-analgesicos-no-opioides-en-espana-durante-el-periodo-2010-2018/?lang=en (Accessed on September 2020).

178. Ternes, T. A. Occurrence of drugs in German sewage treatment plants and rivers. *Water Res.* **32**, 3245–3260 (1998).

179. Reddersen, K., Heberer, T. & Dünnbier, U. Identification and significance of phenazone drugs and their metabolites in ground- and drinking water. *Chemosphere* **49**, 539–544 (2002).

180. Zühlke, S., Dünnbier, U. & Heberer, T. Detection and identification of phenazone-type drugs and their microbial metabolites in ground and drinking water applying solid-phase extraction and gas chromatography with mass spectrometric detection. *J. Chromatogr. A* **1050**, 201–209 (2004).

181. Gómez, M. J., Sirtori, C., Mezcua, M., Fernández-Alba, A. R. & Agüera, A. Photodegradation study of three dipyrone metabolites in various water systems: Identification and toxicity of their photodegradation products. *Water Res.* **42**, 2698–2706 (2008).

182. Favier, M., Dewil, R., Van Eyck, K., Van Schepdael, A. & Cabooter, D. High-resolution MS and MS(n) investigation of ozone oxidation products from phenazone-type pharmaceuticals and metabolites. *Chemosphere* **136**, 32–41 (2015).

183. Miao, H. F. *et al.* Degradation of phenazone in aqueous solution with ozone: Influencing factors and degradation pathways. *Chemosphere* **119**, 326–333 (2015).

184. Jiang, B. *et al.* Degradation behaviors of Isopropylphenazone and Aminopyrine and their genetic toxicity variations during UV/chloramine treatment. *Water Res.* **170**, 115339 (2020).

185. Rodil, R., Quintana, J. B. & Cela, R. Transformation of phenazone-type drugs during chlorination. *Water Res.* **46**, 2457–2468 (2012).

186. Uetrecht, J. P., Ma, H. M., MacKnight, E. & McClelland, R. Oxidation of aminopyrine by

hypochlorite to a reactive dication: possible implications for aminopyrine-induced agranulocytosis. *Chem. Res. Toxicol.* **8**, 226–233 (1995).

187. Han, Y. *et al.* Insight into the generation of toxic products during chloramination of carbamazepine: Kinetics, transformation pathway and toxicity. *Sci. Total Environ.* **679**, 221–228 (2019).

188. Vikesland, P. J., Ozekin, K. & Valentine, R. L. Monochloramine decay in model and distribution system waters. *Water Res.* **35**, 1766–1776 (2001).

189. Zhang, X. *et al.* Highly efficient photocatalytic removal of multiple refractory organic pollutants by BiVO4/CH3COO(BiO) heterostructured nanocomposite. *Sci. Total Environ.* **647**, 245–254 (2019).

190. Zuehlke, S., Duennbier, U. & Heberer, T. Investigation of the behavior and metabolism of pharmaceutical residues during purification of contaminated ground water used for drinking water supply. *Chemosphere* **69**, 1673–1680 (2007).

191. Guidance on the Application of the CLP Criteria Extracts of the document in this consultation. Guidance to Regulation (EC) No 1272/2008 on classification, labelling and packaging (CLP) of substances and mixtures. Version 5.0 European Chemicals Agency (2017).

192. 1,3-di-o-tolylguanidine (EC Number: 202-577-6 | CAS Number: 97-39-2) REACH Dossier. European Chemicals Agency (2018)

193. Montes, R., Rodil, R., Cela, R. & Quintana, J. B. Determination of Persistent and Mobile Organic Contaminants (PMOCs) in Water by Mixed-Mode Liquid Chromatography-Tandem Mass Spectrometry. *Anal. Chem.* **91**, 5176–5183 (2019).

194. Hübner, D., Zahn, D., Huppertsberg, S. & Knepper, T.P. Tires and tire wear particles as source of 1,3- diphenylguanidine and other organic micropollutants in the aquatic environment. In: Annual meeting of the German Waterchemical Society, Erfurt (2019).

195. Jaramillo-Loranca, B. E. *et al.* The Sigma Agonist 1 , 3-Di- o -tolyl-guanidine Reduces the Morphological and Behavioral Changes Induced by Neonatal Ventral Hippocampus Lesion in Rats. *Synapse* **225**, 213–225 (2015).

196. Lamy, C., Scuvée-Moreau, J., Dilly, S., Liégeois, J. F. & Seutin, V. The sigma agonist 1,3-di-o-tolyl-guanidine directly blocks SK channels in dopaminergic neurons and in cell lines. *Eur. J. Pharmacol.* **641**, 23–28 (2010).

197. Perrin, D. Dissociation Constants of Organic Bases in Aqueous Solution. IUPAC Publications (1965).

198. Gallard, H. & von Gunten, U. Chlorination of phenols: Kinetics and formation of chloroform. *Environ. Sci. Technol.* **36**, 884–890 (2002).

199. Deborde, M. & von Gunten, U. Reactions of chlorine with inorganic and organic compounds during water treatment-Kinetics and mechanisms: A critical review. *Water Res.* **42**, 13–51 (2008).

200. Pattison, D. I. & Davies, M. J. Absolute rate constants for the reaction of hypochlorous acid with protein side chains and peptide bonds. *Chem. Res. Toxicol.* **14**, 1453–1464 (2001).

201. Heeb, M. B., Criquet, J., Zimmermann-Steffens, S. G. & Von Gunten, U. Oxidative treatment of bromide-containing waters: Formation of bromine and its reactions with inorganic and organic

compounds - A critical review. *Water Res.* **48**, 15–42 (2014).

202. Cimetiere, N., Dossier-Berne, F. & De Laat, J. Monochloramination of resorcinol: Mechanism and kinetic modeling. *Environ. Sci. Technol.* **43**, 9380–9385 (2009).

203. El Najjar, N. H., Deborde, M., Journel, R. & Vel Leitner, N. K. Aqueous chlorination of levofloxacin: Kinetic and mechanistic study, transformation product identification and toxicity. *Water Res.* **47**, 121–129 (2013).

204. Rodil, R. *et al.* Emerging pollutants in sewage, surface and drinking water in Galicia (NW Spain). *Chemosphere* **86**, 1040–1049 (2012).

205. Wilkinson, J., Hooda, P. S., Barker, J., Barton, S. & Swinden, J. Occurrence, fate and transformation of emerging contaminants in water: An overarching review of the field. *Environ. Pollut.* **231**, 954–970 (2017).

206. Quintana, J. B., Weiss, S. & Reemtsma, T. Pathways and metabolites of microbial degradation of selected acidic pharmaceutical and their occurrence in municipal wastewater treated by a membrane bioreactor. *Water Res.* **39**, 2654–2664 (2005).

207. Iovino, P., Chianese, S., Canzano, S., Prisciandaro, M. & Musmarra, D. Degradation of Ibuprofen in Aqueous Solution with UV Light: the Effect of Reactor Volume and pH. *Water. Air. Soil Pollut.* **227**, (2016).

208. Miklos, D. B. *et al.* Evaluation of advanced oxidation processes for water and wastewater treatment – A critical review. *Water Res.* **139**, 118–131 (2018).

209. Mlunguza, N. Y., Ncube, S., Nokwethemba Mahlambi, P., Chimuka, L. & Madikizela, L. M. Adsorbents and removal strategies of non-steroidal anti-inflammatory drugs from contaminated water bodies. *J. Environ. Chem. Eng.* **7**, 103142 (2019).

210. Romeiro, A. *et al.* Titanium Dioxide Nanoparticle Photocatalysed Degradation of Ibuprofen and Naproxen in Water: Competing Hydroxyl Radical Attack and Oxidative Decarboxylation by Semiconductor Holes. *ChemistrySelect* **3**, 10915–10924 (2018).

211. Adityosulindro, S. Activation of homogeneous and heterogeneous Fenton processes by ultrasound and ultraviolet/visible irradiations for the removal of ibuprofen in water. PhD thesis. University of Toulouse (2017).

212. Da Silva, J. C. C., Teodoro, J. A. R., Afonso, R. J. D. C. F., Aquino, S. F. & Augusti, R. Photolysis and photocatalysis of ibuprofen in aqueous medium: Characterization of by-products via liquid chromatography coupled to high-resolution mass spectrometry and assessment of their toxicities against Artemia Salina. *J. Mass Spectrom.* **49**, 145–153 (2014).

213. Georgaki, I., Vasilaki, I. & Katasaris, N. A study on the degradation of carbamazepine and Ibuprofen by TiO2 & ZnO photo catalysis upon UV/Visible-light irradiation. *Am. J. Anal. Chem.* **5**, 518-534 (2014).

214. Lin, L. *et al.* Adsorption and photocatalytic oxidation of ibuprofen using nanocomposites of TiO2 nanofibers combined with BN nanosheets: Degradation products and mechanisms. *Chemosphere* **220**, 921–929 (2019).

215. Slanina, T. & Oberschmid, T. Rhodamine 6G Radical: A Spectro (Fluoro) Electrochemical and Transient Spectroscopic Study. *ChemCatChem* **10**, 4182–4190 (2018).

216. de Wilt, A. *et al.* Enhanced pharmaceutical removal from water in a three step bio-ozone-bio

process. *Water Res.* **138**, 97–105 (2018).

217. Chiron, S. *et al.* Pesticide by-products in the Rhône delta (Southern France). The case of 4-chloro-2-methylphenol and of its nitroderivative. *Chemosphere* **74**, 599–604 (2009).

218. McNeill, K. & Canonica, S. Triplet state dissolved organic matter in aquatic photochemistry: Reaction mechanisms, substrate scope, and photophysical properties. *Environ. Sci. Process. Impacts* **18**, 1381–1399 (2016).

219. Castro, G., Rodríguez, I., Ramil, M. & Cela, R. Evaluation of nitrate effects in the aqueous photodegradability of selected phenolic pollutants. *Chemosphere* **185**, 127–136 (2017).

220. Russo, D. *et al.* Investigation on the removal of the major cocaine metabolite (benzoylecgonine) inwater matrices by UV254/H2O2process by using a flow microcapillary film array photoreactor as an efficient experimental tool. *Water Res.* **89**, 375–383 (2016).

221. Bolton, J. R., Bircher, K. G., Tumas, W. & Tolman, C. A. Figures-of-merit for the technical development and application of advanced oxidation technologies for both electric- and solar-driven systems. *Pure Appl. Chem.* **73**, 627–637 (2001).

222. Zhai, S. Y. *et al.* A compact efficient deep ultraviolet laser at 266 nm. *Laser Phys. Lett.* **10**, 045402 (2013).

223. Fang, Z. *et al.* High-efficiency UV generation at 266 nm in a new nonlinear optical crystal NaSr_3Be_3B_3O_9F_4. *Opt. Express* **25**, 26500 (2017).

224. Lennikov, V. *et al.* Microstructure and transport properties of Bi-2212 prepared by CO2 laser line scanning. *J. Supercond. Nov. Magn.* **26**, 947–952 (2013).

225. Cubero, A. *et al.* Effects of laser-induced periodic surface structures on the superconducting properties of Niobium. *Appl. Surf. Sci.* **508**, 145140 (2020).

226. Wols, B. A. & Hofman-Caris, C. H. M. Review of photochemical reaction constants of organic micropollutants required for UV advanced oxidation processes in water. *Water Res.* **46**, 2815–2827 (2012).

227. Weidauer, C., Davis, C., Raeke, J., Seiwert, B. & Reemtsma, T. Sunlight photolysis of benzotriazoles - Identification of transformation products and pathways. *Chemosphere* **154**, 416–424 (2016).

228. Ryu, J., Monllor-Satoca, D., Kim, D. H., Yeo, J. & Choi, W. Photooxidation of arsenite under 254 nm irradiation with a quantum yield higher than unity. *Environ. Sci. Technol.* **47**, 9381–9387 (2013).

USC
UNIVERSIDADE
DE SANTIAGO
DE COMPOSTELA

ANNEX

USC
UNIVERSIDADE
DE SANTIAGO
DE COMPOSTELA

ANNEX: LIST OF PUBLICATIONS AND CONTRIBUTION STATEMENT

- Benigno José Sieira, Inmaculada Carpinteiro, Rosario Rodil, José Benito Quintana and Rafael Cela. Determination of N-Nitrosamines by Gas Chromatography Coupled to Quadrupole–Time-of- Flight Mass Spectrometry in Water Samples. Separations 7 (2020) 3. DOI:10.3390/separations7010003.
  Impact factor (2019): 1.9 *
  Journal ranking: Analytical Chemistry Q3, 53 of 86 *
  Citations: 1 *
  Contribution statement: I was responsible for performing all lab-experiments, collection and analysis or real samples, partially data treatment, elaboration of a first draft of the manuscript and provision of critical feedback during subsequent manuscript elaboration.

- Benigno José Sieira, José Benito Quintana, Rafael Cela, Rosario Rodil. Reaction of phenazone-type drugs and metabolites with chlorine and monochloramine. Submitted for publication.
  Contribution statement: I was responsible for performing all lab-experiments, kinetic and TP elucidation experiments, partially data treatment, elaboration of a first draft of the manuscript and provision of critical feedback during subsequent manuscript elaboration.

- Benigno José Sieira, Rosa Montes, Arnaud Touffet, Rosario Rodil, Rafael Cela, Hervé Gallard, José Benito Quintana. Chlorination and bromination of 1,3-diphenylguanidine and 1,3-di-otolylguanidine: Kinetics, transformation products and toxicity assessment. Journal of Hazardous Materials 385 (2020) 121590. DOI: 10.1016/j.jhazmat.2019.121590.
  Impact factor (2019): 9.038 *
  Journal ranking: Environmental Science Q1, 8 of 265 *
  Citations: 2 *
  Contribution statement: I was responsible for performing most kinetic and TP elucidation experiments, partially data treatment, elaboration of a first draft of the manuscript and provision of critical feedback during subsequent manuscript elaboration.

- Francisco Rey-García, Benigno José Sieira, Carmen Bao-Varela, José Ramón Leis, Luis Alberto Angurel, José Benito Quintana, Rosario Rodil, Germán Francisco de la Fuente. Can UV-C laser pulsed irradiation be used for the removal of organic micropollutants

from water? Case study with ibuprofen. Science of the Total Environment 742 (2020) 140507. DOI: 10.1016/j.scitotenv.2020.140507.
Impact factor (2019): 6.551 *
Journal ranking: Environmental Science Q1, 22 of 265 *
Citations: 0 *
Contribution statement: I was responsible for measuring the elimination fo ibuporfen, identification of TPs, data treatment and made provision of critical feedback to the published manuscript.

- Benigno José Sieira, Monica Araujo, Rosa Mª Montes, Rosario Rodil, Rafael Cela, José Benito Quintana. Transformation products of the industrial chemicals 1-vinyl-2-pyrrolidinone and 2-piperazin-1-ylethanamine formed during UV photolysis. In preparation.
  Contribution statement: I was responsible for performing most kinetic and TP elucidation experiments, partially data treatment, elaboration of a first draft of the manuscript and provision of critical feedback during subsequent manuscript elaboration.

** Data from Web of Science (Clarivate Analytics) as on October, 2nd 2020.*

USC
UNIVERSIDADE
DE SANTIAGO
DE COMPOSTELA